Towards new roles for cytochrome P450s and strigolactones in Fusarium Head Blight of Brachypodium distachyon

Valentin Changenet

université PARIS-SACLAY

NNT : 2018SACLS354

Thèse de doctorat

UNIVERSITÉ PARIS SUD

Comprendre le monde, construire l'avenir

Towards New Roles for Cytochrome P450s and Strigolactones in Fusarium Head Blight of *Brachypodium distachyon*

Thèse de doctorat de l'Université Paris-Saclay

préparée à l'Université Paris-Sud

École doctorale n°567

Sciences du végétal: du gène à l'écosystème (SDV)

Spécialité de doctorat: Biologie

Thèse présentée et soutenue à Orsay le 1er octobre 2018 par

Valentin Changenet

Composition du Jury :

Grégory Mouille Directeur de recherche, INRA (IJPB)	Président
Sofie Goormachtig Directrice de recherche, Université de Gent (VIB)	Rapportrice
Harro J. Bouwmeester Professeur, Université d'Amsterdam (SILS)	Rapporteur
Ludovic Bonhomme Maître de Conférences, Université Clermont Auvergne (GDEC)	Examinateur
Marie Dufresne Professeure, Université Paris-Sud (IPS2)	Directrice de thèse

ACKNOWLEDGEMENTS

First of all, my sincerest thanks go to all the members of my thesis jury for agreeing to read and evaluate my work. Thank you to SOFIE GOORMACHTIG, HARRO BOUWMEESTER, LUDOVIC BONHOMME and GRÉGORY MOUILLE, I wish you a pleasant reading.

Merci à MICHEL DRON et MARTIN CRESPI de m'avoir accueilli au sein de l'IBP puis de l'IPS2.

Je remercie MARIE de m'avoir intégré au sein de l'équipe et d'avoir accepté d'encadrer mes travaux de recherche en stage puis en thèse. Merci pour la confiance et la flexibilité que tu m'auras accordées, depuis notre pas de côté vers les strigolactones jusqu'à la rédaction de ce manuscrit. Merci également de m'avoir transmis ta fibre enseignante en soutenant mon choix de vouloir participer aux enseignements à l'université et en me permettant, au laboratoire, d'encadrer des stagiaires.

Merci infiniment à l'ensemble des membres de l'équipe Cerepath. Merci CATHERINE pour ton travail en amont du projet et ton aide au long cours en BM, transfo d'*Arabido*, de *Brachy*… Merci surtout pour ton attention permanente et ton soutien amical tout au long du projet! Merci TRACY pour tes coups de main, ta bonne humeur communicative et tes doigts de fée pour revigorer les souches de *Fusa*. Merci JEAN-MARC pour les discussions personnelles ou professionnelles, ton soutien pour le présent et le futur, ton ouverture d'esprit légendaire et tes ravitaillements réguliers en dattes et autres clémentines. Merci également aux 'anciens' de l'équipe. MIRIAM, merci pour ta personnalité hors-norme et les bons moments à la paillasse comme sur les pistes de ski ! JULIE, merci pour ta fine oreille sur laquelle je continue de beaucoup compter. AUDREY, merci pour les quelques fous rires au labo et l'important soutien amical en dehors. Enfin, PATRICK, merci de l'attention régulière que tu auras porté à ce projet ainsi que pour tes nombreux conseils notamment au moment de la préparation du concours. Merci SOPHIE M, certes en dehors de l'équipe, mais naturellement associée à ce paragraphe étant données ta gentillesse et ton écoute. Je remercie également l'ensemble des stagiaires qui auront contribué à ce projet de recherche : MATHIEU, TANGUY, CLAIRE, NOLWENN, MELANIE, MARGAUX, CLEMENT ainsi que les étudiants de l'UE AOM. Merci de nous avoir aidés à explorer un maximum d'hypothèses, ce fut un plaisir de pouvoir travailler avec vous tous.

Je tiens à remercier chaleureusement les nombreuses personnes qui ont collaboré avec nous sur ce projet de recherche. Sans votre expertise, vos conseils et votre aide technique, nous aurions encore butté quelques années sur la fonction de notre P450 d'intérêt. DANIELE WERCK et HUGUES RENAULT d'abord, merci de m'avoir accueilli à l'IBMP de Strasbourg durant mon M2 pour produire le P450 recombinant. Merci Danièle d'avoir accepté de participer à mon premier comité de thèse. Merci à SANDRINE BONHOMME et CATHERINE RAMEAU de l'IJPB de Versailles pour les discussions autour des strigolactones et les semences d'*Arabidopsis*. Merci Catherine d'avoir suivi avec attention l'avancée de mon projet au travers de ta participation à mon comité. Merci également à STEPHANIE BOUTET-MERCEY et GREGORY MOUILLE, également de l'IJPB, pour le grand travail de détection et quantification des strigolactones chez *Brachypodium*. Stéphanie, merci pour tes analyses chromatographiques d'une rapidité déconcertante, ton

attention permanente au bon déroulement de notre projet et tes conseils amicaux. Grégory, merci d'avoir participé à mes comités et de confirmer ton soutien au travers de ta participation à mon jury. Merci à SOPHIE BERNAD et EDDINE BRICK de m'avoir accueilli au sein des labos du Master MEEF PC afin de réaliser l'une des premières extractions de strigolactones chez *Brachypodium*. Enfin, merci à BENOIT LEFEBVRE, MEGANE GASTON et LUIS BUENDIA du LRSV de Toulouse pour votre accueil sur place et pour l'initiation au subtil art de la mycorhization chez *Brachypodium*.

Je remercie toutes les personnes avec qui j'ai pu interagir au cours de mes activités d'enseignement. Mes chef.fe.s d'abord : CELINE CHARON, MATHIEU JOSSIER, MICHEL MENOU, MARTINE THOMAS et MARIE DUFRESNE, une nouvelle fois. Merci pour l'accueil au sein de vos équipes respectives ainsi que de votre confiance. Ce fut une expérience extrêmement enrichissante et qui va me manquer. Merci également à tous les collègues : SOPHIE, NATALIA, MARJORIE, AXEL, BENOIT, ALEXIS, BERTRAND, FLORENCE, RICHARD, CAMILLE et beaucoup d'autres pour votre gentillesse et votre bonne humeur depuis les réunions de début d'année jusqu'aux examens finaux. Merci évidemment à MARIE B, SYLVIE, VERONIQUE et CLAUDINE de leur aide en TP (merci Sylvie et Véro pour les nombreux dépannages de matériels !).

Je remercie sincèrement l'ensemble du personnel de l'IPS2 et surtout les services communs pour leur aide quotidienne : merci au service culture, à la laverie, à l'administration, au magasin, au service technique et aux services informatiques.

Merci à JACQUI, MARIANNE et MARTINE de l'ED SDV pour leur écoute et leur disponibilité tout au long du projet. J'en profite également pour remercier JEAN COLCOMBET d'avoir représenté l'ED durant mes comités de thèse mais surtout pour son soutien scientifique et humain.

Un grand merci va à tous les copains de Doc' en Herbe, passés, présents et futurs, pour leur engagement dans ce beau projet. Merci les présidentes : FATIMA, SOV' et PILONE ainsi que tous les membres des bureaux successifs. Un merci particulier ira à ma 'thesis mate', Pilone, un soutien humain de premier ordre et qui a apaisé bon nombre de petits (et grands !) tracas. Très grand merci Pilone, je te souhaite plein de belles découvertes et de réussite pour cette dernière ligne droite !

Merci aux amis de toujours, aux plus récents et à ma famille d'avoir accompagné ce projet avec beaucoup de bienveillance : SALICETI, LULU LT, LULU PFEIFER, LULU CHANGENET, CLARA, ANIS RUPAUL JR., NICOUD, JUANITO, MAËL, CECILOU, CAM', VLAD, YANPEI, merci à vous ! Merci AUREL, silver quail de compétition et indéfectible soutien…

Enfin, je souhaitais terminer ces remerciements par JEAN-CLAUDE PASQUET. Jean-Claude a participé à l'initiation du pathosystème *Brachypodium*/*Fusarium* à l'IBP puis à l'élaboration de tous les projets de recherches qui se sont succédé, et donc au mien. Durant les quelques mois de mon stage M1 puis M2, il m'aura appris toutes les techniques routinières du laboratoire, mais aussi la rigueur, la discipline et l'envie nécessaire à la réussite du projet. Son absence ces trois années aura laissé un grand vide que nous aurons surmonté tant bien que mal. C'est avec beaucoup de fierté que je lui adresse ce manuscrit, en reconnaissance de son important travail.

ABBREVIATIONS

ABA	Abscisic Acid	**ha**	hectare
ABC	ATP-Binding Cassette	**hpi**	hour post-infection
AMF	Arbuscular Mycorrhizal Fungus	**IDM**	Integrated Disease Management
ATP	Adenosine Triphosphate	**JA**	Jasmonic Acid
AUC	Area Under the Curve	**L**	Liter
BC	Before Christ	**LC-MS/MS**	Liquid Chromatography coupled to double Mass Spectrometry
BR	Brassinosteroid		
cDNA	complementary DNA		
CDS	Coding DNA Sequence	**M**	Molar
CK	Cytokinin	**Mbp**	Megabase pair
cm	centimeter	**mg**	milligram
CMS	Cytoplasmic Male Sterility	**Mha**	Million hectares
d	day	**min**	minute
DAB	Diaminobenzidine	**mL**	milliLiter
DAF	Day After Fecundation	**mm**	millimeter
DAG	Day After Germination	**mM**	milliMolar
DEG	Differentially Expressed Gene	**mol**	mole
DNA	Deoxyribonucleic Acid	**MS**	Murashige and Skoog
DON	Deoxynivalenol	**Mt**	Million tons
dpi	day post-infection	**MWC**	Modern Wheat Cultivar
FAD	Flavin Adenine Dinucleotide	**MRM**	Multiple Reactions Monitoring
FHB	Fusarium Head Blight		
FW	Fresh Weight	**Myr**	Million years
FX	Fusarenon X	**N**	North
g	gram	**NAD**	Nicotinamide Adenine Dinucleotide
g	gravitational force		
gDNA	genomic DNA	**NADH**	reduced NAD
GA	Gibberellin	**NIL**	Near Isogenic Line
GFP	Green Fluorescent Protein	**NIV**	Nivalenol
GST	Glutathione-*S*-Transferase	**nm**	nanometer
h	hour	**P450**	Cytochrome P450

PCD	Programmed Cell Death	**ssp**	subspecies
pCMA	*p*-Chloro-*N*-Methylaniline	**t**	ton
PCR	Polymerase Chain Reaction	**TAD**	Take-All Decline
PDA	Potato Dextrose Broth	**T-DNA**	Transfer-DNA
pmol	picomole	**TCT(B)**	(Type B) Trichothecene
PR	Pathogenesis-Related	**TILLING**	Targeting Induced Local
qPCR	quantitative PCR		Lesions in Genomes
RGSV	Rice Grassy Stunt Virus	**UGT**	Uridine diphosphate
RIL	Recombinant Inbred Line		Glycosyltransferase
RNA	Ribonucleic Acid	**UK**	United Kingdom
RNAi	RNA interference	**USA**	United States of America
ROS	Reactive Oxygen Species	**v/v**	volume/volume
rpm	revolutions per minute	**wpi**	week post-infection
RT	Revers Transcription	**WT**	Wild Type
s	second	**ZEA**	Zearalenone
S	South	**°**	degree
SA	Salicylic Acid	**µL**	microLiter
SL	Strigolactone	**µM**	microMolar
sp	species	**µmol**	micromole

LIST OF FIGURES

CHAPTER I | INTRODUCTION

CHAPTER II │RESULTS (1/3)

CHAPTER III │RESULTS (2/3)

CHAPTER IV │RESULTS (3/3)

CHAPTER V │DISCUSSION

LIST OF TABLES

CHAPTER I | INTRODUCTION

CHAPTER II | RESULTS (1/3)

CHAPTER III | RESULTS (2/3)

TABLE OF CONTENT

CHAPTER I | INTRODUCTION

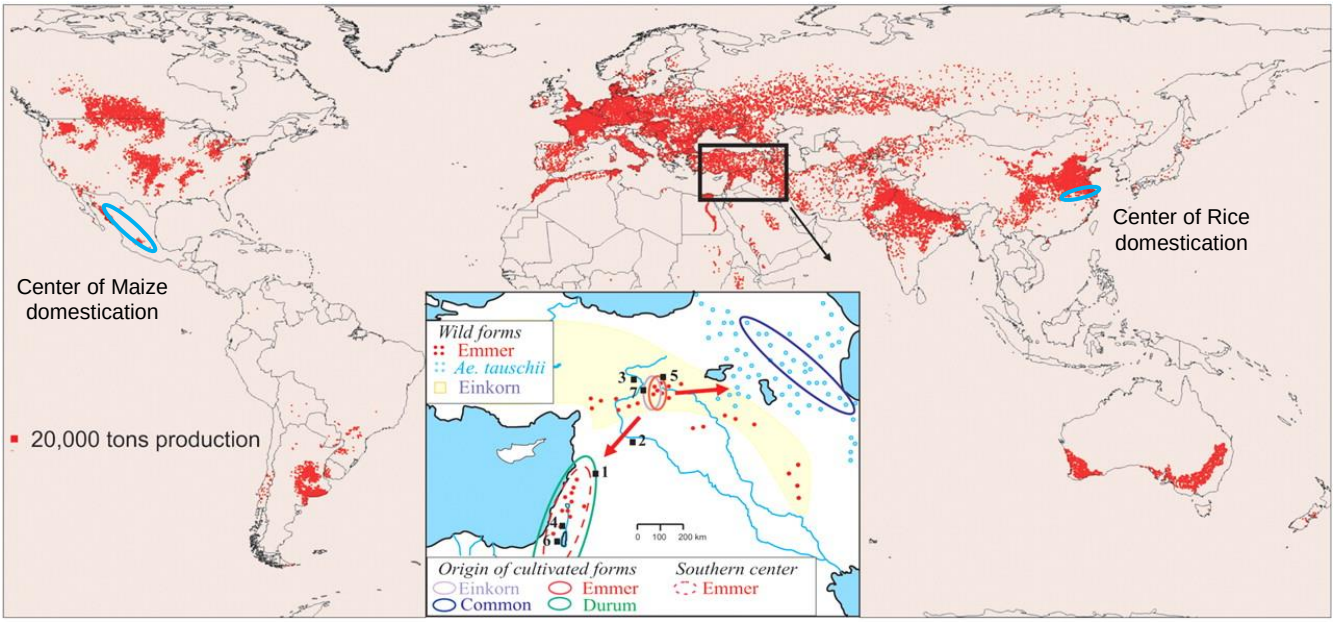

Figure 1.1: The origin and current distribution of wheat. Red dots indicate wheat production sites. In the inset, solid lines indicate origins of cultivated forms of Einkorn (*T. boeticum*), Common wheat (hexaploid common wheat, *T. aestivum*), Emmer (*T. dicoccum*), Durum wheat (tetraploid common wheat, *T. durum*) and dotted line indicate a center of domesticated Emmer diversity. Origins of wild forms of wheat (inset) and centers of Maize and Rice domestication (light blue solid lines on the world map) are also indicated (adapted from Salamini et al., 2002).

A. THE BREAD WHEAT

Plant domestication was one of the most important human developments. It marks the Neolithic Revolution resulting in a lifestyle transition from hunting and food gathering to agriculture and settling. Very few species received this initial attention from human. Wheat was one of them, and ten thousand years later it continues to be the center of all cares. In addition to being a worldwide staple food for millennia, wheat is also used as a feed grain and its processing into starch and gluten allows the production of various industrial products such as alcohol, cosmetics or rubber. It is therefore easily understandable that wheat has become a central element in various lifestyles, cultures and of course in the globalized economy. The aim of this first section is to draw a general overview on wheat in the 21st century. After a general description of wheat domestication, breeding programs and worldwide production, we will go further into the modern and future challenges that surround wheat growing. Among them, disease management is a major issue and we will see how a model temperate cereal, *Brachypodium distachyon*, could help us to improve wheat disease resistance in a context of a world growing population and climate change.

A.1. From ancestral domestication to future breeding

Among the cultural, societal and economic changes that defined the Neolithic Revolution, domestication of plants was a forerunner (Bar-Yosef, 1998). It took place approximately at the same time (8,000 – 10,000 BC) in three locations: the south of present Mexico, the Yangtze Valley of China today and the Fertile Crescent in the Middle East. There, a set of factors including ideal climatic conditions allowed the domestication of maize, rice and temperate cereals, respectively (**Figure 1.1**; Feldman, 2001; Matsuoka et al., 2002; Molina et al., 2011). The Fertile Crescent concentrated 5 ancestral species of the modern temperate cereals: *Triticum urartu* (*T. urartu* Tuman., genome AA), wild emmer (*T. turgidum* L. ssp. *dicoccoides* Aschers., genome AABB), wild einkorn (*T. monococcum* L. ssp. *boeticum* Boiss., genome AA), wild rye (*Secale cereale* L. ssp. *vavilovii* Grossh., genome RR) and wild barley (*Hordeum vulgare* L. ssp. *spontaneum* Thell., genome HH; Salamini et al., 2002). The origin of hexaploid bread wheat, which remains partly unclear, depended on two factors: the independent domestication of several wild species (i.e. the human selection of traits of interest) and the hybridization of distinct species (**Figure 1.2**). Tetraploid wild emmer domestication led to the development of several domesticated species including durum wheat (*T. turgidum* L. ssp. *durum* Desf., genome AABB) which is still currently used for making

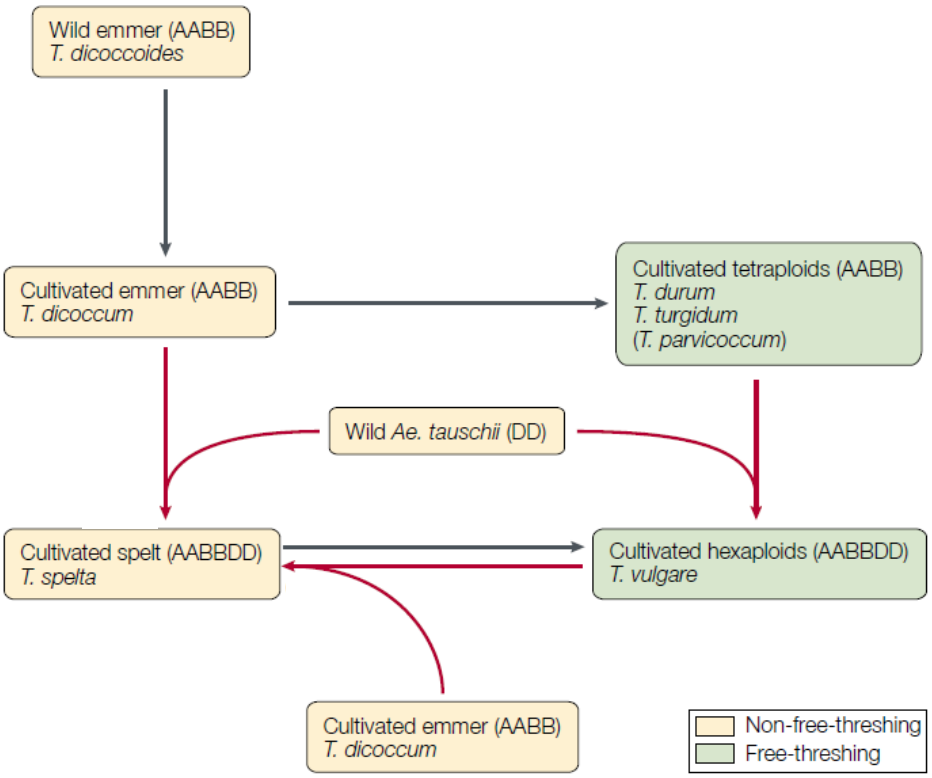

Figure 1.2: Model of origin of polyploid wheats. Hybridization events (red arrows), domestication events (black arrows) and genome formulas are indicated. Background colors differentiate free-threshing (green) and non-free-threshing (yellow) grains. *T.*: *Triticum*; *Ae.*: *Aegilops* (Salamini et al., 2002; adapted).

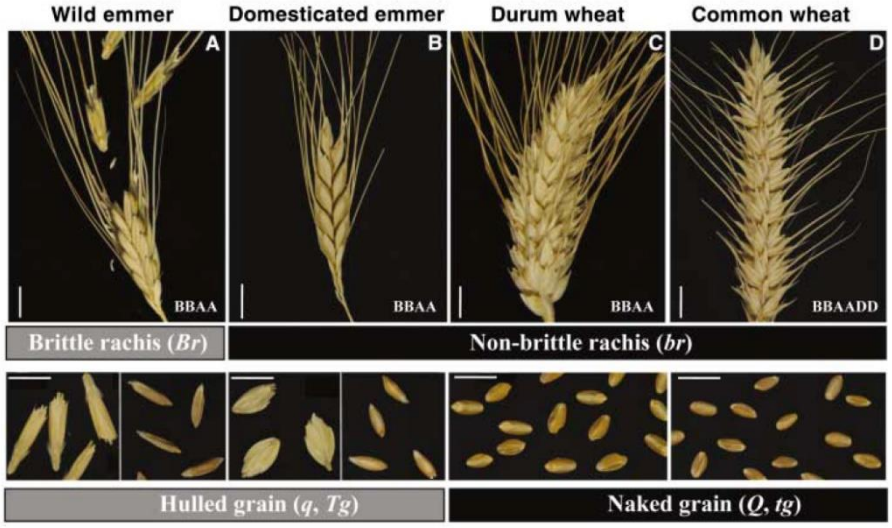

Figure 1.3: The wheat domestication syndrome. Wheat spikes showing (A) brittle rachis. (B to D) non-brittle rachis. (A and B) hulled grain. and (C and D) free-threshing grain. Genome formula of the different types of wheat together with genotype on the *Br* (*brittle rachis*). *Tg* (*tenacious glume*) and *Q* (*square head*) loci are indicated. Bars = 1 cm. (Dubcovsky and Dvorak, 2007).

pasta or semolina. A hybridization between *T. turgidum* and the wild diploid grass *Aegilops tauschii* (also called *T. tauschii*, genome DD) finally led to the emergence of the hexaploid bread wheat (*T. aestivum* L. ssp. *vulgare* Host., genome AABBDD) about 9,000 years ago (Feldman, 2001; Salamini et al., 2002; **Figure 1.2**)

Two major traits differentiate domesticated wheats from wild ones: spike shattering and glume adhesion to the grain (Shewry, 2009). The first one is governed by the *Br* (*brittle rachis*) loci which originally allowed effective seed dispersal at spike maturity through the formation of a fracture zone on the rachis. In an agricultural context and to limit seed loss at harvesting, recessive alleles of the *Br* loci were selected (Nalam et al., 2006). The second trait, glume adhesion to the grain, evolved from adherence in wild species to free-threshing in cultivated cereals. Also selected for facilitating the harvest, this trait is determined by the *tenacious glume* loci (*Tg*) and the *Q* (*square head*) gene (Simons et al., 2006; **Figures 1.2-1.3**). Many other traits are associated with the so-called wheat 'domestication syndrome' including increased seed size, reduced tillering or reduced seed dormancy (Dubcovsky and Dvorak, 2007). In addition to these characteristics shared by all domesticated wheats, more recent efforts have been conducted to generate thousands of bread wheat varieties able to grow from south of Norway at 65°N to south of Argentina at 45°S (Feldman, 1995; Dubcovsky and Dvorak, 2007).

Until the 19th century, crops varieties were considered as 'land races' since they had all evolved, mainly naturally, in the area where they were grown. It is only in the early 1870's that efforts were made to improve wheat varieties through breeding programs (Lupton, 1987). In France, Henry de Vilmorin initiated the work on wheat hybridization in 1873 in order to obtain high yield, high grain quality and drought-tolerant wheat varieties (Vilmorin, 1880). His first commercial hybrid variety, Dattel, was released in 1883 and encountered a remarkable success because of its developmental and stress-tolerant qualities. Simultaneously, hybrids were developed in other European countries, North America, Australia and others with more and more the same goal of getting semi-dwarf high-yielding varieties (Lupton, 1987). Since the middle of the 20th century, modern wheat cultivars (MWCs) were developed thanks to the setting up of wheat germplasm banks, for example, by the International Maize and Wheat Improvement Center (Reif et al., 2005; CIMMYT, 2018). Using this genetic diversity, scientists had the opportunity to cross lines with interesting traits (e.g. biotic or abiotic stress tolerance) with local elite variety, hence to propose cultivars highly adapted to specific local issues.

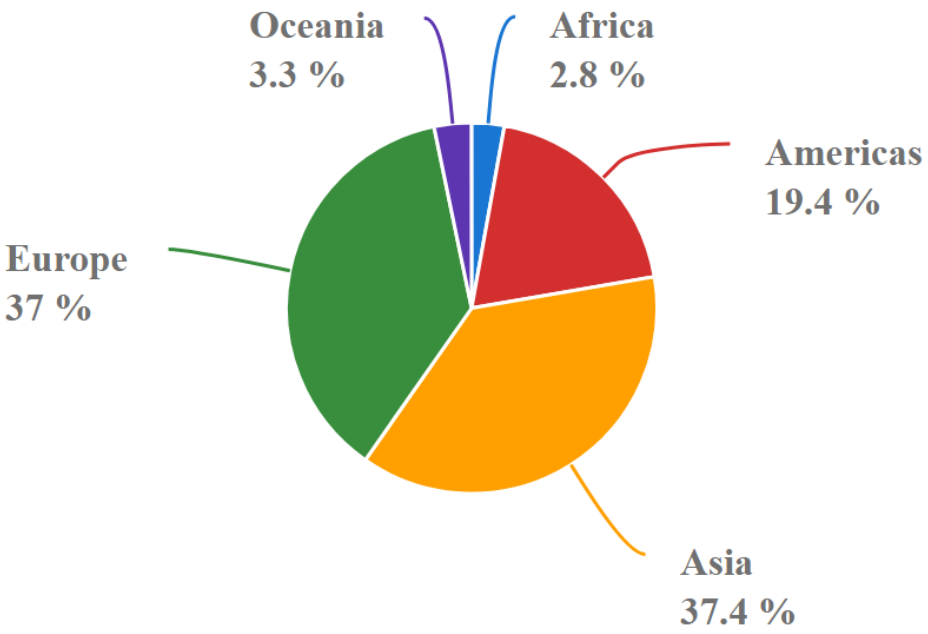

Figure 1.4: Production share of wheat by region. Average of production share between 1961 and 2016 (FAO, 2018).

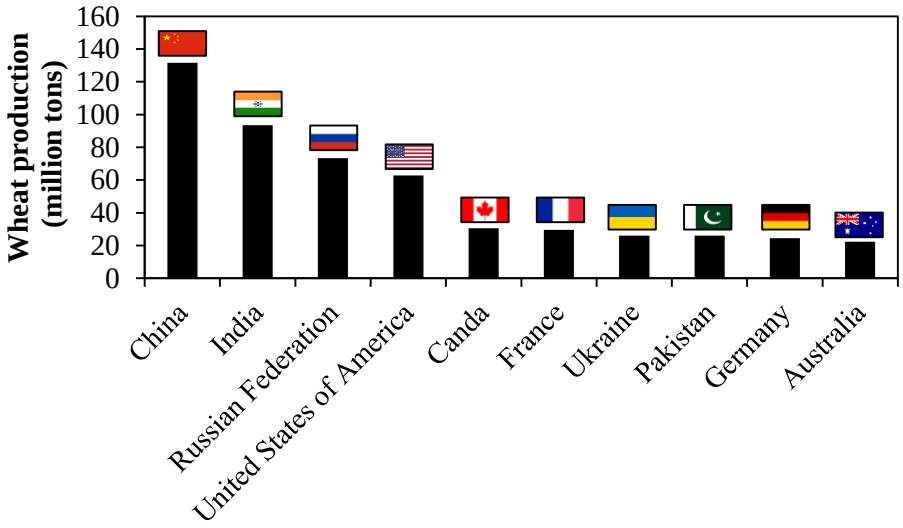

Figure 1.5: Top 10 producers of wheat in 2016. (FAO, 2018; adapted).

Most of the wheat varieties grown nowadays are inbred lines. Indeed, hybrid (F1) wheat lines are much more complicated to obtain on a large scale than for other species for which breeders take advantage of cytoplasmic male sterility (CMS) to produce F1 and benefit from heterosis. In wheat, it has been shown that hybrids present increased yield stability as compared with inbred lines (Mühleisen et al., 2014). It has been therefore proposed as a future goal in breeding programs to facilitate the production of wheat hybrids. This could be done, for example, by screening for morphological traits of interest (e.g. anther extrusion) or by mapping potential CMS systems in the wheat genome. Together with a better use of available genetic resources in germplasm banks, this strategy might contribute to significantly increase wheat yields what will be necessary to support the growth of the world population (Longin, 2016).

A.2. The global wheat production and its challenges

Among crops, wheat has a very special position. According to the Food and Agriculture Organization of the United Nations (FAO), wheat was ranked third in weight produced in 2016, after maize and sugar cane, with nearly 750 million tons (Mt) and it is grown on extended land areas than any other crop with more than 220 million hectares (Mha; **Figure 1.1**; FAO, 2018). Its world trade is also considered as greater than for all other crops combined (Curtis, 2004). This is consistent with the fact that approximately one-fifth of the world's food depends on wheat (Enghiad et al., 2017). Asia is responsible for most of the production with an average of 37.4% of total production between 1961 and 2016 (**Figure 1.4**). Indeed, the biggest producers are China and India with 131.7 and 93.5 Mt produced in 2016, respectively (**Figure 1.5**). The average worldwide yield was 3.36 $t.ha^{-1}$ in 2016, about 3 times more compared to 1961, but it is very variable depending on the geographic area and could reach 9 to 10 $t.ha^{-1}$, for example, in Ireland and in New Zealand (FAO, 2018).

Agriculture is facing new challenges today. These can be summarized into three current finding: world population is growing very rapidly and might reach 9 million people in 2050, competition for land, water and energy is becoming increasingly difficult and finally, climate change could make it more difficult to grow crops (Godfray et al., 2010). The general objective is, therefore, to increase agricultural production by improving yields in a sustainable way. Regarding wheat, it is still complicated to clearly evaluate the future impact of climate change but data collected since 1980 indicate a slight decrease of wheat yield mostly due to the temperature elevation (Lobell et al., 2011). Among numerous aspects which should be

Table 1.1: Major wheat fungal diseases in Europe and their estimated impact on yield losses (t.ha^{-1}) in different countries. (ENDURE. 2018; adapted).


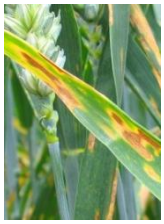
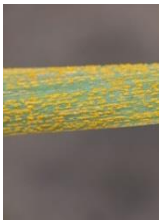



Fungal Pathogen	*Tapesia yallundae*	*Zymoseptoria tritici*	*Puccinia striiformis*	*Puccinia triticina*	*Fusarium* spp.	*G. graminis*[a]	*Blumeria graminis*
Plant organ	Stem base	Leaf	Leaf	Leaf	Spike	Root	Leaf
Disease	Eyespot	Septoria leaf blotch	Yellow rust	Brown rust	Fusarium Head Blight	Take-all	Powdery mildew
France	0.3	1.5	0	1	0.2	0-2	0.1
Germany	n.d.[c]	0.32	0.25	0.27	0.04	n.d.[c]	0.17
UK[b]	0.2	1	0.1	0.1	0.05	0.8	0.1
Netherlands	0.1	0.5	0.1	0.1	0.2	0.1	0.1
Poland	0.5	0.4	0.1	1	0.1	1.2	n.d.[c]
Denmark	0.2	0.8	0.1	0.1	0.1	0.3	0.2

[a]*Gaeumannomyces graminis*

[b]United Kingdom

[c]Not determined

studied in parallel to ensure the increase of global quality wheat production, disease management remains specifically challenging, in particular in the context of climate change (Chakraborty and Newton, 2011).

A.3. Wheat diseases

Among the nearly 200 wheat diseases and pests referenced, 50 are considered economically important (Singh et al., 2016). They can affect all plant parts and occur additively on the same plant but their importance is highly variable depending on geographical area. Despite crop protection practices, all combined biotic stress (weeds, animal pests, pathogenic microorganisms and viruses) are responsible for 28.2% of yield losses worldwide (Oerke, 2006). Most of these losses (36.1% of total losses) are due to microorganisms, mainly pathogenic fungi. As illustrated in **Table 1.1**, major wheat fungal pathogens cause losses in Europe ranging from 0.04 to 1.5 and even 2.0 $t.ha^{-1}$. With respect to yield losses but also grain quality, septoria leaf blotch, brown rust, take-all and Fusarium Head Blight are considered as the most important wheat diseases in Europe (ENDURE, 2018) and the first three are briefly discussed under.

A.3.1. The main wheat fungal diseases

- **Septoria leaf blotch:** Caused by *Zymoseptoria tritici* (*Zt*), septoria leaf blotch is the most economically important disease of wheat with approximately €1 billion investment in fungicide each year. *Zt* exhibits a hemibiotrophic lifestyle initiated by germinating spores infection at the leaf surface through natural openings (stomata; Kettles and Kanyuka, 2016). The biotrophic phase (asymptomatic phase) generally last 7 to 10 days followed by a sharp increase of fungal biomass. Interestingly, it coincides with host activation of programmed cell death (PCD) which results in cell wall degradation and the release of nutrients into the apoplastic compartment (Keon et al., 2007). During this necrotrophic phase, symptoms rapidly spread as a blotch on leaves surface until the production of macro- and/or micro- pycnidiospores. It marks the end of the asexual lifecyle of *Zt*, approximately 2 to 3 weeks after infection (Rudd et al., 2015). *Zt* also produces sexual ascospores which allow over-seasoning and long distance dispersion (Steinberg, 2015). It is interesting to notice that whatever the infection stage, especially during its necrotrophic phase, the fungal pathogen only grows intercellularly within host tissues, which

constitutes a singular strategy. *Zt* also produces a high diversity of secreted effectors and somehow behaves more as an obligate biotroph (Dean et al., 2012).

- **Brown rust:** Also known as leaf rust, brown rust caused by *Puccinia triticina* Erikss. (*Pt*) is the most important rust disease on wheat in terms of regularity and spatial distribution (Bolton et al., 2008). The causal agent has a broad host range among wild and cultivated wheats. Like all the other *Puccinia* species, *Pt* is an obligate (biotrophic) and heteroecious fungus, which means that it needs two botanically different species to complete its sexual lifecycle (Zhao et al., 2016). The complex lifecycle of *Pt* starts on the telial host (wheat) and allows the production of urediniospores which can reinfect the host plant indefinitely. It also leads to the production of teliospores, themselves involved in basidiospores production. These will then infect the pycnial host (*Thalictrum speciosissimum* or *Isopyrum fumaroides*), and this results in the production of haploid mobile pycniospores. The mating of compatible receptive hyphae with a pycniospore generates dikaryotic mycelium which proliferates and produces aeciospores. The lifecycle ends with the germination of dikaryotic aeciospores on the telial host (Bolton et al., 2008).

- **Take-all:** *Gaeumannomyces graminis* var. *tritici* (*Ggt*) is the causal agent of the most important root disease of wheat worldwide, take-all. Indeed, *Ggt* has developed the ability to infect wheat grown both in moist or dry conditions (Kwak and Weller, 2013). *Ggt* is homothallic and its unisexual reproduction on host plant leads to the formation of ascospores which constitute the secondary inoculum (Roach et al., 2014). It survives between two seasons in a saprophytic state on debris or on other susceptible grasses and infects wheat through a mycelial invasion of the root system. Diseased plants usually exhibit root rot, stunting and nutrient deficiency which could lead to a premature death of the plant (Kwak and Weller, 2013). As other soilborne diseases, take-all remains difficult to manage because of the lack of resistant wheat cultivars. Most of the growers depend on the spontaneous take-all decline (TAD) to limit the impact of the disease when crop rotation is not possible. This is a specific case of suppressive soil in which a set of microorganisms (here rhizobacteria) compete with the soilborne pathogen and limit its growth (Cook, 2003).

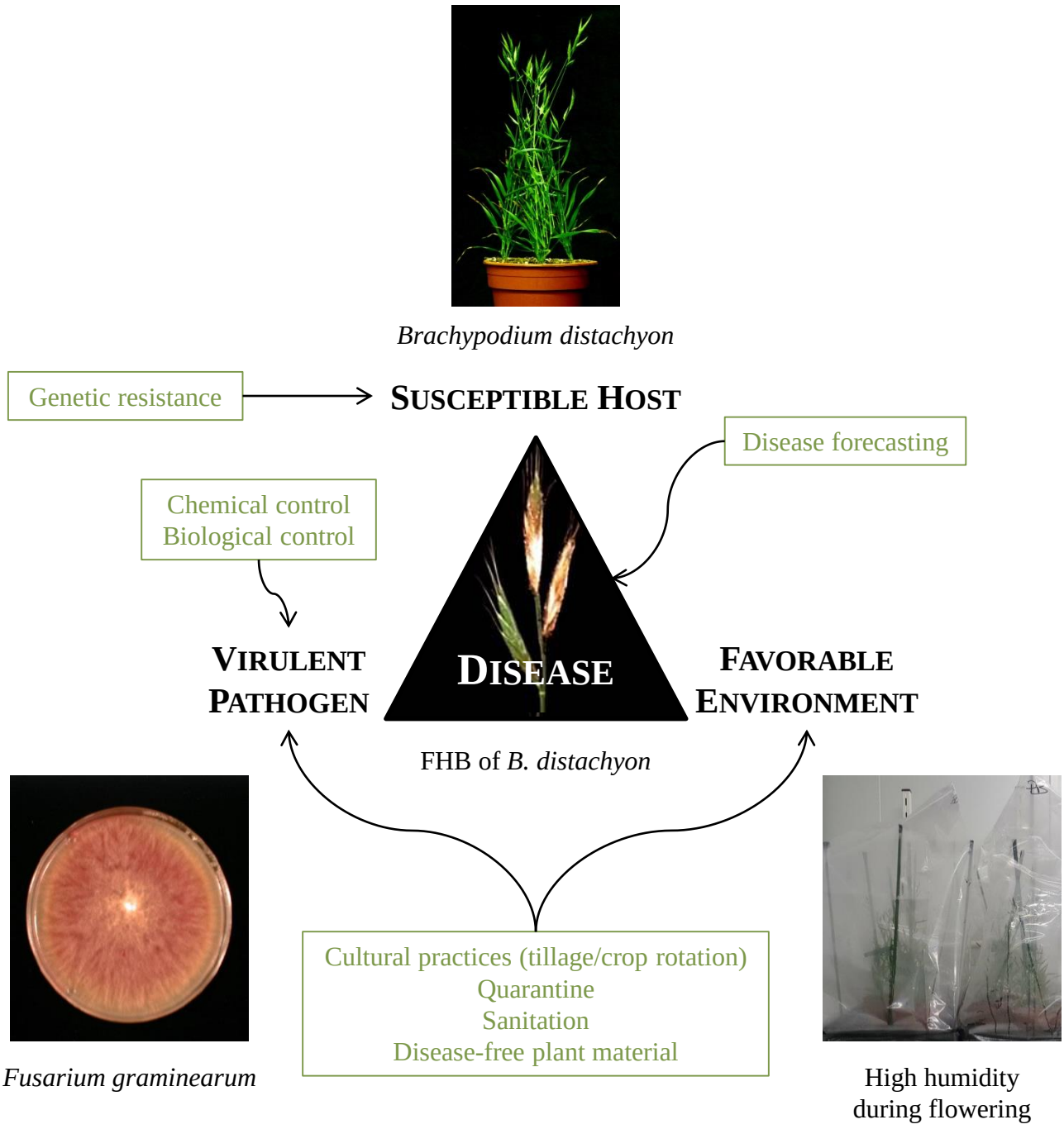

Figure 1.6: The disease triangle and the main disease management strategies. The black arrows indicate which management strategy (in green) impacts which disease factor (in black). An example is given with the disease context related to FHB on *B. distachyon*.

A.3.2. Wheat diseases management strategies

Modern agriculture promoted disease development for all crops, mainly because of the growing need to cultivate genetically homogenous plants in large areas. In that context, development and improvement of diseases management strategies have become necessary (Fry, 1982). Several approaches have been developed to prevent diseases emergence and/or to limit their development. Disease forecasting is the earlier and is based on the "disease triangle" paradigm in which plant affliction emergence depends on three factors: a susceptible host, a virulent pathogen and a favorable environment (**Figure 1.6**; Francl, 2001). In that context, numerous models for wheat disease forecasting are developed and improved and this results in the provision to farmers of several prevention tools adapted to local issues (e.g. CropMonitor™ CHAP, 2018 in the United Kingdom or Baromètre Maladies Arvalis, 2018 in France). In the same perspective, diagnosis tools have also been developed. Recent efforts have, for example, made it possible to directly analyze photos of symptoms taken directly in the field to make a diagnosis (Lu et al., 2017). Altogether, this information can guide farmers in choosing whether to conduct a preventive or curative fight against a potential disease.

Since the beginning of the 20th century, four disease management principles are generally accepted: (1) exclusion and (2) eradication of plant pathogens, (3) protection and (4) resistance of the host plant (Maloy, 2005). The first one, exclusion (1), refers to methods that prevent disease development through the maintenance of a zero inoculum. These include quarantine: the closure of a more or less large area to material/species considered as potentially contaminated; sanitation: the use of technics to limit disease spreading especially through the decontamination of agricultural equipment; and the use of disease-free propagating plant material for example by decontaminating wheat seeds in hot water prior sowing (Ogle, 1997). Despite these precautions, if there is an outbreak of a plant disease, the eradication (2) should be considered to stop disease development and, ideally, go back to a zero inoculum situation. It mainly consists of the destruction of all plants in a defined perimeter and it was for example used to manage stem rust of wheat caused by *P. graminis* Pers. (*Pg*) in the USA. Indeed, an eradication campaign against the common barberry (*Berberis vulgaris* L.), the pynial host of *Pg*, efficiently disturbed the pathogen lifecycle and resulted in a significant (but not utter) reduction of the virulent inoculum in the USA since the beginning of the 20th century (Roelfs, 1982). The protection principle (3) includes all technics allowing the establishment of a chemical, physical or spatiotemporal barrier between the pathogen and its host. We have mentioned above, for example, that the use of a biocide, as fungicide, could be tremendous in

Table 1.2: Biological traits comparison between three model plants and wheat. (Draper et al., 2001; adapted).

Bars: 10 cm




	Arabidopsis thaliana	**Rice (*O. sativa*)**	***Brachypodium distachyon***	**Wheat (*T. aestivum*)**
Plant family	Crucifereae	Oryzoideae	Pooideae	Pooideae
# Chromosomes	10 (2n)	24 (2n)	10 (2n)	42 (6n)
Genome size	157 Mbp	389 Mbp	272 Mbp	15,345 Mbp
Amount of repetitive DNA	16 %	20 %	12-15 %	80 %
Breeding strategy	Self-fertile	Outbreeder	Self-fertile	Self-fertile
Life cycle (weeks)	8-10	20-30	8-18	20-35
Height at maturity	20 cm	1-1.2 m	20 cm	0.7-1 m
Seed yield per plant	Thousands	Thousands	Hundreds	Thousands
Lab growth requirements	Simple	Relatively specialized	Simple	Simple
Transformation efficiency	0.5-4 % (Floral dipping)	3-8 % (Agrobacterium-mediated callus transformation)	5 % (Agrobacterium-mediated callus transformation)	< 1 % (Biolistic-mediated callus transformation)

septoria leaf blotch management (Torriani et al., 2015). But protection also includes the use of biocontrol agents or cultural practices such as tillage, rotation to nonsusceptible crop or modification of the soil structure and composition (Maloy, 2005). Finally, major efforts have and will be done to improve wheat genetic resistance to diseases. Indeed, this aspect belongs to the priorities of the actual breeding program led by CIMMYT but was also of special interest in the characterization of the first wheat hybrids at the beginning of the last century (Guzman et al., 2016). Interestingly, hexaploid wheat is not the sole source of resistance genes. Currently used rusts resistance genes, for example, have been obtained from wild relatives (*T. spelta* L., *T. monococcum*…) L. but also from other genera (*Aegilops* or *Secal*; Mondal et al., 2016). Bioinformatics tools and facilitation of gene introgression technics will probably accelerate this trend by enlarging the pool of putative genes of interest regardless of the ecological classification of the donor organism. Though most of wheat disease management lies in improving protection and resistance, the integration of several methods and practices through the Integrated Disease Management (IDM) concept is taking more interest. Unfortunately, although this method has been proven for a long time and has shown good results, it remains poorly used in the fields (El Khoury and Makkouk, 2010).

In order to improve existing diseases management strategies and develop new ones on a large scale, direct studies on wheat are limited for different reasons including its long lifecycle, size and above all its complex genome. A growing need in a lab-friendly wheat model of the same family finally led to the use of a small grain cereal suitable for translational biology: *Brachypodium distachyon*.

A.4. *Brachypodium distachyon*: a model cereal for bread wheat

Since the 1980's, *Arabidopsis thaliana* (L.) Heynh. is considered as the most successful plant model system. Indeed, this eudicotyledonous plant possesses a range of lab-compatible traits such as a short lifecycle, a small size and a small well-sequenced diploid genome which facilitated the establishment of a devoted scientific community worldwide (**Table 1.2**; Meinke, 1998; The Arabidopsis Genome Initiative, 2000). Nevertheless, *A. thaliana* is clearly phylogenetically distant to the Poaceae family which contains the world's major cereals crops and forage grasses; hence it raised the need for a new model species closer to the cultivated cereals in particular. This situation led to the emergence of rice (*Oryza sativa* L.) as a potential Poaceae model, especially for cereal genomics studies and because of its status of worldwide staple food (Goff, 1999). However, growing rice in the lab is very

technical and this species behaves quite differentially than temperate cereal crops, this is why Draper et al. (2001) first proposed *Brachypodium distachyon* as a potential model for functional genomics of the temperate cereals and forage grasses (**Table 1.2**).

Brachypodium distachyon (L.) P.Beauv., named from Greek βραχύς (brachys) short, and πόδιον (podion) foot, in reference to the small pedicels of its spikelets, has been firstly described in 1812 by the French naturalist Ambroise Marie François Joseph Palisot de Beauvois (1752 – 1820; Palisot de Beauvois, 1812; IPNI, 2018). Commonly known as purple false brome, *B. distachyon* is a C3 grass of relatively short height (15-20 cm), self-fertile and has a short annual lifecycle (8-12 weeks excluding the vernalization period) suitable for high throughput studies. When grown in very long day conditions (≥ 20 h day), several inbred lines, including the fully sequenced Bd21 ecotype, do not need vernalization to induce flowering, which greatly facilitates the culture (Vogel and Bragg, 2009; The International Brachypodium Initiative, 2010). In the wild, *B. distachyon* is found in the middle-east and throughout the Mediterranean region (Li et al., 2012). It belongs to the same order (Poales), family (Poaceae) and sub-family (Pooideae) as wheat, rye, oat or barley (Pimentel et al., 2017; Soreng et al., 2017). Finally, the divergence between *B. distachyon* and wheat has been estimated 32-39 Myr ago whereas rice diverged earlier from wheat (40-53 Myr ago; Vogel et al., 2010).

Beside these biological traits, *B. distachyon* has been mainly selected as a model grass for its genetic and genomic features. Indeed, it possesses a relatively small, simple and well sequenced diploid genome of 272 Mbp (2n = 10) as compared to the hexaploid and 15,345 Mbp (2n = 6x = 42) one of *T. aestivum* (The International Brachypodium Initiative, 2010; Zimin et al., 2017). Moreover and despite numerous intraspecific genome rearrangements, a relatively high degree of synteny could be found between *B. distachyon* and wheat genomes (The International Brachypodium Initiative, 2010; Brutnell et al., 2015). Thenceforth, numerous tools have been developed to use this grass as a model for functional genomics of temperate cereals among which an efficient *Agrobacterium*-mediated transformation system (Vogel and Hill, 2008), a T-DNA insertional (Bragg et al., 2012) and a TILLING (Dalmais et al., 2013) mutants collection, germplasm banks of inbred lines and RIL (recombinant inbred lines; e.g. Vogel et al., 2009; Garvin, 2016) and a range of bioinformatics tools (Mochida and Shinozaki, 2013). Altogether, these traits made *B. distachyon* a strongly interesting intermediary between basic (*A. thaliana*) and cultivated (wheat and barley) species, in a context of translational biology (Girin et al., 2014).

Table 1.3: List of cereal pathogens tested on *B. distachyon.* (Fitzgerald et al., 2015).

	Pathogen	Cereal host	Reference
Bacterial	*Xanthomonas translucens*	Wheat, barley	Fitzgerald et al. (unpublished results)
Fungal	*Colletorichum cereale*	Rye, wheat, oat	Sandoya and Buanafina (2014)
	Fusarium culmorum	Wheat, barley	Peraldi et al. (2011)
	Fusarium graminearum	Wheat, barley	Peraldi et al. (2011)
	Fusarium pseudograminearum	Wheat, barley	Powell et al. (2017)
	Gaeumannomyces graminis	Wheat	Sandoya and Buanafina (2014)
	Bipolaris sorokiniana	Wheat, barley	Falter and Voigt (2014)
	Magnaporthe oryzae	Rice	Routledge et al. (2004)
	Oculimacula acuformis	Wheat	Peraldi et al. (2013)
	Oculimacula yallundae	Wheat	Peraldi et al. (2013)
	Puccinia graminis f. sp. *tritici*	Wheat	Ayliffe et al. (2013)
	Puccinia striiformis f. sp. *avenea*	Oat	Ayliffe et al. (2013)
	Puccinia striiformis f. sp. *tritici*	Wheat	Ayliffe et al. (2013)
	Puccinia triticina	Wheat	Ayliffe et al. (2013)
	Ramularia collo-cygni	Barley	Peraldi et al. (2013)
	Rhizoctonia solani AG 8	Wheat, barley	Schneebeli et al. (2014)
	Pyrenophora teres	Barley	Falter and Voigt (2014)
	Stagonospora nodorum	Wheat	Falter and Voigt (2014)
Oomycete	*Pythium aphanidermatum*	Maize	Sandoya and Buanafina (2014)
Viral	*Barley stripe mosaic virus*	Barley	Cui et al. (2012)
	Panicum mosaic virus	Pearl millet	Mandadi and Scholthof (2012)
	Wheat streak mosaic virus (WSMV)	Maize, wheat, barley	Mandadi et al. (2014)
	Brome mosaic virus (BMV)	Barley, wheat, maize	Mandadi et al. (2014)
	Sorghum yellow banding virus (SYBV)	Maize, sorghum	Mandadi et al. (2014)
	Foxtail mosaic virus (FoMV)	Foxtail, sorghum, wheat	Mandadi et al. (2014)

We described in **section A.3.2.** that cereals (and more specifically wheat) diseases management remains a strong challenging goal especially regarding the improvement of genetic quantitative or qualitative resistance. Since its introduction as a model temperate cereal, an increasing number of pathosystems involving *B. distachyon* as a host plant have been studied with a special attention given to the degree of similarity between the infection strategy of the pathogen on crops *versus* model (Fitzgerald et al., 2015). Indeed, despite the close phylogenetic relationship between wheat and *B. distachyon*, the compatibility of the interaction (i.e. the ability of the pathogen to complete its lifecycle on the host) is not ensured. For example, among the three main wheat fungal pathogens described in **section A.3.1.**, *Z. tritici*, the causal agent of septoria leaf blotch of wheat, is unable to sporulate on a range of *B. distachyon* ecotypes, therefore considered as a non-compatible host (O'Driscoll et al., 2015). Similarly, *B. distachyon* is considered a nonhost for brown rust caused by *P. triticina*, but also for all other wheat rust pathogens (Ayliffe et al., 2013). However, non-compatible interactions remain of interest for the identification of efficient host defense mechanisms. Indeed, the exploitation of differential level of resistance of several ecotypes against a pathogen gives the opportunity to rapidly and finely map resistance loci of interest (Fitzgerald et al., 2015). A range of pathogens including insects, fungi, oomycete, virus and bacteria have been tested on *B. distachyon* and a synthesis is presented in **Table 1.3**. This includes one of the most devastating wheat fungal pathogen: *Fusarium graminearum*.

B. FUSARIUM HEAD BLIGHT

At the end of the 17th century, several farmers reported the arrival of new wheat, barley and rye common disease in the United Kingdom. The first collected and described wheat sample in 1884 came from the county of Norfolk, England. At that time, no explicit name was given to this affliction but symptoms were described: ‹‹ (…) *pale yellow-orange gelatinous stratum over the ears or some portions of the ears. It glues the spikelets together and stops the growth of the grain* ›› (Smith, 1884). With the support of drawings of detailed observations of the symptoms and fungal structures, there is no longer any doubt today that this was the first description of Fusarium Head Blight (FHB). One hundred and thirty years later, the situation has greatly evolved: epidemics were found almost worldwide and are responsible for economic losses amounting millions of dollars (Goswami and Kistler, 2004). This section will first present general information on the main causal agent of FHB and the associated problems of mycotoxins. We will then describe the actual management strategies

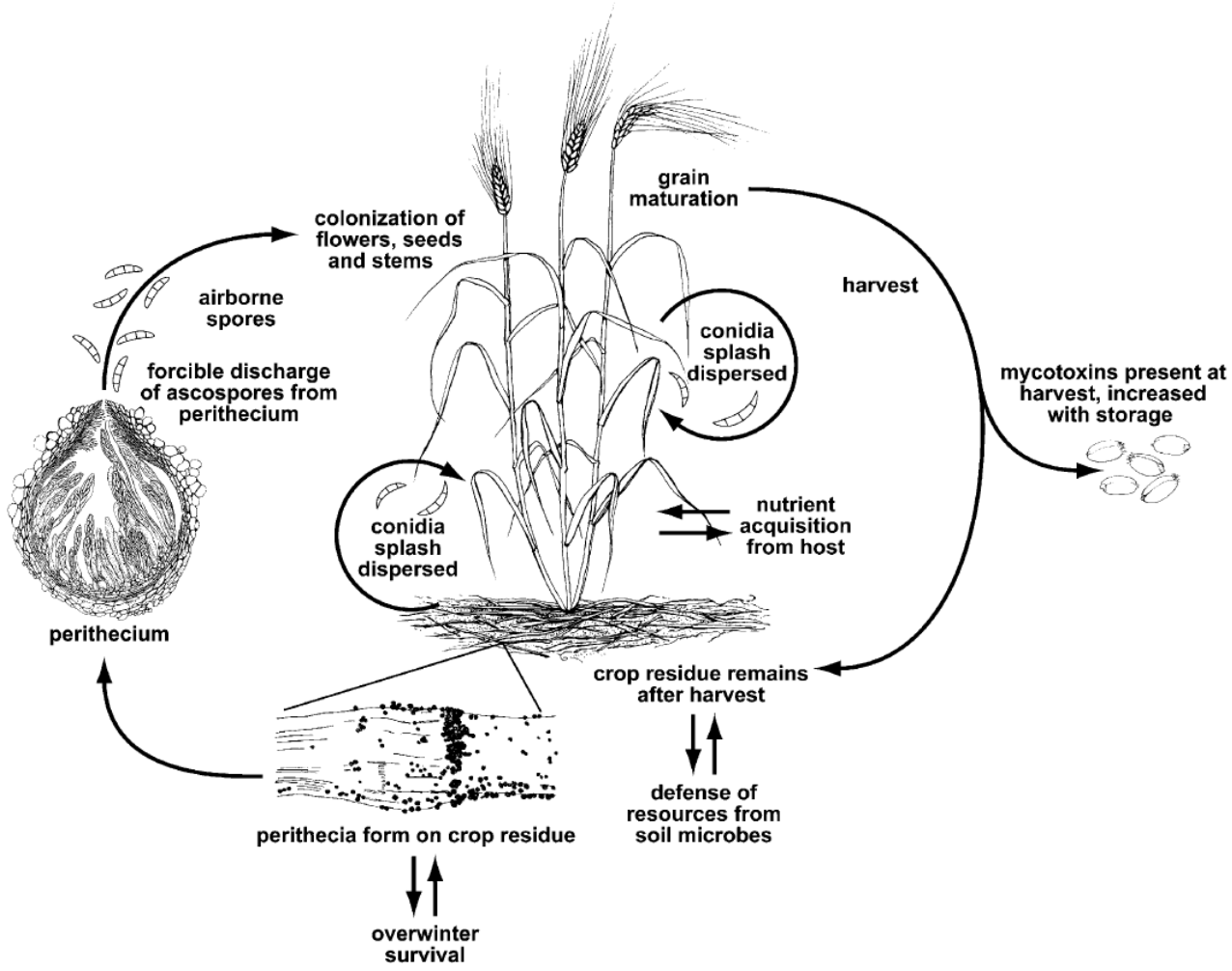

Figure 1.7: ***Fusarium graminearum*** **lifecycle.** (Trail, 2009).

for FHB with an emphasis on genetic resistance of wheat cultivars. We will conclude on the interest of transcriptomic studies to improve plant resistance towards the disease.

B.1. The main causal agent of FHB: *Fusarium graminearum*

The first records of FHB (also known as Fusarium ear blight or scab) in the UK or in the USA during the late 17th century attributed the disease to the fungus *Fusisporium culmorum* Wm.G. Sm. now known as *Fusarium culmorum* (W.G. Sm.) Sacc. (Smith, 1884; Parry et al., 1995; IMA, 2018). Since then, numerous species from the genus *Fusarium* and *Microdochium* have been associated to FHB but *Fusarium graminearum* Schwabe. (telomorph *Gibberella zeae* (Schweinitz) Petch) is the most common causal agent in Europe and North America (Parry et al., 1995; Goswami and Kistler, 2004; Walter et al., 2010). *F. graminearum* belongs to the largest group of fungi, Ascomycota, and therefore exhibits two distinct states: a perfect (sexual) state called teleomorph and an imperfect (asexual) state called anamorph (**Figure 1.7**; Andrews, 2017). Wheat infection in the field is initiated by airborne ascospores (sexual spores) which germinate on spikes and penetrate the plant through natural openings such as stomata, *via* the basis of the sterile parts of the wheat flowers (palea and lemma) or through the anthers (Guenther and Trail, 2005; Trail, 2009). Flowering is, therefore, the maximum susceptibility stage of the plant and infection is promoted by warm moist weather conditions (Goswami and Kistler, 2004). The fungus first grows intercellularly at the infection front and does not elicit symptoms on the plant during a phase generally referred as biotrophic despite the formation of intracellular structures (Trail, 2009; Brown et al., 2010). The fungus spreads up and down into the wheat spike by colonizing the rachis after vascular tissues invasion which could be responsible for the blight of the upper part (Brown et al., 2010). First symptoms are observed 4 to 5 days post-infection (dpi) as water soaking and chlorosis behinds the infection front (Guenther and Trail, 2005). They are caused by the intracellular growing of *F. graminearum* which results in the necrosis of the contaminated plant cells (necrotrophic phase). Fungal spreading causes a premature bleaching of the spike which is characteristic of FHB. *F. graminearum* then completes its asexual reproduction through the production of numerous macroconidia dispersed in short-distance *via* rain-splashes and constituting the secondary inoculum (Trail, 2009). The sexual reproduction is initiated by the dikaryotic (binucleate) phase and results in the production of fruiting bodies (perithecia). Together with the binucleate mycelium in a saprophytic state on debris, perithecia are used as winter survival structures by the fungus. Ascospores formed in

Estrogenic

Type B Trichothecenes (TCTBs)

Zearalenone
(ZEA)

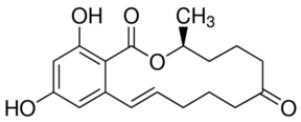

Deoxynivalenol
(DON)

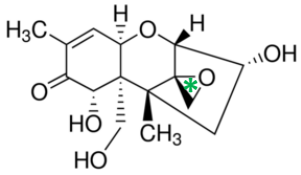

Nivalenol
(NIV)

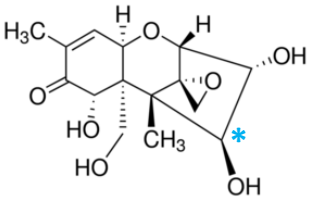

3-acetyldeoxynivalenol
(3-ADON)

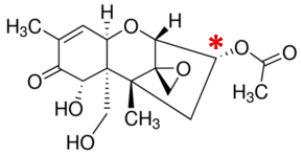

4-acetylnivalenol
(4-ANIV)

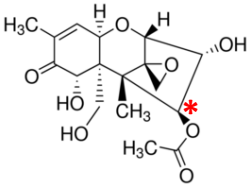

15-acetyldeoxynivalenol
(15-ADON)

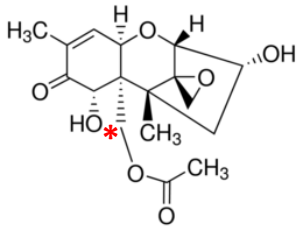

4,15-diacetylnivalenol
(4,15-diANIV)

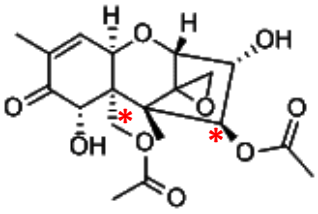

Figure 1.8: The mycotoxins produced by *Fusarium graminearum*. Estrogenic (ZEA) and Type B Trichothecenes (DON, NIV and acetylated derivatives) formulas are presented. Green star indicate the epoxide ring of TCTBs carried by C12 and C13. Blue star indicate the additional hydroxyl group of NIV and acetylated derivatives carried by C4. Red stars indicate acetyl groups carried by the acetylated derivatives of DON and NIV.

perithecia are then discharged during the next season (Guenther and Trail, 2005). *F. graminearum* causes direct yield losses due to the premature stop of kernel development and because infected kernels are stunted and light (badly filled). The sowing of these contaminated seeds generally leads to seedling damping. Discoloration of seeds is also often observed (McMullen et al., 2012). Finally, *F. graminearum* is also responsible for head blight on barley, rice, oat and stalk or ear rot of maize and as previously mentioned, *F. graminearum* is also able to infect spikes from *B. distachyon* and is responsible for the development of highly similar symptoms compared to wheat (**Figure 1.6**; Peraldi et al., 2011).

B.2. The mycotoxins produced by *F. graminearum*

The average economic impact of FHB on wheat has been estimated $245 million annually between 1998 and 2000. A portion of that amount comes from yield losses mentioned above but most of it is due to price discounts of infected grains (Nganje et al., 2002). Indeed, *F. graminearum* (as other *Fusarium* species and few additional fungal genera) is able to produce fungal toxins (mycotoxins), a class of low molecular weight secondary metabolites with a deleterious impact on human and animal health (Soares et al., 2018). Among the most prevalent mycotoxins, we can quote aflatoxins produced by *Aspergillus* species, present almost everywhere, and causing liver illness such as cancer (Williams et al., 2004); ochratoxin A produced by *Aspergillus* and *Penicillium* species with numerous toxicological effects (e.g. nephrotoxic, hepatotoxic, neurotoxic…; El Khoury and Atoui, 2010); and fumonisins produced by *F. verticillioides*, *F. proliferatum* and *Alternaria alternata* which disrupt sphingolipid metabolism resulting in cell cycle damages (Soriano et al., 2005).

F. graminerarum produces the estrogenic mycotoxin zearalenone (ZEA) and sesquiterpenic type B trichothecenes (TCTBs; **Figure 1.8**; Goswami and Kistler, 2004; Soares et al., 2018). Although ZEA does not appear to be phytotoxic (McLean, 1995), it has endocrine-disrupting properties in human and animal because of its structural similarity to estrogen (Kowalska et al., 2016). Therefore, as for other mycotoxins (including TCTBs presented below), and because of the substantial risks to public health, maximum contamination levels in food and feed products have been established, for example by the European Commission (2006), the Food and Drug Administration of the USA (FDA, 2010) and many other countries (Mazumder and Sasmal, 2001). Unlike ZEA, TCTBs have been shown to be involved in virulence of *F. graminearum* (e.g. Jansen et al., 2005) and will, therefore, be presented in more detail.

A

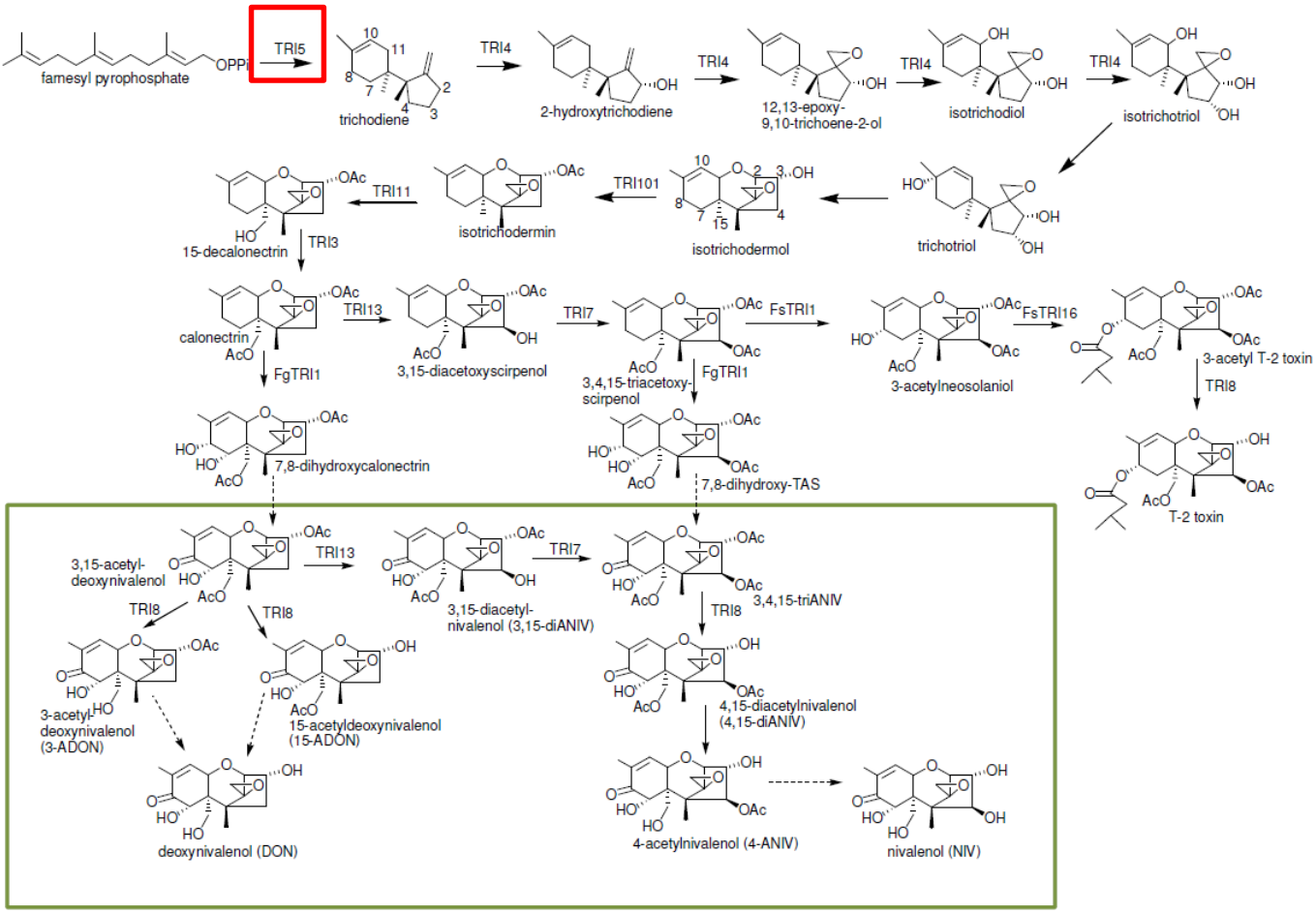

B

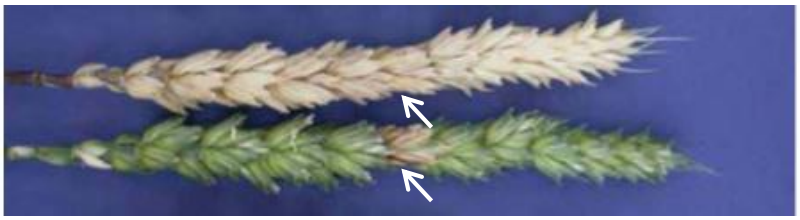

WT (Fg^{TOX+})

Δ*tri5* (Fg^{tox-})

Figure 1.9: Trichothecenes biosynthetic pathway in *Fusarium* sp. and involvement in pathogenicity of *F. graminearum*. **A**, TRI enzymes involved in the biosynthetic pathway of TCTs are indicated. Green box identifies Type B Trichothecenes and red box identifies TRI5, the first enzyme of the biosynthetic pathway (McCormick et al., 2011; adapted). **B**, Spikes of the cultivar Monk 3 wpi with a WT strain (Fg^{TOX+}, upper spike) or with a Δ*tri5* strain (Fg^{tox-}, lower spike) of *F. graminearum*. White arrows indicate sites of point inoculation (Maier et al., 2006; adapted).

B.3. Structure, synthesis and toxicity of type B trichothecenes

Trichothecenes (divided into four different groups from A to D) are defined by their tricyclic nucleus of 15 carbons, their epoxide ring in C12 and C13 (Desjardins et al., 1993) and differ in structure by functional groups on the skeleton (oxygenation, acetylation, acylation). TCTBs are defined by a keto function (R^1-CO-R^2, where R^1 and R^2 are carbon chains) at C8 and a hydroxyl function (-OH) at C7 (Alexander et al., 2011). They include deoxynivalenol (DON), nivalenol (NIV) and their acetylated derivatives: 3-acetyldeoxynivalenol (3-ADON), 15-acetyldeoxynivalenol (15-ADON), 4-acetylnivalenol (4-ANIV, also known as fusarenon X, FX) and 4,15-diacetylnivalenol (4,15-ANIV) for which one or two acetyl groups are added to a carbon (**Figure 1.8**; Alexander et al., 2011).

F. graminearum strains are generally producing one major TCTB, which specify their chemotype: the first group producing DON and its acetylated forms (which could be furtherly divided into 3-ADON and 15-ADON producing groups), and the second producing NIV and/or 4-ANIV. This trait is determined by two genes, *Tri13* and *Tri7*, encoding a cytochrome P450 and an acetyltransferase, respectively, required for the conversion of DON into NIV. Insertion on or deletion of these genes, therefore, leads to a DON chemotype (**Figure 1.9A**; Pasquali and Migheli, 2014). As for most of the genes encoding enzymes involved in secondary metabolite biosynthesis in fungi, those involved in TCTBs are grouped in clusters (Keller et al., 2005). TCTBs biosynthesis requires 15 *Tri* genes located in 3 different clusters in *F. graminearum* genome (McCormick et al., 2011) and is initiated by the cyclization of farnesyl pyrophosphate into trichodiene by the terpene cyclase trichodiene synthase Tri5 (**Figure 1.9A**; Hohn and Vanmiddlesworth, 1986). A mutant strain (Δ*tri5*) for this enzyme, therefore, fails to produce any TCTB (**Figure 1.9B**; Cuzick et al., 2008).

Many studies have shown that environmental factors could modulate TCTBs production. *In vitro*, reactive oxygen species (ROS; Ponts et al., 2007), temperature, (Schmidt-Heydt et al., 2008) or acidic pH (Merhej et al., 2010) have been shown, for example, to induce TCTBs biosynthesis both on the transcriptional and metabolic levels. Interestingly, the two major transcriptional regulators of trichothecenes biosynthetic genes expression, Tri6 and Tri10, are encoded by genes belonging to the *TRI* loci. Their disruption results in an almost total reduction of TCTBs production and, as for Δ*tri5* strain, a reduction of fungal virulence *in planta* (Maier et al., 2006; Seong et al., 2009). *In planta*, TCTBs biosynthesis seems to be induced very early in the infection process (24 hpi) but do not

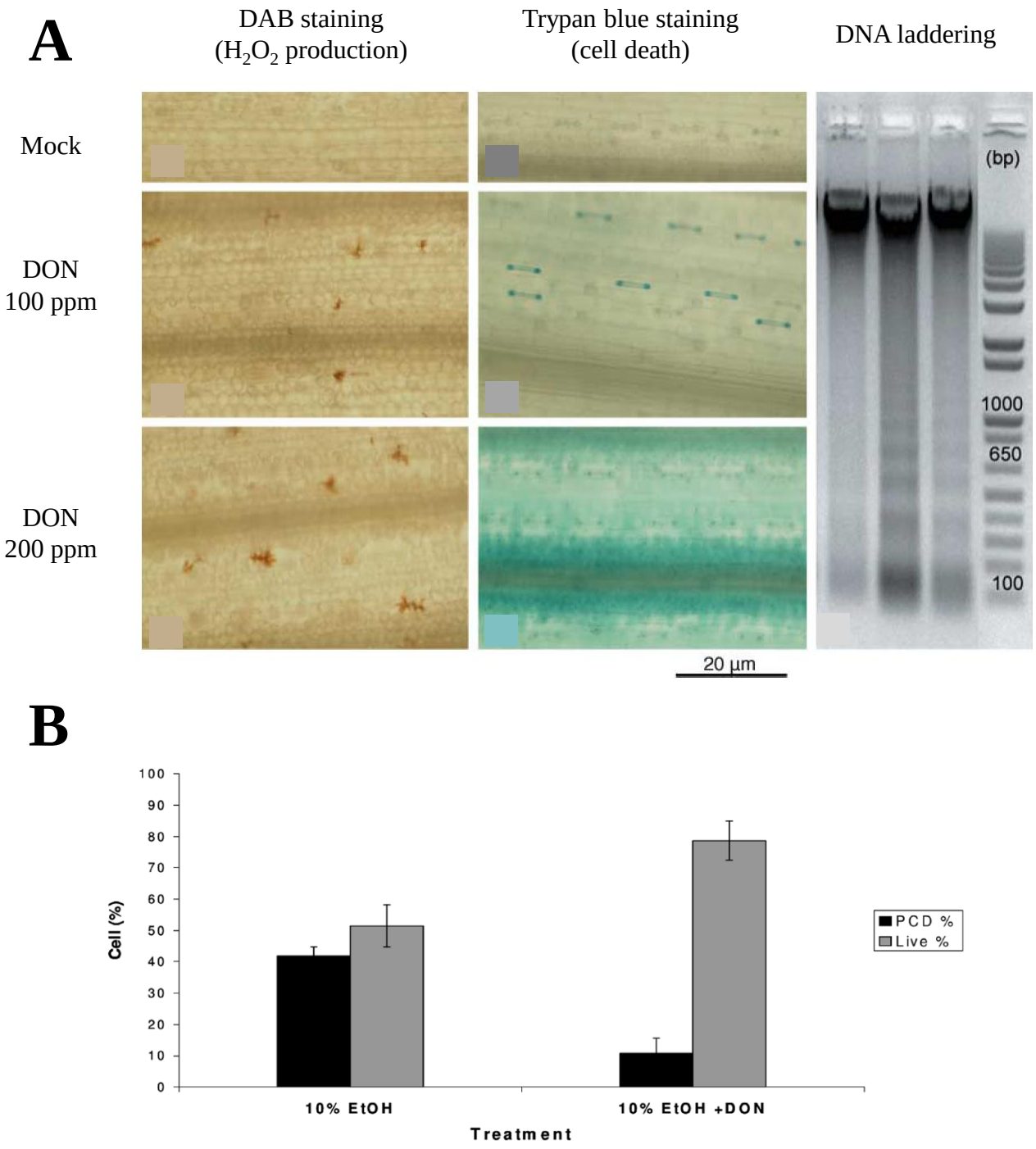

Figure 1.10: Differential impacts of DON on plant cells. A, **High concentrations of DON induces ROS production, cell death and DNA laddering in wheat leaf tissues.** Six left panels: DAB and trypan blue staining of wheat leaves showing H_2O_2 production and cell death, respectively, 6 h after infiltration of water (mock), 100 or 200 ppm of a DON solution using vacuum for DAB staining or 24 h after the same inflitrations for trypan blue staining. Right panel: genomic DNA laddering in wheat leaves 24 h after infiltration with mock solution (first lane), 100 ppm DON (second lane), 100 ppm DON combined with 7 $g.L^{-1}$ ascorbic acid (third lane) and DNA size ladder (fourth lane; Desmond et al., 2008; adapted). **B, A low concentration of DON inhibits ethanol-induced apoptosis-like PCD (programmed cell death) on *A. thaliana* cell suspension culture.** Percentage of living (live) and apoptosis-like PCD entered (PCD) cells 24 h after treatment with (10 % EtOH + DON) or without (10 % EtOH) 10 ppm DON followed by 4-5 h treatment with 10 % EtOH (Diamond et al., 2013)

determine initial infection success. In contrast, colonization efficiency of wheat tissues depends on the strong transcriptional activation of *TRI* genes, and therefore in TCTBs synthesis (**Figure 1.9B**; Boenisch and Schäfer, 2011). Finally, quantification of the spatial and temporal expression of the *Tri5* gene, used as a marker of TCTBs biosynthesis activity, in wheat infected spikes indicates a strong activation in the asymptomatic colonization front rather than in symptomatic zones (Hallen-Adams et al., 2011).

TCTs toxicity lies in their ability to bind, through their epoxide ring, the 60S subunit of eukaryotic ribosomes and inhibit protein synthesis. This will cause a number of disturbances at the cellular level including oxidative stress, DNA damage, cell-cycle perturbations or alterations of membranes (Arunachalam and Doohan, 2013; Payros et al., 2016). In animals, and more specifically in human, TCT ingestion is responsible for severe gastrointestinal symptoms, anaemia, necrotic lesions on the gastrointestinal and airways tracts… (Sudakin, 2003). These molecules are stable to heat or food processing, it is therefore easily understandable that contamination threshold discussed before have been established (Rocha et al., 2005). In plants, DON application leads to contrasting results depending on its concentration. At high concentration, between 100 and 200 ppm, DON triggers H_2O_2 production in 6 h and cell death in 24 h on wheat leaves (**Figure 1.10A**; Desmond et al., 2008). However, at low concentration (10 ppm), DON inhibits apoptosis-like PCD (programmed cell death) on *A. thaliana* cell suspension cultures (**Figure 1.10B**; Diamond et al., 2013). This supports the hypothesis of a dual role of DON during the interaction: first, low concentrations could help initial spreading of the fungus during the biotrophic phase; then, higher concentrations initiate the necrotrophic phase, allowing nutrient release from dead host cells (Diamond et al., 2013). DON is also known to inhibit root growth, a trait often used to compare the general tolerance or sensitivity of different plant lines towards the mycotoxins (Masuda et al., 2007; Pasquet et al., 2016).

B.4. FHB management strategies

Several strategies for the management of FHB have been developed and follow the general principles exposed in **section A.3.2.**. They include a set of cultural practices, chemical and biological control, disease forecasting and the use of genetic resistances. We will briefly discuss each of them independently in this section but as discussed above, the combination of several of these strategies in an IDM system appears to be more efficient than the use of a single strategy (McMullen et al., 2008).

B.4.1. Cultural practices

Agronomic practices mostly used to reduce FHB intensity and DON (TCTBs) accumulation are tillage and crop rotation. They both aim to reduce primary inoculum incidence. Although tillage alone does not appear to efficiently reduce the impact of FHB (Teich and Nelson, 1984; David Miller et al., 1998), buried residues from wheat have shown a greater decomposition rate compared to soil-surface residues and this is positively correlated with a reduction in the colonization of residues by *F. graminearum* (Pereyra et al., 2004). However, in combination with crop rotation with a non-host species, a significant reduction of FHB prevalence has been reported. A study conducted in the Minnesota (USA) in the 1990s related that disease incidence and severity were reduced by 14.1% and 11.7%, respectively, when wheat was grown after soybean and following moldboard plow treatment in comparison with wheat grown after corn and without any soil treatment (Dill-Macky and Jones, 2000). Irrigation management also appeared to significantly reduce FHB severity and TCTB accumulation since moisture is one the most important factor in disease development, moreover decreased watering during and after anthesis gave significant results (Lacey et al., 1999; Cowger et al., 2009).

B.4.2. Chemical and biological control

Fungicide application is often used to control FHB since the late 1990s. Triazoles, belonging to demethylation inhibitor (DMI) class (also known as sterol biosynthesis inhibitor class), are probably the most efficient in reducing symptoms and mycotoxin content (Paul et al., 2007). A combination of prothioconazole and tebuconazole, for example, has been shown to efficiently suppress FHB and DON (52% and 42%, respectively, compared to control; Paul et al., 2008; McMullen et al., 2012). The methyl benzimidizole carbamates (MBCs) such as benomyl is another class of fungicides also known for their effectiveness against the disease (Jones, 2000). Nevertheless, decline sensitivity and resistant strains to triazoles and MBCs have been described (Li et al., 2003; Klix et al., 2007; Becher et al., 2010). The development of novel active molecules might, therefore, constitute a headlong rush. Fungicides application timing is also an important factor in disease management efficiency and that complicates their use in the fields. Indeed, the short time window of anthesis, corresponding to few days in the wheat lifecycle, is the only one that gives effective disease control (Jones, 2000). However, a

later application, up to 20 days after anthesis, might be a good option for TCTBs control but without any effect on the disease itself (Yoshida et al., 2012).

With the growing desire to reduce inputs and to offer cheaper and more sustainable agriculture, numerous biological control agents (BCAs) where investigated towards FHB. Among them, plant growth promoting (PGP) bacteria from the *Bacillus* genus received a special attention because of their stress-resistant traits, their ubiquity, their lack of pathogenicity and the ease of their conditioning (Khan et al., 2017). Strains of *Streptomyces* spp. or *Pseudomonas* spp. and fungal strains of *Trichoderma* spp. or *Cryptococcus* spp., for example, where also selected for their antagonist effect against *F. graminearum* (Gilbert and Haber, 2013; Wegulo et al., 2015) but up to now, commercially available products are still extremely rare.

B.4.3. Disease forecasting

Disease forecasting tools have been developed to help growers in estimating risks of FHB and DON outbreaks, hence to optimize the use of fungicides. The FHB prediction center in the USA (http://www.wheatscab.psu.edu/), the DONcast® model in Canada (http://weathercentral.ca/wheat2.cfm), the FusaProg system in Switzerland (http://www.fusaprog.ch/) or the Baromètre Maladies in France (http://www.barometre-maladies.arvalis-infos.fr/bletendre/) have all been developed based on actual and forecast weather data. They also include wheat varieties, soil treatments and crop rotations employed by the growers and therefore constitute efficient tools to reduce fungicide application and minimize losses.

B.4.4. Genetic resistance

Wheat resistance towards FHB is dominant and quantitative meaning that no gene-for-gene resistance (immunity) has been described yet (Foroud and Eudes, 2009). Resistance is therefore carried by quantitative trait loci (QTLs) and could be divided into two mechanisms: passive tolerance, related to morphological traits of wheat cultivars; and active tolerance, involving physiological processes (Mesterhazy, 1995). Passive resistance is mostly determined by the morphology and the positioning of spikes influencing the humidity level, the stature of the cultivar and the grain filling maturation time. However, these traits are considered of minor interest compared to active (physiological) resistance and are not always compatible with other cultural issues (Rudd et al., 1993). Active resistance has been divided

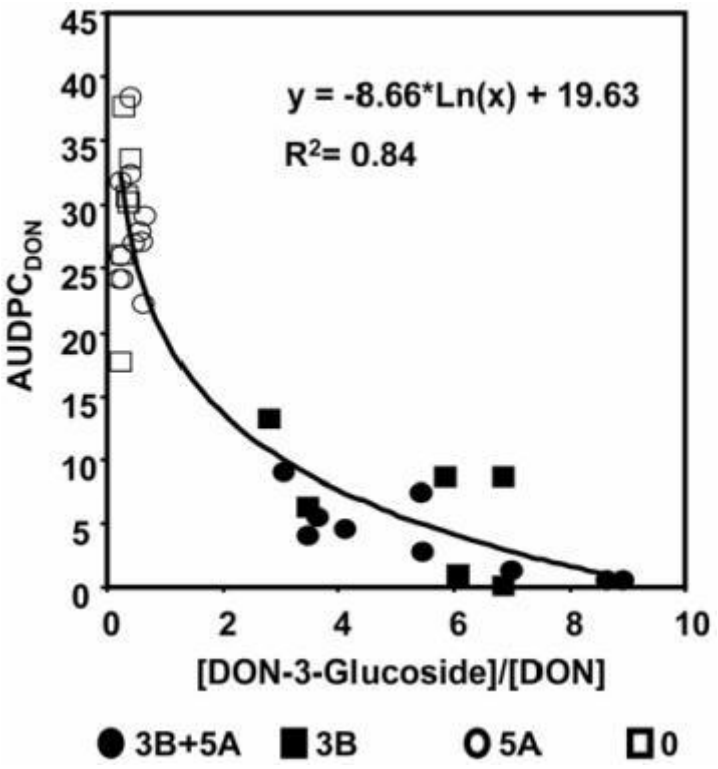

Figure 1.11: QTL *Fhb1* (*Qfhs.ndsu-3BS*) confers tolerance to DON and it is positively correlated with a better ability to glycosylate DON in wheat. Relation between DON tolerance (area under the disease progress curve corresponding to DON-bleached spikes over time, $AUDPC_{DON}$) and the D3G/DON ratio in DON-treated spikes (17 dpi with 20 µL of 10 ppm DON and 16 dpi with 2 ppm DON compared to control condition (0.1 % Tween 20)). Filled circles, wheat lines with *Qfhs.ifa-5A* and *Qfhs.ndsu-3BS* (*Fhb1*); filled squares, lines with *Qfhs.ndsu-3BS* (*Fhb1*) only; open circles, wheat lines with *Qfhs.ifa-5A* only; open squares, lines lacking both QTLs (Lemmens et al., 2005).

into five different types by Mesterhazy (1995): type I corresponding to resistance to initial infection, type II to disease spread along spike, type III to grain infection, type IV corresponding to a tolerance to FHB and TCTBs and finally, type V which refers to resistance to TCTBs through the limiting of their synthesis or *via* their detoxification. Among these, types I and II are the most characterized and used by actual breeding programs to improve cereal resistance against FHB (Bai and Shaner, 2004). An increasing number of QTLs affecting FHB are described from various sources and are localized on every wheat chromosome (Buerstmayr et al., 2009; Gilbert and Haber, 2013). Initially, sources of resistance were studied in Asian cultivars such as 'Sumai 3', 'Ning 7840' or 'Ning 8331' which result from ancient breeding programs for FHB resistance due to regular FHB epidemics in this area (Buerstmayr et al., 2009). As an example, one of the first QTL identified, *Fhb1* (synonym *Qfhs.ndsu-3BS*), derived from 'Sumai 3' and is localized on chromosome *3BS*. It was first associated to type II resistance (Buerstmayr et al., 2003) and later to the ability of wheat lines carrying *Fhb1* to convert DON into less toxic DON-3-*O*-glucoside (D3G; **Figure 1.11**; Lemmens et al., 2005). More recently, *Fhb1* was finally cloned from 'Sumai 3' and was shown to carry a pore-forming toxin-like (*PFT*) encoding gene conferring FHB resistance and the previously reported hypothesis on DON glycosylation was assigned to not yet identified uridine diphosphate glycosyltransferases (UGTs) encoding genes located near *PFT* (Rawat et al., 2016). Numerous other QTLs have been and continue to be extensively studied, both by researchers and breeders. Indeed, genetic resistance appeared to be the most cost-effective FHB management strategy especially since multiple resistance alleles introgression into elite cultivars was shown to increase resistance level (McCartney et al., 2007; Wegulo et al., 2015).

B.5. Improve FHB resistance: benefit from transcriptomic data

As we have just discussed, genetic resistance currently constitutes the most promising FHB management strategy in terms of efficiency, durability, environmental preservation, ease of use and cost. However, the levels of resistance displayed by MWCs are often moderate, partly because of the putative very high number of genes involved in small effects acting additively and quantitatively (Bai and Shaner, 2004). Major efforts are therefore employed to identify wheat candidate genes with high impacts on FHB resistance. One of the best strategies which already gave significant results and have been exploited to generate wheat lines with a high level of DON and/or FHB resistance is the use of transcriptomic data

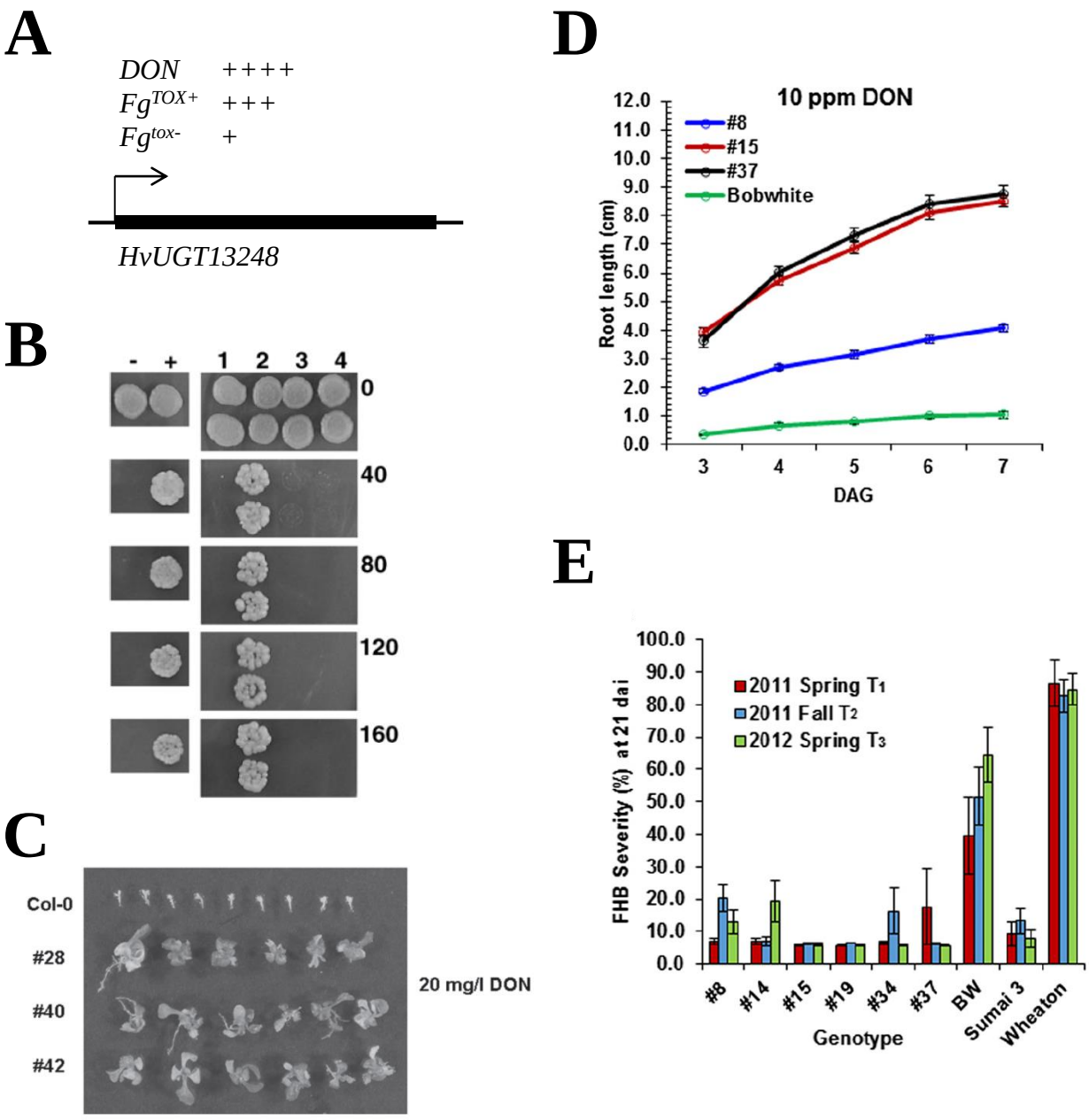

Figure 1.12: Barley UGT HvUGT13248 is transcriptionally induced by DON confers mycotoxin tolerance in yeast, *A. thaliana* and wheat. A, *HvUGT13248* transcriptional induction during FHB in barley is mostly dependent on the mycotoxin. **B**, DON-tolerance phenotype of barley UGT-expressing yeasts on DON – containing media (mg.L^{-1}); - = empty vector (negative control); + = DON-metabolizing *DOGT1* expression vector (positive control); 1-4: candidate UGT-expression vectors with 2 = *HvUGT13248*. **C**, DON-tolerance phenotype of *HvUGT13248* expressing lines of *A.thaliana* (#28, #40, #42) compared to WT line (Col-0; DAG: days after germination). **D**, Root growth inhibition by DON of wheat lines expressing *HvUGT13248* (#8, #15, #37) compared to WT line (Bobwhite). **E**, Disease symptoms of susceptible (BW, Wheaton), resistant (Sumai 3) and susceptible transgenic lines expressing *HvUGT13248* (#8-#37) 21 days after point inoculation with a *Fg*$^{TOX=}$ strain of *F. graminearum*. (Boddu et al., 2007; Gardiner et al., 2010; Schweiger et al., 2010; Shin et al., 2012; Li et al., 2015; adapted).

(Kazan and Gardiner, 2017). Indeed, a better understanding of the host plant transcriptional changes during the interaction with *F. graminearum* give the opportunity to identify genes acting as resistance factors, or on the contrary, as susceptibility determinants.

B.5.1. Available data and example of use

Numerous transcriptomic analyses of the interaction between cereals (mostly wheat) and *F. graminearum* have been conducted these ten last years and most of these have been recently reviewed by Kazan and Gardiner (2017). These analyses have been conducted in various conditions especially regarding host wheat genotypes. Differentially expressed genes (DEGs) have been for example identified between mock *versus* inoculated plants, between resistant and susceptible cultivars, or between near-isogenic lines (NILs) carrying or not a QTL of interest. It is therefore often challenging to compare these studies due to the heterogeneity in wheat lines, methodology and analyses heterogeneity (Nussbaumer et al., 2015). However, recurrent transcriptional changes are observed for genes involved in numerous processes such as photosynthesis, primary metabolisms of carbohydrates and nitrogen, hormone biosynthesis and signaling, phenylpropanoid biosynthesis, regulation of ROS burst, synthesis of pathogenesis-related (PR) proteins, UGTs or ATP-binding cassette (ABC) transporters and others (Kazan and Gardiner, 2017).

One of the most successful stories of transcriptional screening which led to the generation of wheat resistant lines was initiated in barley in 2007 (**Figure 1.12**). Boddu et al. (2007) examined the transcriptional impact of barley infection by a wild-type (TCTBs producing) strain of *F. graminearum*, compared to an infection with a Δ*tri5* (TCTBs non-producing) strain in order to target expression genes specifically modified by the mycotoxins, and not by the infection itself. The contig *Contig13248_at* encoding a UGT putatively involved in TCTBs detoxification was shown to be transcriptionally induced 48 and 96 hpi both by WT and mutant strains compared to water treatment, but in a more significant way in the case of the infection by the WT strain (13.8 and 1.5 fold-change, respectively). These results were confirmed a few years later in another experimental set-up: *Contig13248_at* was shown to be highly transcriptionally induced (more than 1500 fold change, qPCR data) 1 hour after barley spikes inoculation with DON compared to control treatment (**Figure 1.12A**; Gardiner et al., 2010). The same year, it was shown that ectopic expression of this UGT encoding gene (subsequently named *HvUGT13248*) confers DON-tolerance to yeast and results in the accumulation of D3G (**Figure 1.12B**; Schweiger et al., 2010). Similar results

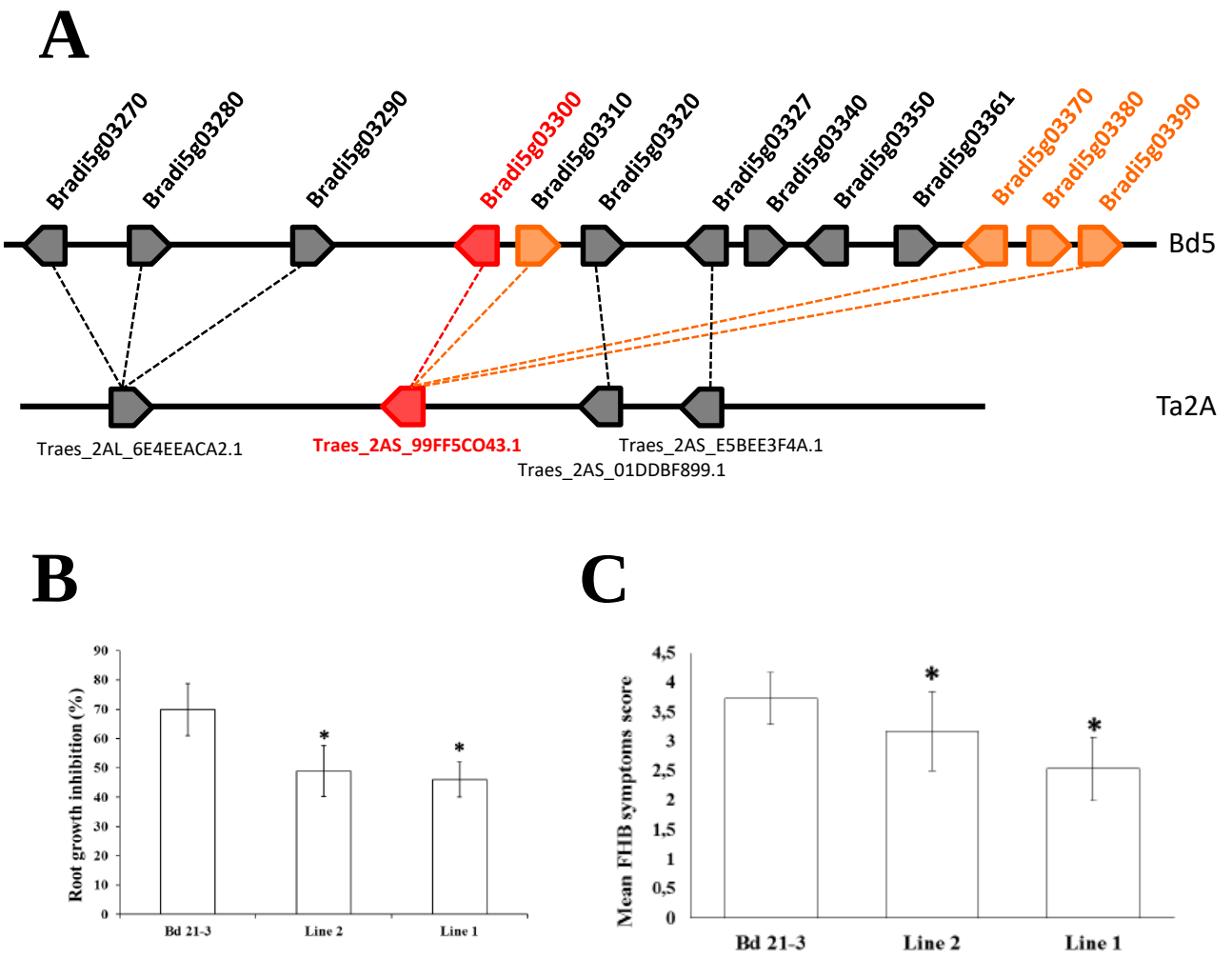

Figure 1.13: Translational biology between *B. distachyon* and wheat allowed the identification of a wheat UGT that confers DON-tolerance and FHB-resistance. A, Syntenic approach between *B. distachyon* and wheat (and transcriptional data, not shown) allowed the identification of *Traes_2BS_14CA35D5D.1*, as the ortholog of UGT-encoding *Bradi5g03300* which metabolizes DON and confers mycotoxin tolerance and FHB resistance in *B. distachyon*. **B**, Root growth inhibition of *B. distachyon* WT (Bd21-3) and transgenic (1-2) lines expressing *Traes_2BS_14CA35D5D.1* on DON-containing medium (50 µM) compared to control medium. **C**, Disease symptoms 7 dpi (point inoculation) of the same *B. distachyon* lines with a Fg^{TOX+} strain of *F. graminearum.* Asterisk indicate statistically significant differences between lines ($p < 0,05$; Student test; Gatti, 2017; adapted).

were obtained when *HvUGT13248* was expressed in *A. thaliana* (**Figure 1.12C**; Shin et al., 2012). More recently, *HvUGT13248* was expressed in two susceptible wheat cultivars: 'Bobwhite' and 'CBO 37' (Li et al., 2015). Transgenic wheat seedlings were shown to be more tolerant to DON (root length 3 to 8 times longer at 10 ppm; **Figure 1.12D**) and to exhibit a higher D3G/DON ratio (5 times higher at 14 dpi) following spikes inoculation with DON compared to WT lines. Moreover, transgenic lines exhibited up to 8 times fewer symptoms 21 dpi with a toxin-producing strain of *F. graminearum* and, therefore, show up the possibility to provide FHB genetic resistance through the metabolism of TCTBs **(Figure 1.12E**; Li et al., 2015). In parallel to this study, the *B. distachyon* ortholog of *HvUGT13248* and *A. thaliana* DON-metabolizing *DOGT1* (**Figure 1.12B**; Poppenberger et al., 2003), *Bradi5g03300*, was identified based on phylogenetic and transcriptional data (Schweiger et al., 2013a). Its overexpression in *B. distachyon* also conferred DON tolerance and FHB resistance (Pasquet et al., 2016). Very recently, *Bradi5g03300* was used as bait to identify UGTs of interest in bread wheat. A synteny approach allowed the identification of the wheat orthologous gene which also confers resistance to FHB in *B. distachyon* (**Figure 1.13**; Gatti, 2017).

B.5.2. Promising fields of investigation

The story described above supports the strategy of TCTBs targeting (detoxification) to improve wheat resistance towards FHB in addition to propose an efficient way to manage mycotoxin contaminations. The large number of plant or fungal genes differentially expressed during the plant-pathogen interaction allowed the development of many other strategies to limit the impact of *F. graminearum* infection. As an example, we could cite the recent studies aiming to silence target virulent fungal gene through RNA interference (RNAi)-plant mediated systems (Machado et al., 2017). Moreover, this confirms the interest of using *B. distachyon* as a model for functional genomic of cereal-pathogen interactions. In this perspective, a transcriptomic study has also been conducted on the model grass in response to the infection by DON-producing or non-producing strains of *F. graminearum* or in response to DON treatment (Pasquet et al., 2014; Pasquet, 2014). Among the DEGs identified, several are involved in pathways already described as mobilized during the interaction between wheat and *F. graminearum* such as photosynthesis, primary metabolism (carbohydrates), plant defense responses, response to ROS, phenylpropanoid pathway… The authors also notice the upregulation of 53 genes encoding enzymes functionally involved in general detoxification

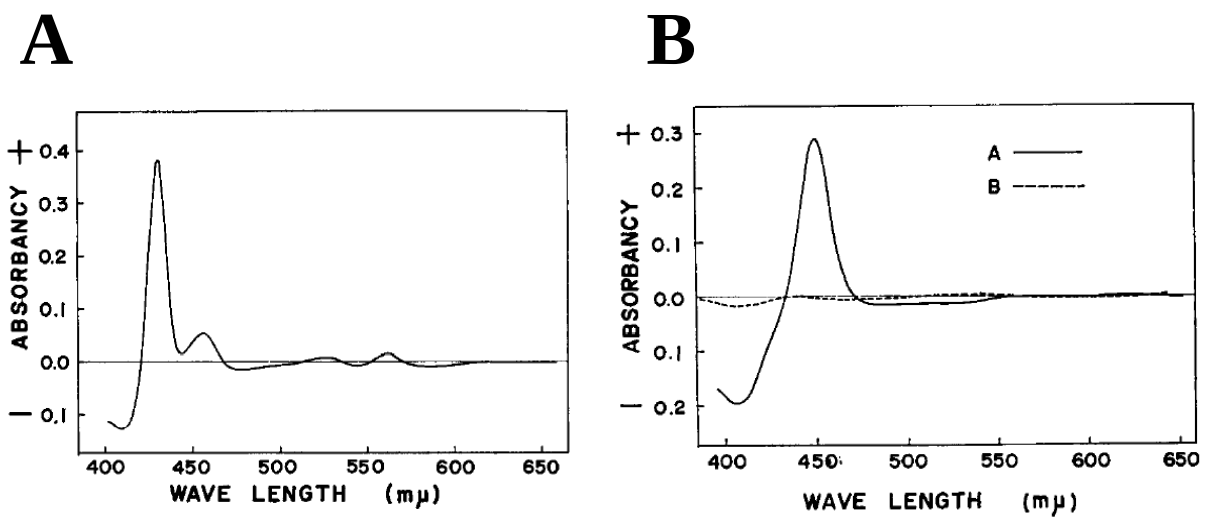

Figure 1.14: CO binding leads to the shift of maximum absorption from 420 to 450 nm of reduced P450s. Differential absorption spectra of liver microsomes carrying P450s in reduced state (dithionite treatment) without (**A**) or with (**B**, line A) CO treatment. B, line B: aerobic microsomes, negative control (Omura and Sato, 1964; adapted).

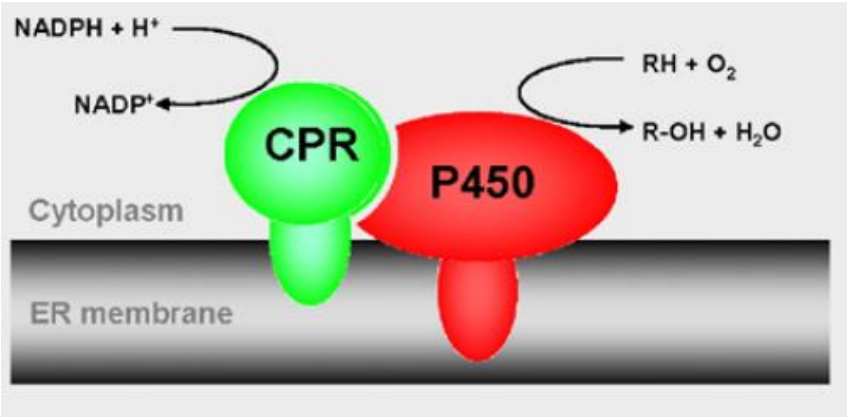

Figure 1.15: Catalytic cycle of plant P450s. Monooxygenation catalyzed by P450 and electron transfer chain between CPR and P450 are shown (Hannemann et al., 2007; adapted).

pathways (see **section C.3.2.**; Coleman et al., 1997). Among these, 16 cytochrome P450s (P450s) are transcriptionally induced, of which two specifically by the mycotoxin and constitute an intriguing category because of the diversity of biosynthetic, catabolic and detoxification pathways in which they participate.

C. CYTOCHROME P450S: A SOURCE OF RESISTANCE TO FHB?

It is exactly 60 years since Cytochrome P450s have been discovered in rat liver microsomes (Klingenberg, 1958). Since then, their study has always brought together an increasingly large community, in particular because of the potential interest of their use in the synthesis of chemicals (Li et al., 2018) or because of their benefit in evolution studies (Nelson and Werck-Reichhart, 2011). Indeed, the diversity of their biochemical functions together with the very high number of gene copies has established an almost limitless field of investigation (Schuler and Werck-Reichhart, 2003). The aim of this section is to briefly describe the genetic, protein and biochemical properties of plant P450s. We will then describe few metabolisms involving P450s in order to hypothesize a potential role of P450s in the interaction between *B. distachyon* and *F. graminearum*.

C.1. Biochemical properties of plant P450s

P450s are enzymes complexed to an iron ion (hemothiolate enzymes) classified as monooxygenases because of the reaction they mostly catalyze: the activation and cleavage of a dioxygen (O_2) molecule with the insertion of one atom on a substrate and reduction of the other into water (Bak et al., 2011). When a P450 is in a reduced state, its heme has a maximum of absorption at 420 nm which shifts to 450 nm after complexation with a carbon monoxide (CO) molecule (which prevents O_2 binding and therefore inhibits P450 activity), and is at the origin of their name ("P" stands for "Pigment"; Omura and Sato, 1964). This property is still exploited to evaluate the functionality and the level of expression of recombinant expressed P450s. Indeed, the amplitude of the peak at 450 nm of the differential absorption spectrum between reduced (often by dithionite treatment) and CO-complexed reduced forms of the recombinant P450 is indicative of the ectopic expression efficiency (**Figure 1.14**; Omura and Sato, 1964). The catalytic cycle of P450s is well described and needs electrons from NADPH to activate O_2. These are transferred by the NADPH-cytochrome P450 reductase (CPR), some-times with the help of cytochrome b_5 and cytochrome b_5 reductase which has the ability to recover electrons from NADH and improve

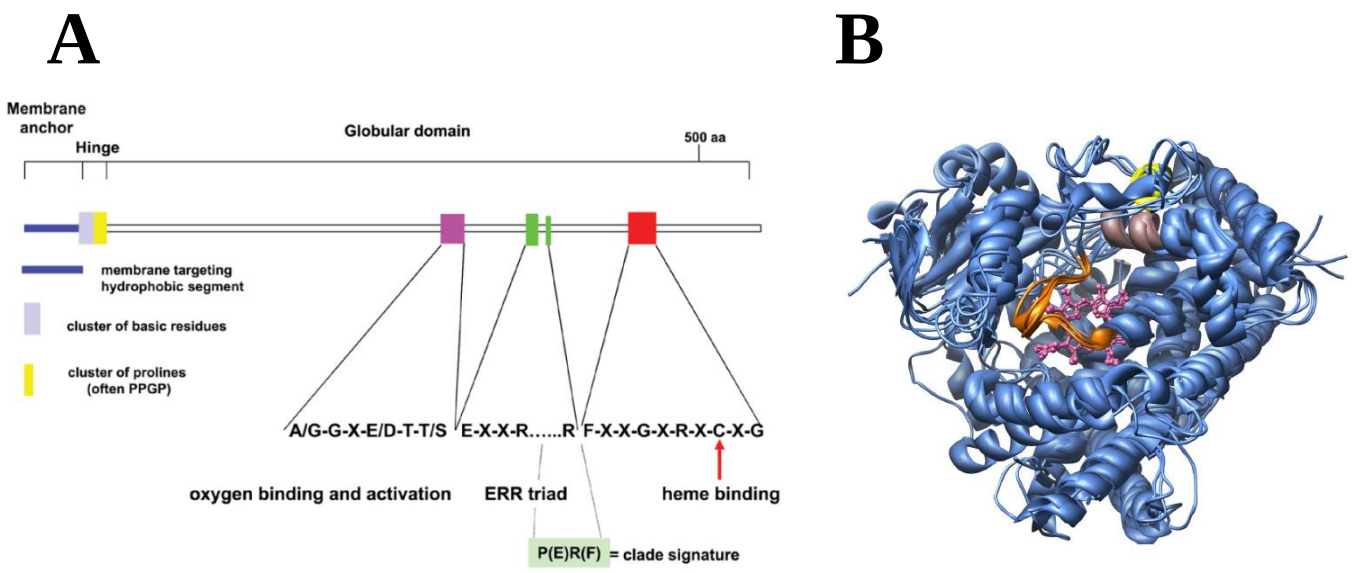

Figure 1.16: Structures of P450s. Two-dimensional (**A**) and three-dimensional (**B**) structures of P450 showing conserved domains in colors. **B**, color key: backbone structure in blue, K-helix consensus in brown, heme-binding loop consensus in orange, PERF domain consensus in yellow, heme in pink (Bak et al., 2011; adapted).

the catalytic cycle efficiency **(Figure 1.15**; Guengerich, 2001). Although most of P450 activities are cytosolic, in plants, all these enzymes need to be anchored to membranes, usually endoplasmic reticulum, to be active. The N-terminus hydrophobic segment of P450s is responsible for this anchoring (**Figures 1.15, 1.16A**; Bak et al., 2011). P450 activity often results in carbon hydroxylation but the diversity of catalyzed reaction is still growing and includes heteroatom hydroxylation, dealkylation or monooxygenation for the most common ones (Guengerich, 2001).

C.2. Structures of P450s

Only two domains, at the protein level, are conserved among plant P450s: the E-R-R (Glutamine-Arginine-Arginine) triad, first, which ensure the stabilization of the core enzyme structure; second, the heme binding loop, a sequence surrounding a strictly conserved Cysteine that acts as the thiolate ligand to the heme iron (**Figure 1.16**; Guengerich, 2001; Bak et al., 2011). Outside of these domains, the sequences are extremely divergent. The nomenclature of P450s is first based on protein sequence identity: following the CYP- prefix, a number indicates the family in which members share at least 40% of homology, (e.g. CYP1), then a letter for the subfamily in which members share at least 55% of identity (e.g. CYP1A). Another number allows the discrimination between isoforms (e.g. CYP1A1). Phylogenetic relationship between P450s and gene organization could also be used by the nomenclature committee led by David Nelson (University of Tennessee, Memphis, USA) to assign names (Nelson, 2009). So far, more than 20,000 P450s have been annotated in all the kingdoms of life, and amino acid sequences are available on the 'Cytochrome P450 Homepage' (http://drnelson.uthsc.edu/cytochromeP450.html; Nelson, 2009).

At the genomic point of view, P450s constitute, by far, the largest multigenic family of enzymes in plants and the third largest family of plant genes following F-box proteins and receptor-like kinases (Nelson and Werck-Reichhart, 2011). For example, *A. thaliana* genome contains about 246 full-length copies and 26 pseudogenes, rice genome contains 328 full-length copies and 99 pseudogenes, *B. distachyon* carries 252 full-length copies and 27 pseudogenes (Nelson, 2004; Nelson, 2009). In 2011, Nelson and Werck-Reichhart performed a phylogenetic analysis of plant P450s copies then available and counted 127 families (from CYP71 to CYP99 and from CYP701 to upper; Bak et al., 2011) grouped into 11 clans. Each derived from one ancestral gene highlighting their very complex evolutionary history with successive gene duplications and family blooms, even from a small-time scale point of view

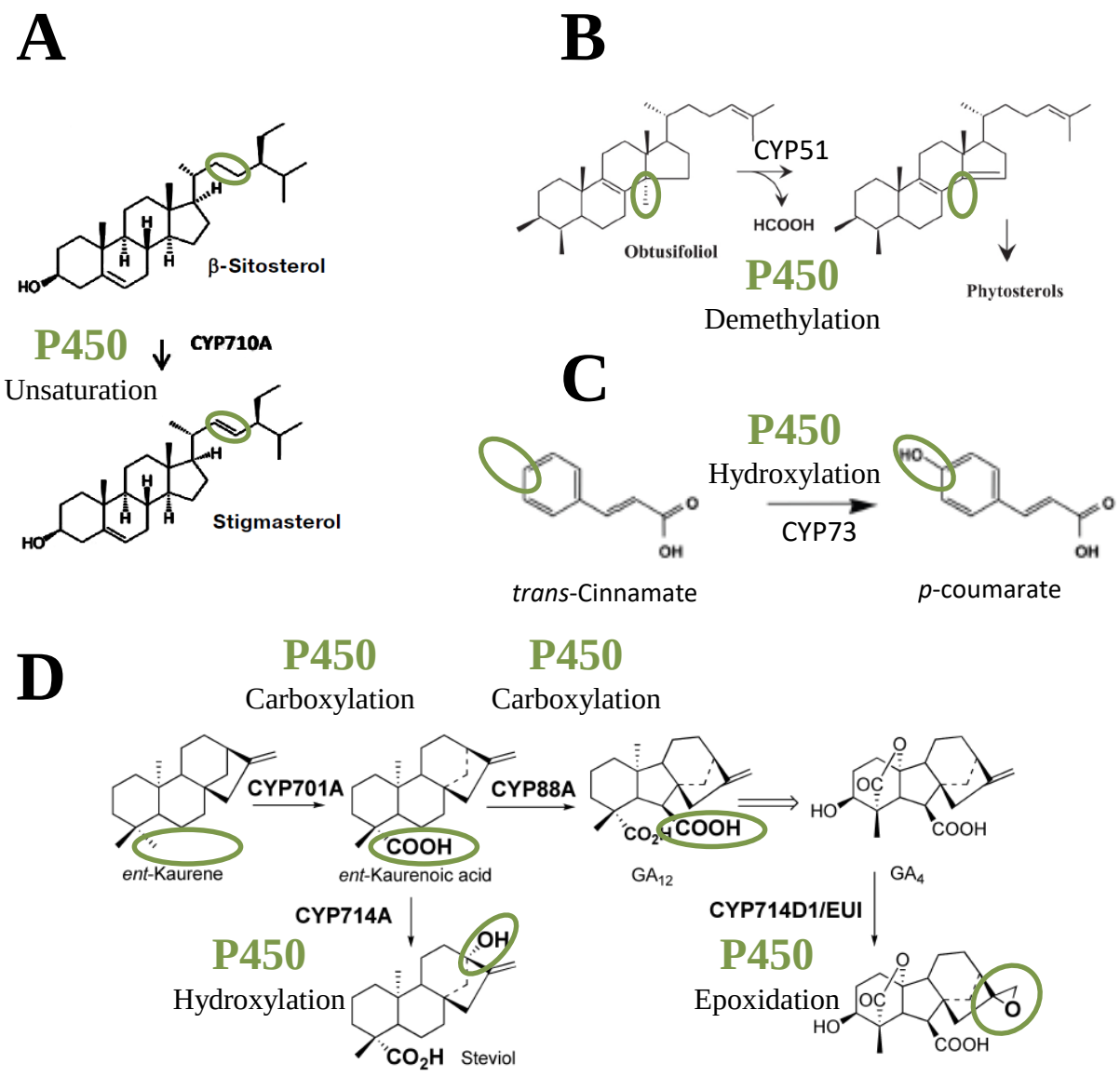

Figure 1.17: Examples of P450 activities on endogenous substrates. A, CYP710As catalyze desaturation of β-Sitosterol into Stigmasterol in the sterol biosynthetic pathway. **B**, CYP51s catalyze demethylation of Obtusifoliol into Phytosterols in the sterol biosynthetic pathway. **C**, CYP73s (Cinnamic acid 4-hydroxylase, C4H) catalyze hydroxylation of *trans*-Cinnamate into *p*-Coumarate in the phenylpropanoid pathway. **D**, Several P450s are involved in the synthesis and catabolism of GAs (Bak et al., 2011; Mizutani et al., 2012; Valitova et al., 2016; adapted).

(Nelson and Werck-Reichhart, 2011). This tremendous diversification of plant P450s copies is now assumed to be a driving force in the diversification of metabolic pathways during land-plant evolution (Mizutani, 2012).

C.3. Plant metabolisms involving P450s

P450s are involved in the metabolization of two kinds of substrates: endogenous or physiological substrates and exogenous or xenobiotic substrates (Bak et al., 2011). This section will provide few examples of P450-mediated metabolisms for each type of substrates.

C.3.1. Endogenous substrates of plant P450s

Plant P450s catalyze biosynthetic or catabolic reactions on a wide variety of endogenous substrates belonging to primary and secondary metabolisms. First, P450s are involved in the synthesis of sterols, which are key components of biological membranes, precursors of brassinosteroids (BRs) and participate in transmembrane signal transduction through the formation of lipid microdomains ('lipid rafts') in the membranes (**Figure 1.17A**; Valitova et al., 2016). The essential 14α-demethylation of obtusifiliol step in sterol biosynthesis is catalyzed by the members of the CYP51 family which, interestingly, is the only one conserved between plants, fungi and animals (**Figure 1.17B**; Bak et al., 1997; Bak et al., 2011). Although copies present in other kingdoms do not catalyze exactly the same reaction, they are all involved in the same biological pathway and therefore are considered as orthologs. CYP710s also participate in sterol biosynthesis (Morikawa et al., 2006). P450s (CYP97s) are also involved in the synthesis of xanthophylls, derived from carotenes and which are components of the photosynthetic complexes playing a role in light-harvesting and photoprotection (Kim et al., 2010). On the border between primary and secondary metabolism, the phenylpropanoid pathway is responsible for the production of a broad range of molecules from structural components (lignin) to UV protectants (flavonoids), antioxidants (polyphenols) or antimicrobials (coumarins, lignans, isoflavonoids). The second step of the biosynthetic pathway, from cinnamate to *p*-coumarate is catalyzed by the cinnamic acid 4-hydroxylase (C4H) a P450 from the first P450 plant family functionally characterized in the 1990s: CYP73 (**Figure 1.17C**; Teutsch et al., 1993; Fraser and Chapple, 2011). Another core metabolic pathway involving P450s concerns the hydroxylation of fatty acids which leads to the synthesis of cutin or suberin for example. A large number of P450s from various plant species have been characterized for their role in fatty acid metabolizing by allowing their

condensation and elongation (Pinot and Beisson, 2011). These elements highlight the role of P450s in the core metabolism of plants and therefore in their normal growth and development.

The biosynthesis and catabolism of several hormones are also dependent on P450 activities. Gibberellins (GAs) are involved in the stimulation of plant organs growth, and the synthesis of the GA_{12} compound, the common precursor for all GAs in plants, is dependent on 6 oxidative steps catalyzed by P450s (CYP701A and CYP88A; **Figure 1.17D**; Hedden and Thomas, 2012). In the case of brassinosteroids, Successive oxidations of campesterol which lead to BRs synthesis are catalyzed by several P450s: CYP85A, CYP90A, CYP90B, CYP90C, CYP90D, and CYP724B (Mizutani, 2012). Moreover, the inactivation (catabolism) of BRs appeared also to be dependent on P450 activities. Indeed, CYP734As catalyze the C26 hydroxylation of the two BRs mostly responsible for growth promoting: brassinolide and castasterone (Thornton et al., 2011). In addition to GAs and BRs, the biosynthesis of auxin, cytokinins (CKs), abscisic acid (ABA), oxylipins, jasmonate (JA) and strigolactones (for which a particular attention is given below) and the catabolism of GAs and ABA recruit P450 activities (Bak et al., 2011). Finely regulated homeostasis of plant hormones which explains the domestication of lands by plants, therefore, appears to partly takedown from P450s evolution (Mizutani and Ohta, 2010).

The reactions discussed above are mostly catalyzed by P450s more or less well conserved across plant species. Although family membership does not determine P450 activity, in the case of primary metabolism, phylogenetic relationships between P450s is an important clue to assign a function to an uncharacterized copy. On the contrary, most of the plant P450s involved in secondary metabolism are much less conserved; hence, their functional characterization remains challenging. Secondary metabolism is expected to comprise more than 200,000 different metabolites which diversity comes from a large variety of enzymes required for their biosynthesis. Among these, P450s are the most divergent class of enzymes (Mizutani, 2012) and therefore explain much of secondary metabolites diversity. We will not detail here the tremendous numbers of secondary metabolic pathways which involve P450s but the three major groups of secondary metabolites (flavonoids and phenolic compounds, terpenoids and nitrogen/sulfur-containing compounds), as defined by Crozier et al. (2007), require P450s for their synthesis. P450 catalyzed reactions in secondary metabolism are extremely diverse and their study often reveal unusual/new P450-associated biochemical functions (Mizutani and Sato, 2011).

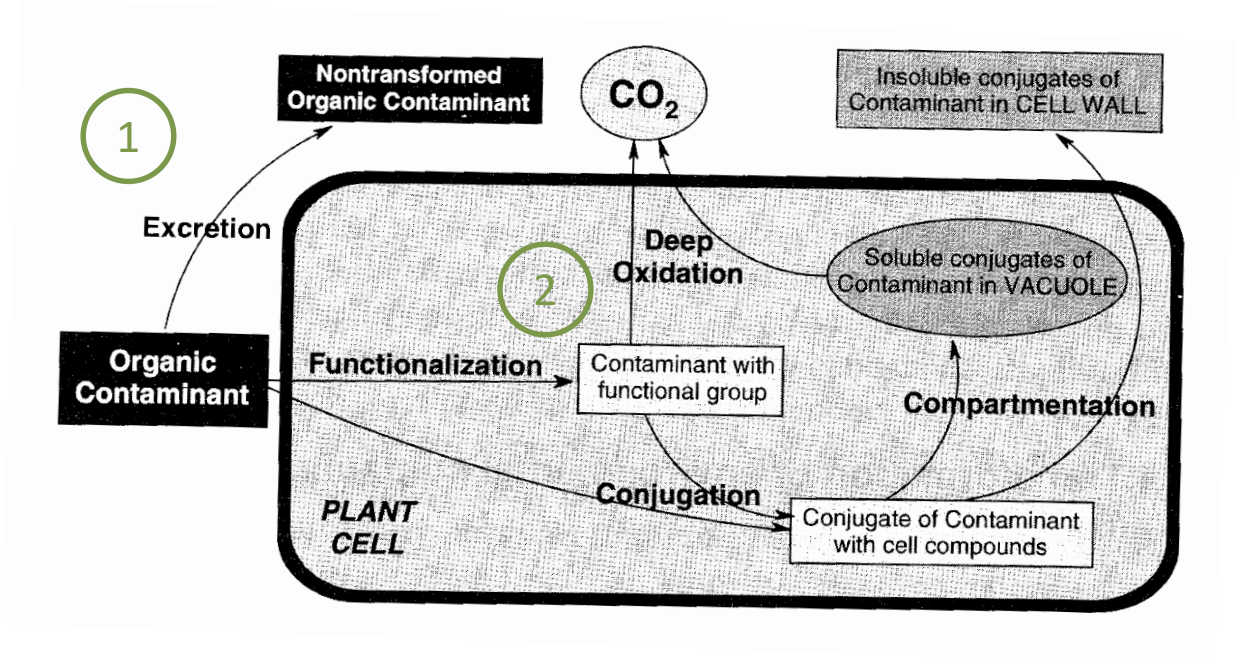

Figure 1.18: Management strategies of xenobiotics by plants. The two main strategies adopted by plants (excretion (1) and metabolization (2)) are indicated (Kvesitadze et al., 2009; adapted).

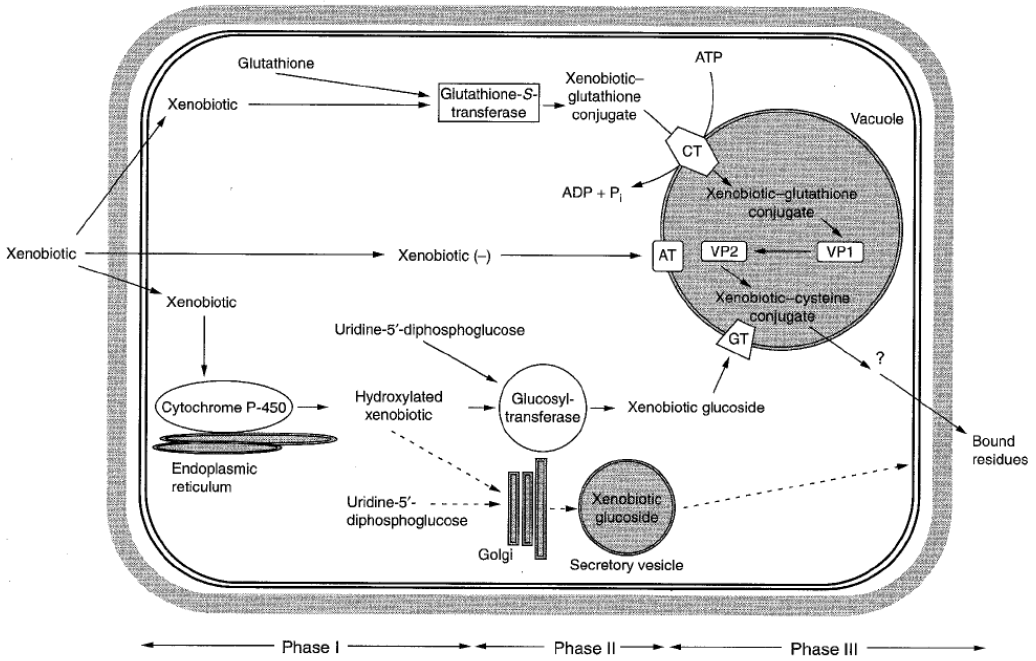

Figure 1.19: Enzymes involved in active xenobiotic detoxification pathways in plants. CT: Glutathion-conjugate transporteur; AT: ATP-dependent transporter; GT: ATP-dependent glucoside-conjugate transporter; VP: Vacuolar peptidase (Coleman et al., 1997).

C.3.2. Exogenous substrates of plant P450s

In addition to the numerous physiological pathways which require P450s for normal plant growth, development and adaptation to external stimuli, detoxification pathways of exogenous or xenobiotic compounds also recruited these enzymes. Before a description of the few well-characterized P450 isoforms involved in the metabolization of foreign compounds, we will briefly expose the general paradigm of plant xenobiotic detoxification.

C.3.2.1. Xenobiotics detoxification by plants

As sessile organisms, plants had to evolve in order to develop sophisticated mechanisms to manage environmental fluctuations. Among these potential hazards, plants are faced with numerous natural or synthetic exogenous molecules which cannot be used as a source of energy and with potential phytotoxic activities: xenobiotics. A general metabolic pathway has been therefore assigned to detoxify these molecules, although this pathway is highly adaptable depending on the compound (Coleman et al., 1997). Following their entry in plant cells, xenobiotics can be taken over by two different pathways **(Figure 1.18)**. First, the pollutant can directly be excreted by the plant, a strategy used only at a high concentration of mobile compounds because of the maintenance of toxicity (Kvesitadze et al., 2009). Second, xenobiotics could be metabolized through successive steps referred to as the so-called 'green liver' in reference to the xenobiotic metabolism in the mammalian liver **(Figure 1.19**; Sandermann, 1992). This second option represents the fate of most of the contaminants. Three successive steps are generally accepted: (1) functionalization, (2) conjugation and (3) compartmentation (Kvesitadze et al., 2009). Functionalization (1) allows the xenobiotic acquisition of a hydrophilic functional group which increases its molecular reactivity for further transformation. A variety of enzymes participate in the first modifications of foreign compounds and include oxidases (P450s, peroxidases, catalases, phenoloxidases, laccases…), reductases, dehalogenases and esterases (Kvesitadze et al., 2006). Conjugation (2) refers to the coupling of the xenobiotic (which has or has not undergone step 1) with a cell endogenous compound such as amino acids and their associated forms (peptides and proteins), organic acids, sugars… This mostly allows the increase of xenobiotic hydrophilicity and therefore decreases its ability to bind biological membranes (Coleman et al., 1997; Kvesitadze et al., 2006). Glutathione-*S*-transferases (GSTs), UGTs, and a range of other transferases catalyze this second step. Finally, the compartmentation step (3) refers to the process of xenobiotic accumulation in the vacuole or in the apoplast, facilitated by transporters (ATP dependent

Table 1.4: Plant P450s shown to be involved in xenobiotic detoxification (continued on next page).

Isoforms	Plant species	Substrats	Catalyzed reactions	Products	Endogenous substrats	References
EgP450 (CYP71A)	*Elaeis guineensis* Jacq. (Oil palm)	isoproturon (IPU)	?	?	?	Phongdara et al., 2012
CYP71A1	*Persea americana* (Avocado)	*p*-chloro-*N*-methylaniline	*N*-dealkylation	*p*-chloroaniline	?	Bozak et al., 1992
CYP71A10	*Glycine max* (Soybean)	fluometuron	*N*-demethylation	*N*-demethyl-fluometuron	?	Siminszky et al., 1999
		linuron (LIN)	*N*-demethylation and *O*-demethylation	*N*-demethyl linuron and *O*-demethyl-linuron	?	
		chlorotoluron (CTU)	*ring*-methyl-hydroxylation and *N*-demethylation	*ring*-hydroxymethyl-chlorotoluron and *N*-demethyl-chlorotoluron	?	
		diuron	*N*-demethylation	*N*-demethyl-diuron	?	
CYP71AH11 (former CYP71A11)	*Nicotiana tabacum* L. cv. Samsun (Tobacco)	7-ethoxycoumarin	*O*-deethylation	7-hydroxycoumarin (umbelliferone)	?	Yamada et al., 2000
		chlorotoluron (CTU)	*N*-demethylation	N-demethyl-chlorotoluron	?	
CYP71C6v1	*Triticum aestivum* (wheat)	chlorosulfuron	hydroxylation	5-hydroxy-chlorosulfuron	?	Xiang et al., 2006
		triasulfuron	hydroxylation	5-hydroxy-triasulfuron	?	
		metsulfuron-methyl	?	?	?	
		bensulfuron-methyl	?	?	?	
		tribenuron-methyl	?	?	?	
CYP73A1	*Helianthus tuberosus* (Jerusalem artichoke)	7-ethoxycoumarin	*O*-deethylation	7-hydroxycoumarin (umbelliferone)	4-hydroxylation of *trans*-cinnamic acid into p-coumaric acid (phenylpropanoid pathway) (Gabriac et al., 1991 ; Teutsch et al., 1993) ; O-de-methylation of 7-methoxycoumarin (herniarin) into 7-hydroxycoumarin (umbelliferone) (Pierrel et al., 1994)	Pierrel et al., 1994 ; Schalk et al., 1997
		p-chloro-N-methylaniline	*N*-demethylation	*p*-chloroaniline		
		chlortoluron (CTU)	*ring*-methyl-hydroxylation	*ring*-methyl-hydroxychlorotoluron		
		1-aminobenzotriazole	?	?		
		2,4-dichlorophenoxypropyne	?	?		
		2-naphthoic acid	hydroxylation	6-hydroxy-2-naphthoic acid		Schalk et al., 1997
CYP76B1	*Helianthus tuberosus* (Jerusalem artichoke)	7-ethoxycoumarin	*O*-deethylation	7-hydroxycoumarin (umbelliferone)	O-de-methylation of 7-methoxycoumarin (herniarin) into 7-hydroxycoumarin (umbelliferone) (Robineau et al., 1998)	Batard et al., 1998
		chlortoluron (CTU)	di-*N*-demethylation	di-demethyl-chlortoluron (DDM-CTU via DM-CTU)		Robineau et al., 1998 ; Didierjean et al., 2002

glutathione pump, ABC transporters or multidrug and toxic compound extrusion (MATE) transporters; **Figure 1.19**; Kvesitadze et al., 2009; Pasquet, 2014). The detoxification pathway does not involve necessarily these three steps and multiple fates could be observed for one xenobiotic. For example, we already discussed the glycosylation of DON into D3G as a detoxification process (see **section B.4.4.**; Lemmens et al., 2005), but 8 other DON-derived products have been also characterized in wheat treated by the mycotoxin, highlighting complex and multiple detoxification processes developed by wheat towards the mycotoxin (Kluger et al., 2015).

C.3.2.1. P450s in plant xenobiotic detoxification (**Table 1.4**)

The first study underlying the putative role of plant P450s in xenobiotic detoxification was performed at the end of the 1960s and showed *in vitro* metabolism of herbicides from phenylurea family (i.e. substituted 3-(phenyl)-l-methylureas) *via N*-demethylation in cotton seedlings (Frear et al., 1969). However, the first characterization of a P450 isoenzyme able to metabolize a xenobiotic (CYP71A1) was only performed in 1992 mainly because of the low expression level of P450 in plant tissue making their isolation intricate (Bozak et al., 1990; Bozak et al., 1992). The ectopic yeast expressed CYP71A1 from ripe avocado (*Persea americana*) was shown to actively demethylate *p*-chloro-*N*-methylaniline (pCMA) used as a model molecule for studying *N*-demethylation by oxidases (Young and Beevers, 1976; Dohn and Krieger, 1984; O'keefe and Leto, 1989). This activity will also be associated to CYP73A1 firstly isolated from the wound- and Mn^{2+}-induced Jerusalem artichoke tuber tissues (*Helianthus tuberosus*) (Gabriac et al., 1991; Pierrel et al., 1994) for which many endogenous and exogenous substrates have been tested for the first time. This P450 was originally identified as a cinnamate 4-hydroxylase (C4H), the second enzyme of the phenylpropanoid pathway as discussed above (Teutsch et al., 1993). On the 22 xenobiotics tested, 6 were actively metabolized by CYP73A1 through the catalysis of at least 4 different chemical reactions highlighting multiple and redundant activities of plant P450s. Among the detected activities, *ring*-methyl-hydroxylation of the phenylurea herbicide chlorotoluron was suggested as a source of resistance despite the apparent low efficiency of the reaction. Finally, 3 dimensions molecular structure should be considered as an important factor in the identification of putative P450 substrates since all chemicals metabolized by CYP73A1 share small and planar conformation, allowing to predict that 2-Naphtoic acid is a xenobiotic substrate (Schalk et al., 1997).

Table 1.4: Plant P450s shown to be involved in xenobiotic detoxification (continued from the previous page).

Isoforms	Plant species	Substrats	Catalyzed reactions	Products	Endogenous substrats	References
CYP76B1	*Helianthus tuberosus* (Jerusalem artichoke)	isoproturon (IPU)	di-*N*-demethylation	di-demethyl-isoproturon (DDM-IPU via DM-IPU)	O-de-methylation of 7-methoxycoumarin (herniarin) into 7-hydroxycoumarin (umbelliferone) (Robineau et al., 1998)	Robineau et al., 1998
		7-methoxyresorunfin	*O*-demethylation	resorufin (7-hydroxyresorufin)		
		7-ethoxyresorunfin	*O*-dealkylation	resorufin (7-hydroxyresorufin)		
		linuron (LIN)	*N*-demethylation	demethyl-linuron (DM-LIN)		Didierjean et al., 2002
CYP76C1	*Arabidopsis thaliana*	chlorotoluron (CTU)	*ring*-methyl hydroxylation and *N*-dealkylation	*ring*-hydroxymethyl-chlorotoluron and *N*-demethyl-chlorotoluron	hydroxylation of linalool into 9-OH-linalool and 8-OH-linalool, hydroxylation of citronellol into 8-OH-citrinellol, hydroxylation of lavandulol into 7-OH-lavandulol, hydroxylation of α-terpineol into 10-OH-α-terpineol (Höfer et al., 2014)	Höfer et al., 2014
		isoproturon (IPU)	hydroxylation and *N*-dealkylation	hydroxyisopropyl-isoproturon and *N*-demethyl-isoproturon (DM-IPU)		
		linuron (LIN)	?	?		
		metobromuron	?	?		
		metoxuron	?	?		
		monolinuron	?	?		
		monuron	?	?		
		diuron	?	?		
CYP76C2	*Arabidopsis thaliana*	chlorotoluron (CTU)	*ring*-methyl hydroxylation and *N*-dealkylation	*ring*-hydroxymethyl-chlorotoluron and *N*-demethyl-chlorotoluron	hydroxylation of nerol into 9-OH-nerol and 8-OH-nerol, hydroxylation of linalool into 9-OH-linalool and 8-OH-linalool, epoxydation of linalool into 1,2-epoxylinalool, hydroxylation of citronellol into 9-OH-citronellol and 8-OH-citrinellol, epoxydation of citronellol into 6,7-epoxycitronellol, hydroxylation of lavandulol into 8-OH-lavandulol and 7-OH-lavandulol (Höfer et al., 2014)	Höfer et al., 2014
		isoproturon (IPU)	hydroxylation and *N*-dealkylation	hydroxyisopropyl-isoproturon and *N*-demethyl-isoproturon (DM-IPU)		
		linuron (LIN)	?	?		
		metobromuron	?	?		
		metoxuron	?	?		
		monolinuron	?	?		
		monuron	?	?		
		diuron	?	?		
CYP76C4	*Arabidopsis thaliana*	chlorotoluron (CTU)	*ring*-methyl hydroxylation and *N*-dealkylation	*ring*-hydroxymethyl-chlorotoluron and *N*-demethyl-chlorotoluron	hydroxylation of geraniol into 9-OH-geraniol and 8-OH-geraniol (Höfer et al, 2013) ; hydroxylation of nerol into 9-OH-nerol and 8-OH-nerol, hydroxylation of linalool into 9-OH-linalool and 8-OH-linalool, epoxydation of linalool into 1,2-epoxylinalool, hydroxylation of citronellol into 9-OH-citronellol and 8-OH-citrinellol, hydroxylation of lavandulol into 8-OH-lavandulol and 7-OH-lavandulol, hydroxylation of α-terpineol into 10-OH-α-terpineol (Höfer et al., 2014)	Höfer et al., 2014
		isoproturon (IPU)	hydroxylation and *N*-dealkylation	hydroxyisopropyl-isoproturon and *N*-demethyl-isoproturon (DM-IPU)		
		linuron (LIN)	?	?		
		diuron	?	?		
CYP81B1	*Helianthus tuberosus* (Jerusalem artichoke)	chlorotoluron (CTU)	*ring*-methyl hydroxylation	*ring*-hydroxymethyl-chlorotoluron	hydroxylation of fatty acids (C10:0; C12:0 and C14:0) (Cabello-Hurtado et al., 1998 ; Didierjean et al., 2002)	Cabello-Hurtado et al., 1998 ; Didierjean et al., 2002
CYP81B2	*Nicotiana tabacum* L. cv. Samsun	7-ethoxycoumarin	*O*-deethylation	7-hydroxycoumarin (umbelliferone)	?	Yamada et al., 2000
		chlorotoluron (CTU)	*ring*-methyl hydroxylation	*ring*-hydroxymethyl-chlorotoluron	?	

Chlorotoluron is one of the well-studied xenobiotic substrates and it has been shown to be metabolized by 9 P450s from various plant species. Interestingly, metabolization of this foreign compound occurs through at least 3 different ways (*ring*-methyl-hydroxylation, *N*-demethylation and di-*N*-demethylation) which might be explained by the complex evolutionary history of P450s as we discussed before. While *ring*-methyl-hydroxylation and di-*N*-demethylation lead to a strong decrease of intrinsic phytotoxicity of chlorotoluron, which easily explains why these activities have been selected through evolution, metabolite produced by simple *N*-demethylation remains partially toxic (Siminszky et al., 1999; Yamada et al., 2000). It was then suggested that the expression profile of several genes encoding P450s involved in partial detoxification of xenobiotic, and more specifically their strong induction in the response of their substrate, could explain their selection (Yamada et al., 2000). Moreover, a single P450 could catalyze diverse modifications on chlorotoluron (e.g. CYP71A10 from soybean, CYP76C1, C2 and C4 from *A. thaliana*) and this highlights the extraordinary complex P450 biochemistry, probably greater considering exo- than endogenous substrates (Schuler and Werck-Reichhart, 2003). Multiple detoxification pathways could also be observed for other phenylurea family members such as linuron and isoproturon but have not been described for another xenobiotic. This can probably be explained by the extensive use of phenylurea herbicides as model substrates for P450s unlike many other xenobiotics less often studied.

In some cases, only exogenous substrates have been identified for P450s (e.g. CYP71A10 from Soybean, CYP71A11 and CYP81B2 from *Nicotiana tabacum*). On the contrary, several plant P450s metabolizing both endo- and exogenous substrates have been identified: CYP73A1, CYP76B1 and CYP81B1 from Jerusalem artichoke and CYP76C1, 2 and 4 from *A. thaliana*. Therefore, it remains unclear whether P450s are always involved in endogenous metabolic pathways, or if specific isoenzymes are only responsible for detoxifying foreign compounds (Schuler and Werck-Reichhart, 2003). However, enzymatic parameters should carefully be considered to assign biological functions to P450s: indeed some catalytic activities described might result from the ability of the xenobiotic substrate to fit into the catalytic site *in vitro* and without any competitor but could fail to efficiently chemically convert the substrate *in planta*.

To the best of our knowledge, only 12 P450s from various plant species were, at least, partially characterized as enzymes able to metabolize 19 different xenobiotic substrates (**Table 1.4**). Interestingly, these P450s all belong to the CYP71 clan (also known as "A-type" clan), containing more than 50% of the plant P450s. This clan presents a complex

evolutionary history with successive gene duplications and family blooms even from a small-time scale point of view (Nelson and Werck-Reichhart, 2011). It contains enzymes assumed to mainly participate in the synthesis of secondary metabolites which explain the lower selection pressure on this clan as compared to those involved in the synthesis of essential compounds of the primary metabolism (Schuler and Werck-Reichhart, 2003; Bak et al., 2011). A high frequency of gene duplication and rapid neofunctionalization of P450s, therefore, allow plants to develop, from a common and reduced core set of genes, an arsenal of detoxifying enzymes which then have been selected independently among species. Although this suggests a possible management of a very wide variety of exogenous substrates, it also makes it more complex to study the detoxification of xenobiotics by P450s on a large scale.

C.4. FHB and P450s

Numerous studies reported the transcriptional activation of plant P450-encoding genes in response to the infection by *F. graminearum*, or in response to DON treatment. We already briefly discussed the transcriptome of *B. distachyon* in these conditions (**section B.5.2**.; Pasquet, 2014; Pasquet et al., 2014), but many other transcriptomic studies have been performed for various conditions or plant species.

The first evidence of the involvement of wheat P450s in the FHB context came in 2005 with the observation of the early induction of *CYP709C3v2* in response to fungal infection of both a resistant ('Ning 7840') and a susceptible ('Len') cultivars compared to water treatment (qPCR data; Kong et al., 2005). Two years later, a first microarray analysis was then performed and reported the up-regulation of three P450 genes in 'Ning 7840' before or during early (0-6 hpi) infection and then their down-regulation compared to the susceptible 'Clark' cultivar. The authors made assumptions about the role of one of those P450s from the CYP71C subfamily as an enzyme involved in DIMBOA biosynthesis (Bernardo et al., 2007). Although this antimicrobial compound is metabolized by *F. graminearum*, it was shown to limit fungal growth *in vitro* (Glenn et al., 2001). The up-regulation of wheat P450-encoding genes was then reported several times, in various context, with sometimes an increasing number of genes, probably because of the improvement of transcriptomic methodologies (Li and Yen, 2008; Jia et al., 2009; Steiner et al., 2009; Li et al., 2010; Gottwald et al., 2012; Muhovski, 2012; Kugler et al., 2013; Schweiger et al., 2013b; Ha et al., 2015; Kosaka et al., 2015; Hofstad et al., 2016). Transcriptomic studies have also been performed in response to a

Table 1.5: Two P450-encoding genes from *B. distachyon* are transcriptionally induced during FHB, in a DON-dependent manner.

Bd Genes	DON	Bon.	Fg^{DON+}	Bon.	Fg^{DON-}	Bon.	NCBI Annotations
Bradi1g75310	14.96	0	121.84	0	1.70	1	BdCYP711A29
Bradi2g44300	17.03	0	30.41	0	2.21	1	BdCYP72A168

Gene expression fold-changes following DON treatment (DON, 12 h after point inoculation of 2 µg of the mycotoxin) or 96 hpi (point inoculation) with a toxin-producing strain (Fg^{TOX+}) or with a non-toxigenic strain (Fg^{tox-}) of *F. graminearum* compared to control conditions. Bon.: *p* value of Bonferroni test (Pasquet et al., 2014; Pasquet, 2014; adapted).

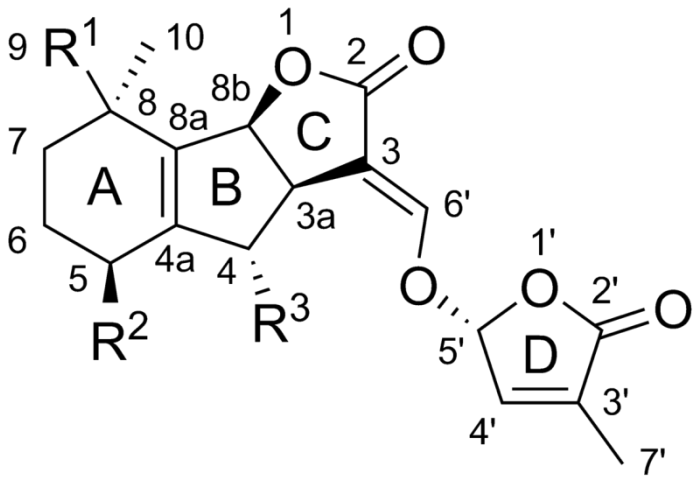

Figure 1.20: Core chemical structure of SLs.

direct application of DON (Li et al., 2010; Walter and Doohan, 2011; Hofstad et al., 2016) or DON-containing fungal crude extract (Sorahinobar et al., 2017). This also led to the identification of early transcriptional activation of P450-encoding genes. Finally, studies have been also performed on other hosts of *F. graminearum*, barley (Boddu et al., 2006; Boddu et al., 2007; Gardiner et al., 2010; Jia et al., 2011) and *B. distachyon* (Pasquet et al., 2014; Pasquet, 2014) and they have once again confirmed the involvement of P450s in the response to infection. Given the numerous metabolic processes involving P450s, in particular in response to stresses, and the high transcriptional regulation of these enzymes, it is not surprising to observe differential expression of plant genes encoding P450s in response to *F. graminearum* infection or DON treatment. In contrast and as discussed above, functional characterization of that kind of genes is intricate precisely because of their wide variety of activities. To the best of our knowledge, no P450 has been functionally characterized in the FHB context so far.

Several microorganisms were shown to metabolize DON and even use the mycotoxin has a carbon source (Ito et al., 2013). In order to elucidate the enzymes involved in these metabolic pathways, Ito et al. (2013) screened a cosmid library of DON-utilizing KSM1 bacterium strain genomic DNA for DON metabolization. A cosmid clone transforming DON was isolated and the *ddnA* sequence responsible for this activity was shown to encode a P450. The reaction product was characterized and *ddnA* was shown to catalyze 16-hydroxylation of DON to form 16-hydroxydeoxynivalenol (16-HDON). Finally, 16-HDON phytotoxicity was evaluated and high concentrations (100 µM) were shown not to affect wheat seedling growth (Ito et al., 2013). The ectopic expression of *ddnA* into wheat could, therefore, constitute a promising strategy to improve DON tolerance and FHB resistance (Gunupuru et al., 2017).

The transcriptomic study performed in our lab aimed to identify *B. distachyon* (ecotype Bd21-3) DEGs during the interaction with *F. graminerarum* DON-producing (Fg^{DON+}; PH-1) or -non producing (Fg^{DON-}; PH-1Δ*tri5*) strains and following direct treatment with DON (Pasquet et al., 2014; Pasquet, 2014). This experimental set-up allowed the identification of a pool of genes specifically induced by the mycotoxin and not by the infection itself (i.e. genes induced in Fg^{DON+} and DON conditions but not in Fg^{DON-} condition compared to control conditions). Seventeen P450s were shown to be differentially expressed between Fg^{DON+} and Fg^{DON-} conditions (Pasquet et al., 2014). Among them, 16 are induced among which two are also regulated by the mycotoxin: *Bradi1g75310* and *Bradi2g44300* which encode CYP711A29 and CYP72A168, respectively (**Table 1.5**; Nelson, 2009; Pasquet, 2014; unpublished results). The expression profiles of these two genes suggest a putative

Figure 1.21: Examples of natural SL chemical structures. Examples of both canonical (strigol- and orobanchol-types) and non-canonical chemical structures are presented (Wang and Bouwmeester, 2018; adapted).

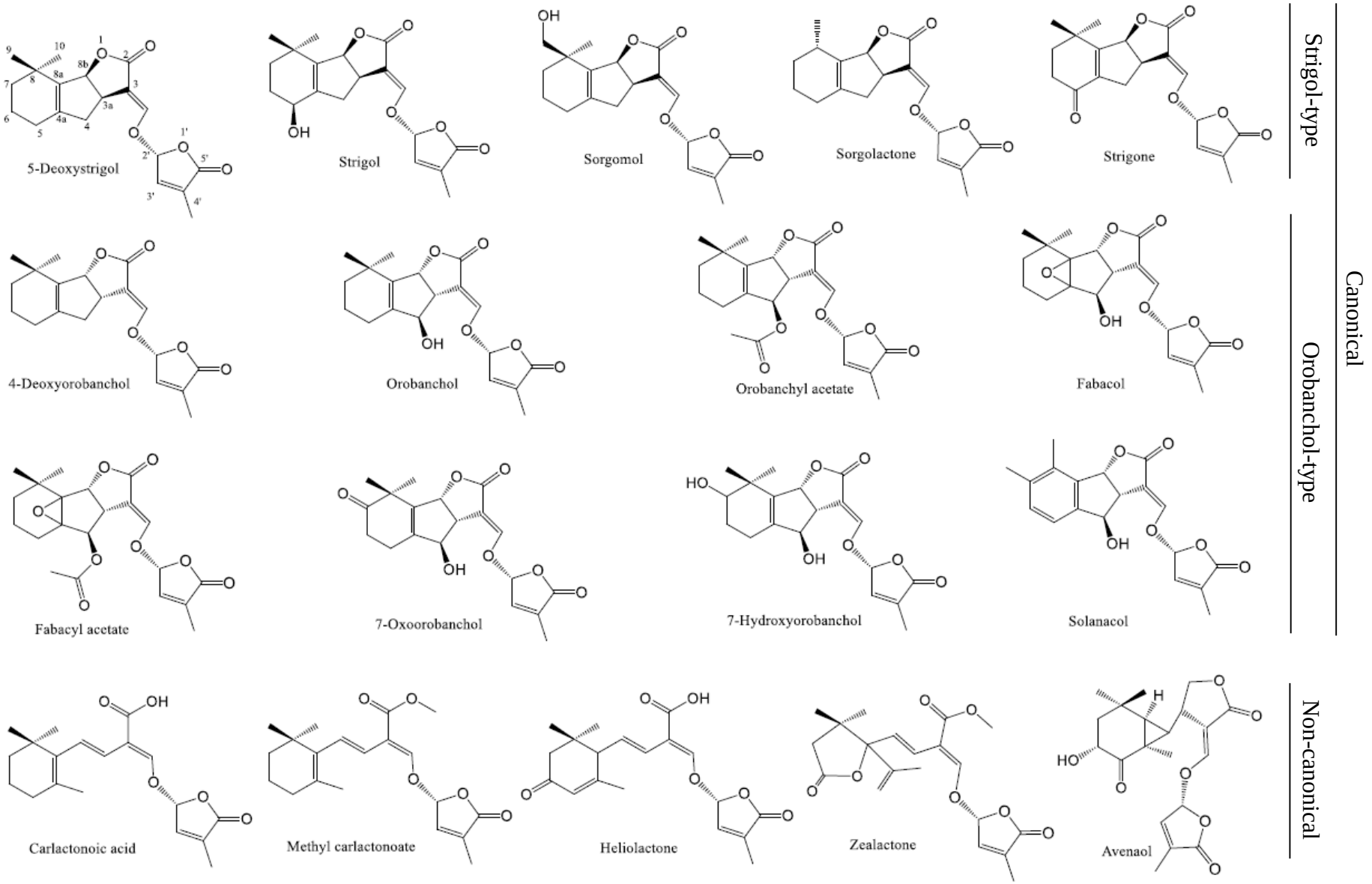

involvement of the two encoded P450s in metabolic pathways mobilized by the host plant in response to the mycotoxin. Because *Bradi1g75310* (*CYP711A29*) was shown to be more induced during the interaction compared to *Bradi2g44300* (*CYP72A168*), likely reflecting a stronger involvement in the interaction, we decided to focus our efforts on the functional characterization of this gene. Interestingly, several P450s of the CYP711A subfamily were shown to be involved in the biosynthesis of a class of plant hormones: the strigolactones (Bak et al., 2011).

D. THE STRIGOLACTONES AS NATURAL CHEMICALS WITH PLEIOTROPIC ACTIVITIES

In 1957 and for a period of over 50 years, parts of North and South Carolina (USA) were quarantined in order to prevent the spreading throughout the USA of a parasitic plant, witchweed (*Striga* sp.). The previous year, an Indian student who knew the ravages of this weed in his home country was the first to recognize the species in North Carolina. His warning and the US Department of Agriculture's still ongoing eradication program have probably saved millions of dollars losses (Zimdahl, 2018). It also accelerated research programs on witchweed and finally led to the discovery of strigolactones (SLs), a class of plant hormones with pleiotropic endo- and exogenous activities. The aim of this section is to describe the chemical diversity of this class of molecules; we will then present their biosynthetic pathway and discuss their numerous endogenous and rhizospheric roles. To conclude, we will propose a comprehensive analysis of the literature on the involvement of SLs in plant interactions with detrimental microorganisms.

D.1. Chemical diversity of SLs

Strigolactones (SLs) are carotenoid-derived lactones composed of a tricyclic ABC ring system, with the ketone function on the C ring, linked to a butenolide D-ring *via* an enol-ether bridge. Natural SLs are divided into (+)-strigol- and (-)-orobanchol-type SLs that differ in the stereochemistry of the C-ring: 3a*R*, 8b*S* in strigol-type (β orientation) and 3a*S*, 8b*R* in orobanchol-type (α orientation) with an *R* configured D-ring (**Figure 1.20**; Wang and Bouwmeester, 2018). Canonical SLs are those exhibiting the 4 rings but there are also non-canonical forms, discovered more recently, lacking one or more of the first three rings but still biologically active. Hence, Wang and Bouwmeester (2018) proposed to redefine SLs as ‹‹ *a carotenoid derived molecule with a butenolide D-ring* ›› to no longer distinguish between

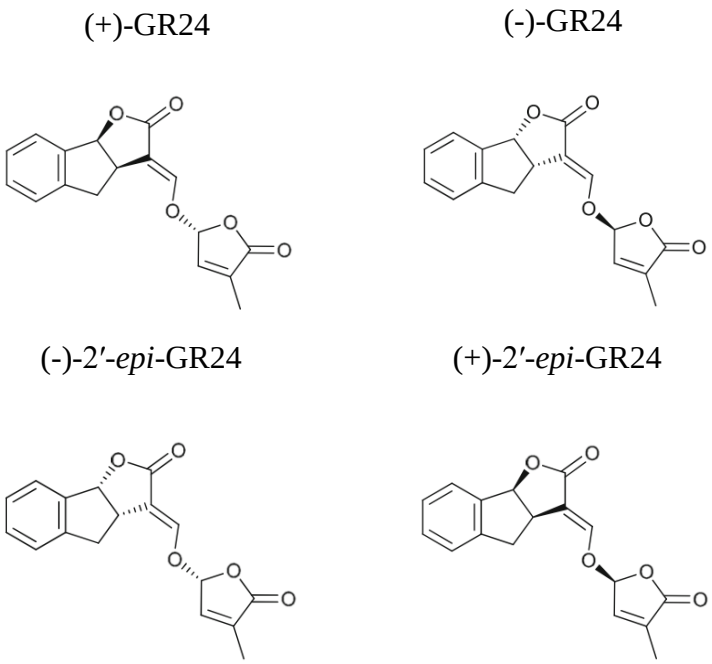

Figure 1.22: Chemical structure diversity of the synthetic SL GR24.

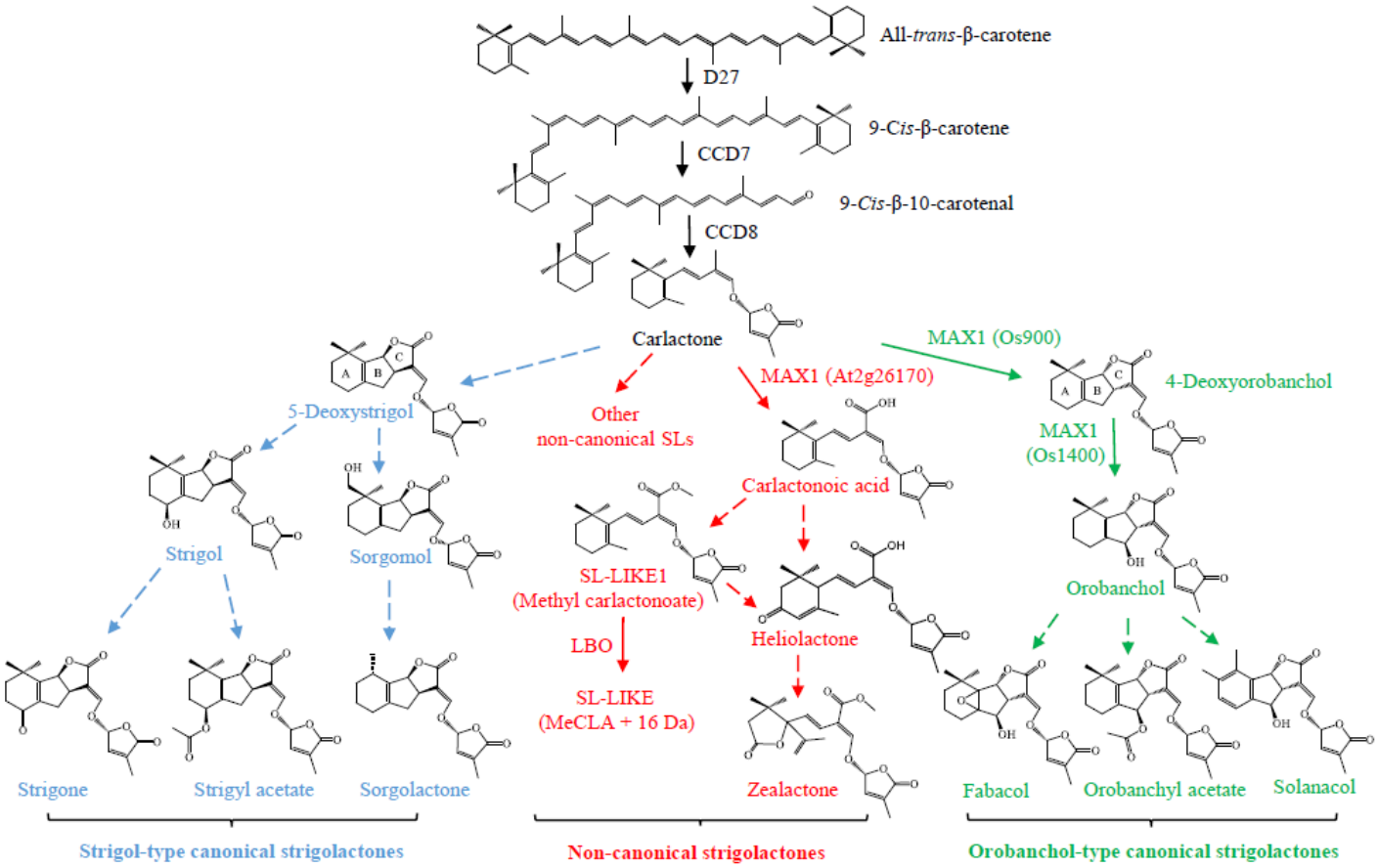

Figure 1.23: SLs biosynthetic pathway. The core biosynthetic pathway producing carlactone is shown in black, the putative pathways responsible (1) for the production of Strigol-type SLs is presented in blue, (2) for the production on non-canonical SLs is presented in red and (3) for the production of orobanchol-type SLs is presented in green (Wang and Bouwmeester, 2018).

canonical and non-canonical forms. Chemical diversity of canonical-SLs is given by several modifications on AB-rings: demethylation, hydroxylation, epoxidation, acetoxylation and ketolation (Al-Babili and Bouwmeester, 2015). To date, over 20 natural molecules have been classified as SLs and it is now generally accepted that this diversity might result from multiple endo- and exogenous roles of SLs (**Figure 1.21**; Wang and Bouwmeester, 2018).

The part of SLs needed for normal or basic bioactivity (bioactiphore) is the CD-part. Hence, a set of SL synthetic analogs with a simplified AB-part have been constructed (Zwanenburg and Blanco-Ania, 2018). Among them, (+)-GR24, a modified (+)-strigol with an aromatic A-ring, is the most commonly used by scientists because of the relative ease of its synthesis and its high level of bioactivity (Johnson et al., 1976). Although synthetic molecules have been firstly validated as SL-analogs for their ability to induce seed germination of parasitic weeds, numerous other biological activities seem to depend on other chemical properties (Zwanenburg and Blanco-Ania, 2018). Moreover, GR24 is often synthesized and used as a racemic mixture of 2 to 4 stereoisomers ((+)-GR24, (-)-GR24, (+)-2'-*epi*-GR24, (-)-2'-*epi*-GR24) in which *S* configured D-ring (2'*S*) forms exhibit distinct biological activities compared to 2'*R* naturally configured molecules (**Figure 1.22**; López-Ráez et al., 2017). When possible, physiological effects of SLs might, therefore, be studied with enantiopure material (Akiyama et al., 2010).

D.2. SLs core biosynthetic pathway

The biosynthesis of SLs is divided into a well-conserved core biosynthetic pathway which is responsible for the transformation of all-*trans*-β-carotene into carlactone (CL) a non-canonical SL considered as the common intermediate of all SLs, and a less-conserved diversification pathway of CL into one of the numerous known SLs (**Figure 1.23**). The elucidation of the core biosynthetic pathway has been mostly performed thanks to *A. thaliana*, rice, petunia (*Petunia hybrida*) and pea (*Pisum sativum*) because of the diversity of branching mutants available in these species linked to *MORE AXILLARY GROWTH* (*MAXs*), *DWARF/HIGH TILLERING DWARF* (*D/HTDs*), *DECREASED APICAL DOMINANCE* (*DADs*) and *RAMOSUS* (*RMSs*) genes, respectively (**Table 1.6**; Saeed et al., 2017). Indeed, as discussed later, a well-described endogenous role of SLs is their ability to inhibit shoot branching.

The precursor of SLs, all-*trans*-β-carotene, was identified in 2005 with the use of carotenoid biosynthesis inhibitors on maize, cowpea and sorghum which, in these conditions,

Table 1.6: Genes involved in the synthesis and the signaling of SLs in four model plants. (Wand and Bouwmeester, 2018; adapted).

Role	Protein identity/Function	*A. thaliana*	Pea	Petunia	Rice
Synthesis	9-*cis*/all-*trans*-β-Carotene isomerase	*AtD27*			D27
	Caroteinoid cleavage dioxygenase (CCD7)	*MAX3*	*RMS5*	*DAD3*	*HTD1*/*D17*
	Caroteinoid cleavage dioxygenase (CCD8)	*MAX4*	*RMS1*	*DAD1*	*D10*
	Cytochrome P450 (CYP711A)	*MAX1*		*PhMAX1*	*Os01g0700900* (*Carlactone oxidase*), *Os01g0701400* (*Orobanchol synthase*), *Os01g0701500*, *Os02g221900*, *Os06g0565100*
	Fe(II)-dependent dioxygenase	*LBO*			
Signaling	α/β-Hydrolase	*AtD14*	*RMS4*	*DAD2*	*D14/D88/HTD2*
	F-box protein	*MAX2*	*RMS3*	*PhMAX2A*, *PhMAX2B*	*D3*
	Class I Clp ATPase protein	*SMXL6*, *SMXL7*, *SMXL8*			*D53*, *D53-LIKE*

exhibit a reduced ability to induce seed germination of parasitic weeds (*S. hermonthica* and *Orobanche crenata*; Matusova et al., 2005). The extensive study of *max*, *d*/*htd*, *dad*, and *rms* mutants was then powerfully achieved using grafting technics and allowed the sequential characterization of the SLs biosynthetic pathway (Al-Babili and Bouwmeester, 2015). The first enzyme involved in the core biosynthetic pathway of SLs is DWARF27 (D27), firstly identified in rice because of the phenotype of the corresponding mutant line *d27*: increased shoot branching reversible with GR24 treatment, no SL detected in roots, inability to induce seed germination of the parasitic weed *Orobanche crenata* (Lin et al., 2009). The expression of D27 in *Escherichia coli* and its incubation with all-*trans*-β-carotene then elucidated its enzymatic activity as an all-*trans*/9-*cis*-β-carotene isomerase (Alder et al., 2012). The homolog of rice D27 has been also identified in *A. thaliana* (AtD27; Waters et al., 2012) but not yet in pea and petunia, the two other plant species for which the SLs biosynthetic pathway is well-described (**Table 1.6**). The product of D27 catalysis, 9-*cis*-β-carotene, is then cleaved by the CAROTENOID CLEAVAGE DIOXYGENASEs 7 and 8 (CCD7-8). CCDs are a class of non-heme iron-dependent enzymes able to catalyze the selective cleavage of carotenoids through a dioxygenase mechanism (Harrison and Bugg, 2014). CCD7, one of the five CCDs present in all plant species, catalyze the isomerization of the C9-C10 double bond (cleavage) of 9-*cis*-β-carotene (C40) into 9-*cis*-β-apo-10´-carotenal (C27) and β-ionone (C13). The C27 product is further transformed into carlactone (CL) by the action of CCD8 which also has the ability to slowly catalyze the formation of β-apo-13-carotenone (Alder et al., 2012). Unlike D27, CCD7 and CCD8 have been characterized in *A. thaliana* (MAX3, MAX4; Sorefan et al., 2003; Booker et al., 2004), pea (RMS5, RMS1; Alder et al., 2012), petunia (DAD3, DAD1; Snowden et al., 2005; Drummond et al., 2009) and rice (HTD1/D17, D10; **Table 1.6**; Zou et al., 2006; Arite et al., 2007). Interestingly, SLs biosynthetic or signaling mutants from various species were shown to overexpress genes encoding the CCDs, then to recover WT level of genes expression after SL exogenous treatment, suggesting a negative feedback control of these genes by SLs. These genes could, therefore, be used as transcriptional markers of the SLs biosynthetic pathway (Foo et al., 2005; Snowden et al., 2005; Arite et al., 2007; Umehara et al., 2008). At the end of this core biosynthetic pathway, CL already contains a D-ring and the enol-ether bridge typical of SLs and could, therefore, exhibit similar activities as GR24, for example (Alder et al., 2012). The next step of the biosynthetic pathway is considered less conserved and involves the activity of one or more P450s.

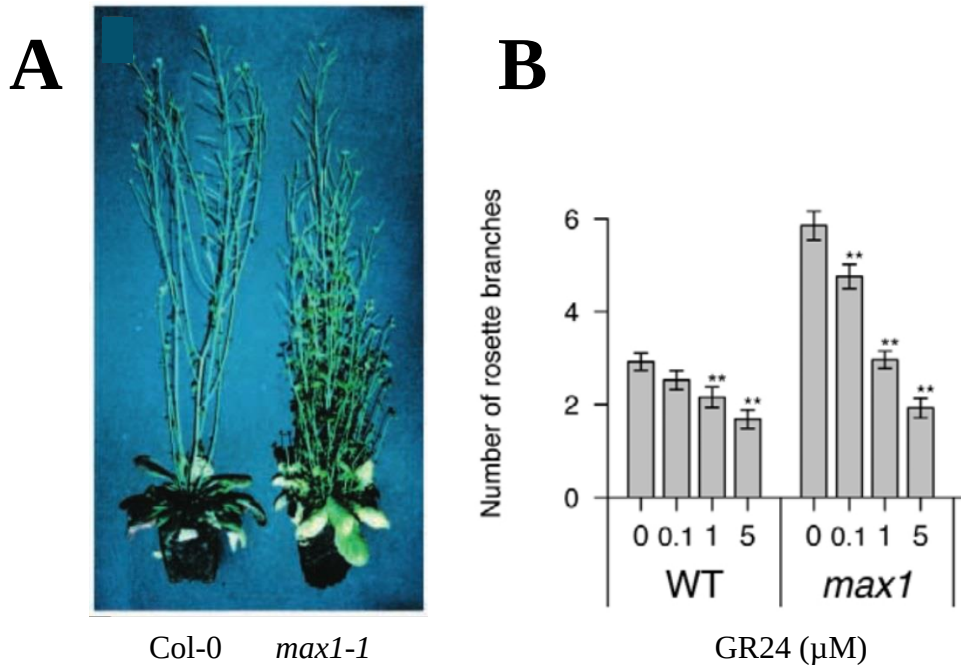

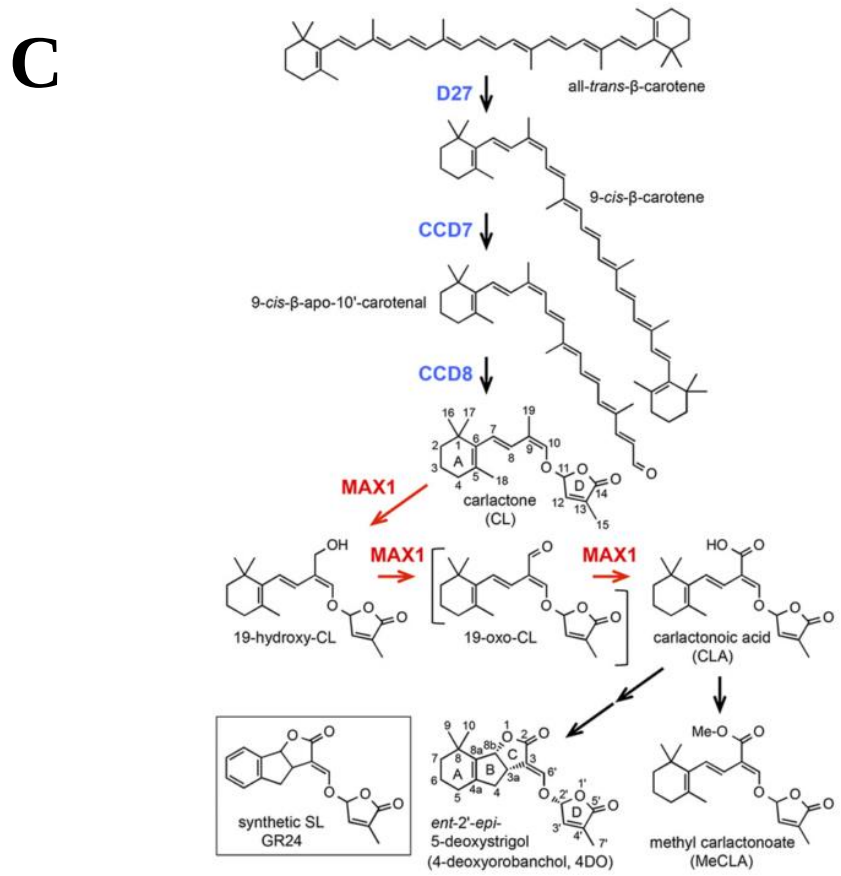

Figure 1.24: Involvement of MAX1 (AtCYP711A1) in the biosynthesis of carlactonoic acid in *A. thaliana*. A, shoot phenotype of the *max1-1* line compared to WT (Col-0; Stirnberg et al., 2002); **B**, Reduction of the number of max1-1 mutant line rosette branches after GR24 treatment (0 to 5 µM) compared to WT (Col-0; Crawford et al., 2010); **C**, Role of MAX1 in SL biosynthesis in *A. thaliana* (Abe et al., 2014).

D.3. CYP711As and SLs diversification

The first evidence of P450 involvement in SL biosynthesis came in 2005 with the functional characterization of *A. thaliana MAX1* gene (Booker et al., 2005). First, MAX1 was shown to act downstream of MAX3 and MAX4 through grafting experiments. Indeed, *max1* rootstock restores the WT branching pattern in *max3* and *max4* shoots, meaning that shoot localized MAX1 can transform a mobile signal from the root into a branching inhibitory factor. *MAX1* was then mapped as *At2g26170* and the corresponding protein finally classified as a P450: CYP711A1. Moreover, the authors used a promoter-GUS reporter construct (*MAX1*::*GUS*) and showed that *MAX1* was predominantly expressed in vascular tissues throughout the plant supporting the hypothesis of an activity of MAX1 on a mobile signal (Booker et al., 2005). The significantly increased shoot branching of the *max1 A. thaliana* mutant (**Figure 1.24A**) has been also shown to be fully rescued after a GR24 treatment of 1 µM, a phenotype associated to all SL-deficient mutants (**Figure 1.24B**; Crawford et al., 2010). Almost ten years after the first characterization, MAX1 was shown to metabolize ^{13}C labelled CL ((*R*)-[1-$^{13}CH_3$]-CL) into an unknown SL-like compound ([^{13}C]-SL-LIKE1) exhibiting an SL characteristic product ion peak at *m/z* ~97 (derived from the D-ring part) in LC-MS/MS analysis (Seto et al., 2014). The same year, the recombinant expression of MAX1 in yeast microsomes finally elucidated the mode of action of MAX1: it catalyzes three consecutive oxidations on CL to successively form 19-hydroxy-CL, 19-oxo-CL and carlactonoic acid (CLA) in which the carboxylic acid is derived from the C-19 methyl group of CL (**Figure 1.24C**). Previously reported SL-LIKE1 was identified as methyl carlactonoate (MeCLA) because of its mass properties. However, ^{13}C labeled carlactonoic acid (CLA) feeding experiment showed that MeCLA derived from CLA in a MAX1 independent manner (Abe et al., 2014).

In parallel to these crucial confirmation steps of MAX1 involvement in SLs biosynthesis in *A. thaliana*, several MAX1 functional homologs in various plant species have been characterized, first, for their ability to rescue the shoot branching phenotype of *Atmax1* mutant line (often *max1-1*; Stirnberg et al., 2002). This is the case for rice Os02g0221900 (OsCYP711A5), Os06g0565100 (OsCYP711A6; Challis et al., 2013), Os01g0701400 (OsCYP711A3) and Os01g0700900 (OsCYP711A2; Cardoso et al., 2014); petunia PhMAX1 (no CYP annotation but highly suspected to belong to the CYP711A subfamily; Drummond et al., 2012), poplar (*Populus trichocarpa*) PtrMAX1a (PtCYP711A8) and PtrMAX1b (PtCYP711A7; Nelson, 2009; Czarnecki et al., 2014), *Selaginella moellendorffii* SmMAX1

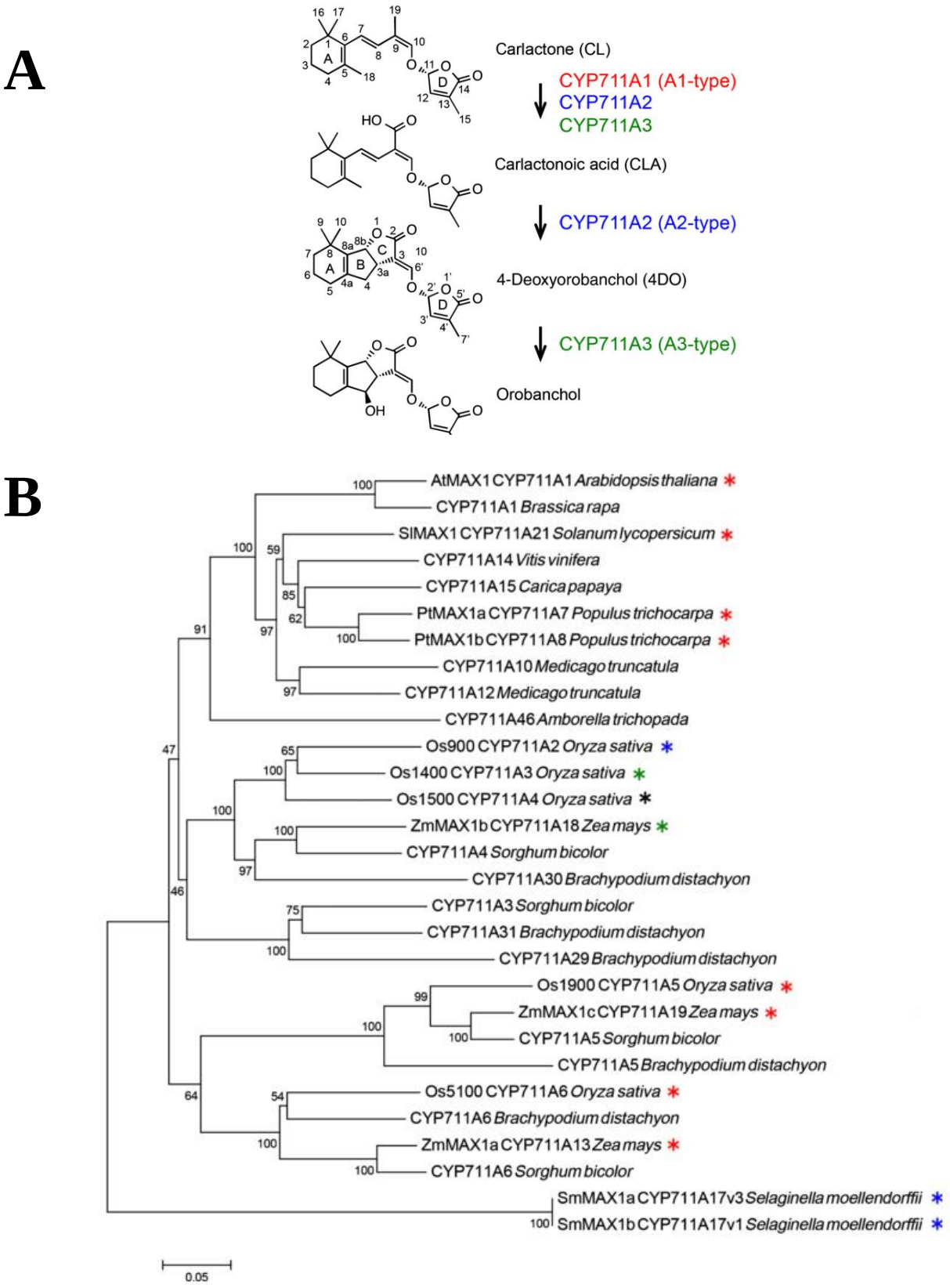

Figure 1.25: MAX1 functional homologs can be divided into three groups depending on their biological activities. A, proposed MAX1s classification using *A. thaliana* (CYP711A1) and rice (CYP711A2 and CYP711A3) as examples. **B**, phylogenetic tree of MAX1 homologs in various species. Stars indicate the type of functionally characterized MAX1 copies: red type 1, blue type 2, green type 3 and black non-functional (Yoneyama et al., 2018; adapted)

(SmCYP711A17, Nelson, 2009; Challis et al., 2013), white spruce (*Picea glauca*) PgMAX1 (identification based on sequence homology with AtMAX1, Challis et al., 2013), *Medicago truncatula* Medtr3g104560 (MtCYP711A12; Nelson, 2009; Challis et al., 2013) and tomato (*Solanum lycopersicum*) SlMAX1 (SlCYP711A21; (Nelson, 2009; Zhang et al., 2018). Interestingly and as previously discussed, these MAX1 functional homologs in various plant species all belong to the CYP711A subfamily, therefore suggesting an ancient specialization of this subfamily conserved across the plant kingdom. Indeed, a first phylogenetical analysis of CYP711As revealed that they are present in angiosperms and conifers but not in the moss *Physcomitrella patens*; hence, this family acquisition which might have occured after Tracheophyta branching (Nelson et al., 2008). This hypothesis was later supported by the identification of a MAX1 functional homolog in *S. moellendorffi* on the basis of vascular plants (Challis et al., 2013). The authors also noticed that most of the vascular plant genomes carry a single CYP711A copy, unlike grasses for which analysis suggest the evolution of three subtypes (divided into 3 copies in maize and 5 copies in rice) likely supporting specialized functions (Nelson et al., 2008). This point has also been investigated by Challis et al. (2013) and led to the same conclusion for a much larger number of monocot species. Furthermore, the authors showed that functional complementation of the *Atmax1* mutant line by several orthologs in other species was unequal depending on the phenotype considered. For example, although both OsCYP711A5 and OsCYP711A6 are able to restore shoot branching of *Atmax1*, OsCYP711A5 failed to rescue all of the leaf phenotypes of the *A. thaliana* mutant line. The authors, therefore, hypothesized on a functional diversity of MAX1 homologs which could explain the structural diversity of SLs (Challis et al., 2013). This was partly confirmed by the functional characterization of two rice copies, OsCYP711A2 shown to catalyze the oxidation of CL into *ent*-2′-*epi*-5-deoxystrigol (also known as 4-deoxyorobanchol, 4DO) and OsCYP711A3 shown to catalyze *ent*-2′-*epi*-5DS transformation in orobanchol (Zhang et al., 2014). Very recently, a new set of CYP711As copies from *A. thaliana*, rice, maize, tomato, poplar and *S. moellendorffi* were biochemically characterized. It revealed the conservation of the CL oxidation function into CLA among CYP711A copies firstly described in *A. thaliana* (Abe et al., 2014), and the additional acquisition of a CLA oxidation in 4DO or 4DO transformation in orobanchol activities by several CYP711A copies. This allowed the authors to propose a classification of MAX1 homologs into three groups: A1-type converting CL to CLA, A2-type converting CL to CLA then CLA to 4DO and A3-type converting CL to CLA and 4DO to orobanchol (**Figure 1.25**; Yoneyama et al., 2018).

Five CYP711A copies are present in *B. distachyon* genome: BdCYP711A5, BdCYP711A6, BdCYP711A30, BdCYP711A31 and, as previously discussed BdCYP711A29 encoded by the *Bradi3g08360*, *Bradi1g37730*, *Bradi4g08970*, *Bradi4g09040* and *Bradi1g75310* genes, respectively (Nelson, 2009). Hence, as for other grasses, *B. distachyon* exhibits several copies of CYP711As compared to the single one present in most of other angiosperms (**Figure 1.25B**). This particular situation might result from a duplication of ancestral *MAX1* copy between the last common ancestor of angiosperms and the last common ancestor of monocotyledons in addition to the complex species-dependent evolutionary history of this P450 subfamily which is well described but less understood (Challis et al., 2013). So far, no study focused on the characterization of *B. distachyon* copies.

D.4. Other partners involved in SLs biosynthesis and signaling

In addition to MAX/RMS/DAD/HTD/D previously described as key enzymes in SLs biosynthesis, another partner from the oxidoreductase family of enzymes has been recently identified in *A. thaliana*. Indeed, *LBO* (*LATERAL BRANCHING OXIDOREDUCTASE*) was screened based on microarray experiments and its expression in *E. coli* followed by incubation of recombinant enzyme with MeCLA led to the production of an unknown SL-like compound (MeCLA + 16 Da) with the characteristic product ion peak at *m/z* ~97 (Brewer et al., 2016). It, therefore, constitutes another clue to explain strigolactone diversity, in particular concerning non-canonical forms of SLs but further studies are needed to precise the function of LBO and the nature and activity of the unknown product.

SLs signaling is not fully characterized but several protein partners have been identified in *A.thaliana* and rice and is based on the same mechanism described for auxin, JA and GA: a Skp1-Cullin-F-box (SCF) E3 ubiquitin ligase complex targets protein substrates, catalyzes their polyubiquitination which leads to their 26S proteasome-dependent degradation (Waters et al., 2017). A significant advance was achieved with the crystallization of this SCF complex in *A. thaliana* (Yao et al., 2016). First, SLs bind the receptor AtD14 which belongs to the α/β-hydrolase superfamily and catalyze the hydrolysis of SL into two parts: the ABC moiety and the D-ring. The conformation of AtD14 changes after SL-binding and allows first, the ABC moiety release and the covalent linkage with the D-ring, then, the recruitment of MAX2, the F-box protein of the SCF^{MAX2} complex and likely SMAX1 (SUPRESSOR OF MAX2 1)/SMXL (SMAX1-LIKE)/D53 protein family members. These last enzymes,

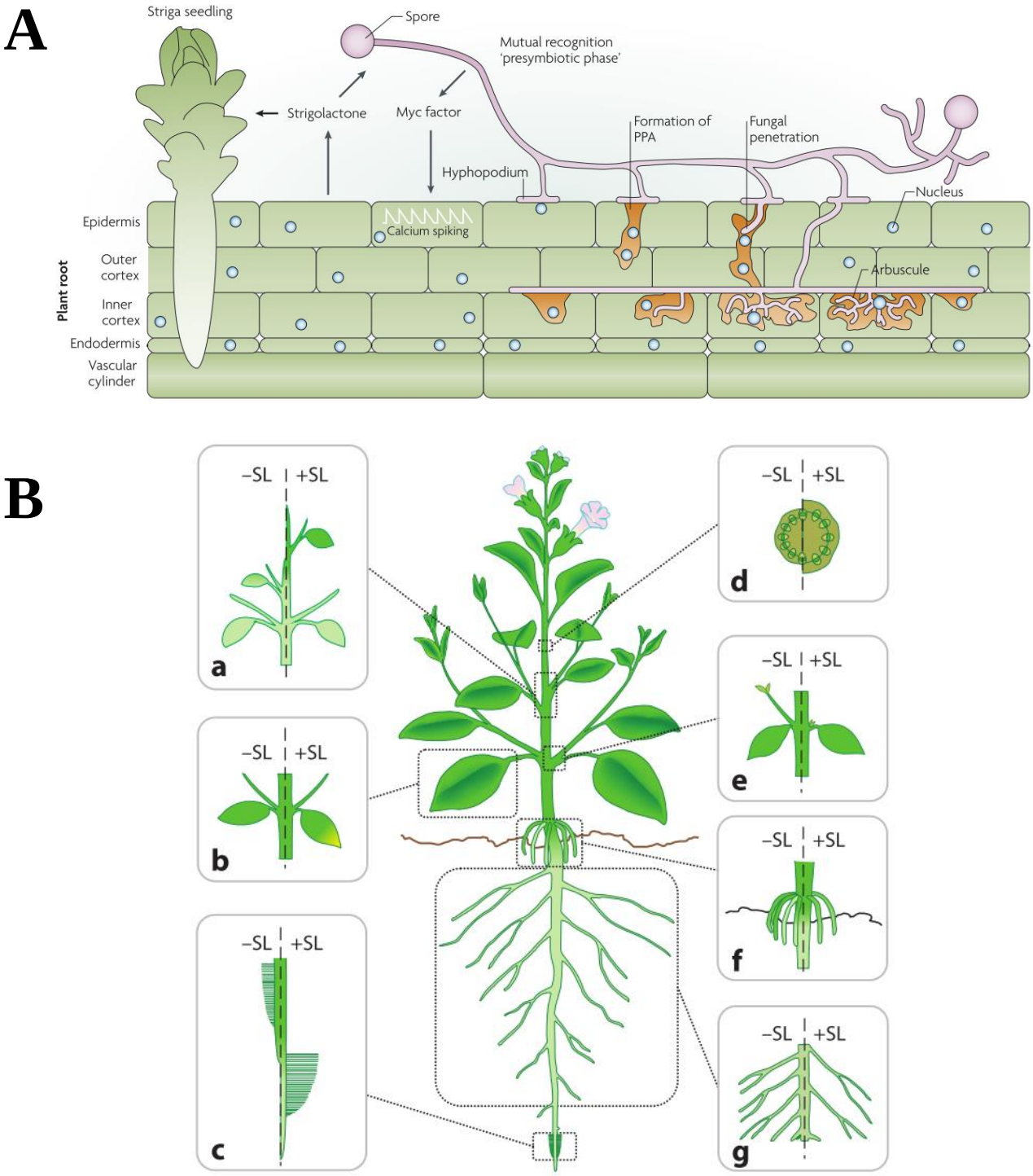

Figure 1.26: Roles of SL in the rhizosphere and in plant development. A, Rizospheric SLs induce seed germination of parasitic weeds and spore germination and hyphal branching of AMF (Parniske, 2008). **B**, Endogenous SLs induce primary shoot growth (a), activate leaf senescence (b), promote primary root and root hair growth (c), induce secondary growth (d), inhibit axillary buds outgrowth (e), inhibit adventious root (f) and lateral root (g) development (Al-Babili and Bouwmeester, 2015).

supposed to be negative transcriptional regulators of SL signaling (Jiang et al., 2013), are then polyubiquitinated and undergo proteasomal degradation (Waters et al., 2017).

D.5. Biological functions of SLs

Historically, that is since 1966, SLs have been associated to the communication between plants and other living organisms such as parasitic weeds and arbuscular mycorrhizal fungi (AMF). Because of their ability to modulate plant development at very low concentrations, they finally have been classified as plant hormones in 2008. Since then, an increasing number of studies focused on SLs in various aspects: crosstalks with other phytohormones, chemical structure and synthesis but also interactions between plant and detrimental microorganisms and others. Before a detailed description of the bibliography on this last point, we will briefly expose in this section the main biological processes involving SLs.

D.5.1. Roles in the rhizosphere

More than 50 years ago, SLs, and more specifically strigol, have been discovered in cotton (*Gossypium hirsutum* L.) root exudates and described as germination stimulants for the root parasitic witchweed *Striga lutea* (Cook et al., 1966). Species from the *Striga* but also *Orobanche, Alectra* and *Phelipanche* genera are a significant threat for worldwide agriculture because they collect some or all their required nutrients from the root of a host plant, including many crops, which often results in important yield losses (Parker, 2009; Al-Babili and Bouwmeester, 2015). Interestingly, various SLs were shown to induce seed germination of several species from these entire parasitic weed genera, with the most important efficiency compared to other rhizospheric plant secondary metabolites also involved in such processes (Cardoso et al., 2011). Although the molecular mechanism which mediates SLs perception and signaling in root parasitic weeds is not fully described, it is now clear that SLs act as molecular clues for parasitic seeds of the presence of a potential host nearby and therefore allow the release of dormancy (**Figure 1.26A**; Cardoso et al., 2011). Current studies on that topic focus on strategies to induce parasitic weed seed germination in the absence of the host (suicidal germination approach) through soil treatments with SLs and SL-like compounds but also on strategies to inhibit seed germination in the presence of the host by limiting/managing SLs exudation by the host (Screpanti et al., 2016).

Because the only biological activity identified for SLs in the rhizosphere was detrimental for plants, it remained unclear during 40 years why plants exude that kind of molecules. The identification of a compound in *Lotus japonicus* root exudate that stimulates arbuscular mycorrhizal fungi (AMF) hyphal branching and its further characterization as 5-deoxystrigol gave a solution to this dilemma (**Figure 1.26A**; Akiyama et al., 2005). AMF are obligate symbiotic microorganisms from the *Glomeromycota* phylum which colonize roots of most of the land plants in order to obtain carbohydrates produced by the photosynthesis, in exchange for phosphate ions, mostly (Schüßler et al., 2001). In addition to promote hyphal branching, SLs were shown to have an impact on mitochondrial activity and density, therefore to affect respiration as well as lipid catabolism of AMF. Given the fact that SLs deficient mutants are poorly able to form a symbiosis with AMF, SLs appear as a key factor in the initiation of mycorrhizas since they are used by fungi to sense a putative host and adapt its metabolism accordingly (Miransari et al., 2014). Because SLs participate in the recruitment of AMF, it has been shown that phosphate starvation is an important factor which promotes SLs synthesis at the transcriptional level and release (Al-Babili and Bouwmeester, 2015). SLs were also shown to promote the interaction between legumes and rhizobia but it concerns endogenous and not exuded SLs (Foo and Davies, 2011).

D.5.2. Roles as plant hormones

In addition to their roles in the rhizosphere as communication molecules, SLs are accepted as plant hormones with numerous developmental effects (**Figure 1.26B**). We already discussed the major phenotype of SLs deficient mutants: a significant increase of shoot branching, but the link between this aberrant developmental phenotype and SLs was only made in 2008. Two concomitant studies showed that highly shoot-branched mutants of pea (Gomez-Roldan et al., 2008) and rice (Umehara et al., 2008) were deficient in SLs and that the shoot phenotype of these lines could be restored through the application of GR24, at micromolar concentrations. Indeed, SLs are now clearly identified as a factor influencing the localization of the auxin export protein PIN1 which mediates auxin gradient and therefore meristems activities (Shinohara et al., 2013), in addition to independently inhibit axillary bud outgrowth (Brewer et al., 2015). Among the other developmental effects of SLs on shoots, we could quote their ability to enhance secondary growth (Agusti et al., 2011), leaf senescence (Snowden et al., 2005) and many others (**Figure 1.26B**; Al-Babili and Bouwmeester, 2015). SLs also mediate belowground architecture of plants mainly through the activation of primary

Table 1.7: Direct effect of SL application on plant pathogen morphology *ex planta*.

Pathogen reign	Trophic lifestyle on host plant	Pathogen species	SLs used in the study	SLs concentrations used in the study	Mode of application of SLs	Results	Reference
Fungus	Biotrophic	*Sporisorium reilianum*	(*rac*)-GR24[a]	10^{-7} M	Embedded in liquid medium	No transition from haploid to solopathogenicity	Sabbagh, 2011
	Hemibiotrophic	*Fusarium oxysporum*	(*rac*)-GR24	10^{-7} M	Microinjection in solid medium	No alteration of the branching pattern	Steinkellner et al., 2007
			(*rac*)-GR24	$3,4.10^{-6}$ to 86.10^{-6} M	Embedded in solid medium	Inhibition of radial fungal growth and increased branching activity	Dor et al., 2011
			(+)-GR24, (-)-GR24, (+)-strigol, (*rac*)-5-deoxystrigol	10^{-7} to 10^{-4} M	Spread on solid medium	No alteration of growth, hyphal branching or spore germination	Foo et al., 2016
		Colletotrichum acutatum	(*rac*)-GR24	$3,4.10^{-6}$ to 86.10^{-6} M	Embedded in solid medium	Inhibition of radial fungal growth and increased branching activity	Dor et al., 2011
	Necrotrophic	*Rhizoctonia solani*	(*rac*)-GR24	10^{-7} M	Microinjection in solid medium	No alteration of the branching pattern	Steinkellner et al., 2007
		Verticillium dahliae	(*rac*)-GR24	10^{-7} M	Microinjection in solid medium	No alteration of the branching pattern	Steinkellner et al., 2007
		Botrytis cinerea	(*rac*)-GR24	10^{-7} M	Microinjection in solid medium	No alteration of the branching pattern	Steinkellner et al., 2007
			(*rac*)-GR24	$3,4.10^{-6}$ to 86.10^{-6} M	Embedded in solid medium	Inhibition of radial fungal growth and increased branching activity	Dor et al., 2011
			(*rac*)-GR24	10^{-8} to 10^{-4} M	Fiberglass discs on medium	No alteration of the growth pattern	Torres-Vera et al., 2014
			(*rac*)-GR24	10^{-8} to 10^{-5} M	Embedded in solid medium	Inhibition of radial fungal growth and increased branching activity	Belmondo et al., 2017
			(-)-*ent*-2'-epi-GR24	10^{-8} to 10^{-5} M	Embedded in solid medium	Inhibition of radial fungal growth	Belmondo et al., 2017
			EGO10	10^{-5} to 10^{-4} M	Embedded in solid medium	Inhibition of radial fungal growth	Belmondo et al., 2017
		Cladosporium sp.	(*rac*)-GR24	10^{-7} M	Microinjection in solid medium	No alteration of the branching pattern	Steinkellner et al., 2007
		Sclerotinia sclerotiorum	(*rac*)-GR24	$3,4.10^{-6}$ to 86.10^{-6} M	Embedded in solid medium	Inhibition of radial fungal growth and increased branching activity	Dor et al., 2011
			(*rac*)-GR24	5.10^{-6} to 50.10^{-5} M	Embedded in solid medium	Inhibition of radial fungal growth	Decker et al., 2017
		Macrophomina phaseolina	(*rac*)-GR24	$3,4.10^{-6}$ to 86.10^{-6} M	Embedded in solid medium	Inhibition of radial fungal growth and decreased branching activity	Dor et al., 2011
		Alternaria alternata	(*rac*)-GR24	$3,4.10^{-6}$ to 86.10^{-6} M	Embedded in solid medium	Inhibition of radial fungal growth and increased branching activity	Dor et al., 2011
		Fusarium solani	(*rac*)-GR24	$3,4.10^{-6}$ to 86.10^{-6} M	Embedded in solid medium	Inhibition of radial fungal growth and increased branching activity	Dor et al., 2011
Oomycete		*Pythium irregulare*	(+)-GR24	10^{-7} to 10^{-4} M	Spread on solid medium	No alteration of growth, hyphal branching or oospore germination	Blake et al., 2016

[a] (*rac*)-GR24 means that authors used a racemic mixture of 2 to 4 stereoisomers of GR24

root development and *via* the inhibition of axillary root formation in a phosphate availability dependent manner (Al-Babili and Bouwmeester, 2015; Sun et al., 2016).

D.6. Roles of SLs in plant interactions with detrimental microorganisms

As discussed before, SLs are involved in the molecular communication between plants and microbes to establish arbuscular mycorrhizal fungi (AMF) symbiosis. Moreover, they act endogenously as a plant hormone to modulate shoot and root architecture, for example. Therefore, it has been proposed that SLs could also play a role in detrimental plant-microbe interactions as other phytohormones shown to impact both endogenous and biotic stress-related mechanisms. Several studies have investigated this hypothesis through various strategies mainly to determine whether SLs could act directly on the pathogen or/and if they are part of the resistance/susceptibility of the host plant metabolism.

D.6.1. Direct impacts of SLs on plant pathogens

One of the well-reported hypotheses is that SLs could act directly on pathogens to promote or inhibit their growth. Indeed, SLs are a class of molecules well-known for their roles *ex planta* because they are widely exuded from the roots. Moreover, not only mycotrophic but also non-mycotrophic plants exude SLs (Yoneyama et al., 2008). It has therefore been proposed that SLs could influence the growth of other rhizospheric microbes such as soil-borne pathogens prior infection of the host plant. The impact of SLs on pathogens infecting organs other than roots has been also studied. All the results discussed below are summarized in **Tables 1.7**-**1.9**.

D.6.1.1. Morphological impacts (**Table 1.7**)

First data on the effect of SLs on the morphology of phytopathogenic fungi were provided in 2007 (Steinkellner et al., 2007). Based on microinjection of (*rac*)-GR24 into Potato Dextrose Agar (PDA) plates (previously described by Nagahashi and Douds, 2000), Steinkellner et al. showed that a 10^{-7} M solution of (*rac*)-GR24 did not influence the branching pattern of soil-borne pathogens (*Rhizoctonia solani*, *Fusarium oxysporum*, *Verticillium dahliae*) nor of pathogens of the aerial plant parts (*Botrytis cinerea* and *Cladosporium sp.*). These results contrast with those obtained on AMF: *Gigaspora margarita* showed an increased hyphal branching in response to synthetic ((*rac*)-GR24) or natural (5-deoxy-strigol, sorgolactone and strigol) strigolactones application (Akiyama et al., 2005).

Therefore, the authors concluded that SLs are specifically involved in communication between AMF and plants but not in other plant-microbe interactions. However, the experimental set-up has been later criticized because of the poor diffusion of GR24 in aqueous agar media due to its lipophilic nature. To ensure homogeneous concentrations of (*rac*)-GR24 in solid media, Dor et al. (2011) proposed to dissolve the mixture directly in hot (60°C) liquid agar media at concentrations ranging from 10^{-5} to 10^{-6} M. Most of the phytopathogenic fungi tested in this study (which included previously tested species, *F. oxysporum* and *B. cinerea*) showed an increased hyphal branching and a decrease in colony size but in various proportion depending on the fungal species (Dor et al., 2011). Hyphal branching in response to (*rac*)-GR24 was the most variable trait from intense to mild and even inhibition of branching but this could not be correlated to the level of inhibition of colony size. Finally, the authors could not make generalizations with respect to the response of soil-borne pathogens versus foliar pathogens or with respect to the phylogenetic relationship between species (Dor et al., 2011). This experiment was also conducted by Belmondo et al. (2017) on *B. cinerea* and *Cryphonectria parasitica* with two different synthetic SLs ((*rac*)-GR24 and (-)-*ent*-2'-epi-GR24) and led to the same results. Similarly, (*rac*)-GR24 inhibited the radial growth of *Sclerotinia sclerotiorum* from 10% at 10^{-5} M up to 50% at 5.10^{-5} M (Decker et al., 2017). Interestingly, contrasting responses of *B. cinerea* after (*rac*)-GR24 application were also observed. Torres-Vera et al. (2014) showed that 10^{-8} to 10^{-4} M (*rac*)-GR24 solutions has no impact on fungal radial growth when applied in fiberglass discs predisposed on PDA plates. Nevertheless, diffusion in agar medium of the active molecule is not ensured in that kind of set-up as previously discussed (Steinkellner et al., 2007). Another mode of application of SLs *ex planta* has been tested on the oomycete *Pythium irregulare* (Blake et al., 2016). Spreading of a solution containing (+)-GR24 onto PDA plates did not influence either radial growth or hyphal branching of *P. irregulare*. The germination rate of oospores was also unchanged in the presence of the synthetic SL compared to control condition (Blake et al., 2016). This method has been also used by Foo et al. (2016) on *F. oxysporum* which did not present any alteration of hyphal growth or branching and spore germination after various SL treatments. These data are consistent with those obtained after microinjection of (*rac*)-GR24 into the medium (Steinkellner et al., 2007), but are in disagreement with those obtained after dilution of the synthetic SL into the warm liquid agar medium (Dor et al., 2011; Belmondo et al., 2017). Other SLs-induced morphological changes than colony size and hyphal branching have been investigated on the solopathogenic strain of *Sporisorium reilianum* f.sp *zeae*. No transition from haploid saprophytic sporidial stage to

Table 1.8: Direct effect of SL application on plant pathogen physiology *ex planta.*

Pathogen reign	Trophic lifestyle on host plant	Pathogen species	SLs used in the study	SLs concentrations used in the study	Mode of application of SLs	Results	Reference
Fungus	Biotrophic	*Ustilago maydis*	(*rac*)-GR24[a]	10^{-15} to 10^{-5} M	Embedded in liquid medium	Increase until 10^{-7} M and decrease of cell respiration at 10^{-5} M	Sabbagh, 2008; Mazaheri-Naeini et al., 2015
		Sporisorium reilianum	(*rac*)-GR24	10^{-7} M	Embedded in liquid medium	Increase of cell respiration	Sabbagh, 2011; Sabbagh et al., 2012
	Hemibiotrophic	*Fusarium oxysporum*	(*rac*)-GR24, (*rac*)-5-deoxystrigol, (*rac*)-4-deoxyorobanchol, (+)-strigol	10^{-7} M	Embedded in liquid medium	Significant reduction of SL content in fungal culture	Boari et al., 2016
	Necrotrophic	*Botrytis cinerea*	(*rac*)-GR24	10^{-5} M	Embedded in liquid medium	Oxidizing effect in mitochondria	Belmondo et al., 2016
			(*rac*)-GR24, (*rac*)-5-deoxystrigol, (*rac*)-4-deoxyorobanchol, (+)-strigol	10^{-7} M	Embedded in liquid medium	Significant reduction of SL content in fungal culture	Boari et al., 2016
		Fusarium solani	(*rac*)-GR24, (*rac*)-5-deoxystrigol, (*rac*)-4-deoxyorobanchol, (+)-strigol	10^{-7} M	Embedded in liquid medium	Significant reduction of SL content in fungal culture	Boari et al., 2016

[a] (*rac*)-GR24 means that authors used a racemic mixture of 2 to 4 stereoisomers of GR24

diploid parasitic hyphae, the typical trait of solopathogenic strain, has been observed in (*rac*)-GR24 containing liquid medium (Sabbagh, 2011). Despite the fact that fractions from maize root exudates could induce yeast-hypha transition (Martinez et al., 2001), it appeared that SLs might not be involved in this morphological adaptation. Finally, not any single phytopathogenic bacterial strain has been reported for being tested in that kind of *ex planta* experiment.

Two main conclusions emerge from these data: the sensitivity of plant pathogens to SLs and their morphological adaptation depend both on the pathogen species and on experimental conditions. Microbe behavior changes after SL treatment observed in several independent experiments is indeed a clue to hypothesize that, as AMF or rhizobium, plant microbial pathogens could perceive and morphologically react to the presence of SLs in their environment. Furthermore, this might be the output of a very complex evolutionary history since no clear correlation exists between phylogenic relationship and/or lifestyle and response to SLs between pathogens. The inconsistency of these biological results might also result from heterogeneity of SLs modes of application, thus constituting one of the main limits in *ex planta* experiments. Indeed, chemical properties of synthetic and natural strigolactones make them hard to manage in a biological experiment as mentioned earlier (see **section D.1.**). These limits should also be carefully considered when studies focus on other levels of changes in plant-pathogen interactions following SLs treatment *ex planta*.

D.6.1.1. Physiological impacts (**Table 1.8**)

Modifications at the physiological level of phytopathogenic microbes in response to SLs application were also investigated. In detail, it has been first reported that a 10^{-7} M solution of (*rac*)-GR24 induces a cell respiration burst in the solopathogenic strain of *S. reilianum* which reaches +13% of redox potential 1 hour after treatment (Sabbagh, 2011; Sabbagh et al., 2012). Equivalent results were observed with the closely related biotrophic fungus *Ustilago maydis* (Sabbagh, 2008; Mazaheri-Naeini et al., 2015). On the contrary, a higher concentration (10^{-5} M) seems to inhibit cell redox potential also in *U. maydis* (Mazaheri-Naeini et al., 2015). More recently in order to identify genes involved in responses to SLs, Belmondo et al. (2017) performed a screening of *B cinerea* mutants which do not present any alteration of radial fungal growth after treatment with (*rac*)-GR24. Two mutant strains where shown to be less sensitive to SLs compared to the wild-type strain B05.10: Δ*bcltf1*, knocked-out in the *BcLTF1* gene encoding a light-responsive transcription factor of

Table 1.9: Direct effect of SL application on plant pathogen transcriptome *ex planta*.

Pathogen reign	Trophic lifestyle on host plant	Pathogen species	SLs used in the study	SLs concentrations used in the study	Mode of application of SLs	Results	Reference
Fungus	Biotrophic	*Ustilago maydis*	(*rac*)-GR24[a]	10^{-15} to 10^{-5} M	Embedded in liquid medium	Induction of genes involved in cell respiration	Sabbagh, 2008; Mazaheri-Naeini et al., 2015
		Sporisorium reilianum	(*rac*)-GR24	10^{-7} M	Embedded in liquid medium	Induction of genes involved in cell respiration	Sabbagh, 2011; Sabbagh et al., 2012

[a] (*rac*)-GR24 means that authors used a racemic mixture of 2 to 4 stereoisomers of GR24

the GATA family (Schumacher et al., 2014) and Δ*bctrr1* a knock-out mutant for *BcTrr1*, a thioredoxin reductase encoding gene (Viefhues et al., 2014). Both mutants present an altered Reactive Oxygen Species (ROS) homeostasis with hypersensitivity to oxidative stress and increased production of hydrogen peroxide (Schumacher et al., 2014; Viefhues et al., 2014). Therefore, the authors tested whether the redox status of *B. cinerea* could be modulated after SLs treatment. Using the redox-sensitive GFP (roGFP2), they found that (*rac*)-GR24 exposure leads to a slight oxidizing effect in mitochondria of the wild-type strain of *B. cinerea* which was reduced in Δ*bcltf1*. In spite of limited data on physiological adaptations of plant pathogens towards SLs treatments, it is interesting to notice that (*rac*)-GR24 induces a respiration burst in biotrophic and necrotrophic plant pathogenic fungi in a similar manner as in AMF *Gigaspora rosea* (Besserer et al., 2006) or *G. margarita* (Salvioli et al., 2016). In an interesting way, these observations are supported by transcriptomic data.

In a roundabout way and in order to develop new strategies suitable for parasitic weed management, three phytopathogenic fungal strains were tested for their ability to metabolize SLs (Boari et al., 2016). Interestingly, 2 soil-borne fungi (*F. oxysporum* and *F. solani*) and one pathogen of the aerial part of plants (*B. cinerea*) were shown to actively reduce the SL content (from 37.5 to 57.6% depending on the fungal strain) in fungal cultures supplemented with different SLs. These very interesting results support the hypothesis that fungi other than AMF could detect then metabolize SLs *in vivo*. Indeed the authors showed that the decrease in SLs content is the result of a true cellular catabolism within the fungal mycelium rather than an *ex vivo* degradation by secreted enzymes or a natural degradation in the medium (Boari et al., 2016). Further studies are needed to identify degradation products and to confirm these data.

D.6.1.1. Transcriptomic impacts (**Table 1.9**)

In parallel with studies of physiological changes in *S. reilianum* and *U. maydis* after SLs treatment, transcriptional modifications were also investigated (Sabbagh, 2008; Sabbagh, 2011; Sabbagh et al., 2012; Mazaheri-Naeini et al., 2015). Twenty genes from the haploid strain of *S. reilianum* were shown to be significantly induced 1 h after treatment with (*rac*)-GR24 both in microarray and RT-qPCR experiments (Sabbagh et al., 2012). Gene ontology revealed that 5 of these genes are encoding enzymes involved in cell respiration: 2 succinate dehydrogenases/fumarate reductases, 1 cytochrome-c oxidase, 1 isocitrate dehydrogenase and 1 NAD/FAD-utilizing enzyme which is consistent with the respiration burst observed and

Table 1.10: Roles of SLs in plant response against biotic stress.

Pathogen reign	Trophic lifestyle on host plant	Pathogen species	Plant species	Plant genotype	SLs studied	Experimental set-up	Results	Reference
Virus	Biotrophic	*Rice grassy stunt virus*	Rice (*Oryza sativa*)	WT (Nipponbare)	focus on 2'-*epi*-5-deoxystrigol	Infection followed by gene expression and metabolic analyzes	RGSV suppress SLs synthesis and signaling	Satoh et al., 2013
Bacteria	Biotrophic	*Rhodococcus fascians*	*Arabidopsis thaliana*	WT (Col-0), *max1-1*, *max2-1*, *max3-9*, *max4-1*, *brc1-2*	naturals (*in planta*), (*rac*)-GR24	Infection followed by gene expression and chemical treatments analyzes	SLs-related mutans are more susceptible to *Rf* than WT in a SLs-dependent manner. SLs biosynthetic genes are transcriptionally induced during the interaction in a bacterial-CKs and a plant-auxin depedant manner	Stes et al., 2015
Bacteria	Hemibiotrophic	*Pectobacterium carotovorum*	*Arabidopsis thaliana*	WT (Col-0), *max2-1*, *max2-4*	naturals (*in planta*)	Characterization of *max2* mutant lines (ROS, stomatal conductance), infection followed by gene expression and metabolic analyzes	*max2* is more susceptible to *Pc* because of increased stomatal conductance, decreased tolerance to ROS and dysregulation of auxin signaling	Piisilä et al., 2015
Fungus	Hemibiotrophic	*Pseudomonas synrigae*	*Arabidopsis thaliana*	WT (Col-0), *max2-1*, *max2-4*	naturals (*in planta*)	Characterization of *max2* mutant lines (ROS, stomatal conductance), infection followed by gene expression and metabolic analyzes	*max2* is more susceptible to *Ps* because of increased stomatal conductance, decreased tolerance to ROS and dysregulation of auxin signaling	Piisilä et al., 2015
Fungus	Hemibiotrophic	*Fusarium oxysporum*	*Physcomitrella patens*	WT (Grandsden 2004), Δ*CCD7*, Δ*CCD8*	naturals (*in planta*), (*rac*)-GR24	Infection followed by (*rac*)-GR24 treatment	Δ*CCD7* and Δ*CCD8* are more susceptible to *Fo* compared to WT	Decker et al., 2017
			Pisum sativum L.	WT (Parvus), *ccd8-1* (*rms1-1*)	naturals (in planta)	Infection followed by observation of symptoms	*ccd8-1* does not exhibits defferential symptoms in comparision with WT	Foo et al., 2016
Fungus	Hemibiotrophic	*Fusarium avenaceum*	*Physcomitrella patens*	WT (Grandsden 2004), Δ*CCD7*, Δ*CCD8*	naturals (*in planta*), (*rac*)-GR24	Infection followed by (*rac*)-GR24 treatment	Δ*CCD7* and Δ*CCD8* are more susceptible to *Fa* compared to WT	Decker et al., 2017
Fungus	Necrotrophic	*Sclerotinia sclerotorium*	*Physcomitrella patens*	WT (Grandsden 2004), Δ*CCD7*, Δ*CCD8*	naturals (*in planta*), (*rac*)-GR24	Infection followed by (*rac*)-GR24 treatment	Δ*CCD7* and Δ*CCD8* are more susceptible to *Ss*compared to WT ; same level of resistance as WT could be restored by adding 1 µM (*rac*)-GR24	Decker et al., 2017
Fungus	Necrotrophic	*Botrytis cinerea*	Tomato (*Solanum lycopersicum* L.)	WT (Craigella), *Slccd8* L09	naturals (*in planta*)	Infection followed by gene expression and metabolic analyzes	*Slccd8* is more susceptible to *Bc* than WT because of misregulation of phytohormones homeostasis (especially JA)	Torres-Vera et al., 2014
Fungus	Necrotrophic	*Alternaria alternata*	Tomato (*Solanum lycopersicum* L.)	WT (Craigella), *Slccd8* L09	naturals (*in planta*)	Infection followed by gene expression and metabolic analyzes	*Slccd8* is more susceptible to *Aa* than WT because of misregulation of phytohormones homeostasis (especially JA)	Torres-Vera et al., 2014
Oomycete	Necrotrophic	*Pythium irregulare*	*Pisum sativum* L.	WT (Parvus and Torsdag), *ccd8-1* (*rms1-1*), *ccd8-2* (*rms1-2*T), *ccd7* (*rms5-3*T) *Psf-box* (*rms4-1*)	naturals (*in planta*)	Infection followed by observation of symptoms and gene expression analyzes	All mutants displays similar symtpoms compared to WT ; slight increase of *PsCCD8* expression after *Pi* infection	Blake et al., 2016
Fungus	Opportunictic (saprophytic)	*Apiospora montagnei*	*Physcomitrella patens*	WT (Grandsden 2004), Δ*CCD7*, Δ*CCD8*	naturals (*in planta*), (*rac*)-GR24	Infection followed by (*rac*)-GR24 treatment	Δ*CCD7* and Δ*CCD8* are more susceptible to *Am* compared to WT	Decker et al., 2017
Fungus	Opportunictic (saprophytic)	*Irpex* sp.	*Physcomitrella patens*	WT (Grandsden 2004), Δ*CCD7*, Δ*CCD8*	naturals (*in planta*), (*rac*)-GR24	Infection followed by (*rac*)-GR24 treatment	Δ*CCD7* and Δ*CCD8* are more susceptible to *I* sp. compared to WT	Decker et al., 2017

discussed earlier. Several genes involved in amino-acid and carbohydrate metabolism were also up-regulated (Sabbagh et al., 2012). Similar responses were observed in *U. maydis* (Sabbagh, 2008). Nevertheless, it is not clear whether SLs act as a global metabolism activator and promote infection of root plant or on the contrary if the oxidative burst is an illustration of a fungal stress and therefore the consequence of a plant defense mechanism.

To conclude on direct impacts of SLs on plant-pathogens, it is still very difficult to draw a clear model from perception to adaptation. The lack of a common and reproducible experimental set-up prevents us to conclude that all or only some of the plant pathogens are able to perceive SLs. Because of the heat sensitivity and lipophilic nature of natural and synthetic SLs, this aspect should be studied in liquid conditions to ensure good diffusion while maintaining a good stability of active molecules. Further studies should focus on the impact of SLs *in planta* in plant-pathogen interactions which allows the evaluation of all natural SLs and not only synthesizable ones (natural or synthetic) but also all the molecular partners involved in these processes which might include other phytohormones, plant and pathogen secondary metabolites, ROS and others.

D.6.2. Roles of SLs in plant responses against biotic stress

Several studies aimed to determine whether SLs are involved in the plant defense system against biotic stress. Results of these experiments have been summarized in **Table 1.10**. The first elements supporting the hypothesis of a strigolactone involvement in plant defense responses were observed in rice (Satoh et al., 2013). Following infection by the Rice grassy stunt virus (RGSV), Satoh et al. reported a transcriptional repression of strigolactone biosynthetic (D17/HTD1) and signaling (D14/HTD2 and D3) genes in RGSV-infected plants. Moreover, the amount of exuded 2'-epi-5-deoxystrigol was reduced in infected plants. Therefore, the authors suggested that excess tillering specifically associated with RGSV infection of rice could be partially related to the deregulation of SLs homeostasis (Satoh et al., 2013). Nevertheless, there is no clue about which organism in the interaction is responsible for this dysregulation and thus, if it is part of a defense mechanism of the host plant or if it is a pathway diverted by the pathogen. More recent studies have subsequently attempted to answer this question.

D.6.2.1. SLs are important players in some plant-pathogen interactions…

Most of the subsequent studies took advantage of the availability of SLs deficient mutant lines of several species. Torres-Vera et al. (2014) firstly used the *Slccd8* mutant of tomato, which exhibits a 95% reduction in SLs content (Kohlen et al., 2012) to perform disease bioassays using two necrotophic pathogens: *B. cinerea* and *A. alternata*. Detached leaves of the SL-deficient tomato line *Slccd8* exhibited more severe symptoms than the WT line whatever the inoculum used (germinating spores or growing hyphae). Moreover, metabolic and gene expression analyses revealed a strong deregulation of phytohormones homeostasis in the mutant line compared to the WT line with a significant reduction of JA, SA and ABA content and an inhibition of expression of the *Proteinase inhibitor II* (*PinII*) gene, a marker for the JA-signaling pathway. Therefore, the authors concluded that the increased susceptibility of *Slccd8* to necrotrophic fungi might be due to SL-dependent misregulation of phytohormones signaling pathways, especially of JA which is well known for its role in defense against necrotrophic pathogens (Pieterse et al., 2009). An increased susceptibility of *Arabidopsis thaliana* mutant lines altered in strigolactone biosynthetic (*max1-1*, *max3-9* and *max4-1*) and signaling (*max2-1*, *brc1-2*) genes towards *Rhodoccocus fascians* was also reported (Stes et al., 2015). This biotrophic actinomycete is the causal agent of leafy gall syndrome of dicotyledonous herbs inducing multiple shoots partly due to its ability to secrete CKs which are essential for its pathogenicity (Stes et al., 2013). Interestingly, Col-0 sensitivity to *R. fascians* was almost completely prevented when 1 µM (*rac*)-GR24 was added to the medium. Conversely, 1 µM D2, an inhibitor of MAX3 and MAX4 activity, significantly increased the susceptibility of WT plants to the pathogen. It was therefore concluded that the hypersensitivity of strigolactones mutants is directly dependent on the reduced strigolactone levels (Stes et al., 2015). Molecular analysis revealed that *R. fascians* infection led to an increase of the expression of strigolactone biosynthesis genes at the outset of the interaction followed by a sustainable induction of *BRC1*. This transcriptional activation of the SLs pathway was shown to be due to the release of bacterial CKs followed by the activation of plant auxin synthesis which was already known to transcriptionally induce *MAX3* and *MAX4* gene expression in *A. thaliana* (Hayward et al., 2009). The *A. thaliana max2-1* mutant line (together with *max2-4*) has also been used in the interaction with bacterial phytopathogens *Pseudomonas syringae* and *Pectobacterium carotovorum* (Piisilä et al., 2015). In both cases, the SL-insensitive mutant line was more susceptible than the WT line

mainly because of increased stomatal aperture, decreased tolerance to apoplastic stress-induced ROS and auxin-dependent defense response dysregulation. Nevertheless, MAX2 has been also shown to be essential in karrikins signaling, a class of smoke-derived compounds, (Nelson et al., 2011) and therefore should be considered as a very particular member of the strigolactone signaling pathway with distinct properties rather than a highly specific marker. Interestingly, *max2-1* line does not show differential susceptibility towards *B. cinerea* compared to WT (Piisilä et al., 2015). However, this line exhibits developmental phenotypes such as elongated hypocotyls or longer juvenile leaves petioles (Stirnberg et al., 2002) and specific long day growth conditions seem to induce reduced leaf area (our study). It is therefore often complicated to estimate the true role of the alteration of SLs production or perception due to developmental phenotypes of the mutant lines. SLs involvement has also been studied in the interaction between pathogens and non-angiosperm plants. Indeed, *Physcomitrella patens* mutant lines Δ*CCD7* and Δ*CCD8* exhibited an increased susceptibility towards several fungal pathogens (*Apiospora montagnei*, *Fusarium avenaceum*, *F. oxysporum*, *Irpex* sp. and *S. sclerotiorum*; Decker et al., 2017). Moreover, the application of 1 µM (*rac*)-GR24 in the growth medium could restore the resistance of mutant lines and increase that of the WT. Because higher concentrations are needed to inhibit fungal growth as discussed before (see **section D.6.1.1.**, **Table 1.7**), the authors concluded that complementation of the mutant lines phenotype towards *S. sclerotiorum* infection by (*rac*)-GR24 application is caused by increased plant resistance rather than by a direct impact of the synthetic SL on fungal growth (Decker et al., 2017).

D.6.2.2. … but not in others

Unlike previous studies underlying a putative positive role of SLs in plant defense against various pathogens, two studies have highlighted that they would not be involved in other pathosystems. Indeed, Foo et al. (2016) showed that SL-deficient pea mutant *ccd8-1* (*rms1-1*) do not present any difference or susceptibility upon *F. oxysporum* infection as compared with the WT line. Similar results were obtained in the interaction between pea and the oomycete *P. irregulare* (Blake et al., 2016). Both SL-deficient (*ccd7* and *ccd8*) and -insensitive (*f-box*) mutants exhibit similar symptoms as seen for WT plants. A slight but significant increase of transcription of *PsCCD7* 24 h post-infection of the WT line has been detected but no difference in fabacyl acetate and orobanchyl acetate content has been

observed in root tissues between control and *P. irregulare* inoculated plants (Blake et al., 2016).

The *in silico* analysis of *cis*-regulatory elements present in the promoters of genes belonging to the RMS/MAX/D pathway of rice and *Arabidopsis* showed up the presence of many binding sites for transcription factors involved in the response to biotic stress (Marzec and Muszynska, 2015). However, as observed for the direct impact of SLs on plant pathogens discussed in **section D.6.1.**, it appears tricky to draw a general paradigm of SLs involvement in plant defense against biotic stress. Firstly, SL-deficient mutants exhibit different phenotypes depending on the pathosystem from increased (*e.g.* Torres-Vera et al., 2014; Decker et al., 2017) to equivalent (Blake et al., 2016; Foo et al., 2016) susceptibility compared to WT lines. The same conclusion could be made with respect to SL-insensitive mutants showing lower (Piisilä et al., 2015; Stes et al., 2015) to similar (Blake et al., 2016) level of resistance compared to WT. On top of that, no clear correlation could be observed with respect to the pathogenic microorganism taxonomy or with respect to its trophic lifestyle on the host plant. Even the pathogen species does not seem sufficient to predict its behavior when it colonizes SL-mutants from different plant species as illustrated by *F. oxysporum* pathogenicity on *P. patens* compared to *P. sativum* L. (Foo et al., 2016; Decker et al., 2017). It is interesting to notice that, however, not any study presented SLs as factors involved in the susceptibility and therefore, as potential targets for a pathogen to manipulate the host plant metabolism and promote its development. Secondly, studies supporting the hypothesis of a positive role of SLs in plant defense against pathogenic microorganisms do not provide a perspicuous explanation about the direct or indirect role and mode of action of these hormones. Cross-talks with other phytohormones might be involved, for example with JA and CKs, but we lack information on the level of pathosystem specificity and requirement of these molecular communication processes *in planta* to ensure resistance against pathogenic microorganisms. However, it is now established that SLs are involved in the interaction between plants and detrimental microorganisms but in a much lesser conserved way as compared with their role in communication with AMF or rhizobia. Only an empirical vision on this topic will provide helpful tools to transfer in agricultural practices.

E. OBJECTIVES OF THE PH.D. WORK

The team 'Functional genomics of cereals-pathogen interactions', which hosted my research, uses the model cereal *B. distachyon* to identify genetic resistance towards *F. graminearum* and translate this knowledge to cultivated cereals. It allowed, for example, the identification of a UGT, Bradi5g03300, able to efficiently and precociously metabolize (detoxify) the main mycotoxin produced by *F. graminearum*, DON, and this was positively correlated to the quantitative resistance of *B. distachyon* towards the disease (Pasquet, 2014; Pasquet et al., 2016). Recently, this work was transferred and allowed the screening of the Bradi5g03300 ortholog in wheat, which presents similar activities against DON and also confers resistance to FHB (**section B.5.1.**; Gatti, 2017). During my Ph.D. project, we also wanted to benefit from *B. distachyon* advantages to identify other plant genetic factors involved in the interaction with *F. graminearum*. As presented earlier, we decided to focus on cytochrome P450s for two main reasons: first, we dispose of plant transcriptomic data in response to several conditions (infections with different *F. graminearum* strains and treatment with the mycotoxin, **section C.4.**), second, P450s are known to be involved in a very large amount of metabolic pathways which are all potential factors of resistance (**section C.3.**). The results of the Ph.D. work are presented in **Chapter II** to **IV**. In a first part (**Chapter II**), we present the screening of our gene of interest, *Bradi1g75310*, which exhibits an almost singular expression profile during the interaction. We also present the screening/generation and molecular characterization of *B. distachyon* lines affected in *Bradi1g75310* expression as well as their behavior in response to *F. graminearum* infection or DON treatment. Because BdCYP711A29 belongs to the same subfamily as several P450s involved in SLs biosynthesis in different plant species (**section D.3.**), we focused in a second step on the characterization of the putative functional homology between *Bradi1g75310* and these P450s (**Chapter III**). In the same perspective, we propose the same analysis on *Bradi1g75310 B. distachyon* relatives which also belong to CYP711A subfamily. This work has been performed through a phylogenetic analysis, the functional complementation of the shoot phenotype of *A. thaliana max1-1* mutant line by the four other isoforms and finally, the use of metabolomic equipment to characterize and quantify exuded SLs of several *B. distachyon* lines. In the last part, we propose a preliminary analysis of the involvement of SLs in the interaction between *B. distachyon* and *F. graminearum* focused on the direct impact of SLs on *F. graminearum* growth and on the transcriptional profile of plant genes involved in defense towards pathogens (**Chapter IV**). All the results presented in Chapter II to IV are discussed in

Chapter V which also proposes several perspectives on the future work. The last chapter (**Chapter VI**) lists all the experimental procedures used in this study.

CHAPTER II | RESULTS (1/3)

Involvement of the *Bradi1g75310* gene in the interaction between *B. distachyon* and *F. graminearum*

A. INTRODUCTION

As described in the introduction (**Chapter I, Section B.4.4.4.**), plant genetic resistance towards FHB is quantitative and determined by a growing number of QTLs (Buerstmayr et al., 2009; Gilbert and Haber, 2013). Since genetic resistance appeared as the most cost-effective FHB management strategy (Wegulo et al., 2015), a strong effort has been employed into the functional characterization of the plant genetic factors involved in the interaction between cereals and *F. graminearum*. Because of their biochemical properties, we propose to study the involvement of a specific class of enzymes, cytochrome P450s, in the FHB context. Indeed, this superfamily of enzymes is known to catalyze extremely diverse biochemical reactions and to metabolize both endo- and exogenous substrates (**Chapter I, Section C.3.**; Bak et al., 2011). Moreover, several transcriptomic studies reported the transcriptional activation of wheat, barley and *B. distachyon* P450s in response to the infection by the fungal pathogen *F. graminearum* and/or in response to DON treatment (**Chapter I, section C.4.**). Nevertheless, only one DON/FHB-induced copy from wheat (*CYP709C1*) has been functionally characterized as a fatty acid hydroxylase even if its physiological role during FHB remains unclear (Li et al., 2010; Pinot and Beisson, 2011). Altogether, these characteristics make P450s a promising open field of investigation, especially in the FHB context.

The objective of this first part was to perform a screening of the *B. distachyon* P450 encoding genes in order to identify the FHB- and DON-responsive copies. Based on a transcriptomic study, we were able to focus our attention on the BdCYP711A29-encoding *Bradi1g75310* gene. We initiated the functional characterization of this gene through the production of *B. distachyon* lines which overexpress the gene of interest and *via* the selection of TILLING mutant lines. Because TCTBs detoxification is one of the most efficient and characterized genetic resistance mechanisms (**Chapter I, Section B.5.1.**) and because P450s are known to be involved in the activation step of xenobiotic detoxification (**Chapter I, Section C.3.2.1.**), we first tested whether the *Bradi1g75310* gene is involved in DON tolerance or sensitivity in *B. distachyon*. We finally performed pathogenicity assays on our different lines of *B. distachyon* with altered *Bradi1g75310* expression/gene sequence using a toxin-producing strain of *F. graminearum* in order to determine the degree of involvement of our gene of interest in FHB. As for the two next chapters, the results are described in the first three parts as texts and figures, and conclusions are made in the final section of this chapter.

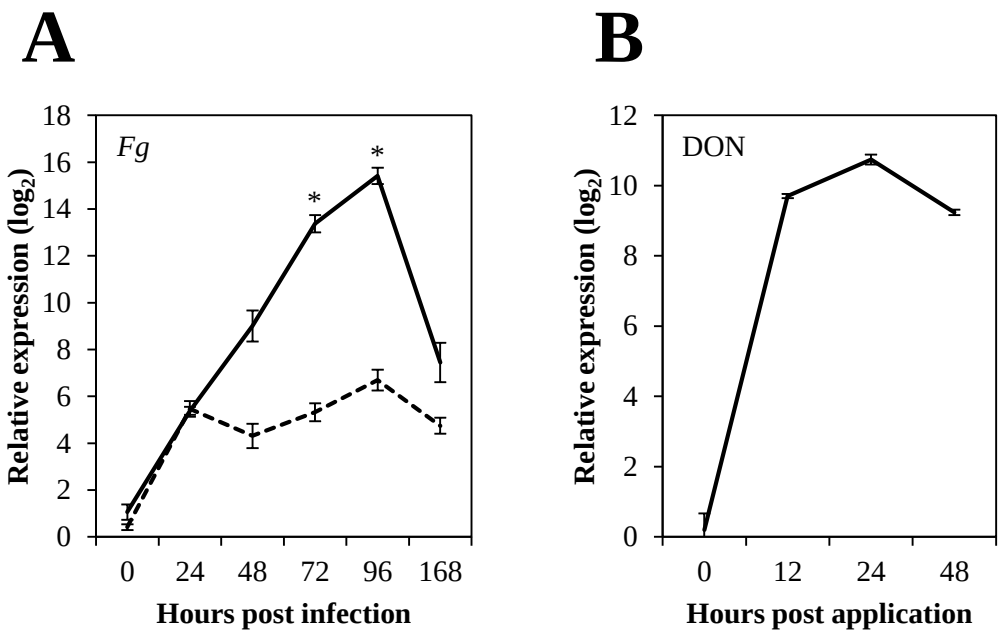

Figure 2.1: The *Bradi1g75310* gene is transcriptionally induced during FHB and following DON treatment. Relative quantification of the *Bradi1g75310* expression level in the Bd21-3 (WT) ecotype of *B. distachyon* following *F. graminearum* infections or following DON treatment. **A**, *Bradi1g75310* expression level (fold-change, $\log_2$) following point infection with the Fg^{DON+} (solid line) or with the Fg^{DON-} (dashed line) strain of *F. graminearum* compared to mock treatment. **B**, *Bradi1g75310* expression level (fold-change, $\log_2$) following DON treatment compared to mock treatment. The relative quantity of *Bradi1g75310* gene transcripts compared to mock condition was calculated using the comparative cycle threshold (Ct) method ($2^{-\Delta\Delta Ct}$). The *B. distachyon UBC18* and *ACT7* genes (*Bradi4g00660* and *Bradi4g41850*) were used as endogenous controls to normalize the data for differences in input RNA between the different samples. Mean of three independent biological replicates ± standard deviation. Asterisks indicate significant differences between conditions, Student test, $P < 0.05$.

B. SCREENING AND FUNCTIONAL VALIDATION OF THE *B. DISTACHYON BRADI1G75310* GENE

B.1. *Bradi1g75310* is transcriptionally activated during FHB

In order to identify a plant P450 encoding gene involved in the interaction between *B. distachyon* and *F. graminearum*, we focused our attention on transcriptomic data obtained by the host team before the beginning of this project and described by Pasquet et al. (2014) and Pasquet (2014; **Chapter I, section C.4.**). These studies allowed the identification of *B. distachyon* wild-type line (Bd21-3) differentially expressed genes (DEGs) in three different conditions: (1) 96 h after the point inoculation of *B. distachyon* spikes with a toxin-producing strain of *F. graminearum* (Fg^{DON+}; PH-1; Goswami and Kistler, 2004) compared to mock treatment (application of 0.01% Tween 20); (2) 96 h after a similar infection but with a toxin non-producing strain (Fg^{DON-}; PH-1Δ*tri5*; Cuzick et al., 2008) of *F. graminearum* compared to mock treatment and (3) 12 h after direct application of DON, the prevalent mycotoxin produced by the Fg^{DON+} strain, also *via* point inoculation and compared to mock treatment (application of a mix of acetonitrile and Tween 20). This experimental set-up gave us the opportunity to identify genes which are specifically responsive to the mycotoxin and not by the infection itself by screening copies which are transcriptionally induced in conditions (1) and (3) but not in condition (2). Among the 252 full-length P450 encoding gene copies present in the *B. distachyon* genome, only two exhibited this pattern of transcriptional expression: *Bradi1g75310* which encodes the BdCYP711A29 protein and *Bradi2g44300* which encodes the BdCYP72A168 protein (**Chapter I, Table 1.5**). As discussed in the introduction (**Chapter I, section C.4.**), *Bradi1g75310* is four times more transcriptionally induced in the interaction context (condition (1)) with a relative expression fold change of 121.84 compared to *Bradi2g44300* which exhibits a 30.41 relative expression fold change. Since the regulation of P450s occurs mainly at the transcriptional level (Bolwell et al., 1994; Guéguen et al., 2006), a higher induction is likely to reflect a greater involvement of the *Bradi1g75310* copy during the interaction. Therefore, we decided to give priority to the functional characterization of this copy.

In order to confirm these data and to get information about the kinetics of transcriptional activation, we performed RT-qPCR experiments in the same initial conditions of *F. graminearum* infection or DON treatment. In the interaction context, *Bradi1g75310* relative expression was determined at 6 time-points between 0 and 168 hpi as compared to control condition (mock treatment; **Figure 2.1A**). Following infection of *B.* distachyon Bd21-3 WT

line with the Fg^{DON+} strain, the transcriptional expression of *Bradi1g75310* increased rapidly from 24 hpi, reached a peak 96 hpi (maximum of 15.41 log_2 fold change) then decreased at 168 hpi. Although transcriptomic studies could not detect a transcriptional activation of *Bradi1g75310* in response to the infection with the non-toxigenic Fg^{DON-} mutant strain of *F. graminearum*, it appeared here that the P450-encoding gene also reacts transcriptionally to this infection set-up, but to a much lesser extent compared to the first condition. Indeed, the transcriptional profile of the *Bradi1g75310* gene is similar to the one previously described but the maximum expression level at 96 hpi only reached 6.70 log_2 fold change. Regarding the mycotoxin treatment, gene expression was followed at 4 time points, between 0 and 48 hpi as compared to mock treatment (**Figure 2.1B**). As observed in the transcriptomic data, the *Bradi1g75310* gene was highly induced by DON from 12 hpi and reached a peak at 24 hpi with a 10.74 log_2 fold change of expression compared to mock condition.

B.2. The *Bradi1g75310* gene encodes a functional Cytochrome P450

The *Bradi1g75310* gene encodes a cytochrome P450 annotated as BdCYP711A29 (Nelson, 2009). This P450 therefore belongs to the only family of the plant CYP711 clan (Bak et al., 2011). As discussed in the introduction (**Chapter I, section C.2.**), P450s are subjected to a high evolutionary frequency as illustrated by their very low degree of amino acid sequence similarity and the number of metabolic pathways which involve P450-mediated biochemical reactions, for example. Overall, the high number of P450s copies in plant genomes, and more specifically the presence of four other copies in the *B. distachyon* CYP711A subfamily which will be discussed in detail in the **Chapter III**, could facilitate neofunctionalization and even loss of function of specific copies. We therefore checked whether BdCYP711A29 encoded by the *Bradi1g75310* gene is functional. To do this, we cloned the coding sequence (CDS) of *Bradi1g75310* from Bd21-3 *F. graminearum*-infected spike cDNAs, added flanking restriction sites and ligated the modified sequence in the pYeDP60 vector. In that construction, *Bradi1g75310* is placed under the control of the *GAL10-CYC1* hybrid promoter which is repressed by glucose used to support the yeast exponential growth phase but inducible by galactose in the stationary phase (**Appendix 1**; Pompon et al., 1996). The resulting pYeDP60 modified vector has then been transformed into *Saccharomyces cerevisiae* strain WAT11 which expresses the *ARABIDOPSIS CYTOCHROME REDUCTASE 1* (*ATR1*, *At4g24520*) gene from *A. thaliana* encoding a P450 reductase (CPR; Pompon et al., 1996). After the induction of production, a microsomal

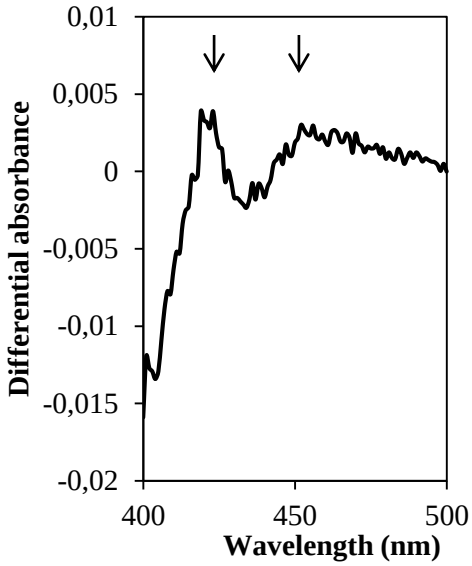

Figure 2.2: Differential CO-reduced versus reduced UV-Vis absorption spectrum of the microsomal membranes prepared from yeasts expressing the *Bradi1g75310* gene. The amplitude of the pic at 450 nm is indicative of the level of *Bradi1g75310* expression (Omura and Sato, 1964). The spectrum presented corresponds to the mean of ten measures of one representative biological replicate among three independent experiments. Arrows indicate the peaks of maximum absorption at 423 nm and 452 nm.

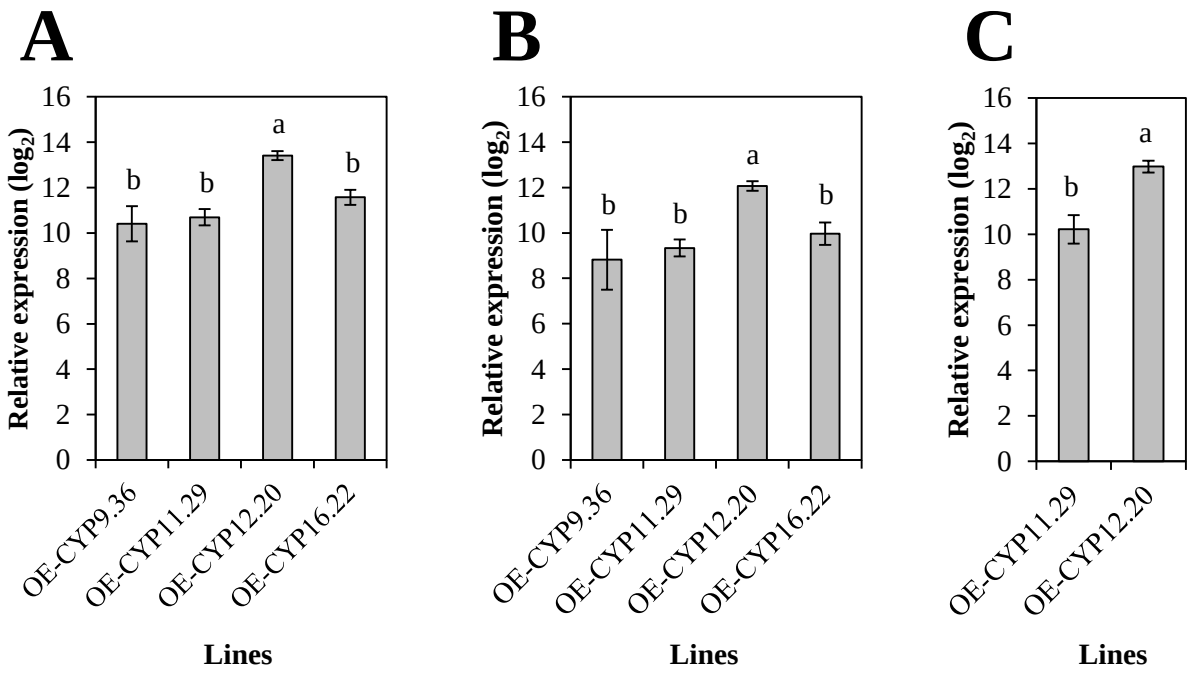

Figure 2.3: Molecular characterization of *B. distachyon* lines overexpressing the *Bradi1g75310* gene. Relative expression of the *Bradi1g75310* gene in spikes (**A**) and leaves of overexpressing lines OE-CYP9.36, OE-CYP11.29, OE-CYP12.20 and OE-CYP16.22 (**B**) and roots (**C**) of overexpressing lines of overexpressing lines OE-CYP11.29 and OE-CYP12.20. The relative quantity of *Bradi1g75310* gene transcripts (fold-change, $\log_2$) of OE lines as compared with the Bd21-3 WT line was calculated using the comparative cycle threshold method ($2^{-\Delta\Delta Ct}$). The *B. distachyon UBC18* and *ACT7* genes (*Bradi4g00660* and *Bradi4g41850*) were used as endogenous controls to normalize the data for differences in input RNA between the different samples. Data represent mean values of three independent biological experiments (n = 3) and two technical repetitions ± standard deviation. Different letters indicate significant differences between conditions, Student test, $P < 0.01$.

fraction could easily be obtained by ultracentrifugation composed of biological membranes carrying both BdCYP711A29 and ATR1. Thus, the optimized redox environment allows the direct use of these microsomes in subsequent enzymatic assays. To check the functionality of BdCYP711A29, we performed a differential absorption spectrum analysis as describe above (**Figure 2.2**, **Chapter I, section C.1.**, Omura and Sato, 1964). The presence of a peak at 452 nm indicates that a portion of ectopic expressed P450 was able to bind CO, a trait specifically linked to functional P450 because it reflects the correct anchorage and positioning of the heme iron. Although, maximum differential absorption was reached at 423 nm, which indicates that most of ectopic expressed protein cannot bind CO and therefore appeared nonfunctional, it is good enough to conclude that BdCYP711A29 is a functional cytochrome P450 (H. Renault and D. Werck, pers. comm.).

C. OBTAINING *B. DISTACHYON* LINES ALTERED IN THE *BRADI1G75310* GENE EXPRESSION

C.1. Four *B. distachyon* independent lines highly and constitutively express the *Bradi1g75310* gene

To achieve the *in planta* functional characterization of the *Bradi1g75310* gene, we generated *B. distachyon* lines which highly and constitutively express our gene of interest. The *Bradi1g75310* CDS was cloned into the pIPKb002 vector which is suitable for *A. tumefasciens*-mediated cereal transformation. In that construction, the *Bradi1g75310* gene is placed under the control of the strong and constitutive promoter of *Z. mays* ubiquitin (ZmUbi1, **Appendix 1**; Himmelbach et al., 2007). In addition, the T-DNA carries an expression cassette containing the *HYGROMYCIN PHOSPHOTRANSFERASE* (*Hpt*^{r}) gene which confers plant resistance towards hygromycin and allows dominant selection of primary transformants. Following Bd21-3-derived callus transformation, plant regeneration and segregation analysis, 4 independent lines carrying a single locus of insertion were selected: OE-CYP9.36, OE-CYP11.29, OE-CYP12.20 and OE-CYP16.22. As a negative control, we also selected a line sensitive to hygromycin, CYP11.26, which therefore has not integrated the construction but undergone the same regeneration processes. The level of expression of the *Bradi1g75310* gene was quantified in spikes and leaves of 4.5 weeks old plants of the 4 resistant lines as compared to WT (Bd21-3) by RT-qPCR (**Figures 2.3A and B**). Both in spikes and leaves, the 4 independent resistant lines strongly overexpress the *Bradi1g75310* gene. In spikes, the lower level of expression is found in OE-CYP9.36 (10.40 ± 0.78 $\log_2$ fold

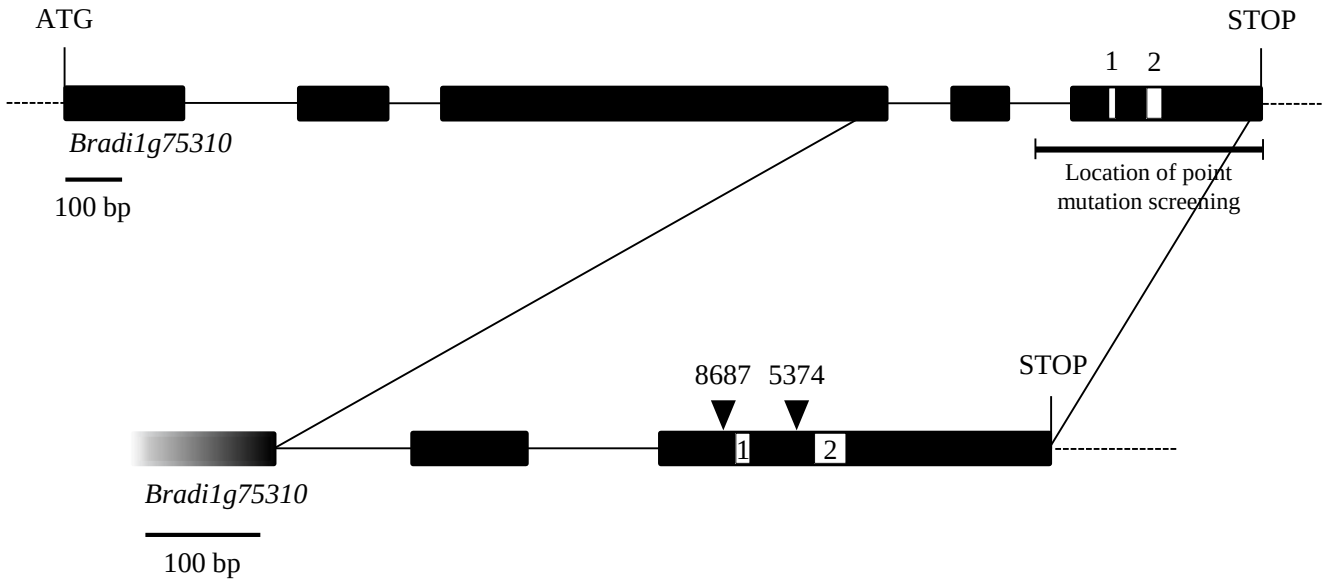

Figure 2.4: Design of the TILLING mutant screening strategy and location of two point mutations on the *Bradi1g75310* gene. Black boxes and solid lines symbolize exons and introns, respectively. The 400 bp region screened for point mutations is indicated on the upper panel. The two open boxes in the last exon indicate the location of regions encoding two consensus sequences for P450s: 1, PERF domain; 2, Heme binding loop. A close-up of the region encoding for the C-terminal part is shown in the lower panel and positions of point mutations carried by 8687 and 5374 TILLING mutant families are indicated.

Table 2.1: Characteristics of the mutant families identified in the *Bradi1g75310* gene following screening of the Bd21-3 (WT) TILLING mutant collection.

Family name	Nucleic acid transition[a]	Amino acid substitution[b]	Type of Mutation	SIFT Score[c]
7758	G1803A	G421G	Silent	1
8687	**C1831T**	**P431S**	**Missense**	**0**
7708	G1855A	E439K	Missense	0
-	G1857A	E439E	Silent	1
5374	**C1888T**	**R450***	**Stop**	**0**
7424	C1940A	P467H	Missense	0,02
8496	C1941T	P467P	Silent	0,06
7123	G1944A	G468G	Silent	1
6511	C1972T	L478F	Missense	0,08
7846	C2034T	P498P	Silent	1
8480	C2076T	G512G	Silent	1

[a]Location of the point mutation is settled from the starting ATG on the gDNA sequence.
[b]Location of the amino acid substitution is settled from starting methionine of the encoded protein.
[c]'Sorting Tolerant From Intolerant' score. The amino acid substitution is predicted damaging if the score is lower than 0.05.

change) followed by OE-CYP11.29 (10.69 ± 0.36 log_2 fold change) and OE-CYP16.22 (11.57 ± 0.33 log_2 fold change) as compared to Bd21-3. The OE-CYP12.20 line exhibits a higher level of expression (13.41 ± 0.19 log_2 fold change) and a statistical analysis supported this difference since OE-CYP12.20 is the only line with a significantly different level of expression of the *Bradi1g75310* gene as compared with the 3 other lines (**Figure 2.3A**). Concerning the expression level of our gene of interest in leaves, the hierarchy between lines is maintained although a slight decrease of overall gene expression level has been observed (**Figure 2.3B**). Since OE-CYP9.36, OE-CYP11.29 and OE-CYP16.22 lines do not present significantly different expression level of the *Bradi1g75310* gene, we decided to focus our effort on two independent lines exhibiting contrasted *Bradi1g75310* overexpression levels: The OE-CYP11.29 and the OE-CYP12.20 lines. Subsequently, we also quantified the relative expression level of our gene of interest in roots of hydroponically grown 3 weeks old OE-CYP11.29 and OE-CYP12.20 plants. Levels of expression are similar to those found in spikes and once again, we observed a statistically significant difference expression level between these two lines with OE-CYP12.20 exhibiting the higher level of overexpression (**Figure 2.3C**).

C.2. Four *B. distachyon* independent mutant families carry potentially deleterious point mutations in the *Bradi1g75310* gene

In order to obtain mutant lines for the *Bradi1g75310* gene, as no T-DNA insertional mutant was available (https://jgi.doe.gov/our-science/science-programs/plant-genomics/brachypodium/brachypodium-t-dna-collection/) we decided to screen the *B. distachyon* TILLING mutant collection generated by sodium-azide mutagenesis (Dalmais et al., 2013). This part of the project has been made in collaboration with MARION DALMAIS and KEVIN MAGNE at the Institute of Plant Sciences Paris-Saclay (IPS2, Orsay, France). The 2.500 mutant families of the collection were screened for point mutation *via* Illumina sequencing of a 400 bp region located at the 3' end of the gene and encoding a region of the C-terminal part of the protein and surrounding two P450 consensus sequences: the PERF domain with the conserved Arginine of the E-R-**R** triad and the heme binding loop (**Figure 2.4**; **Chapter I, section C.2.**). Eleven mutant families were shown to carry point mutations in the locus of interest (**Table 2.1**). A SIFT (Sorting Tolerant From Intolerant) analysis has been performed in order to predict the impact of each point mutation. This analysis is based on the evaluation of the frequency of a point mutation of interest in a single nucleotide polymorphism database.

A

B

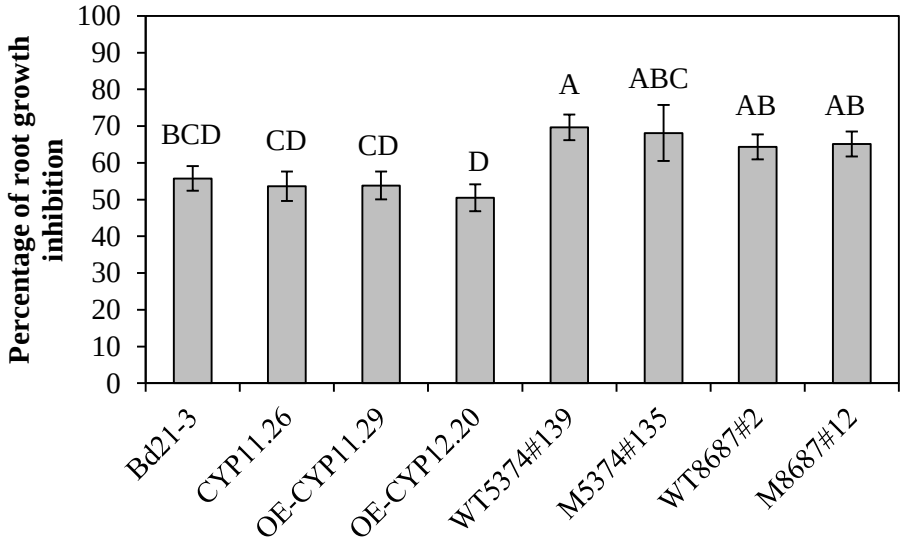

Figure 2.5: Alteration of the *Bradi1g75310* gene expression does not modify root sensitivity of *B. distachyon* towards DON. **A**, Typical root development of plants lines grown 7 d on agar medium containing 30 µM DON. Bar equal 1 cm. **B**, Percentage of root growth inhibition of lines grown 7 d on agar medium containing 30 µM DON compared to control condition. Mean of three independent biological replicates, n = 27, ± standard error. Different letters indicate significant differences between conditions, Student test, $P < 0.05$.

By assuming that essential positions in a protein sequence have been conserved throughout evolution, we conclude that the higher the frequency of a point mutation is, the lower the damage at the protein level (Kumar et al., 2009). Here, a score has been assigned to each point mutation which is predicted as damaging if the score is lower than 0.05. Only four families carry point mutations predicted to affect the protein structure: 8687, 7708, 5374 and 7424. Among them, three carry missense mutations: 8687 (P431S), 7708 (E439K) and 7424 (P467H); and one carries a nonsense mutation: 5374 (R450*; **Table 2.1**). For further experiment, we decided to focus our effort on only two of these families: 5374, for which the point mutation leads to the emergence of a STOP codon upstream the heme binding loop and 8687, which was supposed to carry the stronger missense mutation since it is responsible for the transition between a small amino acid with a particular geometry, Proline, and a tiny polar amino acid with a classical geometry, Serine. Both mutant families were led to homozygosity (giving the lines named M5374#135 and M8687#12) and wild-type (giving the lines named WT5374#135 and WT8687#2) *Bradi1g75310* alleles for each family were also selected since backcrosses are technically long and difficult to set up in *B. distachyon*.

D. ROLE OF THE *BRADI1G75310* GENE IN DON SENSITIVITY AND FHB SUSCEPTIBILITY

D.1. The *Bradi1g75310* gene is not involved in DON tolerance or sensitivity

Evaluation of plant root sensitivity towards DON has been routinely employed in the team to evaluate the general tolerance to the mycotoxin of several *B. distachyon* lines. As an example, this trait has been recently correlated to plant ability to detoxify DON through a glucosylation metabolism (Pasquet et al., 2016). In order to evaluate the role of the *Bradi1g75310* gene in DON tolerance or sensitivity, our different lines of interest were grown on agar medium containing 0 or 30 µM DON, then we measured primary root length 7 d later (**Figure 2.5**). The concentration of mycotoxin used is this experiment has been determined according to Pasquet et al. (2016) as an intermediate between 10 µM (18% of root growth inhibition on Bd21-3) and 50 µM (50% of root growth inhibition on Bd21-3 derived null segregant line). In this condition, we therefore expected to highlight potential increased tolerance or sensitivity towards DON of our different *B. distachyon* lines altered in the *Bradi1g75310* gene compared to control lines. Bd21-3 (WT) line exhibited an inhibition of root growth of 55.56 ± 3.38% on DON containing medium and the null segregant line

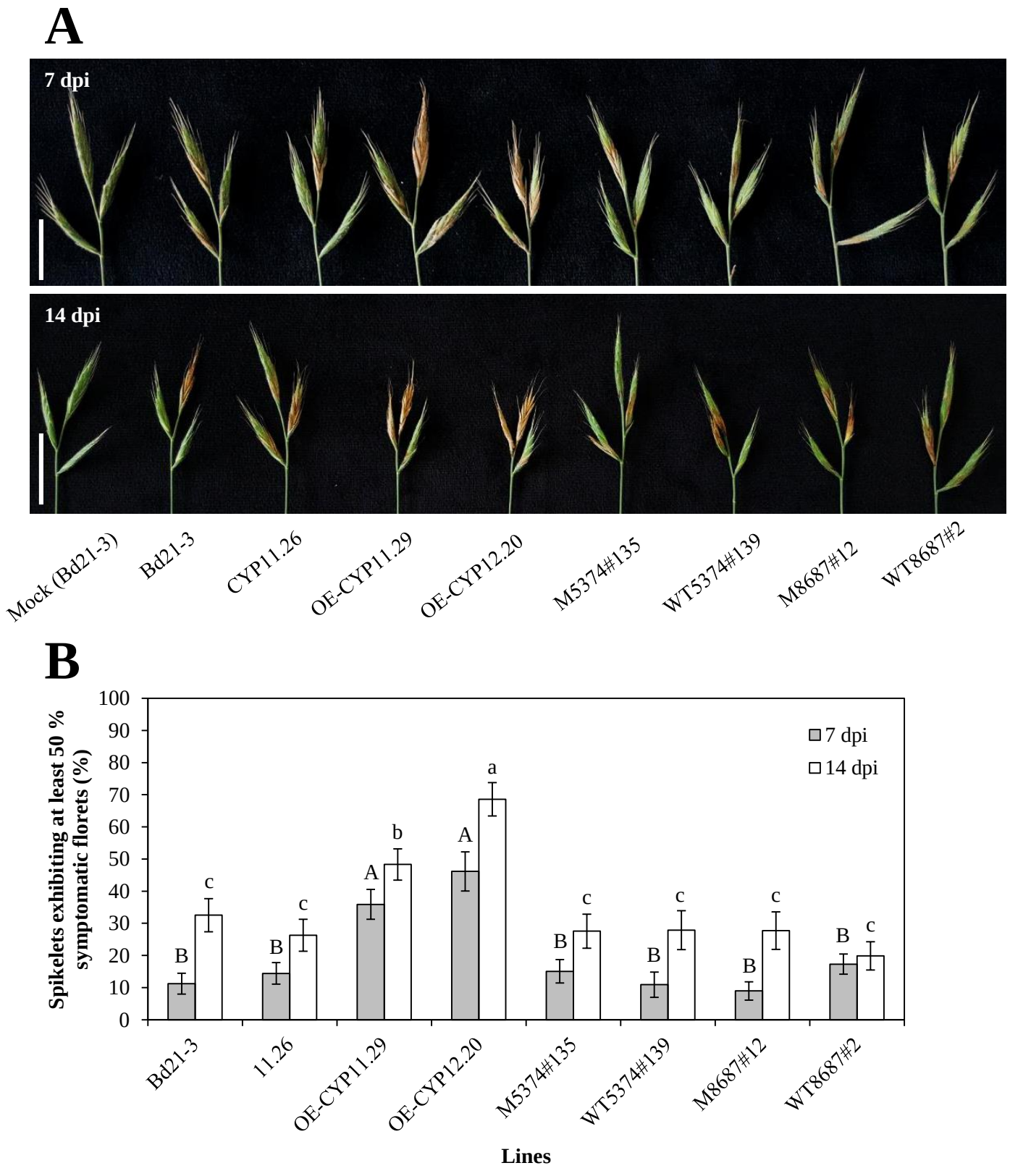

Figure 2.6: Overexpression of the *Bradi1g75310* gene increases FHB susceptibility following spray inoculation of *F. graminearum*. **A**, Typical FHB symptoms at 7 and 14 days following spray inoculation of whole spikes of the different lines by the PH-1 strain (Fg^{DON+}). Bars equal 1 cm. **B**, Percentage of spikelets exhibiting FHB symptoms on at least 50 % of the florets of the inoculated spikes at 7 and 14 dpi by the PH-1 strain. Mean of four independent biological replicates, n = 52, ± standard error. Different letters indicate significant differences between conditions; upper case and lower case letters indicate the statistical comparison at 7 and 14 dpi, respectively. Student test, $P < 0.05$.

CYP11.26 was shown to behave similarly (53.60 ± 4.02%). The percentages of root growth inhibition of the two lines overexpressing the *Bradi1g75310* gene were shown to be non-significantly different from Bd21-3 and CYP11.26 (53.82 ± 3.79 and 50.47 ± 3.65% for OE-CYP11.29 and OE-CYP12.20, respectively). Both TILLING lines carrying a *Bradi1g75310* WT allele presented a slight increase of root sensitivity towards DON (69.66 ± 3.52 and 64.31 ± 3.41% for WT5374#135 and WT8687#2, respectively), but only WT5374#135 was shown to be significantly more sensitive to the mycotoxin compared to Bd21-3. None of the TILLING mutant lines was shown to exhibit a significantly different level of sensitivity towards DON as compared to both their respective TILLING control lines and WT line (68.13 ± 7.63 and 65.14 ± 3.42% for M5374#135 and M8687#12, respectively).

D.2. The *Bradi1g75310* gene is a susceptibility factor of *B. distachyon* towards FHB

In order to determine whether the *Bradi1g75310* gene is involved in the interaction between *B. distachyon* and *F. graminearum*, we performed pathogenicity assays. We conducted spray inoculations of *F. graminearum* strain PH-1 (Fg^{DON+}) spore suspensions on whole spikes of the *B. distachyon* lines described above: WT (Bd21-3), overexpressing lines (OE-CYP11.29 and OE-CYP12.20) and the corresponding null segregant (CYP11.26), TILLING mutant lines for our gene of interest (M5374#135, M8687#12) and their control lines (WT5374#135 and WT8687#2, respectively; **Figure 2.6**). Representative symptoms 7 and 14 dpi for each line are presented in **Figure 2.6A**. We quantified typical FHB symptoms 7 and 14 dpi by counting the number of spikelets exhibiting more than 50% of symptomatic florets over the total number of spikelets (**Figure 2.6B**). The results presented represent the mean of four independent biological replicates. Seven dpi, both overexpressing lines OE-CYP11.29 and OE-CYP12.20 exhibited statistically significant more developed symptoms (35.9 ± 4.7% and 46.2 ± 6.1% of symptomatic spikelets, respectively) as compared to WT (11.2 ± 3.3%) and CYP11.26 (14.4 ± 3.3%). All the TILLING mutant lines, carrying either the mutant or WT allele for the *Bradi1g75310* gene, presented equivalent symptoms as compared to the Bd21-3 line. After another week of disease development (14 dpi), the tendency described above was conserved. Both overexpressing lines presented increased symptoms compared to control lines (48.3 ± 4.9% for OE-CYP11.29 and 68.6 ± 5.2% for OE-CYP12.20 compared to 32.5 ± 5.1% and 26.3 ± 5.0% for Bd21-3 and CYP11.26,

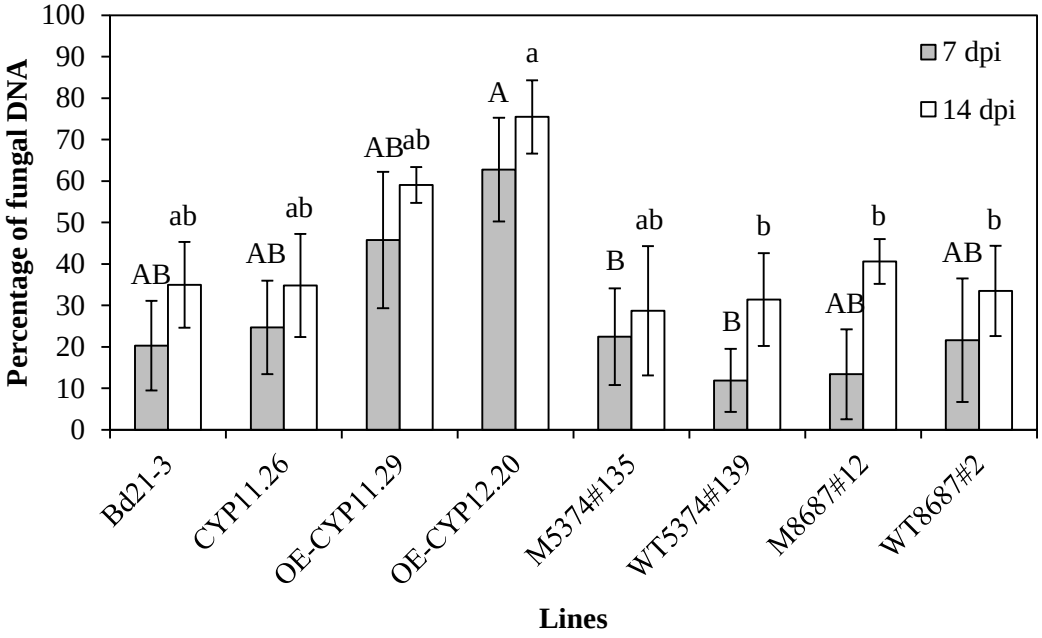

Figure 2.7: Overexpression of the *Bradi1g75310* gene promotes *F. graminearum* development on *B. distachyon* spikes following spray inoculation. Relative quantification of fungal DNA by qPCR compared to total DNA 7 and 14 days after spray inoculation of different *B. distachyon* lines with the PH-1 (Fg^{DON+}) strain of *F. graminearum*. Mean of three independent biological replicates, ± standard error. Different letters indicate significant differences between conditions, Student test, $P < 0.05$.

respectively). The 19.9% differential development of symptoms between the two overexpressing lines has also been shown to be statistically significant. As observed at 7 dpi, all the other TILLING lines did not show any significant difference in the level of symptomatic spikelets as compared to the WT line of *B. distachyon*.

To be able to correlate the differences of disease symptoms described above with a differential fungal development, we quantified by qPCR the relative amount of fungal gDNA depending on the *B. distachyon* lines. On the same material used for symptoms quantification (3 out of 4 biological replicates), we collected 3 to 5 representative spikelets at 7 and 14 dpi for each line and conducted total gDNA extractions. We quantified the relative fungal gDNA amount by qPCR through the determination of the cycle threshold (Ct) of a plant reference gene (*ACT7, Bradi4g41850*) and a fungal reference gene (*R18S*) in each sample and by relating it to a standard curve of plant and fungal gDNA of known relative concentrations. The percentages of fungal DNA are presented in **Figure 2.7**.

Seven dpi, Bd21-3 samples exhibited 20.3 ± 10.8% of fungal DNA and the other control lines oscillate around this value: 24.7 ± 11.3; 11.9 ± 7.6 and 21.6 ± 14.9% for CYP11.26, WT5374#135 and WT8687#2, respectively. Whereas TILLING mutant lines did not presented difference greater than 10% compared to WT and TILLING control lines (22.5 ± 11.6 and 13.4 ± 10.9% for M5374#135 and M8687#12, respectively), both overexpressing lines showed an increased percentage of fungal DNA as compared to Bd21-3 and CYP11.26 (45.8 ± 16.4 and 62.8 ± 12.5% for OE-CYP11.29 and OE-CYP12.20, respectively). This tendency was conserved 14 dpi since all the control lines and TILLING mutant lines ranged from 28.7 ± 15.6 (M5374#135) to 40.6 ± 5.4% (M8687#12), contrary to overexpressing lines which exhibited from around 20 to 45% more fungal DNA (59.0 ± 4.3 and 75.5 ± 8.9% for OE-CYP11.29 and OE-CYP12.20, respectively).

We conducted statistical analyses on these results but data dispersal impeded us to statistically confirm most of the observations reported above. More precisely, both overexpressing lines were not statistically distinguished from WT or CYP11.26 at 7 and 14 dpi. Nevertheless, OE-CYP12.20, which exhibited the highest percentages of fungal DNA at 7 and 14 dpi, was shown to be significantly different to M5374#135 at 7 dpi and to M8687#12 at 14 dpi.

E. CONCLUSION

The first objective of this part was to identify a P450-encoding gene of the model cereal *B. distachyon* exhibiting a specific transcriptional regulation which could therefore be considered as a good candidate to study the involvement of P450s in the FHB context. Based on a transcriptomic study performed in the lab before the beginning of this thesis project, we decided to focus our attention on the *Bradi1g75310* gene which encodes the BdCYP711A29 P450 in *B. distachyon.* Indeed, this gene is highly transcriptionally induced either 96 h following infection with a toxin-producing strain of *F. graminearum* or 12 h following direct application of DON on *B. distachyon* spikes (**Table 1.5**; Pasquet et al., 2014; Pasquet, 2014). This gene appeared to be specifically induced by the mycotoxin produced by the fungus rather than the infection itself. Indeed, the transcriptomic study failed to detect any differential regulation of this gene 96 hpi with a non-toxigenic strain of *F. graminearum*. We performed RT-qPCR experiments in order to validate these data and gain information about the kinetics of the transcriptional activation. We followed the expression of the *Bradi1g75310* gene from 0 to 168 hpi with the two *F. graminearum* strains describe above and from 0 to 48 hpi with DON (**Figure 2.1**). We were able to confirm the transcriptional activation of the *Bradi1g75310* gene in response to Fg^{DON+} and DON treatment and observed maximum expression levels 96 hpi with Fg^{DON+} and 24 hpi with DON. Contrary to what was observed in the transcriptomic experiments, our gene of interest is also transcriptionally induced by the Fg^{DON-} strain. The patterns of gene expression kinetics are similar following Fg^{DON+} or Fg^{DON-} inoculations, but the *Bradi1g75310* gene appeared to be 4 to 8 times less induced following infection with the non-toxigenic strain. We therefore concluded that most of the transcriptional regulation of our gene of interest is dependent on the mycotoxin. Nevertheless, we could not exclude a delayed transcriptional induction of the *Bradi1g75310* gene following infection with the Fg^{DON-} strain since it was shown to have a delayed development on *B. distachyon* but not fully blocked as observed on wheat (Pasquet et al., 2014).

Because P450s constitute a tremendous class of enzymes with complex evolutionary history including duplications and rapid neofunctionalization or even loss of function (Nelson and Werck-Reichhart, 2011), a preliminary study of a specific isoform should include its functional validation. Because P450 activity is dependent on the correct anchorage of the ferric heme to the tertiary structure of the protein and gives it the ability to bind oxygen, we produced the recombinant BdCYP711A29 in yeast in order to record the differential absorption spectrum of the enzyme. A P450 in a reduced state exhibits a maximum of

absorption at 420 nm and if it is correctly folded and therefore carries a functional ferric heme, it can bind carbon monoxide which will lead to the shit of maximum absorption to 450 nm (Omura and Sato, 1964). In our study, we were able to detect a slight peak at 450 nm which allowed us to conclude on the functionality of BdCYP711A29. Nevertheless, the peak with the maximum amplitude was found at 420 nm which indicate that most of the produced proteins are not correctly folded or have been denatured before measurements. Nonetheless, this is a quite common observation in recombinant P450 protein production and therefore it does not impact our conclusion on the functionality of the BdCYP711A29 protein, only a total absence of a 450 nm peak in several independent productions could.

In order to initiate the functional characterization of the *Bradi1g75310* gene *in planta*, we generated *B. distachyon* lines which overexpress our gene of interest. Among the four independent lines we could obtain, we decided to focus on two lines, OE-CYP11.29 and OE-CYP12.20, for further experiments. Indeed, these two lines exhibit significantly different *Bradi1g75310* gene overexpression level in spikes, leaves and roots. In parallel, we screened the TILLING mutant collection available in the institute for point mutations impacting the C-terminal part of the BdCYP711A29 protein and surrounding essential conserved domains (Bak et al., 2011). Among the 11 mutant families carrying point mutations in the target area, we selected two lines predicted to carry a damaged allele of the *Bradi1g75310* gene. One exhibits a missense mutation (M8687#12) and the other one a nonsense mutation (M5374#135), both expected to strongly affect the protein structure and therefore the functionality of BdCYP711A29. Together with controls lines, we therefore obtained a set of *B. distachyon* lines suitable for further experiments needed to functionally characterize the *Bradi1g75310* gene.

One of the well-studied activities of P450s is their role in xenobiotic detoxification. Indeed, several plant P450s were shown to metabolize herbicides from the phenylurea family, for example (Siminszky, 2006). Although not any plant P450 was shown to metabolize DON, a bacterial copy is able to hydroxylate DON into 16-HDON, a derivative with highly reduced phytotoxicity as compared to its parent metabolite (Ito et al., 2013). Because transcriptional activation of the *Bradi1g75310* gene mostly depends on DON and also because enzymes involved in xenobiotic pathways are often transcriptionally induced by their exogenous substrate (Edwards et al., 2011), we were wondering whether BdCYP711A29 P450 could be involved in DON detoxification and therefore in *B. distachyon* tolerance towards the mycotoxin. We tested the root sensitivity of our different *B. distachyon* lines towards 30 µM DON which has been already shown to be a good and simple way to evaluate the overall

tolerance of plants towards a toxic compound (Pasquet et al., 2016). We did not observed any significant difference of percentage of root growth inhibition between lines overexpressing the *Bradi1g75310* gene, TILLING mutant lines and their respective control lines. We therefore concluded that the *Bradi1g75310* gene is not involved in *B. distachyon* tolerance or sensitivity to the main mycotoxin produced by *F. graminearum* and decided to not go deeper into that hypothesis.

Nevertheless, we benefited from our different *B. distachyon* lines to evaluate the putative involvement of the *Bradi1g75310* gene in the level of resistance or susceptibility of the model cereal grass towards the infection by *F. graminearum*. We performed pathogenicity assays and quantified both disease symptoms development and fungal biomass. The results of symptoms quantification indicate that our gene of interest is a plant susceptibility factor during FHB since both overexpressing lines exhibit stronger symptoms 7 and 14 dpi compared to all the other lines. However, TILLING mutant lines did not show enhanced resistance to the disease which might be explained by a functional redundancy between BdCYP711A29 and other *B. distachyon* P450 isoforms. This hypothesis will be explored in detail in the next chapter. The relative quantification of fungal DNA in *B. distachyon* spikes 7 and 14 dpi gave the same tendency of increased *F. graminearum* development on overexpressing lines compared to control lines. Nevertheless, data dispersion limited the statistical validation of this observation, which is a quite common limit in plant-pathogen interaction experiments wherein tendencies but not numeraries are easily repeatable due to environmental fluctuations between different biological replicates. It is also important to notice that the level of disease development achieved in this study for the WT lines Bd21-3 is relatively low compared to other published studies. As an example, the level of symptomatic spikelets of Bd21-3 in our study was 11.2 ± 3.3% at 7 dpi as compared to the almost 60% reached in Pasquet et al. (2016). This difference could be due to a reduction of fungal virulence but is also the consequence of the experimental set-up. Indeed, we thinly managed the pathogenicity assays in order to limit relative hygrometry so as to gain two advantages: we limited the aerial and therefore abnormal development of the pathogen on the host plant surface and get closer to natural conditions, and we also placed in optimal conditions to observe the differential of symptoms development between lines. As a matter of fact, before the 4 independent biological replicates presented in this study, first tuning experiments were conducted in higher hygrometry conditions. The level of disease symptoms observed was comparable to those observed in other studies but somehow rubbed out susceptibility differences between lines (data not shown). Although this does not influence our conclusion

about the role of the *Bradi1g75310* gene in *B. distachyon* susceptibility towards FHB, this requires us to temper it.

To conclude this first results chapter, it appeared that the *Bradi1g75310* gene encodes a functional P450 transcriptionally induced during FHB, mostly by the main mycotoxin produced by *F. graminearum*, and involved in *B. distachyon* susceptibility towards FHB but not in plant tolerance/sensitivity towards DON. We hypothesized that this involvement could be linked to an endogenous role of our P450 of interest. The next chapter will explore this hypothesis, mostly *via* the study of the putative involvement of the *Bradi1g75310* gene in the biosynthesis of a specific class of secondary metabolites: strigolactones.

CHAPTER III | RESULTS (2/3)

Role of the *Bradi1g75310* gene and its homologs in strigolactones biosynthesis

A. INTRODUCTION

The largest family of plant enzymes constituted by P450s is also the less conserved at the level of amino-acid primary sequence and this constitutes the main barrier in P450 functional characterization studies (Mizutani, 2012). Nevertheless, phylogenetic relationships between copies from various plant species, no matter how weak, were also shown to be potential strong evidences to assign an enzymatic activity to an uncharacterized isoform regarding specific biological processes. This situation is plainly illustrated by the CYP51 family for which all full-length copies characterized in higher plants were shown to be obtusifiliol 14α-demethylases. Moreover, the function of this P450 family is globally conserved across kingdoms since all copies were shown to be involved in sterol biosynthesis as 14α-demethylases (Lepesheva and Waterman, 2009). In a more common way, several P450s belonging to the same family have been shown to be involved in the same metabolic pathway: this is the case for CYP90A-Ds which are all involved in brassinosteroids (BRs) biosynthesis although they do not catalyze the same biochemical reaction (Mizutani, 2012). Altogether, these elements have led us to investigate the phylogeny of the *Bradi1g75310* gene as a starting point for its endogenous functional characterization. Because homologous genes are likely to exhibit similar expression profiles, we also benefited from *in silico* and RT-qPCR data to justify our assumptions and start the *in planta* characterization of the *Bradi1g75310* gene.

The objective of this second part was to determine whether the *Bradi1g75310* gene is involved in the metabolization/biosynthesis of an endogenous substrate in *B. distachyon*. As discussed in the introduction, BdCYP711A29 belongs to the same P450 family as copies, from various plant species, showed to participate in strigolactones biosynthesis. Consequently, we specified the ancestral and transcriptional relationships between our gene of interest and the similar ones presented in 2 other model species: *A. thaliana* and rice. Based on strong homology evidences, we pursued the functional characterization of the *Bradi1g75310* gene through the genetic complementation of the *A. thaliana* related mutant line and *via* the detection and quantification of SLs exuded from roots of *B. distachyon* lines.

Four other CYP711A encoding genes are present in the *B. distachyon* genome and none of them have been characterized. We therefore employed the strategy of genetic complementation in order to propose a first characterization of the four other BdCYP711As copies.

Table 3.1: Protein identity matrix (percentages) between CYP711As from *B. distachyon*, *O. sativa*, *A. thaliana* and *S. moellendorffii*.

P450 annotation	Encoding gene	1	2	3	4	5	6	7	8	9	10	11	12
1: SmCYP711A17	***LOC9651576***	100	36,62	37,48	39,8	39,12	40,08	39,27	40,85	38,2	40,51	41,9	40,67
2: BdCYP711A5	***Bradi3g08360***	36,62	100	72,38	55,71	54,19	45,67	50,29	48,16	47,46	46,41	49,52	50,29
3: OsCYP711A5	***Os02g0221900***	37,48	72,38	100	56,73	56,78	46,3	51,54	51,64	47,86	49,81	52,19	51,44
4: BdCYP711A6	***Bradi1g37730***	39,8	55,71	56,73	100	74,61	54,58	60,4	59,14	55,53	58,53	60,54	59,45
5: OsCYP711A6	***Os06g0565100***	39,12	54,19	56,78	74,61	100	53,94	56,97	59,1	56,58	58,98	59,65	60,71
6: BdCYP711A29	***Bradi1g75310***	40,08	45,67	46,3	54,58	53,94	100	72,8	55,8	55,47	56,05	58,27	57,92
7: BdCYP711A31	***Bradi4g09040***	39,27	50,29	51,54	60,4	56,97	72,8	100	59,14	56,83	59,81	63,69	61,72
8: AtCYP711A1	***At2g26170***	40,85	48,16	51,64	59,14	59,1	55,8	59,14	100	57	60,27	62,98	62,38
9: BdCYP711A30	***Bradi4g08970***	38,2	47,46	47,86	55,53	56,58	55,47	56,83	57	100	65,51	67,31	67,83
10: OsCYP711A2	***Os01g0700900***	40,51	46,41	49,81	58,53	58,98	56,05	59,81	60,27	65,51	100	81,94	78,69
11: OsCYP711A3	***Os01g0701400***	41,9	49,52	52,19	60,54	59,65	58,27	63,69	62,98	67,31	81,94	100	82,65
12: OsCYP711A4	***Os01g0701500***	40,67	50,29	51,44	59,45	60,71	57,92	61,72	62,38	67,83	78,69	82,65	100

Matrix based on ClustalW multiple amino-acid sequence alignments.

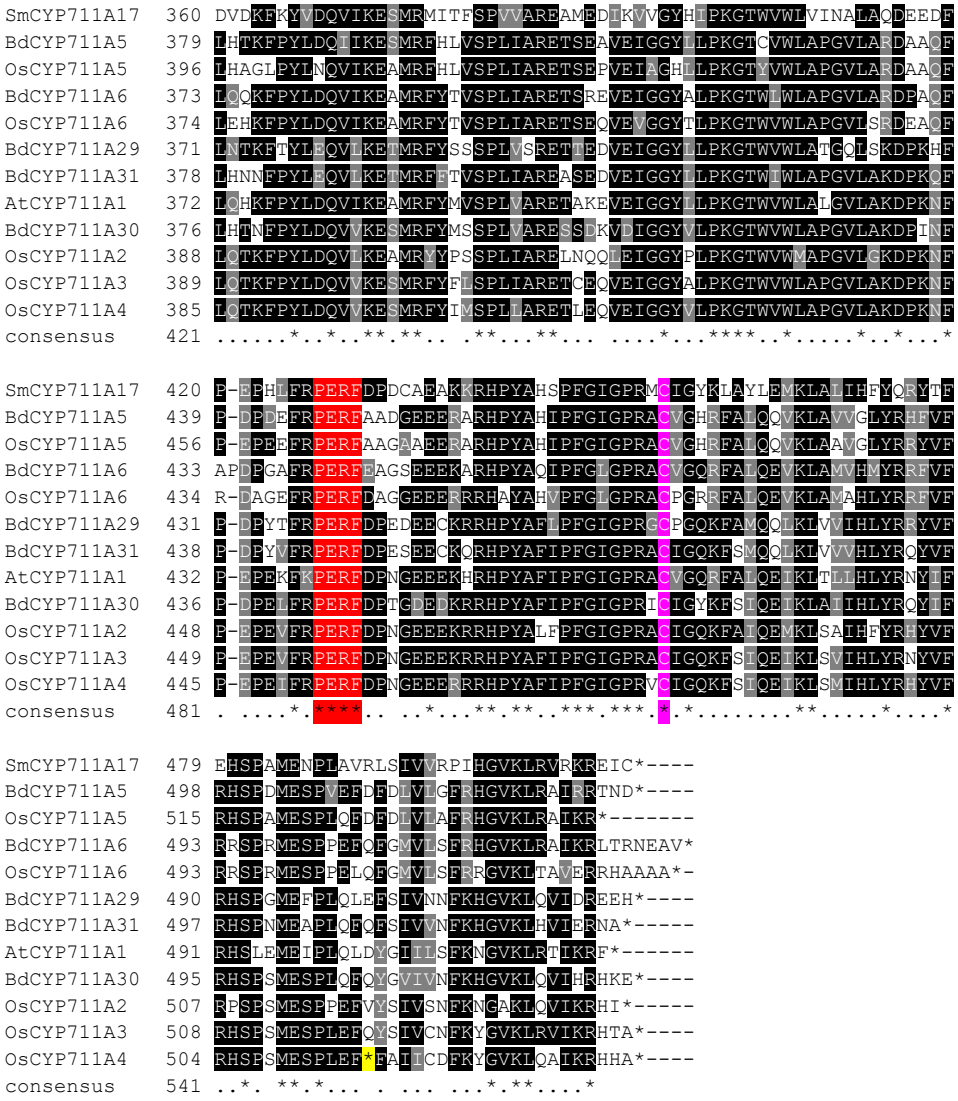

Figure 3.1: Multiple amino-acid sequence alignment of CYP711As from *B. distachyon*, *O. sativa*, *A. thaliana* and *S. moellendorffii*. Multiple sequences alignment was build using the ClustalW program (Thompson et al., 1994). Black, grey and white boxes indicate conserved, similar and non-conserved residues between sequences, respectively. Only the C-terminal part of the alignment is shown. The PERF domain is shown in red, the strictly conserved Cysteine in the heme binding loop is shown in magenta and the premature STOP codon in the OsCYP711A4 sequence (second last line) is shown in yellow. No other premature STOP codon has been observed in the N-terminal part of sequences (data not shown).

B. PHYLOGENETIC AND TRANSCRIPTIONAL RELATIONSHIPS BETWEEN CYP711AS FROM *B. DISTACHYON*, *O. SATIVA* AND *A. THALIANA*

B.1. Phylogenetic analysis of the *B. distachyon*, *O. sativa* and *A. thaliana* CYP711As

The nomenclature of P450s is mostly based on protein sequence identity (Nelson, 2009). Members of a single P450 subfamily are therefore expected to share at least 55% identity which remains quite low and is not indicative enough regarding gene functionality. We recovered the amino-acid sequences of CYP711As protein of rice (*Os01g0700900*, *Os01g0701400*, *Os01g0701500*, *Os02g0221900* and *Os06g565100* encoding OsCYP711A2, A3, A4, A5 and A6 respectively), *A. thaliana* (*At2g26170* encoding AtCYP711A1), *B. distachyon* (*Bradi3g08360*, *Bradi1g37730*, *Bradi1g75310*, *Bradi4g08970*, *Bradi4g09040* encoding BdCYP711A5, A6, A29, A30 and A31 respectively) and from the lycophyte *Selaginella moellendorffii* (*LOC9651576* encoding SmCYP711A17) from 'The P450 Homepage' (Nelson, 2009). We then performed multiple sequence alignments using ClustalW (Thompson et al., 1994). The **Table 3.1** shows a protein identity matrix between these CYP711A copies. Surprisingly, 27 out of 66 possible combinations exhibited a protein identity lower than 55%. Because *S. moellendorffii* does not belong to angiosperms and therefore was the first to diverge from the other angiosperm species studied here, its CYP711A copy was expected to be the less conserved. Indeed, in the case of comparisons involving the *S. moellendorffii* copy, percentages of identity are distributed between 36.62% and 41.9% which is almost insufficient to consider SmCYP711A17 as a CYP711 family member. Obviously, phylogeny and/or gene organization was also used by the P450 nomenclature committee to assign this annotation, a regular option used for plant P450s with complex evolutionary history (Werck-Reichhart et al., 2002). Regarding the copies from angiosperm species, percentages of identity ranged from 45.67% (BdCYP711A5 *vs* BdCYP711A29) and 82.65% (OsCYP711A3 *vs* OsCYP711A4). Interestingly, the five copies from *O. sativa* exhibited higher identity between them (from 49.81 % to 82.65 % with an average of 62.69%) compared to *B. distachyon* ones (from 45.7% to 72.8% with an average of 55.47%), likely to reflect a more complex evolutionary history of the subfamily in the model temperate cereal as compared to rice. At last, BdCYP711A29 encoded by the *Bradi1g75310* gene showed maximum identity with BdCYP711A31 regarding *B. distachyon* copies (72.8%) and OsCYP711A3 regarding copies from all other plant species (58.27%). As discussed in the

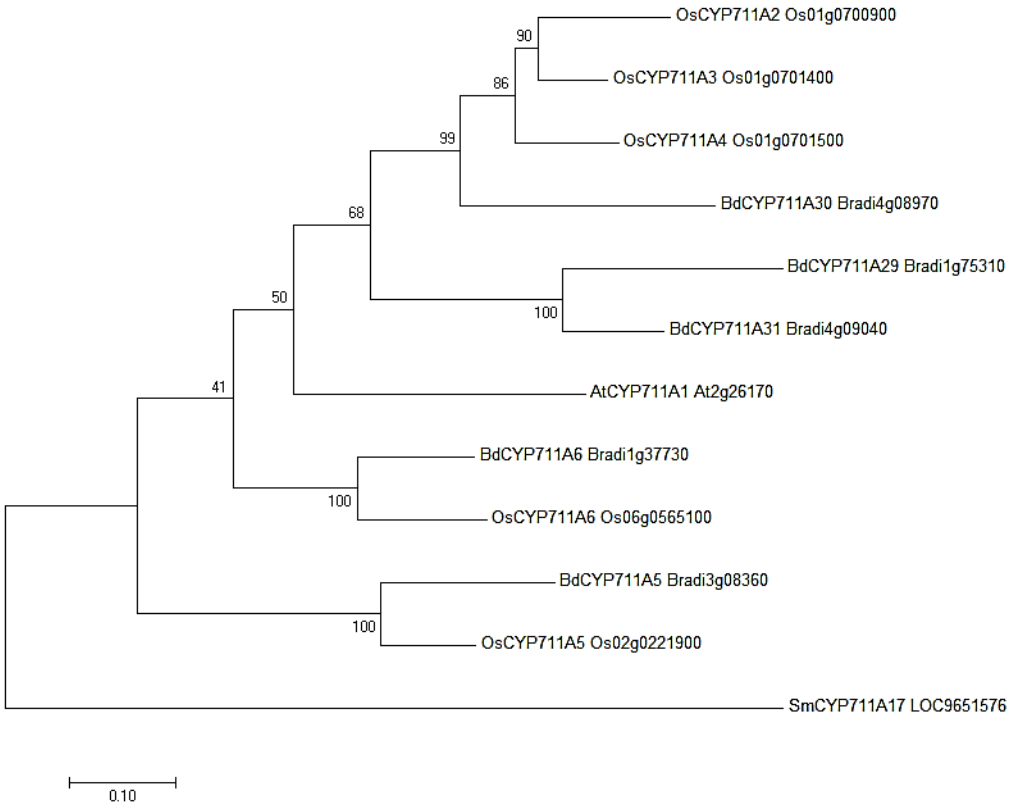

Figure 3.2: Molecular phylogenetic analysis of *B. distachyon, A. thaliana, O. sativa* and *S. moellendorffii* CYP711As. The protein evolutionary history was inferred by using the Maximum Likelihood method based on the JTT matrix-based model (Jones et al., 1992). The percentage of trees in which the associated CYP711A copies clustered together is shown next to the branches (bootstrap value for 100 replicates). The tree is drawn to scale, with branch lengths measured in the number of substitutions per site. Phylogenetic analyses were conducted in MEGA7. The tree has been rooted with *Selaginella moellendorffii* CYP711A17 (SmCYP711A17). Os: *O. sativa*; Bd: *B. distachyon*; At: *A. thaliana*; Sm: *S. moellendorffii*.

introduction, this last copy was shown to catalyze *ent*-2′-*epi*-5DS transformation in orobanchol (**Section I.D.3.**; Zhang et al., 2014).

The OsCYP711A4 copy exhibited the overall highest level of identity with other copies, especially with OsCYP711A2 (78.69%) and OsCYP711A3 (82.65%). Nevertheless, this copy failed to efficiently complement the highly branched developmental phenotype of *A. thaliana max1-1* mutant line (Challis et al., 2013). The authors suggested that a premature STOP codon was responsible for this loss of function and that this copy was under a pseudogeneisation process which is consistent with the functional redundancy observed between other copies (Challis et al., 2013). We studied the *B. distachyon* amino-acid sequences of CYP711As in order to detect such situation in the model cereal but contrary to OsCYP711A4, not any *B. distachyon* CYP711A copies exhibited a premature STOP codon (**Figure 3.1**) hence, none of them should be considered as a pseudogene.

We then generated a phylogenetic tree of the CYP711As from *B. distachyon*, rice and *A. thaliana* based on the multiple sequence alignment described above and using the Maximum Likelihood method of MEGA version 7 (Kumar et al., 2017; **Figure 3.2**). *S. moellendorffii* CYP711A17 sequence was also included as outgroup to root the phylogenetic tree. As expected, copies from different species but sharing the same nomenclature are grouped with a bootstrap value of 100: BdCYP711A5 and OsCYP711A5; BdCYP711A6 and OsCYP711A6. All the other *B. distachyon* and rice copies belong to the same clade as *A. thaliana* AtCYP711A1 and are divided into 3 subclades: one specific to the *A. thaliana* copy, one groups *B. distachyon* BdCYP711A29 and BdCYP711A31 copies, and the last merges rice OsCYP711A2, OsCYP711A3 and OsCYP711A4 with *B. distachyon* BdCYP711A30. Interestingly, the BdCYP711A29 copy is carried by the longest branch and therefore exhibits the highest rate of substitution per site.

B.2. Transcriptional regulation of the *B. distachyon*, *O. sativa* and *A. thaliana* CYP711As

Because homologous genes are more likely to exhibit similar expression patterns, we then focused our study on CYP711As, and more specifically on BdCYP711A29, at the transcriptional level. To precise the relationships between the CYP711A copies from the three model plants, we recovered transcriptomic data of each encoding gene (except *Os01g0701500* the pseudogene encoding the OsCYP711A4 truncated P450 in rice and only *Bradi1g75310* encoding BdCYP711A29 for *B. distachyon* copies) from the PlaNet web service hosted by the

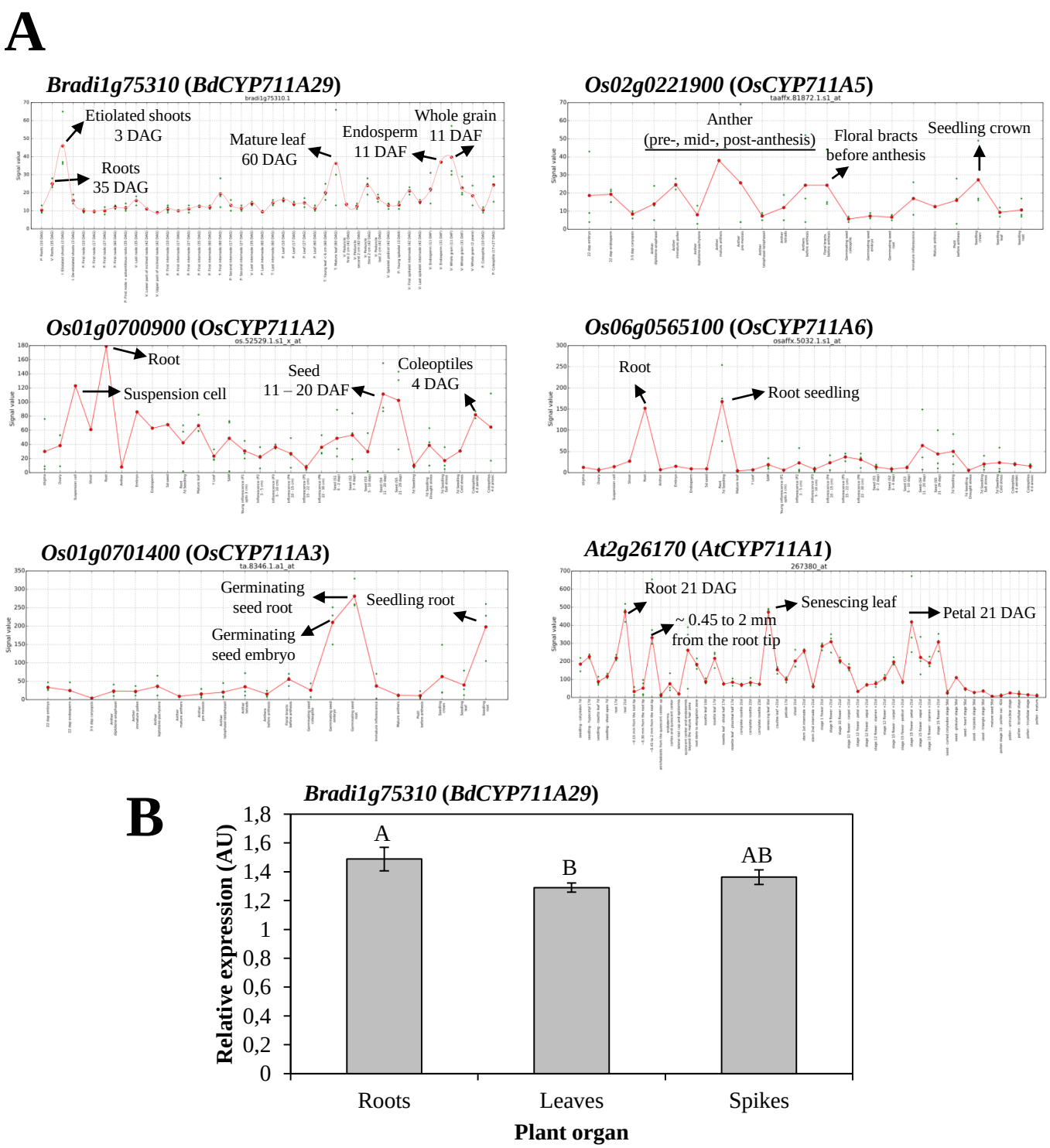

Figure 3.3: Transcriptional regulation of the *Bradi1g75310* gene is comparable to other CYP711A encoding genes from *O. sativa* and *A. thaliana*. A, Transcriptional regulation profiles of *Bradi1g75310* encoding *B. distachyon* BdCYP711A29, 4 *O. sativa* CYP711A encoding genes (*Os01g0700900*; *Os01g0701400*, *Os02g0221900*, *Os06g565100*) and *At2g26170* encoding *A. thaliana* AtCYP711A1 (MAX1). Data were collected from the PlaNet web service hosted by the Max Planck Institute of Potsdam (Germany). Two to four maximum expression levels were specified with arrows. Average expression, green dots: expression from individual microarray/RNAseq experiments. Expansions are presented in Appendix 2. **B**, Relative expression level (Arbitrary Unit, AU) of the *Bradi1g75310* gene in roots, leaves and spikes of 5 w old plants grown hydroponically as compared to *UBC18* and *ACT7* genes (*Bradi4g00660* and *Bradi4g41850*) expression. Mean numbers of n = 3 biological replicates ± standard error, different letters indicate significant differences between conditions, Student test, $P < 0.05$.

Max Planck Institute of Potsdam (Germany; http://aranet.mpimp-golm.mpg.de/; **Figure 3.3A; Appendix 2**). The transcriptional profile of each gene depending on the plant organ or the developmental stage has been recovered and special attention was given to conditions in which maximum expression levels were observed. Regarding *Bradi1g75310* gene, the maximum expression levels were found in grain (whole grain and endosperm, 11 days after formation (DAF)), mature leaf 60 days after germination (DAG) and etiolated shoots 3 DAG. An intermediate level of expression was found in roots 35 DAG, peduncle 42 DAG, and coleoptile (17 + 27 DAG; the last two conditions are not indicated on the figure). Concerning the rice and *A. thaliana* copies, an important level of expression was systematically found in roots but at different developmental stages depending on the plant species or the CYP711A isoform (e.g. 'root' for *Os01g0700900*, 'seedling root' for *Os01g0701400* or 'root' and 'root tip' for *At2g26170*). Nevertheless, data were not collected and presented in the web service with the same manner; hence, it seems difficult to propose an exhaustive comparison of the pattern and/or level of expression of CYP711A encoding genes even within a single plant species. Among the other recurrent organs in which a high expression of CYP711A encoding genes was detected, we could cite the seed and the germinating seed (*Bradi1g75310, Os01g0700900, Os01g0701400*) or the flower (*Os02g0221900, At2g26170*). To complete this information, we performed a relative quantification of the *Bradi1g75310* gene expression in spikes, leaves and roots of 5 w old plants (WT, Bd21-3) grown hydroponically (**Figure 3.3B**). It appeared that the *Bradi1g75310* is not highly regulated in our conditions since levels of relative expression are similar: 1.49 ± 0.09 in roots, 1.29 ± 0.03 in leaves and 1.36 ± 0.05 in spikes. However, statistical analysis revealed that the slightly higher expression in roots compared to leaves is significant ($P = 0.017$).

C. THE *BRADI1G75310* GENE COMPLEMENTS *A. THALIANA MAX1-1* SHOOT PHENOTYPE

The *A. thaliana At2g26170* gene which encodes the AtCYP711A1 is also known as *MAX1* for *MORE AXILLARY GROWTH 1*. MAX1 was shown to catalyze an essential step in strigolactones biosynthesis downstream MAX3 and MAX4 carotenoid cleavage dioxygenases. A knock-out mutant for the *MAX1* gene exhibits a typical phenotype associated to SLs deficient or insensitive mutants: a significant increase of shoot branching due to an activation of axillary bud outgrowth. Based on that observation and to know whether BdCYP711A29 and MAX1 are functional homologs in the *A. thaliana* SLs biosynthetic

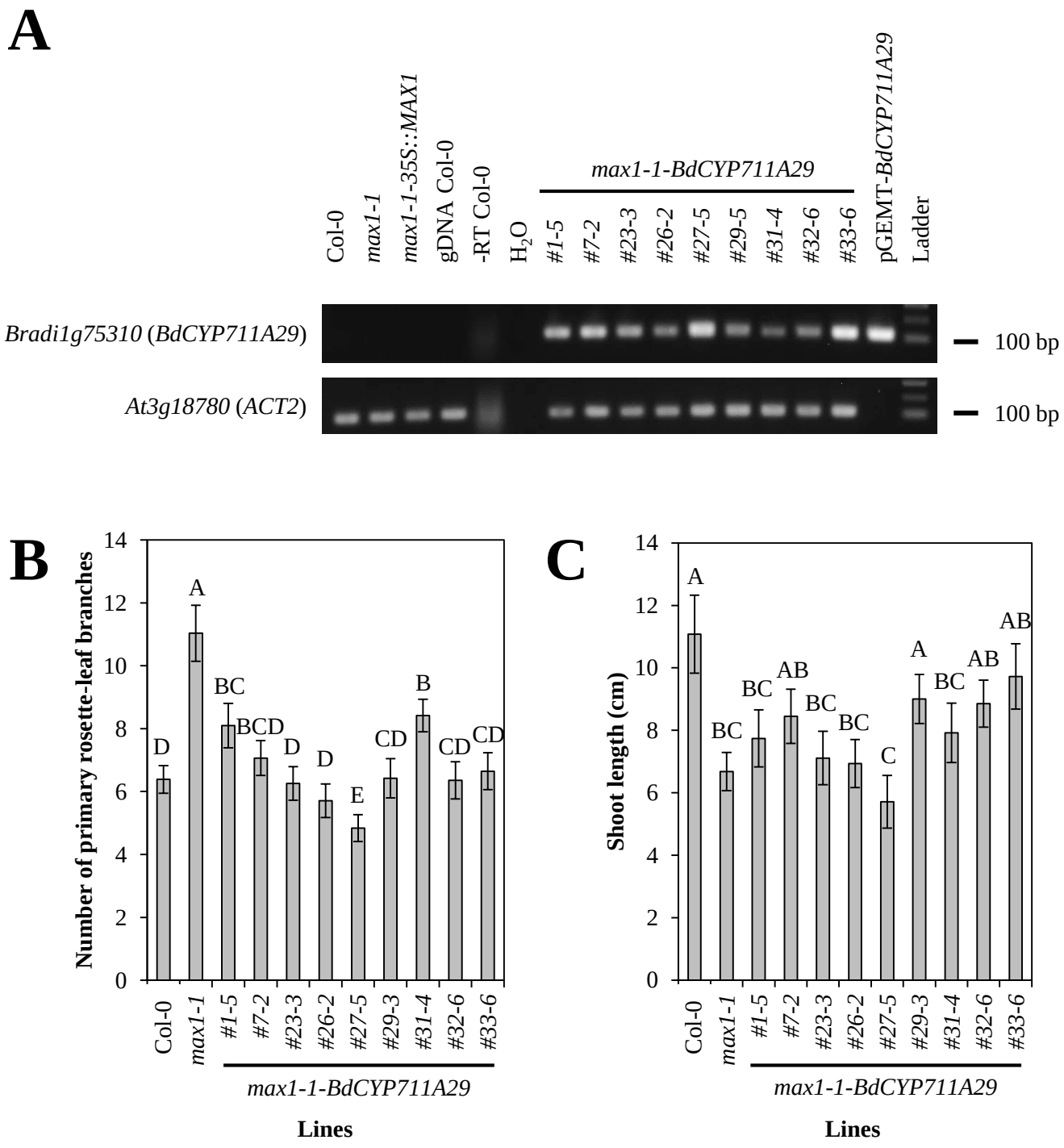

Figure 3.4: Genetic complementation of the *A. thaliana max1-1* mutant with the *B. distachyon Bradi1g75310* gene. A, RT-PCR analysis of the max1-1-BdCYP711A29s (*35S::Bradi1g75310*) lines. Contrast was adjusted based on ladder signal intensity. The Col-0 line (genetic background of the *max1-1* line), *max1-1* and *max1-1-35S::MAX1* were used as negative controls. ADNg of Col-0 and pGEMT-*BdCYP711A29* (pGEMT vector carrying the cDNA of *Bradi1g75310*) were used as positive controls for PCR amplifications of *ACT2* and *Bradi1g75310* genes, respectively. Non-reverse transcribed RNA of Col-0 (-RT Col-0) was used as a negative control for DNAse treatment efficiency following RNA extraction. **B**, Number of primary rosette-leaf branches and **C**, shoot length (cm) of WT (Col-0), mutant (*max1-1*) and transgenic (max1-1-BdCYP711A29s) lines. Mean number from n = 31 individuals ± standard error. Different letters indicate significant differences between conditions, Student test, $P < 0.05$.

pathway, we performed a genetic complementation of the *max1-1* mutant line. This technique has been routinely employed to characterize numerous MAX1 functional homologs. We cloned the *Bradi1g75310* cDNA into the pK7WG2.0 vector and transformed the *max1-1* line. In that construction, the transgene is placed under the control of the cauliflower mosaic virus 35S promoter (**Appendix 1**; Karimi et al., 2002). We characterized the 11 independent recombinant lines we obtained by RT-PCR through the amplification of a portion of the *Bradi1g75310* cDNA (**Figure 3.4A**). We amplified part of the *At3g18780* (*ACT2*) cDNA as a control for reverse transcribed RNA input. The Col-0 line (genetic background of the *max1-1* line), *max1-1* and *max1-1-35S::MAX1* were used as negative controls. This last line corresponds to a *max1-1* mutant line genetically complemented *via* the introgression of the cDNA of *MAX1* placed under the control of the 35S promoter (kindky provided by OTTOLINE LEYSER). Genomic DNA (gDNA) of Col-0 and pGEMT-*BdCYP711A29* plasmid DNA (pGEMT vector carrying the cDNA of *Bradi1g75310*) were used as positive controls for PCR amplifications of *ACT2* and *Bradi1g75310* genes, respectively. Non-reverse transcribed RNA of Col-0 (-RT Col-0) was used as a negative control for DNAse treatment efficiency following RNA extraction. A positive signal for *Bradi1g75310* expression was detected in each independent recombinant line.

We then evaluated the potential restoration of a WT phenotype by the *Bradi1g75310* gene *via* the evaluation of shoot branching of the recombinant lines. Using the decapitation method adapted from Challis et al. (2013) we counted the number of primary rosette-leaf branches per plant and measured plant height (**Figures 3.4B-3.4C**). The *max1-1-35S::MAX1* positive control line, received lately during the project, has not been integrated to that experiment but is presented in **Figures 3.7-3.10**. As expected, we observed a significant increase of shoot branching (11.03 ± 0.90 primary rosette-leaf branches per plant) and reduction of plant height (6.68 ± 0.61 cm) for the *max1-1* line as compared to Col-0 (6.39 ± 0.44 primary rosette-leaf branches per plant and 11.08 ± 1.24 cm). Each independent recombinant *max1-1-BdCYP711A29* lines showed a significant medium to strong reduction of shoot branching as compared to *max1-1*. On one hand, the two *A. thaliana* lines *max1-1-BdCYP711A29#1-5* and *#31-4* exhibited an intermediary level of shoot branching (8.10 ± 0.71 and 8.42 ± 0.52 primary rosette-leaf branches per plant, respectively) compared to Col-0 and *max1-1*. On the other hand, the *max1-1-BdCYP711A29#27-5* line, which seemed to exhibit the highest level of expression of the transgene (**Figure 3.4A**), was shown to be even less branched (4.84 ± 0.43 primary shoot per plant) than Col-0. The results were less clear regarding plant height, mostly due to data dispersal, since only *max1-1-BdCYP711A29#33-6*

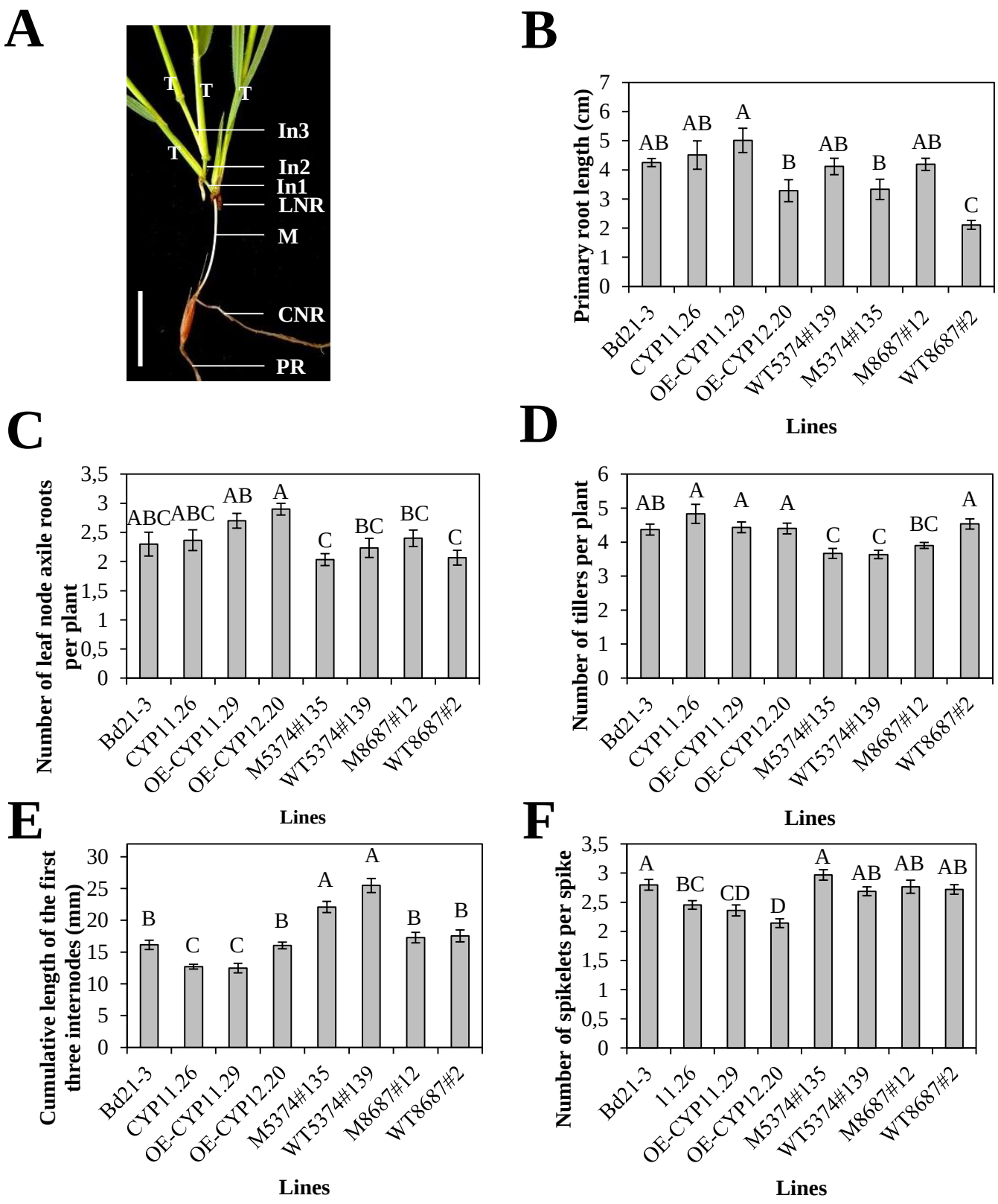

Figure 3.5: Alteration or modification of expression of the *Bradi1g75310* gene induce developmental changes in *B. distachyon*. **A**, Morphological structure of *B. distachyon*, T: tiller; In: internode; LNR: leaf node axile root; M: mesocotyl; CNR: coleoptile node axile root; PR: primary root. **B**, Primary root length of 7 d old plants grown on agar medium; n = 28. **C-E**, Number of LNR, tiller and first three internodes length of 3.5 w old plants grown on soil/perlite (2/1; v/v); n = 30. **F**, Number of spikelets per spikes of 4.5 w old plants grown on soil/perlite (2/1; v/v); n = 64. Mean numbers ± standard error, different letters indicate significant differences between conditions, Student test, $P < 0.01$.

(9.73 ± 1.04 cm) could be statistically distinguishable from *max1-1* but not Col-0. Overall, we observed a global tendency of partial complementation of shoot length for the other recombinant lines.

D. *B. DISTACHYON* LINES AFFECTED IN THE *BRADI1G75310* LOCUS OR GENE EXPRESSION SEEM TO EXHIBIT DIFFERENTIAL DEVELOPMENTAL PHENOTYPES

Strigolactones, as plant hormones, are known to be involved in numerous developmental processes (Al-Babili and Bouwmeester, 2015). Thus, we analyzed several developmental phenotypes in the different *B. distachyon* lines affected in the *Bradi1g75310* gene (TILLING mutant lines) or in its level of expression (overexpressing lines; **Figure 3.5**). For all statistical analyses (Student test), the statistical threshold has been lowered to $P < 0.01$ in order to increase the robustness of the results despite data dispersal and lighten the annotations on the histograms.

First, we measured the primary root (PR) length of 7 d old plants (end of transition between germination and vegetative phase) grown on agar medium (**Figure 3.5B**). Overall, values ranged from 2.11 ± 0.15 cm for WT8687#2 line to 5.01 ± 0.41 cm for OE-CYP11.29. The WT line (Bd21-3) exhibited a PR length of 4.25 ± 0.14 cm and is significantly not different from the two others control lines: CYP11.26 (4.5 ± 0.48 cm) and WT5374#135 (4.11 ± 0.28 cm). On the contrary, in the fourth control line (WT8687#2), PR length is significantly lower than in the three other lines, which suggests that this TILLING mutant family carries one or more point mutations which affect root growth. Each TILLING mutant line exhibited an increased PR length as compared to their own control line (+ 0.79 cm for 5374 and + 2.07 cm for 8687) but the difference was significant only between the two 8687 lines. As regard to overexpressing lines, OE-CYP11.29 exhibited a + 0.50 cm and OE-CYP12.20 a - 1.22 cm as compared to the null segregant CYP11.26. The difference between the two overexpressing lines is significant but both overexpressing lines appeared non-significant compared to their control line, the null segregant CYP-11.26.

We then focused on the vegetative phase of *B. distachyon* lifecycle and evaluated the number of leaf node axile roots (LNR) per plant, one of the two types of axile roots in *B. distachyon*, on 3.5 w old plant (end of the vegetative phase; **Figure 3.5C**; Watt et al., 2009). LNRs correspond to roots starting from the plant first node and, contrary to coleoptile node axile roots (CNRs) can be more than 2 per plant (**Figure 3.5A**). Values ranged from 2.03 ±

0.10 for M5374#135 to 2.90 ± 0.01 LNR per plant for OE-CYP12.20. All the control lines exhibited non-significantly different numbers of LNR (i.e. Bd21-3, CYP-11.26, WT5374#135 and WT8687#2). Therefore, Agrobacterium-mediated transformation, regeneration for the null segregant line and potential background point mutations for TILLING lines do not have any impact on this morphological trait. Not any overexpressing line (OE-CYP11.29 and OE-CYP12.20) or TILLING mutant line (M5374#135 and M8687#12) exhibited a significant difference with its own control line. On the contrary, the clearest difference was observed between the OE-CYP12.20 line which exhibits the highest level of expression of the *Bradi1g75310* gene (2.90 ± 0.01 LNR per plant) and the M5374#135 line which carries the strongest allele for the *Bradi1g75310* gene (2.03 ± 0.10 LNR per plant). Nevertheless, such difference is also observable between the same OE line and the TILLING control line WT8687#2.

The second morphological trait which has been measured at the end of the vegetative phase was the number of tillers per plant (**Figure 3.5D**). We measured between 3.63 ± 0.12 and 4.83 ± 0.28 tillers per plant (WT5374#135 and CYP11.26 respectively). Despite the statistically different reduced number of tillers per plant in the WT5374#135 TILLING control line as compared to the three other control lines (Bd21-3, CYP-11.26 and WT8687#2), no significant difference between a line of interest and its respective control line has been observed, except for M8687#12 mutant line which was significantly less branched as compared to its control line WT8687#2 (3.90 ± 0.01 and 4.53 ± 0.15 tiller per plant, respectively).

We also measured the sum of the length of the first three internodes at the end of the vegetative phase using ImageJ software (Schneider et al., 2012; **Figure 3.5E**). Most of the time, the first internode was not strongly elongated and therefore was not different between lines (data not shown) but the second and third ones were. In this experiment, values ranged from 12.48 ± 0.75 mm for OE-CYP11.29 to 25.47 ± 1.09 for WT5374#135. The WT line (Bd21-3) exhibited a length of 16.13 ± 0.74 mm, which was not significantly different from the other control line WT8687#2 with 17.53 ± 0.92 mm. On the contrary, the first three internodes of CYP11.26 were significantly shorter with 12.69 ± 0.37 mm and those from WT5374#135 TILLING control line were significantly longer with 25.47 ± 1.09 mm. When we payed attention to each individual line as compared to its own control line, we showed that overexpressing line OE-CYP12.20 presented significantly higher values (16.02 ± 0.53 mm) compared to CYP11.26, while OE-CYP11.29 was not significantly different. Concerning TILLING lines, none of mutant line exhibited significant difference with its control line.

Table 3.2: List of characteristic parent and product ions detected during multiple reaction monitoring (MRM) in *B. distachyon* (Bd21-3) exudates.

Hypothetic compounds (parent ion form) detected in MRM	Parent ion *m/z*	Daughter ion *m/z*	RT (min)
4-deoxyorobanchol [M + Na] [a]	353	241	4,2
Solanacyl acetate [M + H] [c, *]	325	97	4,2
Solanacyl acetate [M + H] [c]	325	279	11,5
Sorgomol [M + Na] [e, l, *] / Strigol [M + Na] [d, *]	369	272	5,5
Strigol [M - H_2O] [c]	329	215	5,9
Strigol [M - H_2O] [c, d, *] / Sorgomol [M - H_2O] [*]	329	97	7,4
Sorgomol [M + H] [c] / Strigol [M + H] [c]	347	215	7,5
DidehydroOrobanchol [M + Na] [e, *] / DidehydroStrigol [M + Na] [e, *]	367	270	6,0
DidehydroOrobanchol [M + Na] [*] / DidehydroStrigol [M + H] [*]	345	97	7,4
DidehydroOrobanchol [M + Na] [*] / DidehydroStrigol [M + H] [*]	345	248	9,6
Solanacol [M + Na] [e, n, *]	365	268	7,0
Solanacol [M + H] [*]	343	246	9,6
Orobanchyl acetate (Alectrol) [M + H] [h, m]	389	347	8,1
Orobanchyl acetate (Alectrol) [M + H] [c, d, h, k, m]	389	233	8,9
5-deoxystrigol [M + H] [b, c, d, *]/ Unknown 5 from Maize [M - OH] [b, *]	331	97	8,6
5-deoxystrigol [M + H] [b, c, d, *] / Unknown 5 from Maize [M - OH] [b, *]	331	97	9,5
Carlactonoic acid [M + H] [b, *]	333	97	8,9
Zealactones [M + H] [b] / Unknown 2 from Maize [M + H] [b]	377	345	9,1
Orobanchol [M - H_2O] [*]	329	97	9,2
Orobanchol [M + H] [c, d, h, i, m]	347	205	9,2
Orobanchol [M + H] [c, d, h, m, *]	347	97	9,2
Orobanchol [M + H] [d, h, i, j]	347	233	9,2
Hydroxyorobanchol [M + Na] [f, *]	385	288	9,2
Methoxy-5-Deoxystrigol [M + H] [g, *] / Heliolactone [M + H] [b, d, *] / Unknown 6 from Maize [M + H] [b, *]	361	97	10,7
Unknown 4 from Maize [M - OH] [b]	375	343	10,9

Each transition has been detected at least in 1 out of 3 independent experiments.
The four orobanchol transitions in grey have been validated using a standard in a preliminary experiment.
* SL specific transition: detection or release of a *m/z* 97 fragment.
[a] Boari et al., 2016
[b] Charnikhova et al., 2017
[c] Xie et al., 2015
[d] Iseki et al., 2018
[e] Yoneyama et al., 2008
[f] Khetkam et al., 2016
[g] Cardoso et al., 2014
[h] Kohlen et al., 2011
[i] Boutet-Mercey et al., 2017
[j] Foo and Davis, 2011
[k] Kohlen et al., 2013
[l] Yoneyama et al., 2010
[m] Pavan et al., 2016
[n] Xie et al., 2013

The last morphological phenotype we measured was the number of spikelets per spike at the mid-anthesis developmental stage on 4.5 w old plants (**Figure 3.5F**). The number of spikelets ranged from 2.14 ± 0.08 for OE-CYP12.20 to 2.9 ± 0.09 spikelets per spike for M5374#135. Regarding control lines, the CYP-11.26 null segregant line exhibited a slight and significant reduction of the number of spikelets per spike as compared to WT line (2.45 ± 0.07 and 2.80 ± 0.09, respectively). On the contrary, the TILLING control lines exhibited non-significantly different numbers of spikelets per spike (2.69 ± 0.08 and 2.72 ± 0.08 for WT5374#135 and WT8687#2 lines, respectively). We therefore observed a slight increase of the number of spikelets per spike in the 5374 TILLING mutant line as compared to its control line but it failed to be significantly validated ($P = 0.018$). The 8687 TILLING mutant line was not different from its control line (2.76 ± 0.11 spikelets per spike for the M8687#12 line). For each overexpressing line, we detected a slight to moderate reduction of spikelets as compared to CYP11.26 control line (2.35 ± 0.09 and 2.14 ± 0.08 spikelets per spike for OE-CYP11.29 and OE-CYP12.20 respectively) but statistical analysis confirmed only the difference between CYP11.26 and OE-CYP12.20.

Altogether, these data gave us information on control lines behavior as compared to WT line Bd21-3. First, we observed statistically significant differences between Bd21-3 and all the three control lines (CYP11.26, WT5374#135 and M8687#12) but not in all phenotypical analyses. The CYP11.26 line was significantly different from Bd21-3 when comparing first three internodes length and the number of spikelets per spikes, the TILLING line WT5374#135 was significantly different from Bd21-3 when comparing the number of tillers per plant and the first three internodes lengths and the TILLING line WT8687#2 differentially behaved compared to WT when comparing PR length.

E. OVEREXPRESSION OF THE *BRADI1G75310* GENE INCREASES OROBANCHOL EXUDATION FROM THE ROOTS OF *B. DISTACHYON*

E.1. Detection of SLs exuded from the roots of WT *B. distachyon*

To finalize the functional characterization of the *Bradi1g75310* gene as a partner in SLs biosynthesis in *B. distachyon*, we performed a detection and quantification of SLs exuded from plant roots. We chose to focus this experiment on the WT line (Bd21-3), the overexpressing line with the highest level of expression of the *Bradi1g75310* gene (OE-CYP12.20) and the TILLING mutant line encoding a truncated version of the BdCYP711A29 P450 (M5374#135). Plants were grown hydroponically 4 w in liquid ¼ MS medium then 1 w

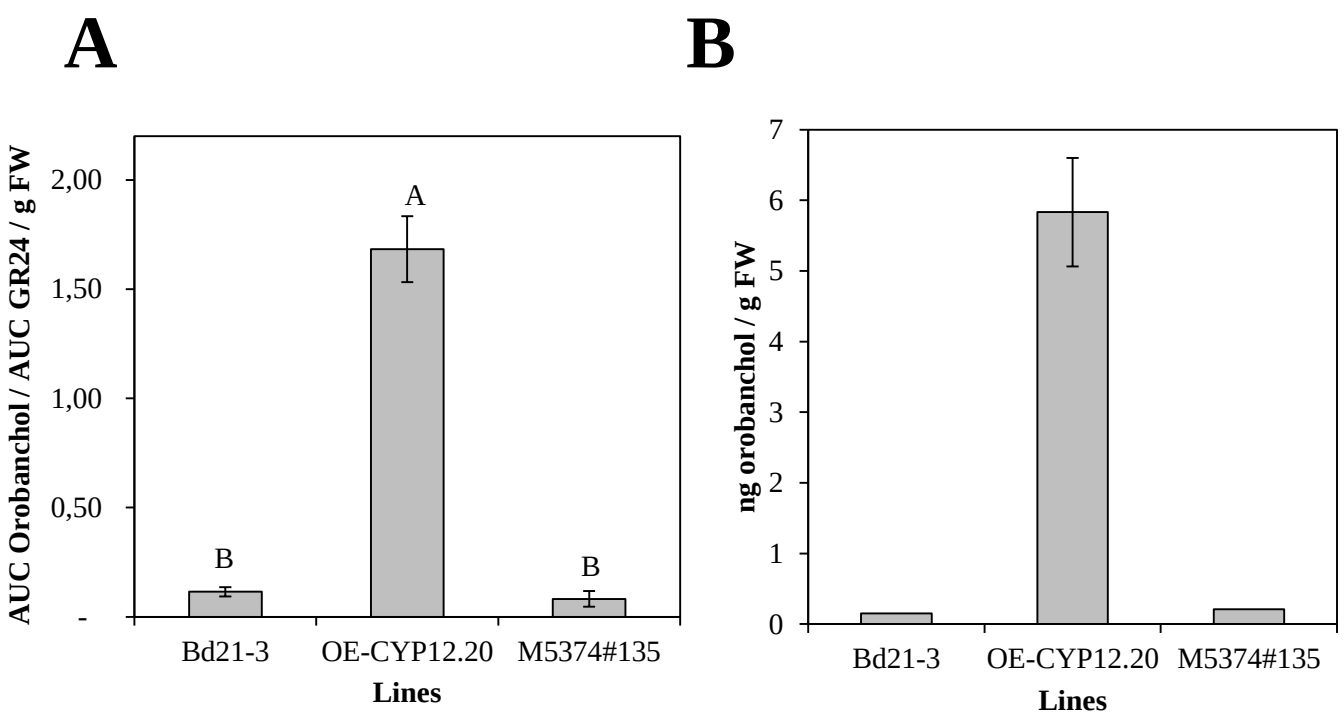

Figure 3.6: Quantification of orobanchol in *B. distachyon* exudates. Relative (**A**) and absolute (**B**) quantification of orobanchol in *B. distachyon* exudates after 7 d phosphorus starvation. AUC: Area under the curve. MRM transitions 321 > 224 and 347 > 97 were used to quantify GR24 and orobanchol signals, respectively. Mean of three biological replicates ± standard deviation. Different letters indicate significant differences between conditions, Mann and Witney test, $P < 0.05$. Statistical analysis have not been conducted for absolute quantification since two out of three biological replicates for Bd21-3 and 5374#135 lines exhibited too weak signals.

in liquid ¼ MS medium depleted in phosphate (-KH_2PO_4) in order to activate SLs biosynthesis. Exudation was performed during 24 h in fresh liquid medium. The recovered *B. distachyon* exudates were then extracted using ethyl acetate, supplemented with 10 ng (*rac*)-GR24 as the internal standard and analyzed by liquid chromatography coupled to tandem mass spectrometry (LC-MS/MS) *via* Multiple Reaction Monitoring (MRM). To the best of our knowledge, this is the first time that such experiments are conducted in *B. distachyon*.

Table 3.2 presents the chromatographic peaks of characteristic *m/z* MRM transitions detected at least in one biological replicate of the WT line as compared to blank sample (liquid ¼ MS –KH_2PO_4). We detected both orobanchol and strigol type SLs but most of detected transitions were not specific to one SL (e.g. 345 > 97, 345 > 248 and 367 > 270 could be linked to both didehydroorobanchol or didehydrostrigol), therefore preventing us from validating the compound detection. We therefore focused on compounds detected through at least two different characteristic transitions: orobanchol, orobanchyl acetate, solanacol and solanacyl acetate and each giving a chromatographic peak at only one RT. Among these, only orobanchol characteristic transitions were recorded at the same RT (9.2 min). An additional experiment on the WT line and conducted in the same conditions allowed us to detect a chromatographic peak with a similar RT (9.2 min) for 3 orobanchol characteristic transitions (347 > 205; 347 > 97 and 347 > 233). Finally, this RT was confirmed by adding orobanchol standard in samples, which resulted in a single peak at this same RT for each transition and similar ratios as in WT line (data not shown). Therefore, following MRM, we were able to confirm the presence of orobanchol in *B. distachyon* WT root exudates.

E.2. Quantification of orobanchol exuded from the roots of lines altered in the *Bradi1g75310* gene

We then quantified the relative amount of orobanchol exuded from the roots of the WT (Bd21-3), overexpressing (OE-CYP12.20) and TILLING mutant (M5374#135) lines by calculating the ratio between the area under the curve (AUC) of the 347 > 97 chromatographic peak, specific to orobanchol, and the AUC of the 321 > 224 chromatographic peak, specific to (*rac*)-GR24 (Boutet-Mercey et al., 2017). We normalized data over root fresh weight (**Figure 3.6A**)**.** We observed a significant increase of about 16 times of the relative quantity of orobanchol in OE-CYP12.20 exudates, as compared to WT and M5374#135 lines. No significant difference was observed between Bd21-3 and the TILLING mutant line. Indeed, a

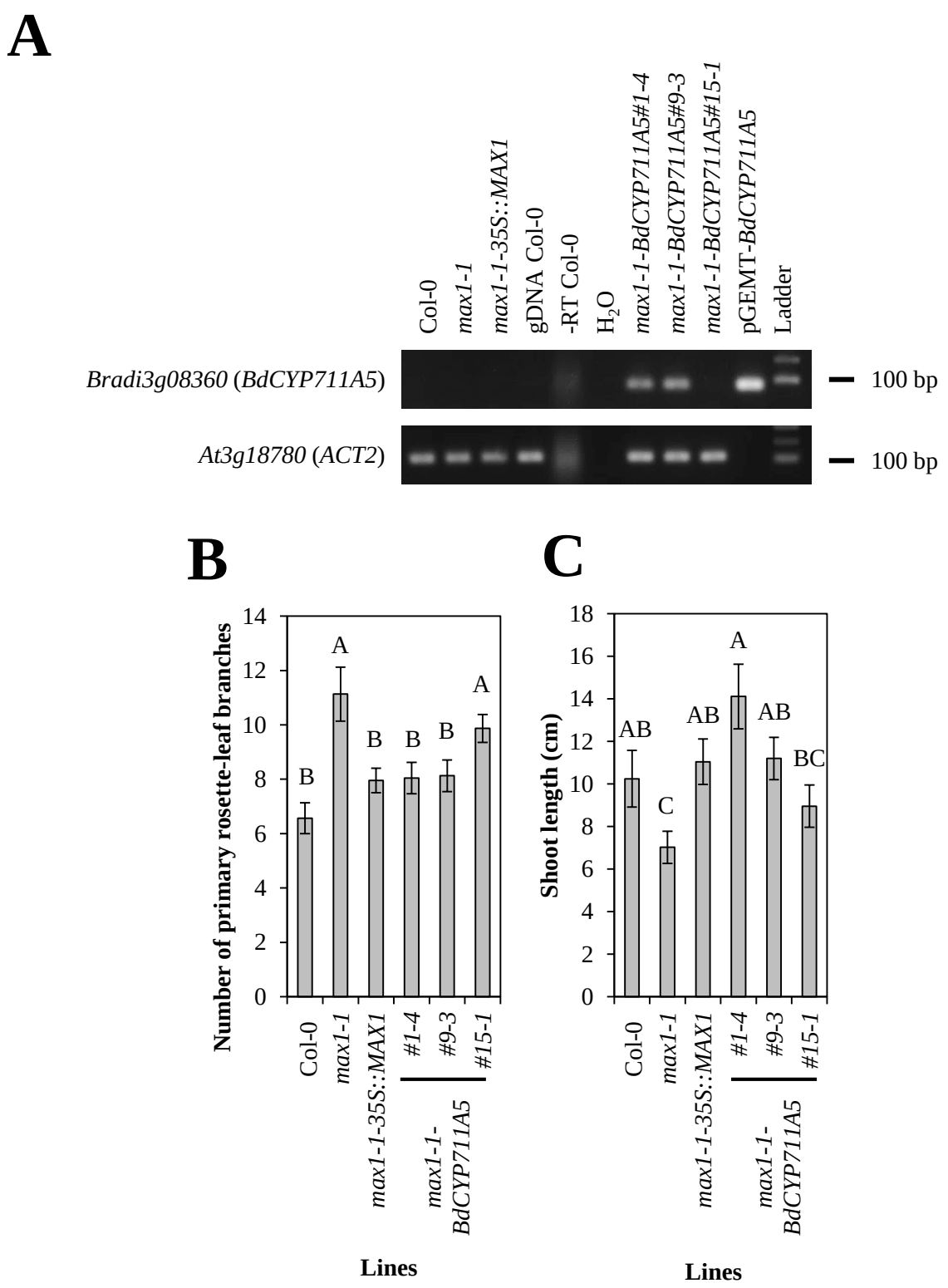

Figure 3.7: Genetic complementation of *A. thaliana max1-1* mutant with *B. distachyon Bradi3g08360* gene. A, RT-PCR analysis of the max1-1-BdCYP711A5s (*35S::Bradi3g08360*) lines. Contrast was adjusted based on ladder signal intensity. The Col-0 line (genetic background of the *max1-1* line), *max1-1* and *max1-1-35S::MAX1* were used as negative controls. ADNg of Col-0 and pGEMT-*BdCYP711A5* (pGEMT vector carrying the cDNA of *Bradi3g08360*) were used as positive controls for PCR amplifications of *ACT2* and *Bradi3g08360* genes, respectively. Non-reverse transcribed RNA of Col-0 (-RT Col-0) was used as a negative control for DNAse treatment efficiency following RNA extraction. **B**, Number of primary rosette-leaf branches and **C**, shoot length (cm) of WT (Col-0), mutant (*max1-1*), complemented (*max1-1-35S::MAX1*) and transgenic (max1-1-BdCYP711A5s) lines. Mean number from n = 23 individuals ± standard error. Different letters indicate significant differences between conditions, Student test, $P < 0.05$.

high coefficient of variation between biological replicates was observed for these two lines (18.3 and 44.0%, respectively) contrary to OE-CYP12.20 (9.0%).

We performed an absolute quantification of orobanchol *via* an internal calibration curve of this specific SL using a series of calibration solutions of orobanchol (10 µg.L^{-1} to 200 µg.L^{-1}) and the addition of the same concentration of reference standard (*rac*)-GR24 (100 µg.L^{-1}) in both calibration solutions and samples (**Figure 3.6B**). Two out of three biological replicates of the WT and TILLING mutant lines gave signals outside (lower than) the calibration curve and were therefore not considered (absence of standard deviation for these two lines). The production of orobanchol in Bd21-3 and M5374#135 were therefore evaluated at 0.149 and 0.212 ng orobanchol / g of roots, respectively, but these results should be considered very carefully. On the contrary, the orobanchol production of OE-CYP12.20 appeared more stable between biological replicates and far more important as compared to the other lines. We evaluated the orobanchol production of this line at 5.83 ± 0.77 ng / g of roots.

F. THE FOUR OTHER BDCYP711AS ARE MAX1 FUNCTIONAL HOMOLOGS

As mentioned in the introduction of this chapter, we also initiated the characterization of the four other BdCYP711A encoding genes present in the *B. distachyon* genome. We employed the same strategy of genetic complementation described above and transformed the *A. thaliana max1-1* mutant line with one of the four corresponding cDNAs of interest placed under the control of the 35S promoter. We generated 3 independent lines carrying the *Bradi3g08360* gene encoding BdCYP711A5, 3 independent lines carrying the *Bradi1g37730* gene encoding BdCYP711A6, 7 independent lines carrying the *Bradi4g08970* gene encoding BdCYP711A30 and 2 independent lines carrying the *Bradi4g09040* gene encoding BdCYP711A31. Transgene expression in each line was evaluated by RT-PCR and the shoot phenotype was evaluated according to the same decapitation method described above. The positive control line *max1-1-35S::MAX1* was included in those experiments.

Among the 3 independent lines carrying the *Bradi3g08360* (*BdCYP711A5*) gene, only two (*max1-1-BdCYP711A5#1-4* and *max1-1-BdCYP711A5#9-3*) were shown to express the transgene since no signal was observed for the third one by RT-PCR (*max1-1-BdCYP711A5#15-1*; **Figure 3.7A**). Regarding shoot phenotypes, as expected and already described, the *max1-1-35S::MAX1* was efficiently genetically complemented by the overexpression of the *MAX1* gene in the *max1-1* mutant genetic background since it exhibited 7.96 ± 0.45 primary rosette leaf branches compared to 11.13 ± 1.00 for *max1-1* (**Figure 3.7B**).

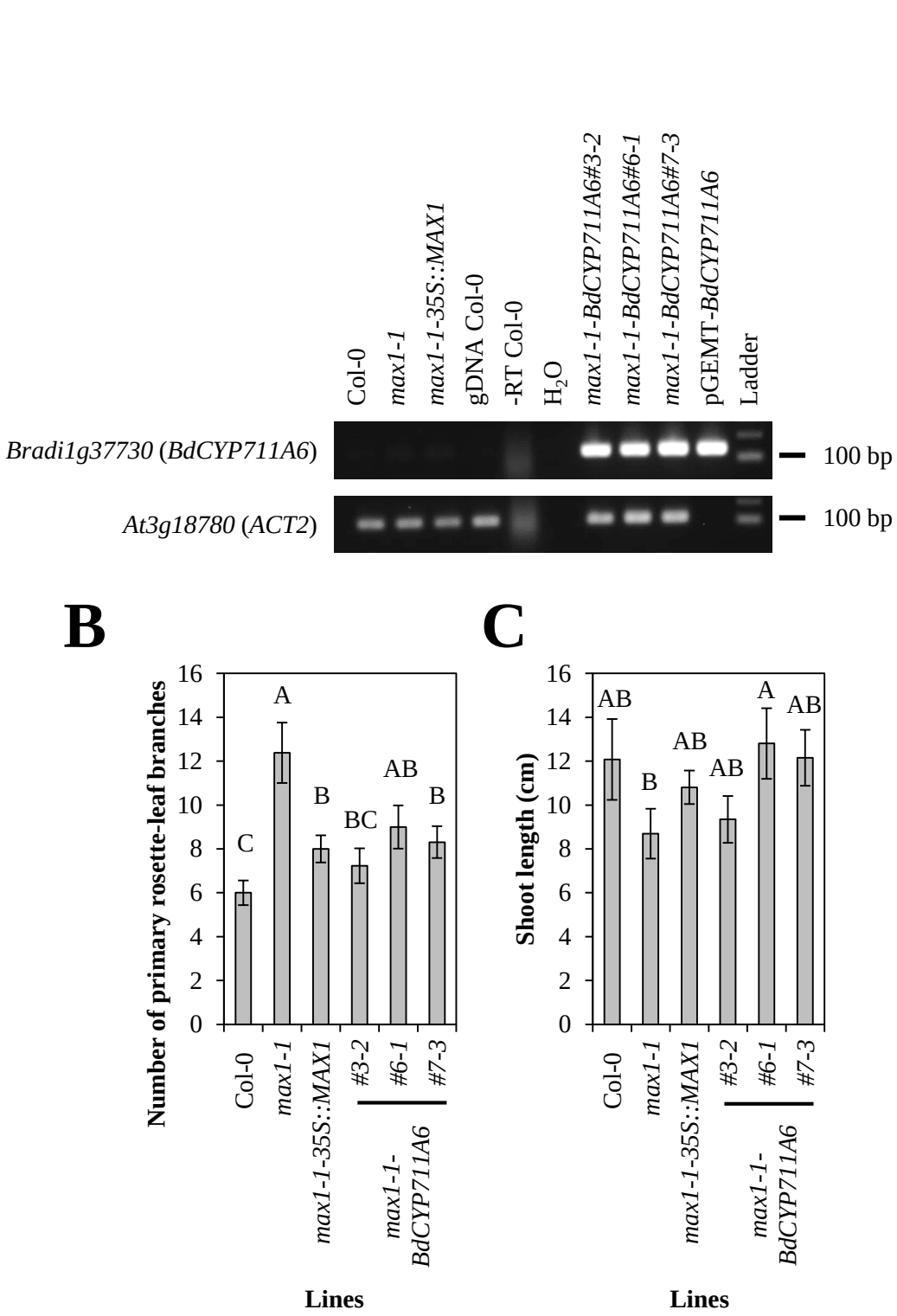

Figure 3.8: Genetic complementation of *A. thaliana max1-1* mutant with *B. distachyon Bradi1g37730* gene. A, RT-PCR analysis of the max1-1-BdCYP711A6s (*35S::Bradi1g37730*) lines. Contrast was adjusted based on ladder signal intensity. The Col-0 line (genetic background of the *max1-1* line), *max1-1* and *max1-1-35S::MAX1* were used as negative controls. ADNg of Col-0 and pGEMT-*BdCYP711A6* (pGEMT vector carrying the cDNA of *Bradi1g37730*) were used as positive controls for PCR amplifications of *ACT2* and *Bradi1g37730* genes, respectively. Non-reverse transcribed RNA of Col-0 (-RT Col-0) was used as a negative control for DNAse treatment efficiency following RNA extraction. **B**, Number of primary rosette-leaf branches and **C**, shoot length (cm) of WT (Col-0), mutant (*max1-1*), complemented (*max1-1-35S::MAX1*) and transgenic (max1-1-BdCYP711A6s) lines. Mean number from n = 13 individuals ± standard error. Different letters indicate significant differences between conditions, Student test, $P < 0.05$.

Moreover, the difference between these two lines has been statistically confirmed whereas Col-0 (6.57 ± 0.57) was not considered different. Among the transgenic lines, both two lines expressing the transgene were shown to group with Col-0 and *max1-1-35S::MAX1* (8.04 ± 0.58 and 8.13 ± 0.58 for *max1-1-BdCYP711A5#1-4* and *max1-1-BdCYP711A5#9-3*, respectively). On the contrary, the one which does not express the *Bradi3g08360* gene (*max1-1-BdCYP711A5#15-1*) was shown to be non-significantly different from the *max1-1* lines (9.87 ± 0.52). A similar tendency was observed for shoot length, but in a less clear manner (**Figure 3.7C**). Indeed, the four lines which grouped together in the previous experiment (WT, complemented and 2 out of 3 transgenic lines; 10.24 ± 1.33; 11.04 ± 1.06; 14.11 ± 1.52 and 11.20 ± 1.00 cm, respectively) were all shown to be significantly higher than the *max1-1* mutant line (7.02 ± 0.76 cm). Nevertheless, the third transgenic line which does not express the transgene (*max1-1-BdCYP711A5#15-1*) was shown to exhibit an intermediary phenotype (8.96 ± 1.00) and was therefore not significantly different from Col-0 or *max1-1* lines but was significantly smaller than *max1-1-BdCYP711A5#1-4*).

The second copy, BdCYP711A6 encoded by the *Bradi1g37730* gene, was also studied thanks to 3 independent transgenic lines (*max1-1-BdCYP711A6#3-2*, *max1-1-BdCYP711A6#6-1* and *max1-1-BdCYP711A6#7-3*) and each of them was shown to express the transgene (**Figure 3.8A**). Each transgenic line was also shown to exhibit a reduced number primary rosette-leaf branches (7.23 ± 0.80; 9.00 ± 0.99 and 8.31 ± 0.73, respectively) as compared to *max1-1* (12.39 ± 1.38; **Figure 3.8B**). Nevertheless, only *max1-1-BdCYP711A6#3-2* was shown to be non-significantly different from Col-0 (6.00 ± 0.57), the two others exhibiting a number of branches closer to the one exhibited by *max1-1-35S::MAX1* (8.00 ± 0.62) shown to have an intermediate phenotype between the WT and the mutant line in this experiment. The *max1-1-BdCYP711A6#6-1* line was even non-significantly different from the *max1-1* line. Again, information gained with shoot length measurements were more heterogeneous, especially regarding this experiment since we were not able to statistically differentiate Col-0 (12.08 ± 1.84 cm) from *max1-1* (8.69 ± 1.14 cm) because of data dispersal, reduced number of measures (n = 13) and despite the mean 3.39 cm difference between those lines (**Figure 3.8C**). Regarding transgenic lines, only *max1-1-BdCYP711A6#6-1* (12.81 ± 1.61 cm) was shown to be significantly higher than *max1-1*. All the other differences between lines height, including positive and negative control lines, were not significant. The two other transgenic lines exhibited a partial or very slight rescue of their shoot length (9.35 ± 1.06 and 12.15 ± 1.27 cm for *max1-1-BdCYP711A6#3-2* and *max1-1-BdCYP711A6#7-3*, respectively).

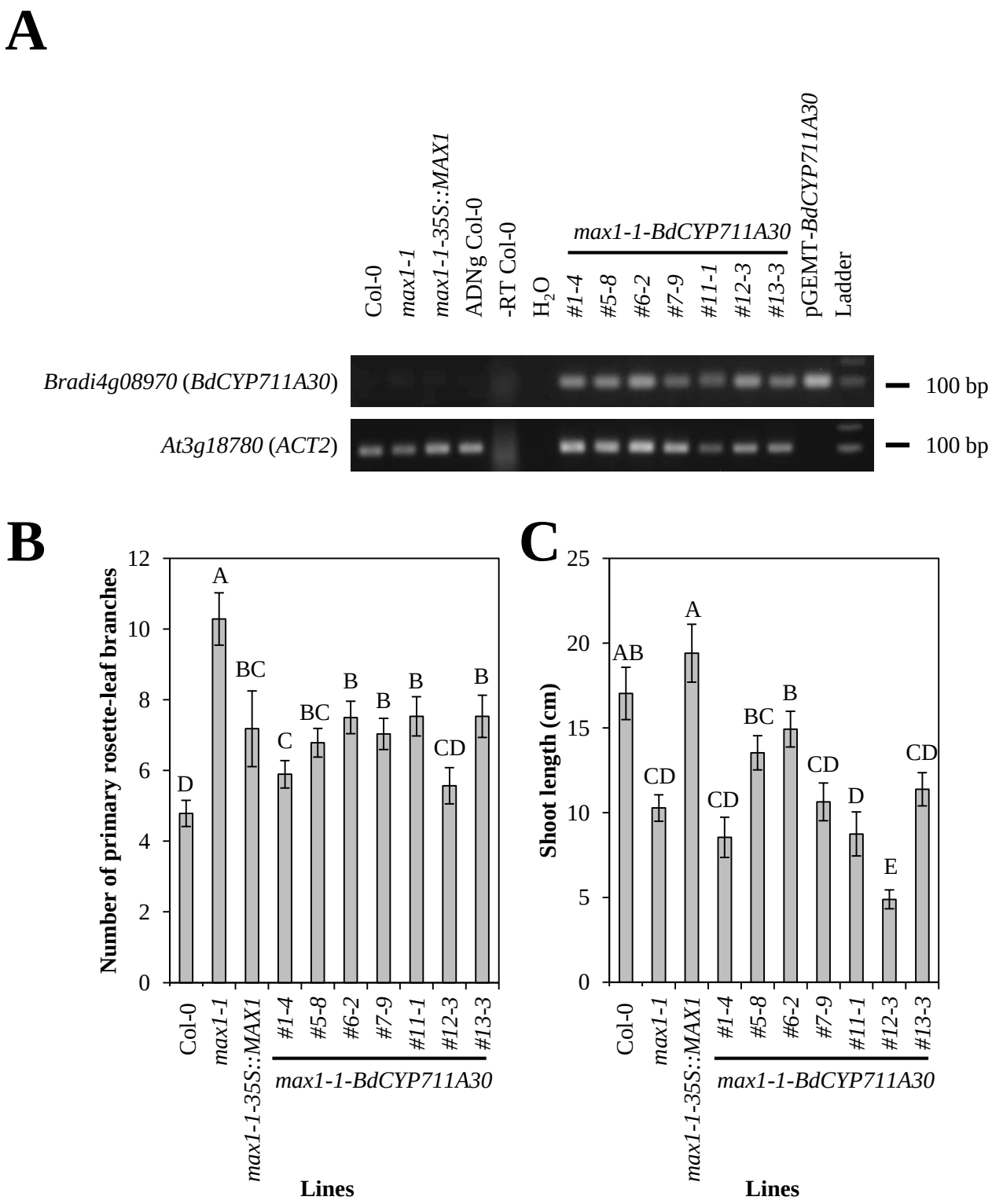

Figure 3.9: Genetic complementation of *A. thaliana max1-1* mutant with *B. distachyon Bradi4g08970* gene. A, RT-PCR analysis of the max1-1-BdCYP711A30s (*35S::Bradi4g08970*) lines. Contrast was adjusted based on ladder signal intensity. The Col-0 line (genetic background of the *max1-1* line), *max1-1* and *max1-1-35S::MAX1* were used as negative controls. ADNg of Col-0 and pGEMT-*BdCYP711A30* (pGEMT vector carrying the cDNA of *Bradi4g08970*) were used as positive controls for PCR amplifications of *ACT2* and *Bradi4g08970* genes, respectively. Non-reverse transcribed RNA of Col-0 (-RT Col-0) was used as a negative control for DNAse treatment efficiency following RNA extraction. **B**, Number of primary rosette-leaf branches and **C**, shoot length (cm) of WT (Col-0), mutant (*max1-1*) and transgenic (max1-1-BdCYP711A30s) lines. Mean number from n = 28 individuals ± standard error. Different letters indicate significant differences between conditions, Student test, $P < 0.05$.

The BdCYP711A30 copy was the one for which we obtained the largest number of independent transgenic lines. Each of the 7 transgenic lines was shown to express the *Bradi4g08970* gene, potentially with various efficiency (**Figure 3.9A**). Similarly to the decapitation experiments in which we tested BdCYP711A29 and BdCYP711A6 copies, the *max1-1-35S::MAX1* line showed an intermediary number of leaf-rosette branches (7.18 ± 1.07) as compared to Col-0 and *max1-1* (4.79 ± 0.37 and 10.29 ± 0.74, respectively; **Figure 3.9B**). The same tendency was observed for each of the transgenic lines with a number of leaf-rosette branches ranging from 5.57 ± 0.51 for *max1-1-BdCYP711A30#12-3* and 7.53 ± 0.60 for *max1-1-BdCYP711A30#13-3*. Statistical analyses confirmed these observations since every transgenic lines were significantly different from both WT and mutant line apart from line max1-1-BdCYP711A30#12-3 which grouped with Col-0. This last line might be the one which expresses the most the transgene according to RT-PCR results (**Figure 3.9A**). We also measured the shoot length of our different lines of interest but, as already observed, data were much more dispersed and only *max1-1-BdCYP711A30#6-2* (14.93 ± 1.06 cm) showed a significantly increased height compared to *max1-1* (10.29 ± 0.78 cm). The other *max1-1-BdCYP711A30* lines exhibited null or weak genetic complementation of their shoot length. Interestingly, the *max1-1-BdCYP711A30#12-3* line (4.90 ± 0.56 cm) was even shown to be shorter than the *max1-1* mutant, which is a contrasting result compared to the number of shoot branches.

We were only able to get 2 independent transgenic lines carrying the last gene of interest, *Bradi4g09040* encoding BdCYP711A31. Both lines were shown to express the transgene (**Figure 3.10A**) and were conducted in a decapitation experiment. Although *max1-1-BdCYP711A31#1-7* was shown to be fully complemented following *Bradi4g09040* introgression and regarding its average number of leaf-rosette branches (7.94 ± 0.46 compared to 7.06 ± 0.69 and 10.88 ± 1.22 for Col-0 and *max1-1*, respectively), *max1-1-BdCYP711A31#5-4* (10.06 ± 5.91) was not significantly different from the mutant (**Figure 3.10B**). Nevertheless, both lines were shown to exhibit a higher shoot height as compared to *max1-1* line and even positive control lines with an average of 15.78 ± 1.08 cm for *max1-1-BdCYP711A31#1-7* and 13.09 ± 1.10 cm for *max1-1-BdCYP711A31#5-4* as compared to 11.21 ± 1.51; 7.13 ± 0.80 and 10.91 ± 0.93 cm for Col-0, *max1-1* and *max1-1-35S::MAX1*, respectively (**Figure 3.10C**). Results appeared therefore clearer regarding shoot height than number of branches unlike previous experiments.

An overview of the genetic complementation experiments of the *A. thaliana max1-1* mutant line by the different *BdCYP711A* genes is shown in **Table 3.3**. It has been built using

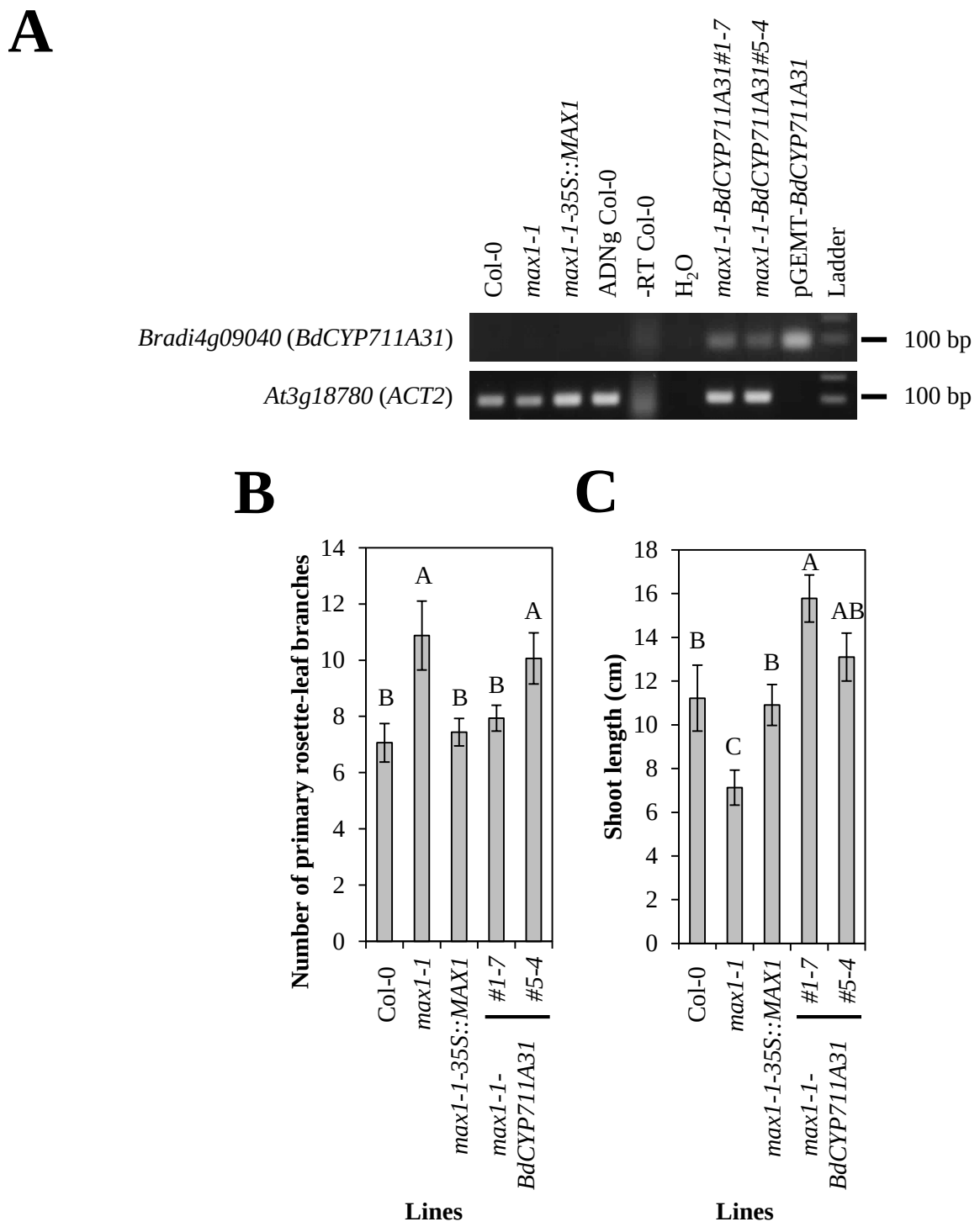

Figure 3.10: Genetic complementation of *A. thaliana max1-1* mutant with *B. distachyon Bradi4g09040* gene. **A**, RT-PCR analysis of the max1-1-BdCYP711A31s (*35S::Bradi4g09040*) lines. Contrast was adjusted based on ladder signal intensity. The Col-0 line (genetic background of the *max1-1* line), *max1-1* and *max1-1-35S::MAX1* were used as negative controls. ADNg of Col-0 and pGEMT-*BdCYP711A31* (pGEMT vector carrying the cDNA of *Bradi4g09040*) were used as positive controls for PCR amplifications of *ACT2* and *Bradi4g09040* genes, respectively. Non-reverse transcribed RNA of Col-0 (-RT Col-0) was used as a negative control for DNAse treatment efficiency following RNA extraction. **B**, Number of primary rosette-leaf branches and **C**, shoot length (cm) of WT (Col-0), mutant (*max1-1*) and transgenic (max1-1-BdCYP711A31s) lines. Mean number from n = 28 individuals ± standard error. Different letters indicate significant differences between conditions, Student test, $P < 0.05$.

lines evaluated to express the most or the less each transgene of interest based on semi-quantitative RT-PCR results. Based on our observations, we could split the five genes of interest into 3 groups depending on their ability to genetically complement one or both of the analyzed shoot phenotypes. The first group is composed by the *BdCYP711A5* gene which appears to partially complement both traits. The second is composed by the *BdCYP711A6*, *A29* and *A31* genes which all showed a better ability to genetically complement shoot branching (number of primary rosette-leaf branches) than shoot length. The last one is composed by the *BdCYP711A31* gene for which an opposite situation emerged: it appeared to better complement shoot height compared to branching.

G. CONCLUSION

The main objective of this chapter was to assign an endogenous function to the P450 encoded by the *Bradi1g75310* gene. Several phylogenetic evidences led us to test whether BdCYP711A29 is involved in SLs biosynthesis in the model temperate cereal *B. distachyon*. First, this P450 belongs to the same subfamily, CYP711A, as copies from various plant species characterized as enzymes involved in the last steps of SLs biosynthesis: AtCYP711A1 (MAX1) from *A. thaliana* or OsCYP711A2, A3, A5 and A6 from *O. sativa* for example. Second, BdCYP711A29 shares between 46.3 and 58.27% of amino acid sequence identity with the copies cited above, a high degree of similarity considering the very high degree of sequence diversity between P450s. This second point is illustrated by our phylogenetic analysis in which BdCYP711A29 appeared in the same clade as two functionally characterized *O. sativa* copies, OsCYP711A2 and OsCYP711A3, shown to be a carlactone oxidase and an orobanchol synthase, respectively. Nevertheless, we also observed a higher rate of polymorphism for BdCYP711A29, likely to reflect a diversification which could lead to either subfunctionalization or neofunctionalization of this copy. Therefore, we also studied *in silico* the expression pattern of our gene of interest as compared to the copies from rice and *A. thaliana* shown to be involved in SL biosynthesis. For each copy, including *Bradi1g75310*, we observed a peak of expression in roots which was furtherly confirmed by our gene expression analysis in spikes, leaves and roots of the *B. distachyon* Bd21-3 line. In addition, expression of our gene of interest was shown to be induced in seed and seedling as the two rice copies encoding CYP711As shown to group in the same phylogenetic clade as *Bradi1g75310*: *Os01g0700900* and *Os01g0701400*. Despite the higher level of polymorphism observed in the BdCYP711A29 sequence, it therefore appeared that the *Bradi1g75310* gene

Table 3.3: Overview of the genetic complementation experiments of *A. thaliana max1-1* mutant line by *BdCYP711A* genes.

***BdCYP711A* copy expressed in *A. thaliana max1-1* line**	**Line with the maximum expression level of the transgene (line max) [a]**	**Line with the minimum expression level of the transgene (line min) [a]**	**Complementation of shoot branching (line max/line min) [b,c,d]**	**Complementation of shoot height (line max/line min) [b,c,d]**
BdCYP711A5	#1-4	#9-3	++/++	++/+
BdCYP711A6	#6-1	#3-2	++/+	++/0
BdCYP711A29	#27-5	#31-4	+++/+	0/0
BdCYP711A30	#5-8	#7-9	+/+	0/0
BdCYP711A31	#1-7	#5-4	++/0	+++/++

[a] Estimation based on RT-PCR signal intensity of the transgene compared to *ACT2*.

[b] Complementation of *max1-1* number of leaf-rosette primary branches and shoot length compared to Col-0.

[c] 0: non complementation (statistically non-different from *max1-1*); +: partial complementation (statistically non-different/between *max1-1* and Col0); ++: total complementation (statistically non-different from Col-0); +++: less branched/higher than Col-0 (statistically different from Col-0).

[d] Colors indicate equivalent (yellow), increased (red) or reduced (blue) level of genetic complementation between phenotypes.

follows a similar general gene expression pattern as compared with the other MAX1 functional homologs.

The genetic complementation of the *A. thaliana max1-1* mutant line is an easy manner to test whether a P450 is a functional homolog of AtCYP711A1. Our transformation of the SL-deficient *A. thaliana* mutant line led us to generate 9 independent transformant lines, each expressing the *Bradi1g75310* transgene under the 35S promoter. The number of primary rosette leaf branches was partly to fully restored in the transformant lines and we observed a clear tendency of increased height as compared to *max1-1* which have often been not statistically confirmed due to data dispersal. However, our results are clear enough to conclude on the functional homology between BdCYP711A29 and AtCYP711A1. MAX1 was shown to catalyze 3 consecutive oxidations on carlactone (CL) to form carlactonoic acid (CLA), a SL which could be directly recognized by the AtD14 SL receptor and which is not furtherly transformed by MAX1 (Abe et al., 2014). BdCYP711A29 might therefore catalyze the same reaction when expressed in *A. thaliana* but we cannot exclude that it catalyzes the transformation of CL into another SL with similar biological activities, especially because most of the transformants exhibited partial complementation of one or two of the evaluated traits.

Because strigolactones are a group of hormones shown to be involved in numerous developmental processes in various plant species, we hypothesized that if the *Bradi1g75310* gene encodes an enzyme involved in SLs biosynthesis, we should observe differential developmental phenotypes between our different *B. distachyon* lines. It is first important to notice that no obvious phenotype has been observed between lines in terms of general appearance (e.g. height or level of branching) and developmental timeline (e.g. time for germination or flowering). Moreover, not any SL-associated phenotype has been described yet in *B. distachyon*. We therefore performed a general phenotyping experiment and focused on several easily quantifiable specific traits. First, we noticed that our different control lines (null segregant and TILLING control lines) do not always behave as the WT line Bd21-3. Indeed, the null segregant line CYP11.26 exhibited shorter internode length and less spikelets per spike as compared to Bd21-3; the TILLING control line WT5374#135 exhibited less tillers per plant and an increased internode length and WT8687#2 showed reduced PR length as compared to Bd21-3. It therefore appeared that the regeneration processes which might induce epigenetic changes in CYP11.26 and the background point mutations for TILLING lines are responsible for differential developmental phenotypes by themselves. When focusing on TILLING mutant lines, it appeared that the two lines of interest mostly behave

differentially, especially with regards to their own control line. The only clear tendency we could observe was an increased primary root (PR) length for M5374#135 and M8687#12 as compared to their respective control lines; nevertheless, statistical analyses only confirmed the difference between the two 8687 lines. OE lines showed more often comparable phenotype as compared to CYP11.26: increased number of leaf node axile roots (LNRs) per plant, increased internode length and reduced number of spikelets per spike. Unfortunately, none of these observations could be fully statistically confirmed especially when considering the OE-CYP11.29 line which exhibited intermediary phenotypes between CYP11.26 and OE-CYP12.20. This situation might reflect, and be correlated to, the overexpression level of the *Bradi1g75310* gene in these lines. Overall, in our conditions, it appeared really complicated to strongly associate a developmental phenotype to the lines altered in the *Bradi1g75310* gene locus or expression. Nonetheless, recurrent observations of differential developmental phenotypes between these lines and the WT Bd21-3 support our conclusion of a *Bradi1g75310* involvement in plant architecture modulation in *B. distachyon*. No information is available about phenotypes associated to SLs deficiency, insensitivity or overproduction in *B. distachyon*; in rice, the phylogenetically closest plant species in which SLs are largely studied, this information is only available for SL deficient and insensitive mutants. These rice mutant plants were shown to exhibit more tillers, a reduced height, enhanced lamina joint inclination, reduced crown root length, delayed leaf senescence and an increased in mesocotyl length (Arite et al., 2009; Arite et al., 2012; Cardoso et al., 2014; Hu et al., 2014; Li et al., 2014; Yamada et al., 2014). Contrary to rice, we did not observe an increased number of tillers in mutant lines. We did not perform an exhaustive quantification of plant height but decided to focus on the first three internode length to avoid misinterpretation of the results and clearly differentiate stem and limb length but no difference between mutant and control TILLING lines has been observed. The last four other phenotypes have not been studied in our work because of the growth conditions needed for evaluate these traits or because of *B. distachyon* specific root and shoot architecture. In conclusion, no clear correlation could be made between rice deficient or insensitive mutant and our *B. distachyon* TILLING mutant lines. Therefore, if the *Bradi1g75310* gene encodes an SLs biosynthetic enzyme, functionally redundant activities in *B. distachyon* could be responsible for these slight and non-homogenous developmental phenotypes between WT and lines altered in the *Bradi1g75310* locus or gene expression.

The detection and quantification of SLs produced by our different lines of *B. distachyon* gave us more clues about the biochemical activities of BdCYP711A29. We were

only able to detect SLs exuded from plant roots grown hydroponically since we obtained weak and unreproducible signals when we tried to detect SLs *in planta* (data not shown). We retrieved 26 *m/z* transitions in MRM which could correspond to 19 different SLs but were only able to confirm the presence of orobanchol. Indeed, 4 specific transitions were detected for this compound in which 3 were specifically confirmed by a preliminary experiment using an orobanchol standard and allowed us to validate the retention time (RT). Orobanchol concentration in root exudates was high enough and quite stable between biological replicates, we therefore had the opportunity to perform an absolute quantification of this compound between our different *B. distachyon* genotypes. Interestingly, we detected 16 times more orobanchol in OE-CYP12.20 as compared to Bd21-3 and M5374#135. The high accumulation of this specific SL might reflect the imbalance generated in the SLs biosynthetic pathway by the overexpression of the *Bradi1g5310* gene and hence that BdCYP711A29 is responsible for orobanchol biosynthesis in *B. distachyon*. Orobanchol is the most abundant naturally occurring SL and in rice it was shown to be mostly synthetized by OsCYP711A3 from 4-deoxyorobanchol (*ent*-2′-*epi*-5deoxystrigol, Zhang et al., 2014; Zwanenburg and Blanco-Ania, 2018). OsCYP711A3 was also shown to catalyze CL conversion into CLA and therefore catalyze the same reactions in SLs biosynthesis as ZmMAX1b from maize (Yoneyama et al., 2018). This observation led the authors to classify these two copies in the A3-type P450s involved in CL oxidation into CLA and in the conversion of 4-DO into orobanchol (**Chapter I, Figure 1.25**). Our study supports the classification of our *B. distachyon* P450 of interest into this category. Indeed, its ability to genetically complement the *A. thaliana max1-1* phenotype and the overproduction of orobanchol by *B. distachyon* overexpressing line OE-CYP12.20 suggest that BdCYP711A29 can catalyze both reactions.

To conclude this chapter, we initiated the functional characterization of the four other BdCYP711A copies *via* their ectopic expression in the *A. thaliana max1-1* mutant line and, as for BdCYP711A29, quantified the number of leaf-rosette primary branches and measured the shoot length of the independent transgenic lines we could obtain for each copy. We were able to include in those experiments the *max1-1* line complemented with the cDNA of the *At2g26170* (*MAX1*) gene placed under the control of the 35S promoter (*max1-1-35S::MAX1*) as a positive control. As previously described by Challis et al. (2013), the overexpression of the *MAX1* gene in the *max1-1* genetic background allowed partial to full complementation of the mutant shoot phenotypes. Apart from one experiment (**Figure 3.8C**), we were able to statistically confirm the genetic complementation of the *max1-1-35S::MAX1* line. We recovered several independent lines for each construction which almost all express the

transgene of interest. Data collected on the number of primary branches were systematically more homogeneous and allowed us to observe, as for *max1-1-35S::MAX1*, a partial to full complementation of the *max1-1* number of branches in all recombinant lines except for *max1-1-BdCYP711A5#15-1* which seemed not to express the transgene, *max1-1-BdCYP711A6#6-1* and *max1-1-BdCYP711A31#5-4*. For the last two lines, fewer shoot branches were observed but this could not be statistically confirmed. Regarding plant height, the genetic complementation of the *max1-1* mutant line was much less obvious. Indeed, in most cases, we were not able to statistically differentiate transgenic lines from the *max1-1* mutant line. No clear correlation appeared between the level of expression of the transgene, the average number of primary branches and the average height which is the reason why, on one hand, we hypothesized that our growth conditions might not have been optimal and hindered shoot elongation but not emergence. On the other hand, contrary to what has been observed for all the other copies, the two *max1-1-BdCYP711A31* recombinant lines showed a very clear complementation of shoot length (**Figure 3.10C)** and less homogeneous complementation of the number of shoot branches (**Figure 3.10B; Table 3.2**). This could reflect a specific activity linked to this copy compared to the other ones. Indeed, because the five *B. distachyon* CYP711A copies can, at least partly, complement the shoot phenotypes of the *max1-1* line, we can assume that they catalyze different reactions, which could explain their maintenance in *B. distachyon* genome. With the same logic and as we discussed in the introduction (**section I.D.1.**), this diversity of chemical reactions and therefore of products (SLs) might reflect the numerous physiological processes involving SLs. We could therefore hypothesize that the product of BdCYP711A31 biochemical activity in *A. thaliana* could have a higher impact on shoot elongation than on branches emergence. Overall, it clearly appeared that the five BdCYP711As are able to, at least partly, complement *max1-1* mutant line phenotypes and might therefore be considered as MAX1 functional homologs although they are likely to catalyze different reactions.

CHAPTER IV | RESULTS (3/3)

Preliminary study of the role of strigolactones in the *B. distachyon – F. graminearum* interaction

A

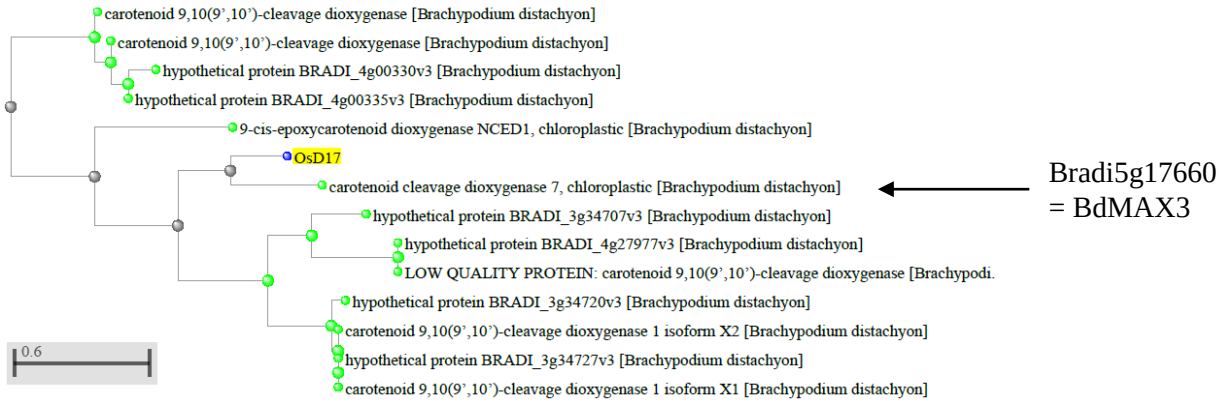

B

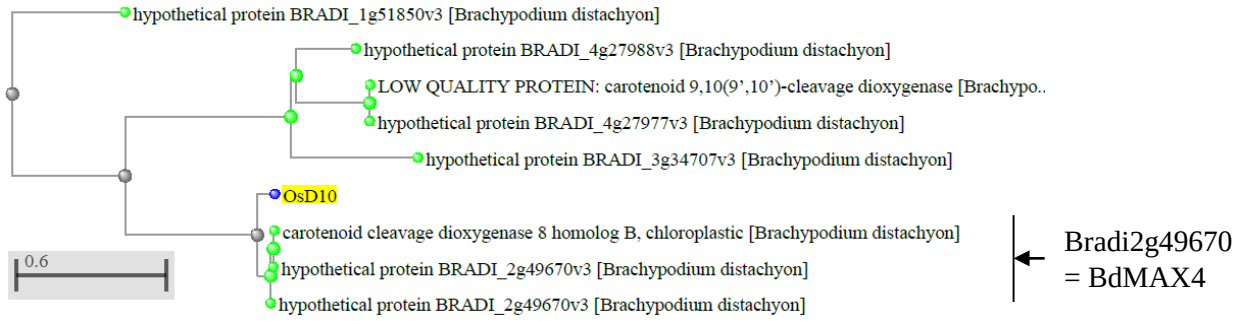

Figure 4.1: Phylogenetic analysis of D17 and D10 *B. distachyon* homologs. Rice amino-acid sequences of D17 (OsCCD7, **A**) and D10 (OsCCD8b, **B**) have been used as bait to identify homologous protein in *B. distachyon* genome using BlastP and design Neighbor Joining phylogenetic trees. The tree is drawn to scale, with branch lengths measured in the number of substitutions per site. Analyses were conducted using the NCBI BLAST webtool.

A. INTRODUCTION

We recorded in the introduction (**Chapter I, section D.6.**) that SLs are not only studied in beneficial plant-microbe interactions but more and more when plants face detrimental microorganisms. Nevertheless, no paradigm for SLs involvement in plant-pathogen interactions emerged yet. First, pathogens behavior towards SLs appears to be highly variable depending on the microorganism species; then, several results could not be confirmed in independent studies probably because of the importance of the experimental set-up. Indeed, the direct impact of SLs on pathogen morphology *ex planta* was shown to vary between no effect and inhibition of radial growth concomitant with the activation of hyphal branching (these experiments have been conducted only on fungi and oomycetes, **Chapter I, Table 1.7**). At the physiological point of view, SLs were shown to impact mitochondrial metabolism of pathogenic fungi since studies reported the alteration of cell respiration (**Chapter I, Table 1.8**). The use of SL deficient or insensitive plant mutants gave also contrasting results regarding SL involvement in plant resistance/susceptibility towards pathogenic microorganisms. A number of plant-pathogen combinations have been tested and studies seems to converge into two main but different conclusions: whether SLs seem not involved in the interaction, or SLs participate in a direct or indirect plant defense mechanism towards the pathogen (**Chapter I, Table 1.10**).

In our study, we already showed that the *Bradi1g75310* gene is highly transcriptionally induced during FHB and that it constitutes a susceptibility factor of *B. distachyon* towards *F. graminearum* infection. Our functional study of BdCYP711A29 allowed us to conclude on its homology with the phylogenetically related P450 MAX1 from *A. thaliana*. Moreover, we showed that the overexpression of the BdCYP711A29-encoding gene in *B. distachyon* was responsible for orobanchol accumulation in root exudates. We were therefore wondering whether the transcriptional activation of the *Bradi1g75310* gene in the FHB context was illustrative of the involvement of SLs in the *B. distachyon* response towards *F. graminearum* infection. We first evaluated if the *B. distachyon* SLs core biosynthetic pathway is activated during FHB; then tested whether SLs, and more specifically orobanchol, had an impact on *F. graminearum* growth *ex planta*. We conclude this chapter with the transcriptional study of defense related genes in our different *B. distachyon* lines in response to FHB.

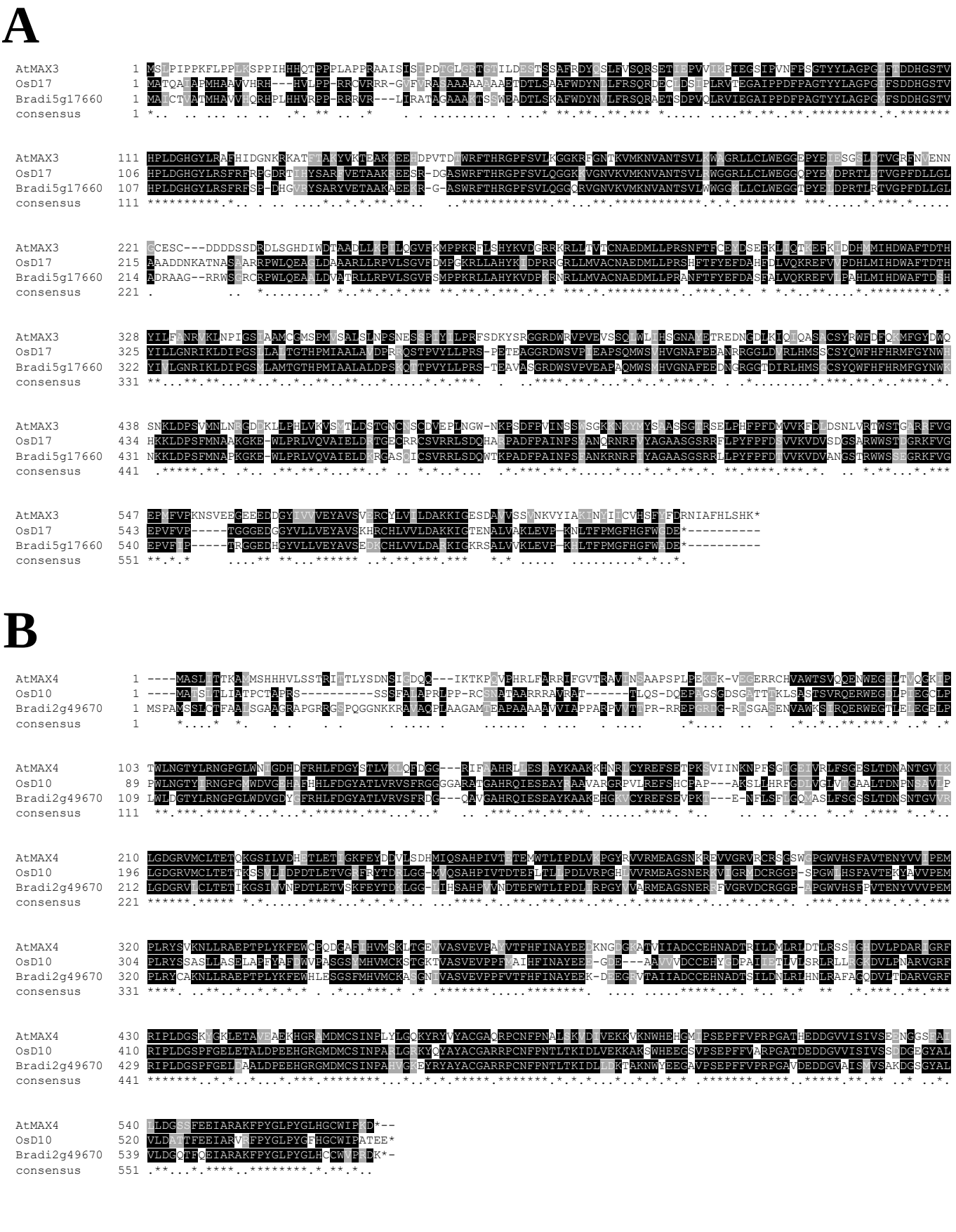

Figure 4.2: Multiple amino-acid sequence alignment of MAX3 and MAX4 orthologs from *B. distachyon*, *O. sativa* and *A. thaliana*. **A**, Multiple amino-acid sequence alignment between AtMAX3, OsD17 and Bradi5g17660. **B**, Multiple amino-acid sequence alignment between AtMAX4, OsD10 and Bradi2g49670. Both alignments were build using ClustalW program. Black, grey and white boxes indicate conserved, similar and non-conserved residues between sequences, respectively.

B. *B. DISTACHYON* SLS BIOSYNTHETIC PATHWAY IS ACTIVATED DURING FHB

As described in the introduction (**Chapter I, section D.2.**) the two genes encoding the carotenoid cleavage dioxygenases CCD7 and CCD8 in the core biosynthetic pathway have been shown to be upregulated in SLs deficient or insensitive mutants and that a SL treatment could restore WT expression levels due to a a negative feedback control of these genes by SLs. The transcriptional regulation of these two genes is therefore a clue to evaluate SLs production in specific conditions and they are often used as markers indicative of the overall functional status of the whole biosynthetic pathway. We identified the homologs of these two genes in *B. distachyon* genome *in silico* to follow their transcriptional profile during FHB.

CCD7 and CCD8 are two enzymes involved in the metabolization of 9-*cis*-β-carotene, the product of the 9-*cis*-/all-*tran*-β-carotene isomerase D27 activity, into carlactone (CL), the last common parent molecule of SLs. *CCD7* genes are, to date, found in a single copy in plant genomes, contrary to *CCD8* genes which exhibit a more complex evolutionary history since 4 copies are found in rice, 2 in maize, 6 in sorghum and only one in *A. thaliana* genome (Vallabhaneni et al., 2010). The rice copy *OsCCD8b* (*D10*) was shown to use two β-apo-10´-carotenal isomers to form β-apo-13'-carotenone from all-*trans*-β-10'-carotenal and carlactone from 9'-*cis*-β-apo-10'-carotenal (Alder et al., 2012). We therefore used the OsCCD7 (D17) and OsCCD8b (D10) amino-acid sequences from rice as baits to identify putative functional homologs in *B. distachyon*. For each rice protein, we were able to identify a single homolog in *B. distachyon* with clear phylogenetic relatedness. We confirmed our prediction using the reciprocal BLAST method. Indeed, OsCCD7 exhibited a close phylogenetic relationship with Bradi5g17660 (therefore named BdMAX3) and OsCCD8b with Bradi2g49670 (therefore named BdMAX4) proteins (**Figure 4.1**). The high degree of protein sequence homology between *A. thaliana*, rice and *B. distachyon* CCD7 and CCD8 proteins is illustrated by multiple sequence alignments in which BdMAX3 and BdMAX4 appeared as full-length copies (**Figure 4.2**).

We benefited from the characterization of *BdMAX3* and *BdMAX4 in silico* to test whether their transcriptional profile was affected in healthy spikes of the different lines altered in the *Bradi1g75310* locus or gene expression. We quantified the relative amount of *BdMAX3* and *BdMAX4* transcripts by RT-qPCR as compared to the WT line (**Figure 4.3**). A slight but significant reduction of *BdMAX3* expression was observed in OE-CYP11.29 as

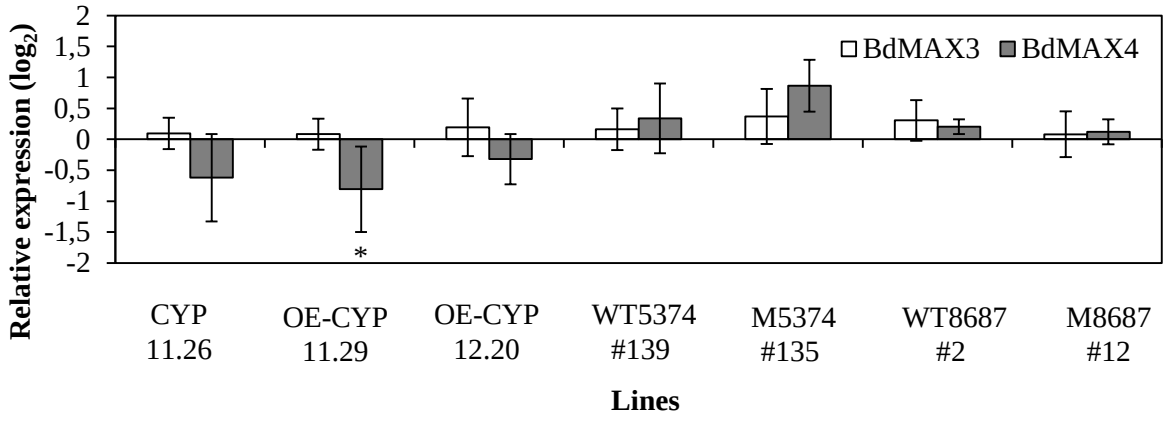

Figure 4.3: Relative expression of *BdMAX3* and *BdMAX4* in spikes is not significantly modified in lines altered in the *Bradi1g75310* locus or gene expression. Relative quantification (log_2 fold change) of the *Bradi5g17660* (*BdMAX3*) and *Bradi2g49670* (*BdMAX4*) expression levels in spikes of the lines altered in the *Bradi1g75310* locus of gene expression as compared to WT (Bd21-3) line. The relative quantity of gene transcripts compared to mock condition was calculated using the comparative cycle threshold (Ct) method ($2^{-\Delta\Delta Ct}$). The *B. distachyon UBC18* and *ACT7* genes (*Bradi4g00660* and *Bradi4g41850*) were used as endogenous controls to normalize the data for differences in input RNA between the different samples. Mean of three independent biological replicates ± standard deviation. Asterisks indicate significant differences compared to Bd21-3. Student test, $P < 0.05$.

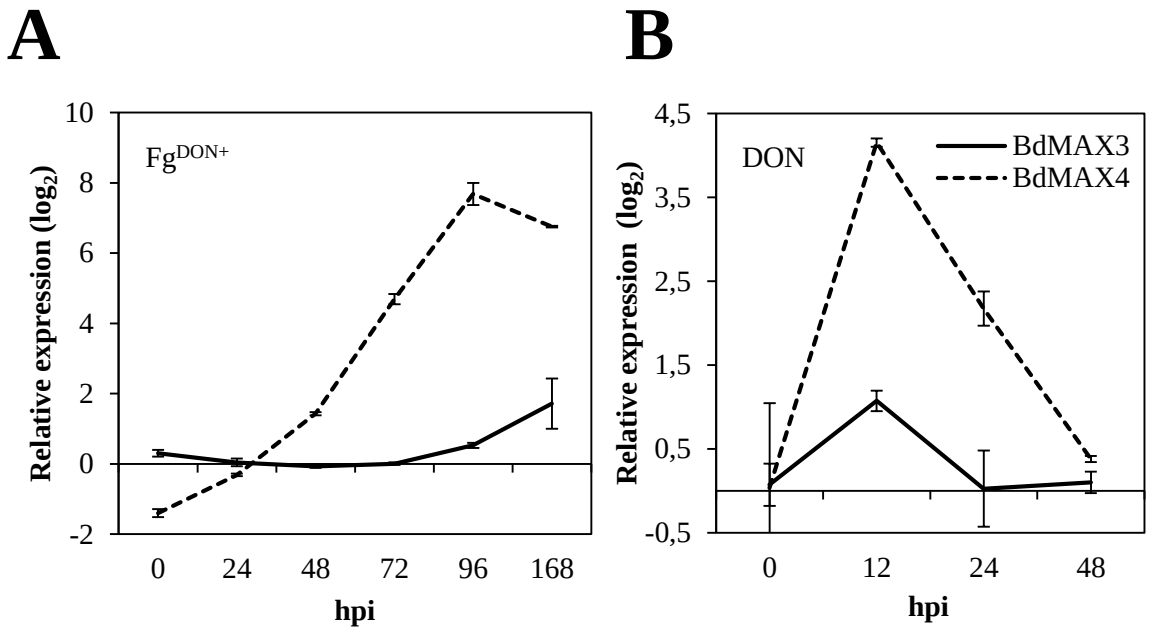

Figure 4.4: The *B. distachyon* SLs core biosynthetic pathway is transcriptionally activated following *F. graminearum* inoculation or DON application. Relative quantification of the *Bradi5g17660* (*BdMAX3*; solid line) and *Bradi2g49670* (*BdMAX4*; dotted line) expression levels in spikes of the Bd21-3 (WT) ecotype of *B. distachyon* following *F. graminearum* infections (**A**; Fg^{DON+} strain) or following DON treatment **(B)** compared to mock treatment. The relative quantity of gene transcripts compared to mock condition was calculated using the comparative cycle threshold (Ct) method ($2^{-\Delta\Delta Ct}$). The *B. distachyon UBC18* and *ACT7* genes (*Bradi4g00660* and *Bradi4g41850*) were used as endogenous controls to normalize the data for differences in input RNA between the different samples. Mean of three independent biological replicates ± standard deviation.

compared to Bd21-3 (-0.92 ± 0.20 log_2 fold-change). No other significant modification has been observed

Following *in silico* prediction of BdMAX3 and BdMAX4 proteins, we followed the transcriptional regulation of the respective encoding genes during the interaction between *B. distachyon* and *F. graminearum* and following direct application of DON by RT-qPCR in the WT line Bd21-3 (**Figure 4.4**). Following infection with *F. graminearum* strain Fg^{DON+}, we observed a rapid induction of the *Bradi2g49670* (*BdMAX4*) gene expression which reached a maximum expression level 96 hpi (7.68 ± 0.32 log_2 fold-change compared to mock condition) before a slight decrease at 168 hpi. The *Bradi5g17660* (*BdMAX3*) gene also exhibited a transcriptional induction following *F. graminearum* inoculation but to a much lesser extent. The maximum expression level was reached later, at 168 hpi, with 1.71 ± 0.72 log_2 fold-change compared to mock condition (**Figure 4.4A**). Interestingly, we also observed a transcriptional induction of these two genes in response to direct application of the main mycotoxin produced by *F. graminearum* (**Figure 4.4B**). Both genes exhibited maximum expression level 12 hours after DON treatment and a similar gap between levels of expression of the two genes was observed: 4.15 ± 0.05 and 1.07 ± 0.12 log_2 fold-change compared to mock condition for *BdMAX4* and *BdMAX3*, respectively.

C. OROBANCHOL SEEMS TO INFLUENCE EARLY GROWTH OF *F. GRAMINEARUM EX PLANTA*

To evaluate the direct impact of SLs, and more specifically orobanchol, on *F. graminearum*, we set up an experiment of *ex planta* fungal growth in liquid medium containing (*rac*)-orobanchol. From a spore suspension of the Fg^{DON+} strain, we followed fungal growth by absorption measurements at 405 nm between 0 and 96 hpi in 96-well plates. We were therefore able to test the impact of media containing from 10^{-12} M to 10^{-4} M of (*rac*)-orobanchol (**Figure 4.5**). Twenty-four hours post inoculation of the medium with *F. graminearum* spores, we observed a slight but significant increase of fungal growth when (*rac*)-orobanchol concentration was between 10^{-6} M and 10^{-12} M compared to the control condition (0 M). We did not observe such statistically confirmed differences at later points for any orobanchol concentration ranging from 10^{-5} M to 10^{-12} M. On the contrary, the medium containing 10^{-4} M of (*rac*)-orobanchol induced a slight reduction of fungal growth at 48 and 72 hpi (294.2 ± 23.6 and 708.2 ± 40.1%, respectively) compared to the control medium (361.1 ± 37.7 and 764.0 ± 19.3%, respectively). After 96 h of growth, not any difference was shown

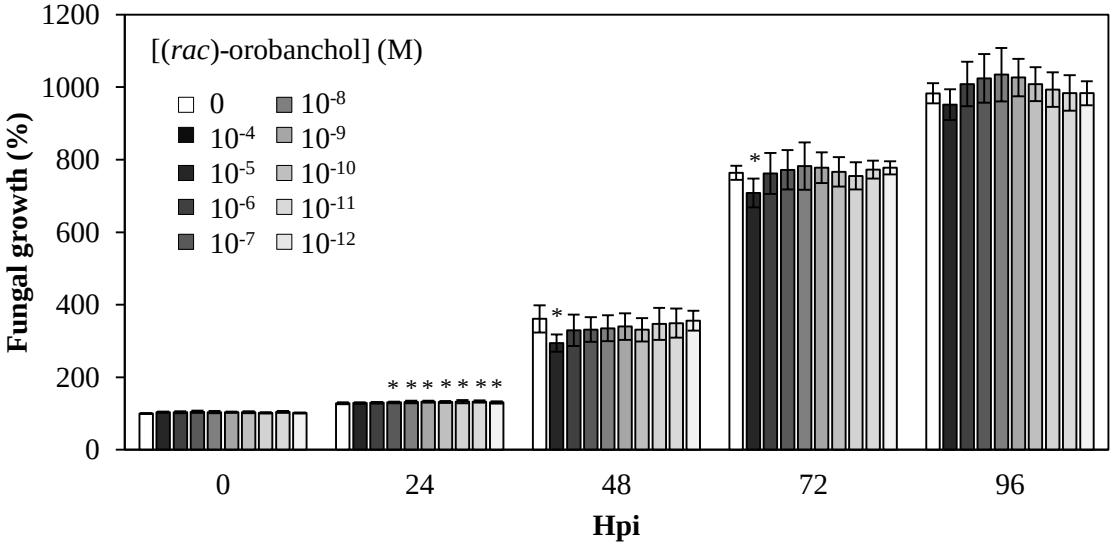

Figure 4.5: Impact of (*rac*)-orobanchol on *F. graminearum* (strain PH-1, Fg^{DON+}) growth. Percentage of fungal growth at 5 time points between 0 and 96 hpi of *F. graminearum* strain PH-1 in presence of (*rac*)-orobanchol ranging from 10^{-12} to 10^{-4} M + 0.01 % DMSO compared to control (0.01 % DMSO, 0 hpi). Liquid cultures have been conducted in 96-well plates with 10^5 spores grown in PDB and growth was followed by 405 nm absorbance measurements. The 100% growth has been set on the 0 M (*rac*)-orobanchol, 0 hpi condition. Mean of 8 technical replicates split into 2 independent experiments ± standard deviation. Asterisks indicate significant differences compared to 0 M condition. Student test, $P < 0.05$.

to be statistically significant. Nevertheless, an interesting distribution of fungal growth values was observed since maximum growth was quantified in 10^{-7} M orobanchol (1034.5 ± 73.6%) at 96 hpi whereas in higher or lower concentrations of (*rac*)-orobanchol, values were systematically weaker, gradually, as concentrations move away from this optimum until reaching a minimum growth of 982.9 ± 27.7% at 10^{-4} M and 983.3 ± 33.2% at 10^{-12} M.

D. OVEREXPRESSION OF THE *BRADI1G75310* GENE SEEMS TO INCREASE DEFENSE MAKER GENES EXPRESSION

To evaluate the general status of biotic stress related defenses in our different *B. distachyon* lines altered in the *Bradi1g75310* locus or gene expression, we followed by RT-qPCR the level of expression of the *Bradi1g39190* and *Bradi3g47110* marker genes in response to the infection by *F. graminearum*. The *Bradi1g39190* (*PR9*) ant the *Bradi3g47110* (*PAL6*) genes encode a peroxidase and a phenylalanine ammonia lyase, respectively, both shown to be highly induced in the WT line of *B. distachyon* following infection with *F. graminearum* strain Fg^{DON+} (Pasquet et al., 2014). The expression level of these two genes was followed at 0, 48 and 96 hpi compared to mock condition (spraying with Tween 20, 0.01%; **Figure 4.6**).

First, we confirmed the transcriptional activation of the *PR9* gene in response to *F. graminearum* infection in *B. distachyon* WT line Bd21-3 with the observation of an approximate 180-fold-change induction between 0 and 96 hpi. At 0 hpi, we observed a significant higher expression of *PR9* in the null segregant control line CYP11.26 as compared to Bd21-3 (2.05 ± 0.47 and 0.29 ± 0.25 $\log_2$ fold-change, respectively) but this difference was not maintained at later time points. All the other lines were shown to behave similarly to Bd21-3 (**Figure 4.6A**). After 48 h of infection, the line which exhibits the highest level of overexpression of *Bradi1g75310,* OE-CYP12.20, showed a significant highest induction of *PR9* expression as compared to Bd21-3 (6.39 ± 0.13 and 0.53 ± 1.41 $\log_2$ fold-change, respectively). This difference was maintained at 96 hpi since OE-CYP12.20 exhibited a 12.15 ± 1.62 $\log_2$ fold-change whereas Bd21-3 showed only 7.49 ± 0.19 $\log_2$ fold-change compared to Tween condition. No other significantly different gene expression levels between the other lines have been detected. Due to data dispersal, it seems important to focus on differences confirmed by statistical analysis. Nevertheless, it is interesting to notice that at 48 hpi, the two mutant lines and the control line WT8687#2 exhibited *PR9* expression values between -1.05 and -1.74 $\log_2$ fold-change likely to reflect a non-activation and even a repression of this

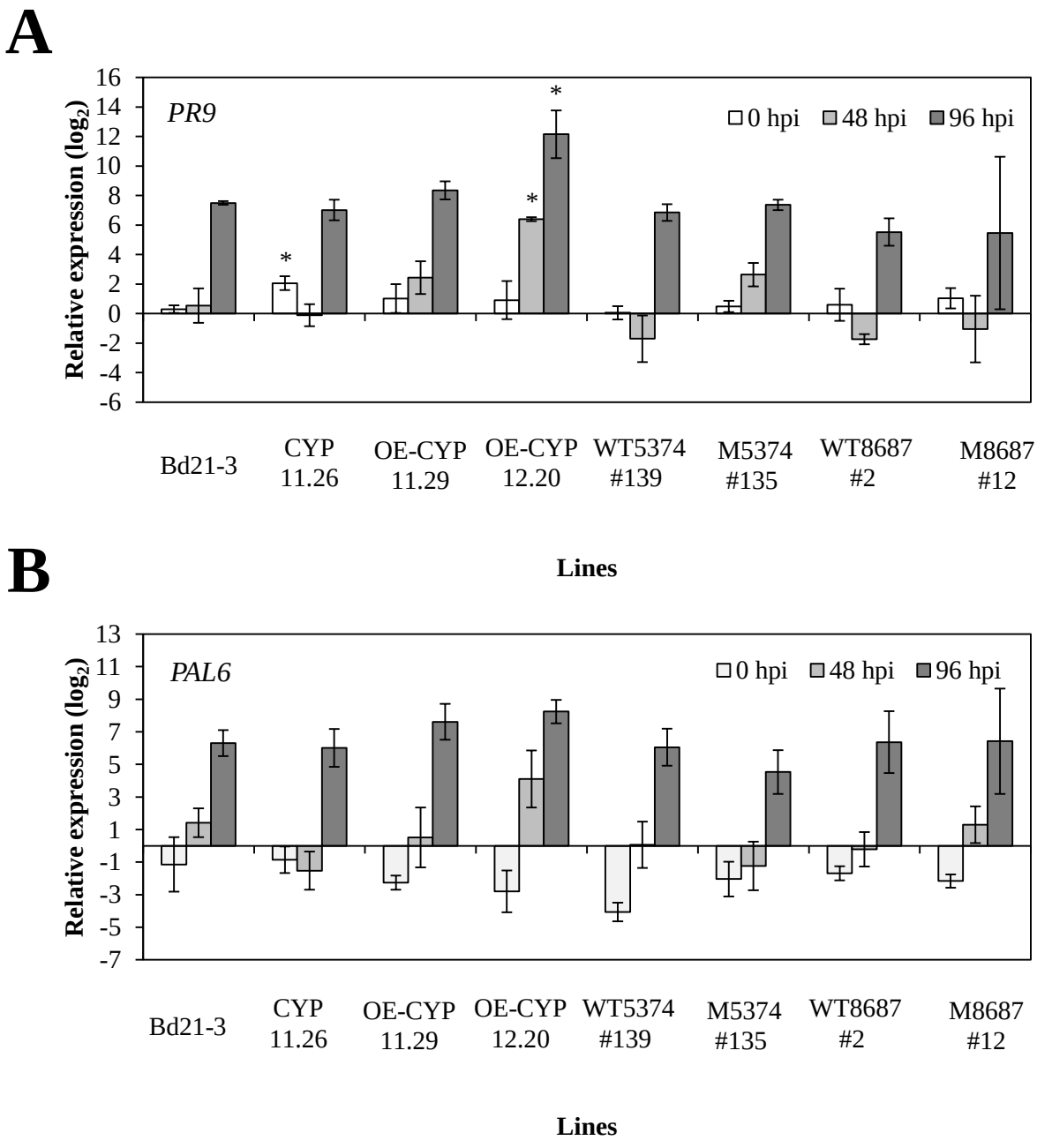

Figure 4.6: Relative defense gene expression in *B. distachyon* lines altered in *Bradi1g75310* following *F. graminearum* infection compared to mock condition. Relative quantification (fold-change, $\log_2$) of the *Bradi1g39190* (*PR9*, **A**) and *Bradi3g47110* (*PAL6*, **B**) expression levels in the *B. distachyon* lines altered in the *Bradi1g75310* locus or gene expression following *F. graminearum* infection (Fg^{DON+} strain) compared to mock treatment. The relative quantity of gene transcripts compared to mock condition was calculated using the comparative cycle threshold (Ct) method ($2^{-\Delta\Delta Ct}$). The *B. distachyon UBC18* and *ACT7* genes (*Bradi4g00660* and *Bradi4g41850*) were used as endogenous controls to normalize the data for differences in input RNA between the different samples. Mean of three independent biological replicates ± standard deviation. Asterisks indicate significant differences compared to Bd21-3 (WT) line. Student test, $P < 0.05$.

defense marker gene, possibly driven by the pathogen. On the contrary, both overexpressing lines exhibited values higher than 2, which could be interpreted as a fastest induction of gene expression compared to the other lines.

Regarding the *PAL6* gene, the transcriptional induction in Bd21-3 was also confirmed, this time with an approximate 110 fold-change (6.30 log_2) induction between 0 and 96 hpi (**Figure 4.6B**). At 0 hpi, all the lines exhibited a negative log_2 fold-change of expression compared to Tween condition which could reflect an inhibition of *PAL6* gene expression at the very beginning of the interaction. This transcriptional repression was also be observed at 48 hpi since most of the lines exhibited weak or negative log_2 fold-change of expression, except for the OE-CYP12.20 line which exhibited a 4.10 ± 1.75 log_2 fold-change of gene expression. We finally observed a similar gene expression level by the different line at 96 hpi ranging from 4.53 ± 1.34 to 8.25 ± 0.72 log_2 fold-change for WT5374#135 and OE-CYP12.20, respectively. Statistical analysis did not reveal significant differences between the different lines and Bd21-3 at each time point.

Interestingly, for both genes, OE-CYP12.20 exhibited the maximum expression level at 48 and 96 hpi (respectively 6.39 ± 0.13 and 12.15 ± 1.62 for *PR9* and 4.10 ± 1.75 and 8.25 ± 0.72 for *PAL6*). At the latest time point, OE-CYP11.29 was systematically found in second position with 8.35 ± 0.62 and 7.61 ± 1.1 log_2 fold-change for *PR9* and *PAL6*, respectively. This specific behavior of the overexpressing lines of the *Bradi1g75310* gene could reflect either a change of expression at the basal level or a faster induction of these two defense marker genes in the interaction context. To test these hypotheses, we also compared the *PR9* and *PAL6* gene expression levels in non-infected lines altered in the *Bradi1g75310* gene and their respective control lines compared to WT Bd21-3 line (**Figure 4.7**). We used the 0 hpi Tween condition to compare the basal level of expression of these genes in our different lines (**Figure 4.7A; 4.7C**). For both genes, no significant differences of the basal level of expression have been found between lines and Bd21-3 although the WT8687#2 control line exhibited systematically the lowest expression level compared to WT with -1.47 ± 0.49 and -1.44 ± 0.53 log_2 fold-change for *PR9* and *PAL6*, respectively which represents 2 to 3 times less transcripts at the basal level in this line compared to Bd21-3. We also re-analyzed our data following infection using the Bd21-3 line at the same infection time point as reference for determining the level of relative gene expression (**Figure 4.7B; 4.7D**). Regarding *PR9* gene expression in CYP11.26, OE-CYP11.29 M5374#135, WT5374#135 and 8387#12, gene expression fold change was systematically found between -2 and +2 log_2 and were not found significantly different from Bd21-3 (**Figure 4.7B**). The WT8687#2 line was not found

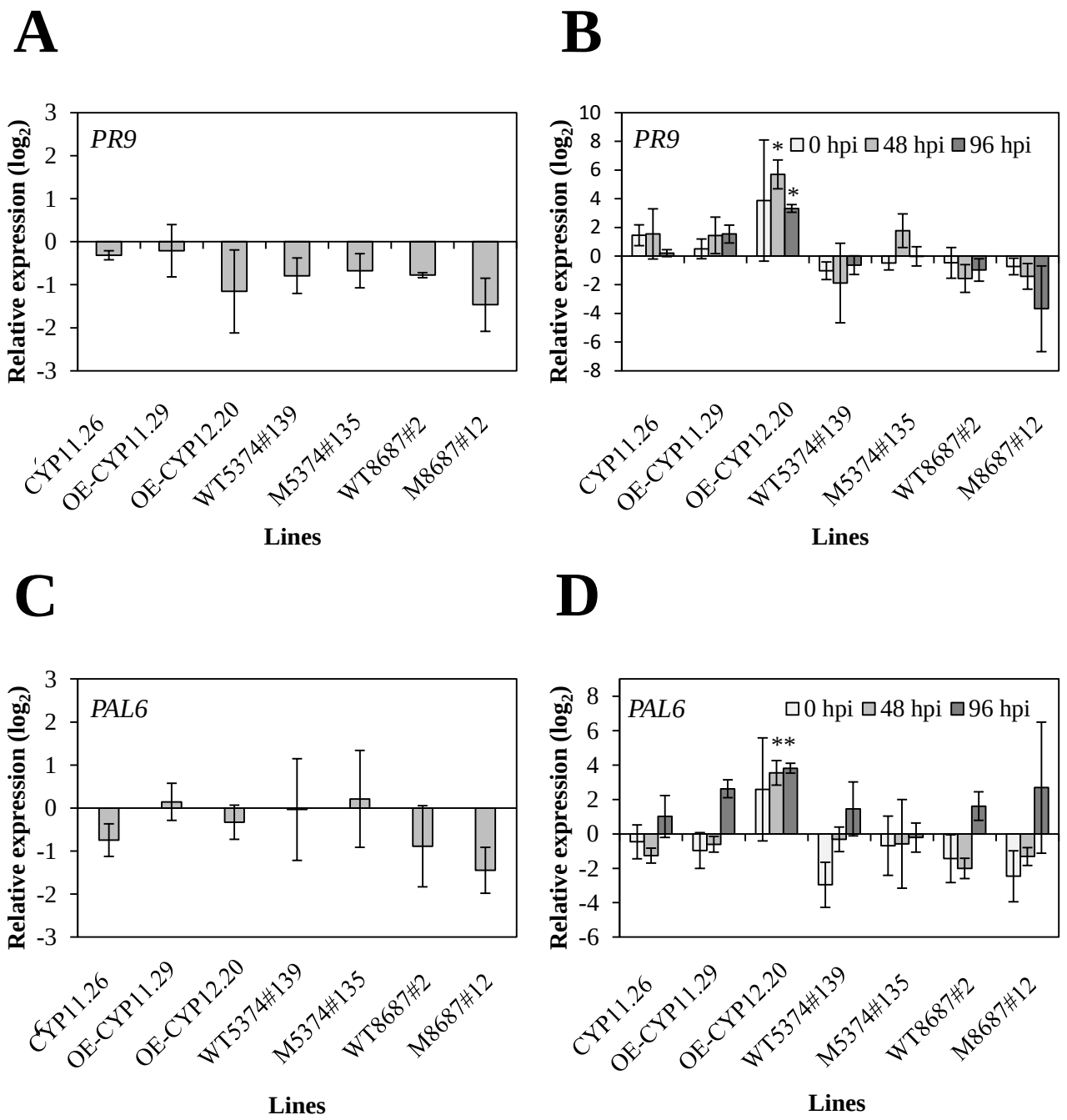

Figure 4.7: Relative defense gene expression in *B. distachyon* lines altered in *Bradi1g75310* following *F. graminearum* infection compared to WT. Relative quantification (fold-change, $\log_2$) of the *Bradi1g39190* (*PR9*, **A-B**) and *Bradi3g47110* (*PAL6*, **C-D**) expression levels in the *B. distachyon* lines altered in the *Bradi1g75310* locus or gene expression in healthy plants (**A**, **C**) or following *F. graminearum* infections (Fg^{DON+} strain) (**B**, **D**) compared to WT line Bd21-3. The relative quantity of gene transcripts compared to mock condition was calculated using the comparative cycle threshold (Ct) method ($2^{-\Delta\Delta Ct}$). The *B. distachyon UBC18* and *ACT7* genes (*Bradi4g00660* and *Bradi4g41850*) were used as endogenous controls to normalize the data for differences in input RNA between the different samples. Mean of three independent biological replicates ± standard deviation. Asterisks indicate significant differences compared to Bd21-3 (WT) line. Student test, $P < 0.05$.

different either, but we observed a gradual reduction of *PR9* gene expression compared to Bd21-3. On the contrary, we observed a significant higher level of expression of the *PR9* gene in the overexpressing line OE-CYP12.20 48 and 96 hpi. The same observation was made for the *PAL6* gene (**Figure 4.7D**) and overall, OE-CYP12.20 exhibited an average of 48.5 and 12.5-fold-change in defense marker gene expression levels compared to Bd21-3 at 48 and 96 hpi, respectively. No other significant differences have been observed.

E. CONCLUSION

The main objective of this chapter was to determine whether the transcriptional activation of the *Bradi1g75310* gene during the interaction between *B. distachyon* and *F. graminearum* was linked to the activity of BdCYP711A29 in SLs biosynthesis. In other words, we wanted to determine if SLs are involved in FHB and if they participate in the increased susceptibility observed for lines overexpressing our gene of interest.

To determine if SLs play a role during the interaction, we first evaluated the level of activity of the core SLs biosynthetic pathway. We decided to focus on the transcriptional level since SLs detection and quantification *in planta* is challenging (**Chapter III**) and because several studies suggested the use of *CCD7* and *CCD8* gene expression levels as markers for the SLs biosynthetic pathway activity. We identified putative homologs of these two enzymes in *B. distachyon in silico* based on sequence identity with the primary amino-acid sequences of the two enzymes already characterized in rice, D17 and D10, respectively. For each rice *CCD* gene, we identifed a single homolog in *B. distachyon*: *Bradi5g17660* and *Bradi2g49670* furtherly named *BdMAX3* and *BdMAX4*, respectively (**Figure 4.1**). As explained in the introduction of this chapter, *CCD7* has been found, so far, in a single copy in plant genomes. Thus, we can be quite confident regarding our prediction. The situation is more complex concerning *CCD8* which has been found in several copies in several plant genomes including rice. We used the deduced protein sequence of the *D10* (*CCD8b*) copy as a bait since it has been shown to catalyze the production of carlactone in rice, but we cannot exclude that the situation evolved differentially in *B. distachyon* and that another CCD8 isoform is now responsible for this activity in the model temperate cereal. Multiple sequence alignment showed a very high degree of sequence identity / homology between the characterized proteins from rice and *A. thaliana* and our predicted homologs in *B. distachyon* were also confirmed both by reciprocal BLAST and a simple phylogenetic analysis (**Figure 4.2**) which further supports our study.

After this identification, we were able to follow the transcriptional expression level of these two genes in spikes of *B. distachyon* in response to the infection by *F. graminearum* or to the direct application of DON (**Figure 4.4**). Interestingly, in both conditions, we observed a slight to important induction of transcription of these two genes compared to the mock control. The transcriptional induction was shown to be faster and more important for *BdMAX4* than for *BdMAX3*. These results suggest an activation of the SLs core biosynthetic pathway in spikes of *B. distachyon* in response to *F. graminearum* infection which seems dependent, at least partly, on the mycotoxin. It is therefore tempting to speculate that *B. distachyon* engage SL biosynthesis in response to *F. graminearum* infection which could result in a general increase of SLs quantity or, at least, a modification of SLs homeostasis. To the best of our knowledge, this is the first time that SLs biosynthetic pathway mobilization is described in the FHB context and more globally in plant response to a plant pathogenic fungus. Only a slight increase of the pea *PsCCD8* expression level in response to *P. irregulare* (oomycete) infection has been described but failed to be correlated to a differential level of resistance or sensitivity of the host plant towards the pathogen (Blake et al., 2016).

Because no major changes in *BdMAX3* and *BdMAX4* transcripts could be found in healthy spikes of the overexpressing lines OE-CYP11.29 and OE-CYP12.20 compared to Bd21-3 or TILLING mutant lines (**Figure 4.3**), we speculated that the global pool of SLs and more specifically CL content might be similar between the different lines altered in the *Bradi1g75310* gene. On the contrary, if BdCYP711A29 efficiently catalyzes orobanchol biosynthesis *in planta*, we could assume that OE lines contain a higher level of this compound in spikes, as we observed in root exudates (**Chapter III**). We were therefore wondering whether potential increased orobanchol content in spikes could be responsible for the differential level of resistance towards the disease we could observe between WT and OE lines. We tested the direct impact of orobanchol on *F. graminearum via* the follow-up of fungal growth in liquid medium containing different concentrations of orobanchol (**Figure 4.5**). Interestingly, at 24 hpi we detected a slight but significant increase of fungal growth in medium containing 10^{-6} to 10^{-12} M orobanchol likely to suggest an activation of an early step of fungal development such as spore germination. At 48 and 72 hpi, we observed a significant reduction of fungal growth in liquid culture containing 10^{-4} M of orobanchol and no other differences have been statistically confirmed. Nevertheless, 96 hpi, our data suggest a slight activation of fungal growth at 10^{-7} M which decreases at higher or weaker concentrations of orobanchol but remain higher than the condition (except for 10^{-4} M). Regarding symbiotic interactions, it has been shown that arbuscular mycorrhizal fungi (AMF)

are stimulated by SLs at concentrations as low as 10^{-13} M which should correspond to the concentrations of these molecules in the rhizosphere (Besserer et al., 2006). The slight repression of growth observed at 10^{-4} M is therefore unlikely biologically relevant in nature. On the contrary, the early activation of fungal growth at concentrations as low as 10^{-12} M we could observed might be more conceivable in nature. Nonetheless, we used a racemic mixture of two stereoisomers of orobanchol including the naturally occurring *ent*-2'-*epi*-orobanchol (3a*R*, 8b*R*, 2'*R*) and its non-natural epimer 2'-*epi*-orobanchol (3a*S*, 8b*S*, 2'*S*; Zwanenburg et al., 2016). These two stereoisomers might have distinct biological activities as already described for GR24 (López-Ráez et al., 2017). Overall, it seems therefore complicated in our conditions to assign a direct biological activity of orobanchol towards *F. graminearum*.

We also tested if the general defense pathways against biotic stresses were altered in our *B. distachyon* lines modified in the *Bradi1g75310* locus and gene expression. To do so, we performed a preliminary analysis and followed the transcriptional profile of two genes which have been already shown to be induced during FHB in *B. distachyon*: *PR9* and *PAL6* (Pasquet et al., 2014; Pasquet et al., 2016). The first one encodes a peroxidase supposed to be involved in ROS-related stresses and the second one encodes a phenylalanine ammonia lyase supposed to act at the basis of the phenylpropanoids biosynthetic pathway. First, we evaluated the expression of these two genes during the interaction with *F. graminearum* as compared to mock control of our lines of interest (**Figure 4.6**). We observed a greater induction of *PR9* but not *PAL6* in OE-CYP12.20 at 48 and 96 hpi as compared to Bd21-3. Although we were not able to statistically confirm this result with the second OE line OE-CYP11.29, it also exhibited a slight increase of expression of this gene compared to WT. No clear difference has been observed for the TLLING mutant lines. To explicit the increased transcription of *PR9* in OE-CYP12.20 and more specifically compare the relative amount of transcript with that in the control line Bd21-3 and not with the mock condition in each genotype, we also analyzed our data using Bd21-3 as a reference (**Figure 4.7**). First, it is important to notice that no significant differences in *PR9* and *PAL6* gene expression level exist between our lines and Bd21-3 at the basal level (Tween, 0 hpi; **Figure 4.7A-4.7B**). Hence, we logically observed anew the increased level of *PR9* transcript in the OE-CYP12.20 line when it was compared to Bd21-3. Similarly, we observed a significant increase of *PAL6* transcript in OE-CYP12.20 as compared to Bd21-3 at 48 and 96 hpi. It therefore appeared that this OE line has a comparable level of expression of these two genes in basal conditions but that their induction in response to *F. graminearum* seems faster and/or stronger compared to the WT line Bd21-3.

Overall, we showed that the SLs core biosynthetic pathway of *B. distachyon* is activated upon *F. graminearum* infection in a DON-dependent manner. The transcriptional induction of the *Bradi1g75310* gene we observed at the beginning of the project might therefore be related to its activity in SLs biosynthesis. Nevertheless, we were not able to conclude on an impact of SLs during the interaction, either directly on *F. graminearum* development, or regarding general defense related genes. We observed a slight increase of defense related-genes in the OE-CYP12.20 line but failed to clearly confirm this result with the other independent overexpressing line OE-CYP11.29 and therefore do not have the ability to conclude firmly on the biological role of SLs induction during FHB leaving us interrogations that we will discuss, among other points, in the next chapter.

CHAPTER V | DISCUSSION

A. A FIRST STEP IN THE CHARACTERIZATION OF FHB-INDUCED P450S

The large diversity of plant metabolic pathways involving P450, their grouping into multigene families but also their poor conservation at the primary amino-acid sequence level make them intricate to study (Bak et al., 2011), but their use as biotechnological tools allowed, for example, the ease production of plant natural products (Renault et al., 2014) or the production of toxin-tolerant plants (Jagtap and Bapat, 2017). Hence, P450s constitute a plant family of enzymes with promising prospects both for fundamental and applied research in many different fields of plant biology. In that context, although the transcriptional activation of plant P450 encoding genes in response to *F. graminearum* infection or DON treatment has been described many times for over 10 years, no study has been able to functionally characterize them in the disease context (**Chapter I, section C.4.**). The aim of this project was, therefore, to identify and characterize a putative interesting P450 candidate to contribute to increasing knowledge concerning the overall plant responses towards FHB and, to ultimately help improve the genetic resistance of *F. graminearum* host plants.

In the FHB context, transcriptomic data are often used as a starting point to identify host resistance or susceptibility genes as well as pathogen virulence factors (Kazan and Gardiner, 2017). Indeed, the transcriptomic methodologies enabled the obtention of enough information to study quantitative resistance to the disease but, of course, remain extremely elusive concerning the characterization of specific biological activities. P450s are known to be mostly regulated at the transcriptional level and the corresponding genes are therefore relevant candidates to search for in transcriptomic data (Bolwell et al., 1994; Guéguen et al., 2006). We used this strategy to identify the *Bradi1g75310* gene encoding the BdCYP711A29 P450 in the model cereal *B. distachyon,* characterized it in response to FHB and assigned it an endogenous activity. Indeed, the *Bradi1g75310* gene was shown to be induced following *F. graminearum* infection, in a DON-dependent manner (**Chapter I, Table 1.5**; **Chapter II, Figure 2.1**). Moreover, we showed that it constitutes a susceptibility factor of *B. distachyon* towards the disease (**Chapter II, Figures 2.6-2.7**). Finally, we demonstrated that the BdCYP711A29 encoded P450 was involved in strigolactones biosynthesis in the model monocotyledonous plant (**Chapter III**). Hence, the present work significantly improved our knowledge about FHB since it is the first to propose a functional characterization of an FHB-induced plant P450 in addition to giving interesting clues about the role of SLs in the disease, which have never been associated to FHB so far.

B. IS A PLANT P450 ABLE TO DETOXIFY DON?

One of the well-described activities of P450s is their involvement in xenobiotic detoxification and more specifically herbicide metabolisation (**Chapter I, section C.3.2.1.**; Siminszky, 2006). They catalyze monooxygenation-based chemical reactions which often result in the adjunction of a hydrophilic residue or the cleavage of a reactive part on toxic foreign compounds (**Chapter I, Table 1.4**). The products of such reactions could exhibit lower, equivalent or higher toxicity compared to the parent molecule. In the first case, P450s provide direct strong tolerance to a specific xenobiotic and this has been exploited to generate plant lines with higher tolerance towards phenylurea herbicides, for example (Didierjean et al., 2002). In the last two cases, P450s often act synergistically with other xenobiotic-metabolizing enzymes such as UGTs and GSTs and are responsible of the adjunction of functional groups on the xenobiotic, making it suitable for glycosylation or glutathionylation. A well-known integrated detoxification process concerns the 2,4-Dichlorophenoxyacetic acid (2,4,D) herbicide which is hydroxylated, then conjugated with glucose and malonyl, and finally exported in the vacuole (Sandermann, 1994). The genetic and biochemical properties of P450s therefore made them central partners in the so called 'green liver' (Coleman et al., 1997).

Recently, several studies reported the plant detoxification of *F. graminearum* mycotoxins as a promising source of resistance towards the pathogenic fungus in *B. distachyon* and wheat (Li et al., 2015; Pasquet et al., 2016; Gatti, 2017). As an example, in *B. distachyon*, the UGT Bradi5g03300 efficiently converts DON into DON-3-*O*-glucoside *in planta* and confers both tolerance to the mycotoxin and resistance to the disease (Pasquet et al., 2016). The transfer of this knowledge into wheat allowed the identification of an orthologous protein with similar properties in wheat which constitutes a relevant candidate to include in selection processes (Gatti, 2017). The diversity of DON-derivatives detected in wheat during toxin detoxification suggests the involvement of numerous plant enzymatic partners in biotransformation processes of the *F. graminearum* mycotoxins, one of them compatible with the involvement of a P450 activity (Kluger et al., 2015).

On one hand, the bacterial P450 DdnA isolated in a *Sphingomonas* sp. strain was shown to catalyze 16-hydroxylation of DON and the product of its activity, 16-HDON, presents a dramatically reduced phytotoxicity as compared to its parent molecule (Ito et al., 2013). Another strain isolated from an agricultural soil (*Devosia mutans*) was also shown to catalyze the oxidation-based epimerization of DON into 3-*epi*-DON, a derivative with

substantial reduced toxicity compared to DON (He et al., 2015). In addition, since more than 30 years, anaerobic bacterial strains from the animal digestive tract were regularly shown to de-epoxidate DON and form deepoxy-deoxynivalenol (DOM-1) with abolished toxicity (Karlovsky, 2011). Although enzyme(s) responsible for such transformations have not been reported yet, this activity could clearly be associated to a P450 enzyme. Nevertheless, no plant P450s have been shown to catalyze any reaction on *F. graminearum* mycotoxins yet. We were therefore wondering whether our P450 of interest in *B. distachyon*, BdCYP711A29, could be involved in such reactions which could explain its transcriptional activation partly dependent on DON during FHB. Our evaluation of root sensitivity towards DON of several *B. distachyon* lines altered in the *Bradi1g75310* locus or gene expression (**Chapter II, Figure 2.5**) allowed us to cancel our assumption. However, we can still wonder if a plant P450 is able to modify the chemical structure of DON in order to decrease its phytotoxicity or to produce the substrate for other detoxification enzymes. DON is a molecule carrying 3 hydroxyl groups on C3, C15 and C7 (**Chapter I**, **Figure 1.8**). C3 and C15 hydroxyl groups are suitable for acetylation to generate 3-ADON and 15-ADON derivatives in *F. graminearum*, for glucosylation to generate D3G and D15G during wheat detoxification processes or for sulfation to generate various combinations of sulfated DON *in vitro* (Fruhmann et al., 2014; Kluger et al., 2015; Schmeitzl et al., 2015). The C7 hydroxyl group is therefore the only appearing unreactive, probably because of its steric hindrance. However, it leaves two hydroxyl groups in C3 and C15, highly reactive for biotransformation. It is therefore unlikely that a P450 participates in the adjunction of a hydroxyl group used by other enzymatic partners to conjugate the hydroxylated DON form with a hydrophilic molecule.

We described above other kinds of reactions on DON which could be catalyzed by P450s. Hydroxylation on other positions, as observed for bacterial DdnA, attack of the alkyl groups in C5 or C9 positions or of the ketone group in C8 position are all putative biochemical reactions which, theoretically, could be catalyzed by a P450 activity. Nevertheless, among the different derivatives of DON found in plant cells, to the best of our knowledge, no analysis reported DON derivatives supporting such a hypothesis. Another kind of reaction, the opening of epoxide group in C12-C13 position necessary for 'DON-2H'-S-glutathione production, could be catalyzed by a plant P450 (Guengerich, 2001; Kluger et al., 2015). Nevertheless, it is also possible that the glutathione-*S*-transferase (GST) which catalyzes gluthationylation and therefore production of this DON-derivate is itself responsible for this epoxide ring opening (Kluger et al., 2015).

Overall, we still miss clues to conclude on the putative involvement of plant P450s in DON detoxification processes. On the contrary, a number of studies reported the detection of numerous glucosylated and glutathionylated forms of DON with, at least for part of them, marked reduced toxicity. From a practical point of view, it is therefore certainly more promising to identify the enzymatic partners (UGTs and GSTs) involved in the second step of xenobiotic detoxification metabolism to, in the long term, exploit these properties in cereal breeding.

C. *B. DISTACHYON*: A MODEL FOR STUDYING SLS DIVERSIFICATION

Based on phylogenetic relationships (**Chapter III, Figure 3.2**) and comparative analysis of transcriptional expression patterns (**Chapter III, Figure 3.3**), we hypothesized that BdCYP711A29 is involved in SLs biosynthesis in *B. distachyon*. Through the genetic complementation of the *A. thaliana max1-1* mutant line (**Chapter III, Figure 3.4**) and the detection and quantification of SLs exuded from the roots of the *B. distachyon* lines altered in the *Bradi1g75310* locus or gene expression (**Chapter III, Figure 3.6**), we were able to assign an endogenous function to BdCYP711A29. In addition to be a functional homolog of *A. thaliana* MAX1 protein, therefore to be able to metabolize carlactone (CL) into a molecule with branching inhibition activity, BdCYP711A29 seems to be involved in orobanchol biosynthesis in *B. distachyon*. Indeed, the *Bradi1g75310* gene allowed full complementation of the highly branched phenotype of *A. thaliana* mutant line and its overexpression in *B. distachyon* led to an accumulation of orobanchol in root exudates. It is therefore likely to hypothesize that BdCYP711A29 is an orobanchol synthase in *B. distachyon* as observed for rice OsCYP711A3 (Zhang et al., 2014) and for maize ZmCYP711A18 (Yoneyama et al., 2018). In *A. thaliana*, MAX1 catalyzes the conversion of CL into carlactonoic acid (CLA; Abe et al., 2014), a reaction which seems conserved across MAX1 homologs (Yoneyama et al., 2018). We could therefore speculate that the genetic complementation of *max1-1* shoot phenotype by the *Bradi1g75310* gene reflects the ability of BdCYP711A29 to oxidize CL into CLA. Only one MRM transition allowed us to detect CLA in our metabolic analysis of *B. distachyon* root exudates (**Chapter III, Table 3.2**). Although it is not enough to confirm the structure of the detected metabolite, a 3-fold increase of AUC CLA (333 > 97) / AUC GR24 / g FW was observed in OE-CYP12.20 exudates compared to M5374#135 and Bd21-3 lines which could reflect an accumulation of this compound (data not shown). Other specific transitions *in planta* and the *in vitro* incubation of BdCYP711A29 with CL followed by

products analysis would be useful to test this hypothesis. Nevertheless, we already gained important clues to classify BdCYP711A29 as an A3-type MAX1 homolog (**Chapter I, Figure 1.25**) involved in both transformations of CL into CLA and 4-DO into orobanchol but not in the CLA – 4-DO transformation (Yoneyama et al., 2018). Interestingly, the two characterized MAX1 A3-type homologs (OsCYP711A3 and ZmCYP711A18) in addition to BdCYP711A29 carry different isoform numbers which reflect the relatively important phylogenetic distance between them, partly supported by several independent phylogenetic analyses (**Chapter III, Figure 3.2**; Challis et al., 2013; Yoneyama et al., 2018). Because P450s are subjected to complex evolutionary history, it seems complicated to determine whether these copies emerged from a common ancestor and evolved rapidly, at the amino-acid sequence level following speciation, or if the orobanchol synthase activity was acquired independently by each A3-type MAX1 homologs. Nevertheless, it clearly appears now that phylogenetic analyses are not informative enough to assign a specific activity in SLs diversification to MAX1 homologs.

In this thesis work, we also presented the preliminary characterization of the four paralogs of the *Bradi1g75310* gene. Each copy was able to genetically complement the shoot phenotype of *A. thaliana max1-1* mutant line suggesting that all the copies are able to metabolize CL. Nevertheless, shoot complementation was not observed with the same efficiency especially depending on the trait considered (**Chapter III, Figures 3.7-3.10**; **Table 3.3**). Overall, while BdCYP711A6, A29 and A30 where shown to efficiently complement the number of leaf-rosette primary branches but not or poorly the plant shoot height, BdCYP711A31 was shown to be more efficient to genetically complement the second trait. Meanwhile, BdCYP711A5 was shown to efficiently complement both mutant phenotypes. Such diversity in *max1-1* genetic complementation has already been described for example by Challis et al. (2013) during their characterization of *Medicago truncatula* MAX1 homologs for which distinct behavior were observed. Indeed, although the *MAX1* homologous gene *Medtr3g104560* was able to fully genetically complement each of the studied phenotypes (branching, height and leaf shape) of the *max1*-1 mutant line, the *Medtr1g015860* paralogous gene was only able to weakly complement some but not all of the phenotypes. This might reflect the biochemical specificity of MAX1 paralogs which should catalyze the production of different SLs with distinct physiological properties within the same species (Challis et al., 2013). During the thesis project, we generated *B. distachyon* lines overexpressing each of the genes encoding the other BdCYP711As. Due to time limitation, we tried to quantify SLs exuded from the roots of M2 (heterozygous or homozygous for the integrated construction)

individual plants but were not able to obtain quantifiable signals (data not shown, collaboration with STÉPHANIE BOUTET-MERCEY and GRÉGORY MOUILLE, IJPB, Versailles, France). This experiment will have to be performed again in optimal conditions and should give very interesting results regarding the biochemical activity of each BdCYP711A copy. Indeed, to the best of our knowledge, *B. distachyon* carries the highest number of functional MAX1 homologs so far. The fact that *B. distachyon* is a monocot species, a class for which a higher number of MAX1 homologs present in the genome is already described (Challis et al., 2013), and that contrary to wheat or rice, it has not undergone a domestication process (**Chapter I, section A.1.**) likely to counter select several developmental phenotypes, could explain this specific situation. This is also particularly interesting regarding the variable number of copies in other plant species (4 + 1 pseudogene in rice, 4 in soybean, 1 in *S. moellendorffii*, 2 in poplar…) which is questioning about the SLs diversity in these species. Indeed, it is still complicated to perform exhaustive detection of SLs *in planta* or *ex planta* and many of the recent studies focused their metabolic analyses on compounds often present in high concentration and detected through several MRM specific transitions. Therefore, we cannot make any correlation between MAX1 paralogs number and SLs diversity within a species. Although other enzymes should be identified as partners in SLs biosynthetic pathways downstream MAX1 (Brewer et al., 2016); we could assume that the higher MAX1 paralogs number a species carries, the higher SLs could diversify. We could also expect that the general diversity is not affected since P450s are often shown to metabolize several substrates with different efficiency, but that the proportion between individual SLs is modified. Indeed, the acquisition of a copy with high ability to produce one specific SL will redirect the biosynthetic pathway to promote the production of this compound. Given the increasing number of biological roles associated to SLs, this could constitute an interesting strategy for plants to adapt to specific conditions. Finally, *B. distachyon* showed interesting biological and genomic features regarding the SLs research topic and might constitute an interesting model especially thanks to the biological material generated during this Ph.D. project.

D. WHY IS THE SLS BIOSYNTHETIC PATHWAY ACTIVATED DURING FHB IN *B. DISTACHYON*?

Although the biological role of SLs in the interaction between plants and parasitic weeds or AM fungi is well described and conserved across plant species (Zwanenburg and

Blanco-Ania, 2018), the involvement of this class of phytohormones during plant interaction with pathogenic microorganisms remains elusive (**Chapter I, section I.D.6.**). Several putative roles for SLs in plant-pathogen interactions were studied thanks to the availability of several SLs deficient or insensitive mutant lines and of a growing number of synthetic and natural SLs (**Chapter I, Tables 1.7-1.10**). We discussed in the introduction the high variability of the results which impeded so far the establishment of a general paradigm for SLs involvement in plant pathogenesis. Indeed, direct impacts of SLs on pathogen growth *ex planta* were different depending on the pathogen species, the SLs mixture used (synthetic/natural, enantiopure/racemic mixture), the different modes of application of SLs… Similarly, SLs mutant plants showed increased to similar resistance level compared to WT plants depending on the pathosystem.

SLs involvement in plant-AMF and plant-parasitic weed interactions in the rhizosphere is, in a sense, coherent with the localization of SLs biosynthesis in plants. Although information about spatiotemporal regulation of SLs biosynthesis are still incomplete, grafting experiments, localization of expression of genes encoding enzymes involved in SLs biosynthesis and localization of these enzymes support the hypothesis of core biosynthetic pathway localized in root cells. On the contrary, the diversification pathway seems to occur throughout the plant since CL and its derivatives are mobile molecules whereas intermediate metabolites upstream CL are not (Kameoka and Kyozuka, 2017). Hence, CL is expected to be transformed by a MAX1 activity (and/or by other enzymatic activity) after having been transported into the plant (Waters et al., 2012). The differential transcriptional regulation of MAX1 (and homologs) between plant organs is therefore a strong evidence to predict the localization of SLs accumulation in organs for which metabolomics analyses are not conclusive (SLs level below the detection limit). Interestingly, *in silico* data recovered during this project show that CYP711A encoding genes in *B. distachyon*, rice and *A. thaliana*, are often found highly expressed in flowers/inflorescences and in the seed (**Chapter III, Figure 3.3A**; **Appendix 2**). More specifically, the *Bradi1g75310* gene was shown to be upregulated in the peduncle, spikelet internode (rachis), endosperm and whole grain. Therefore, it is relevant to consider that spikes and the resulting grains are likely subjected to SLs accumulation and that this particular situation could influence the growth of a pathogen specifically infecting these plant organs such as *F. graminearum* during FHB.

In this thesis work, we observed a significant increase of FHB symptoms 7 and 14 dpi on the two *B. distachyon* lines overexpressing the *Bradi1g75310* gene (**Chapter II, Figure 2.6**) and confirmed this result by the relative quantification of the fungal biomass

(**Chapter II, Figure 2.7**). On the contrary, we did not observe any difference between the WT line and the two TILLING mutant lines altered in the *Bradi1g75310* gene. Given the fact that the SLs core biosynthetic pathway seems not strongly altered in healthy spikes of the different OE and mutant lines compared to WT (**Chapter IV, Figure 4.3)**, we hypothesized that only the pool composition and not the absolute quantity of SLs might be altered in spikes of OE lines (increased proportion of orobanchol) but not in the TILLING mutant lines due to the putative functional redundancy between BdCYP711A paralogs. Therefore, orobanchol might be directly or indirectly responsible for this increase susceptibility of OE lines. This is the first time that SLs are shown as susceptibility factors in FHB.

SLs being susceptibility factors, the transcriptional activation of the SLs core biosynthetic pathway in *B. distachyon* during FHB is likely driven by the pathogen to support its growth *in planta*. The transcriptional modulation of genes involved in SLs core biosynthesis has been reported in very few studies. Only one study reported the transcriptional inactivation of the biosynthetic pathway in rice following RGSV infection likely to induce the excessive tillering observed as a typical symptom in RGSV-infected plants (Satoh et al., 2013). On the contrary, the activation of the same pathway was reported in *A. thaliana* and pea following infection with the biotrophic bacteria *Rhodococcus fascians* and the necrotrophic oomycete *Pythium irregulare*, respectively (Stes et al., 2015; Blake et al., 2016). In the first case, the authors were able to demonstrate the increased susceptibility of SLs deficient and insensitive mutants compared to WT line towards the infection with *R. fascians* and also showed that the transcriptional activation of SLs biosynthetic genes was party dependent on cytokinins produced by the pathogenic bacteria which highlight the high degree of specificity of this induction (Stes et al., 2015). On the contrary, no difference of resistance / susceptibility of pea towards *P. irregulare* infection was observed between WT and SLs deficient or insensitive mutant plants (Blake et al., 2016). We tested whether orobanchol has a direct impact on *F. graminearum* growth *ex planta* and were not able to observe significant growth differences with or without orobanchol at late time points (48-96 hpi, **Chapter IV, Figure 4.5**). A slight inhibition of fungal growth was described at 10^{-4} M orobanchol, a concentration which is unlikely to be found in nature. However, a slight but significant increase of fungal growth was detected for biologically-compatible concentrations as low as 10^{-12} M orobanchol at 24 hpi. This could reflect an activation of the early spore developmental processes as showed for AM fungi; hence, it would be interesting to focus on the impact of SLs on *F. graminearum* spore germination *via* more precise microscopic observations rather than global evaluation of fungal growth. This hypothesis is supported by

recently obtained data showing a positive impact of orobanchol on the number of germinating tubes emerging from *F. graminearum* spores. Indeed, a maximum of 50 % increase of the number of germinating tube was observed when spores were grown on medium containing 10^{-10} M orobanchol compared to the control condition (data not shown).

We also tested whether SLs could influence the expression pattern of defense-related genes *via* the relative quantification of two genes, *PAL6* and *PR9*, encoding a phenylalanine ammonia lyase and a peroxidase, respectively (**Chapter IV, Figure 4.6-4.7**). At the basal level (healthy spikes), no significant difference was observed between our lines altered in the *Bradi1g75310* gene (and more specifically OE lines) and WT line Bd21-3. This suggests that a modification of SLs pool or content does not influence the expression pattern of these two genes. On the contrary, during FHB, we observed a significant increase of expression of these two genes in the OE line which expressed the most the *Bradi1g75310* gene as compared to Bd21-3. This suggests a faster or greater induction of these genes in this OE line which is not consistent, *a priori*, with the above mentioned increased sensitivity. Several hypotheses could explain these contradictory results. First, it is important to notice that we only followed the expression of two genes, known to be induced during the interaction between *B. distachyon* and *F. graminearum* but not functionally characterized. It is therefore necessary to complete this experiment with the follow-up of other defense marker genes. The recent development of a set of defense-associated marker genes in *B. distachyon* might help us in this perspective (Kouzai et al., 2016). Moreover, because *F. graminearum* is a hemibiotrophic pathogen, both pathways involved in defense against biotrophic (generally associated to SA) and necrotrophic (generally associated to JA) pathogens could be mobilized in a spatiotemporal dynamics. The status of genes involved in one or another pathway could therefore give us clues about the role of SLs in defense against *F. graminearum*, depending over time on the given trophic lifestyle of the pathogen on its host plant. Second, we hypothesized that orobanchol might activate *F. graminearum* spore germination and therefore could be considered as a germinant. If it is the case, we could conceive that spores germinate more easily on lines with increased level of orobanchol (OE lines) compared to the others and that this would result in an increased number of infection sites. In other words, primary infection would be promoted in the lines which overexpress the *Bradi1g75310* gene. This promotion of pathogenesis is likely to induce higher plant responses, among them transcriptional induction of defense-related genes, which could explain the results obtained during this project. To test this hypothesis, several microscopic analyses associated to staining methods of ROS (DAB staining) or dead cells (trypan blue staining) or to the use of a *F. graminearum* strain which

constitutively expresses the green fluorescent protein (GFP) could help us to rapidly detect any differences in the early steps of the infection. Finally, numerous crosstalks between SLs and other phytohormones have been described (Cheng et al., 2013) including SA (Rozpądek et al., 2018) and JA (Torres-Vera et al., 2014) generally associated to defense pathways against biotrophic and necrotrophic pathogens, respectively. Moreover, *F. graminearum* has been shown to produce indole-3-acetic acid (IAA), an auxin compound both shown to accumulate in wheat spike during FHB and to be subjected to a SLs-mediated negative feedback *in planta* (Sang et al., 2014; Luo et al., 2016). It would therefore be interesting to conduct metabolomic analyses to compare the phytohormones content in the *B. distachyon* lines altered in the *Bradi1g75310* locus or gene expression to determine whether increased susceptibility of OE lines results from abnormal hormonal content.

E. RESEARCH AND APPLIED PERSPECTIVES OF THE PH.D. WORK

The Ph.D. project allowed the generation of several *A. thaliana* and *B. distachyon* modified lines which will constitute an essential material to go on with the study of SLs and their biosynthesis in the model temperate cereal and the elucidation of the role of SLs during plant-pathogen interactions. Indeed, each *BdCYP711A* gene has been overexpressed independently in both *A. thaliana* and the host species *B. distachyon* and the availability of plasmid constructions carrying *BdCYP711As* genes will allow rapid transfer into a new organism, especially yeast. To finely characterize the five BdCYP711A copies, these three organisms could, indeed, be particularly interesting. The yeast, first, in addition to allowing the functional validation of P450s, constitutes also the easiest way to perform *in vitro* activity assays and therefore finely biochemically characterize the biosynthetic step catalyzed by each copy. The only, but important, limit of this approach is the availability of substrates. Although more and more academic and private laboratories succeed in the synthesis of several SLs or SL-like compounds, their obtention is often limited by low yields, low stability of the molecules and difficulty in obtaining enantiopure compounds. That is why plant material remains of particular interest on two aspects. First, the overexpression approach appeared during this project as an interesting tool to evaluate, *in planta*, the activity of a MAX1 homolog. Although this approach will not allow the listing of all biochemical reactions catalyzed by a MAX1 homolog of interest, it should provide strong evidence on compound(s) predominantly synthetized *in planta*. However, several improvements are needed, such as the possibility to efficiently detect and quantify SLs *in planta* in *B. distachyon* and not only in

root exudates for which SLs composition might be influenced by affinity of SLs with cell membrane exporters, stability of the molecules *ex planta* and others. Second, following the characterization of the SLs pool content, these OE lines could be used in biological experiment to evaluate the role of one or a group of SLs in various biological processes: development, interactions with detrimental or symbiotic organisms, abiotic stress tolerance… Overall, the OE approach appeared as the most promising regarding *B. distachyon* because of the difficulty to obtain KO mutant lines (almost 6 times less insertional mutant line in the *B. distachyon* collection compared to *A. thaliana* Salk T-DNA bank, for example) with clean genetic background (difficulty to perform backcrosses for TILLING mutant lines).

We introduced this thesis manuscript with an overview on wheat history and current challenges that surround wheat growing. Indeed, *B. distachyon* is a species with close phylogenetic relationship with this temperate cereal crop with a high level of synteny, a trait already used successfully by the host team to improve wheat genetic resistance towards FHB based on data acquired on *B. distachyon* (Gatti, 2017). We could therefore consider a transfer of the functional genomic knowledge from the model species to the cultivated cereal in order to modulate several traits related to P450s and SLs, which could generates positive impacts in agriculture: secondary metabolism, tolerance to pollutants, plant architecture, communication with AM fungi or parasitic weed management.

CHAPTER VI | MATERIALS & METHODS

A. PLANT MATERIAL

A.1. Brachypodium lines

A.1.1. Growth conditions

Brachypodium distachyon lines (**Appendix 3**) were cultivated in a growth chamber under a 20 h light period at 23°C ± 2°C under fluorescent light (light intensity in SI unit such as 265 µmol.m^{-2}.s^{-1} at the soil level) followed by a 4 h dark period at 20°C ± 2°C with 60% relative humidity. Prior to sowing, seeds were surface sterilized by incubation in a 0.6% sodium hypochlorite solution for 10 min with gentle shaking followed by three rinses in sterile distilled water. Sterilized seeds were subsequently incubated for 5 d at 4°C in sterile distilled water and in the dark. Plants were grown routinely on a 2:1 mixture of compost (Tref terreau P1; Jiffy France SARL) and standard perlite (Sinclair) and soaked with an aqueous solution containing a carbamate fungicide (Previcur® at 2 mL.L^{-1}; Bayer Crop Sciences) and a larvicide (Hortigard® at 1 g.L^{-1}; Syngenta). Plants were routinely watered in 2 to 3 d intervals using a standard nutritional solution and were never allowed to stand in water.

For molecular and metabolic analyses at the root level, the palea and lemma of each seed was removed and seeds were surface sterilized by incubation in a 0.6% sodium hypochlorite solution for 5 min with gentle shaking followed by three rinses in sterile distilled water. Sterilized seeds were subsequently incubated for five days at 4°C in sterile distilled water and in the dark, then pre-germinated on filter paper soaked with sterile water for three days. Seedlings were transferred on hydroponic boxes (Araponics system) in liquid self-made ¼ Murashige and Skoog medium (**Appendix 4**; Murashige and Skoog, 1962). The medium was changed every three days. For strigolactone detection and quantification assays, plant were grown four weeks in self-made liquid ¼ MS then one week in self-made liquid phosphate deficient (- KH_2PO_4) ¼ MS.

A.1.2. Screening of the TILLING mutant collection

We screened the *B. distachyon* TILLING collection (http://tools.ips2.u-psud.fr/UTILLdb) available at the Institute of Plant Sciences Paris-Saclay (IPS2, Orsay, France) for putative point mutations in a fragment of the *Bradi1g75310* gene encompassing the heme binding loop and the PERF encoding regions. Screening was conducted as described by Dalmais et al. (2013). Specific primers used for the generation of the *Bradi1g75310* PCR product were as follow: CYP711A29-F1 (5'-TTC CCT ACA CGA CGC TCT TCC GAT

CTC GGC CAC ATC AAT TTT CAT T-3') and CYP711A29-R (5'-AGT TCA GAC GTG TGC TCT TCC GAT CTT TAG TGC TCT TCT CGA TCG A-3'; complementary sequences with *Bradi1g75310* gene are underlined). Screened families (**Table 2.1**) were then led to homozygosity for their point mutation of interest, checked at each step by sequencing, before characterization.

A.1.3. Production of Brachypodium overexpressing lines

The cDNAs of interest were amplified from spikelets cDNAs using the primers listed in **Appendix 5** adding restriction sites. The PCR products were purified using the NucleoSpin Gel and PCR Clean-up kit (Macherey-Nagel EURL) using the manufacturer's instructions, and then ligated into the linearized pENTR1A plasmid. The resulting plasmids were then used to transfer cDNA fragments into the pIPKb002 binary vector (**Appendix 1**; Himmelbach et al., 2007) by *in vitro* recombination using the Gateway LR Clonase II Enzyme mix according to the manufacturer's recommendations (Invitrogen, Life Technologies). Constructs were confirmed by sequencing at each step. The pIPKb002 binary vectors containing the cDNAs of interest were then electroporated into *Agrobacterium tumefasciens* (AGL1 strain). The Bd21-3 wild-type line was genetically transformed using a method adapted from that described by Vogel and Hill (2008) and Alves et al. (2009). After selection of transformants in MS agar medium containing 40 $mg.L^{-1}$ hygromycin, segregation analysis was used to identify single-locus insertion lines in the T2 generation.

A.2. Arabidopsis lines

A.2.1. Growth condition

Arabidopsis thaliana lines were cultivated in a growth chamber under a 16 h light period at 20°C ± 2°C under fluorescent light (light intensity in SI unit such as 200 $\mu mol.m^{-2}.s^{-1}$ at the soil level) followed by a 8 h dark period at 18°C ± 2°C with 60% relative humidity. Prior to sowing, seeds were surface sterilized by incubation in a solution containing Bayrochlore mini 83,25 $g.L^{-1}$ (Bayrol)/ethanol 96% (1/9, v/v) for 5 to 10 min with gentle shaking followed by two rinses in ethanol 96% then dried overnight. Plants were grown routinely on sifted compost (Tref terreau P1; Jiffy France SARL) and soaked with an aqueous solution containing a carbamate fungicide (Previcur® at 2 $mL.L^{-1}$; Bayer Crop Sciences) and a larvicide (Hortigard® at 1 $g.L^{-1}$; Syngenta). Plants were routinely watered in 2 to 3 d intervals using a standard nutritional solution.

Branching was assessed using a method adapted from Challis et al. (2013). Briefly, plants were cultivated in short day conditions (8 h light) during 4 weeks, transferred in long day condition (16 h light) until flowering stalks reach approximately 10 to 15 cm. Stalks were then decapitated close to rosette. Branches longer than 0.5 cm were counted and height of the highest flowering stalk was measured 10 d later. The *max1-1_35S::MAX1* line (Challis et al., 2013), kindly provided by OTTOLINE LEYSER and RUTH STEPHENS from Sainsbury Laboratory (John Innes Center, Norwich, UK), was used as a positive control.

A.2.2. Production of Arabidopsis transgenic lines

The cDNAs of interest were amplified, purified and ligated into the linearized pENTR1A plasmid as described above. The resulting plasmids were then used to transfer cDNA fragments into the pK7WG2.0 binary vector (**Appendix 1**; Karimi et al., 2002) by *in vitro* recombination using the Gateway LR Clonase II Enzyme mix according to the manufacturer's recommendations (Invitrogen, Life Technologies). Constructs were confirmed by sequencing at each step. The pK7WG2.0 binary vectors containing the cDNAs of interest were then electroporated into *Agrobacterium tumefasciens* (GV3101 strain). The *max1-1* line (Stirnberg et al., 2002), kindly provided by CATHERINE RAMEAU and SANDRINE BONHOMME from Institut Jean-Pierre Bourgin (IJPB, Versailles, France), was genetically transformed using the floral deep method adapted from that described by Clough and Bent (1998). After selection of transformants in ½ MS medium containing 50 $mg.L^{-1}$ kanamycin, segregation analysis was used to identify 100% resistant lines in the T2 generation.

B. FUNGAL MATERIAL

F. graminearum strain PH-1 (Fg^{DON+}; synonym NRRL 31084; Goswami and Kistler, 2004) and strain PH-1Δ*tri5* (Fg^{DON-}; synonym MU102; Cuzick et al., 2008) were maintained on PDA plates (**Appendix 4**). To obtain fungal spores, 2-4 mm^2 plugs from 15-day old PDA plates were inoculated in liquid mung bean medium (Bai and Shaner, 1996, 10 plugs for 20 mL) and incubated at 150 rpm at 23°C for five to six days. The resulting spore suspension was then diluted ten times in fresh liquid mung bean medium and further incubated for five to six additional days under the same conditions. Spores were further filtrated onto sterile Miracloth (Calbiochem, Toulouse, France) and resuspended in 0.01% Tween 20 at the intended final concentration depending on the assay.

C. EVALUATION OF THE IMPACT OF SLS ON *F. GRAMINEARUM* GROWTH

F. graminearum strain PH-1 (Fg^{DON+}) spore suspension was obtained as described above and resuspended in PDB 2X (**Appendix 4**) at 2.10^5 spores.mL^{-1}. (*rac*)-Orobanchol (OIChemIm) was diluted in DMSO at 1 M, and then diluted at the appropriate concentration in sterile water with a final concentration of 0.01% DMSO in each solution. A solution of 0.01% DMSO was used as a control. In 96-well microtiter plate, 100 µL of spore suspension and 100 µL of SL solution were mixed and incubated in the dark at 26°C. Fungal growth was followed by measuring medium absorbance at 405 nm using a spectrophotometer (Tecan).

D. PATHOGENICITY ASSAY

B. distachyon was inoculated 33-35 days post-sowing at mid-anthesis. Whole spikes were sprayed with the fungal spore suspension (10^5 spores.mL^{-1}) until dripping. During the first 24 h, inoculated heads were kept in the dark under high relative humidity (≈ 90%), then incubated with a photoperiod of 8 h of light and 16 h of darkness at 20°C +/- 2°C with the same light intensity used for the plant development. Application of 0.01% Tween 20 was used as a control. The relative humidity was lowered regularly during the first days until reaching 60% at 7 dpi. Symptoms were evaluated at 7 and 14 days after inoculation by counting symptomatic spikelets over the total numbers of spikelets on each inoculated spike. A spikelet was considered as symptomatic if at least half of its florets were symptomatic.

B. distachyon was inoculated with deoxynivalenol (Sigma-Aldrich) by pipetting into a central floral cavity of the second spikelet starting from the top of the spike of different lines 2 µg of DON in acetonitrile and Tween 20 0.01%. Application of the same solution, without DON, was used as control.

E. *IN VITRO* ROOT ASSAY

For root tests *in vitro* (root tolerance) the palea and lemma of each seed were removed and naked seeds were surface sterilized as previously described. Surface-sterilized seeds were incubated at 4°C for 5 days. Consequently, the sterilized *B. distachyon* grains were sown on Linsmaier and Skoog agar medium (**Appendix 4**, Linsmaier and Skoog, 1965) with 30 µM of deoxynivalenol (Sigma-Aldrich) dissolved at 10 mg.mL^{-1} in methanol. LS medium with the appropriate volume of methanol was used as a control. Plates were incubated for 48 h in the dark at 24°C, then moved under the same conditions described for *B. distachyon* growth. Measures on primary root length were performed after 7 days growth.

F. PHYLOGENETIC ANALYSES

Amino acid sequences were recovered from The Cytochrome P450 Homepage (Nelson, 2009) and phylogenetic analyses were inferred by using the Maximum Likelihood method based on the JTT matrix-based model, conducted on MEGA7 software (Kumar et al., 2017).

G. MOLECULAR BIOLOGY

G.1. DNA extraction

Whole genomic DNA from leaves, healthy or infected spikes and roots of *B. distachyon* or from *F. graminearum* mycelium was extracted using the protocol set up by Atoui et al. (2012).

G.2. RNA extraction

Leaves, roots and healthy or infected spikes from *B. distachyon* were ground in liquid nitrogen, and total RNA was extracted from 100 mg of the resulting powder using 1 ml Trizol (Invitrogen, Life Tech). Samples were centrifuged 10 minutes at 4°C (13000 rpm). The supernatant was transferred into a new 2 ml tube and it was incubated 10 minutes at room temperature. Two hundreds microliters of chloroform was added and samples were homogenized for 15 seconds and they were incubated 3 minutes at room temperature. Samples were centrifuged 15 minutes at 4 ° C (13000 rpm speed). The aqueous phase was transferred to a new tube and this step was repeated twice. Once the last aqueous phase was transferred into a new tube, 350 µl of isopropanol was added to precipitate the nucleic acids. The tube was vortexed and incubated for 10 minutes at room temperature. After the centrifugation for 10 minutes at 4°C (13000 rpm), the supernatant was removed, the pellet was washed with 1 mL of 75% ethanol. Samples were finally vortexed and centrifuged for 10 minutes at 4°C (13000 rpm speed). The ethanol was removed and the pellet was dried briefly and resuspended in 40 µl of RNase water–free.

G.3. cDNA synthesis

After one night at -80°C, a digestion with DNase I RNase free (Ambion) was performed. Four µl and a half of buffer 10X and 1 µl of DNase I were added to each sample.

Samples were incubated for 30 minutes at 37°C and DNase was inactivated by the addition of 5 µl of DNase inhibitor (Ambion). Total RNAs was quantified by spectrophotometry (NanoDrop, Thermo Scientific) at 260 nm. The reverse transcription reaction was carried out with Improm-II ™ (Promega). One microliter of oligo dT (500 µg/ml) and 1 µg total RNA in a final volume of 5 µl was incubated for 5 minutes at 70°C. These 5 µl were supplemented with 15 µl of: 1 µl of dNTP (10 mM each), 1.2 µl of MgCl (25 mM), 4 µl of 5X buffer, 1 µl of reverse transcriptase and 7.8 µl of sterile water. The 20 µl obtained were then subjected to 3 steps: 25°C for 5 minutes, 42°C for 1 hour and 70°C for 15 minutes. The cDNAs were stored at -20°C until use. The product was diluted 10 times in nuclease-free water.

G.4. qPCR

RT-qPCR was performed on 2 µL of the 1/10 diluted cDNA product or on 20 ng of total gDNA using 8 pmol of each specific primer and 10 µL of SYBRGreen Master Mix (Applied Biosystems) in a final volume of 20 µL. Reactions were performed in a LightCycler LC480 real-time PCR system (Roche). After a denaturation step of 10 min at 95°C, samples are subjected to 45 cycles of 15 seconds at 95°C and 40 seconds at 60°C. At the end of the program, the temperature is headed gradually from 65°C to 95°C to acquire the dissociation curve. All (RT-)qPCR were carried out on biological triplicates, each in technical duplicate. To determine the efficiency of primer pairs, a standard range of dilution has been done from a pool of cDNAs or from pure plant or fungal gDNA. The results are analyzed using the LightCycler 3 software (Roche) for the determination of the efficiency (E) and the Ct (Threshold cycle) of the pairs of primers, in different conditions. Relative expression of the gene is calculated using the method of $2^{-\Delta\Delta Ct}$ (Livak and Schmittgen, 2001). Relative quantification was performed to determine the changes in steady-state mRNA levels of the different genes by comparing the levels of two internal control genes (*ACT7* and *UBC18; Bradi4g41850* and *Bradi4g00660*, respectively)

H. RECOMBINANT PROTEIN

This part of the project has been performed in collaboration with DANIÈLE WERCK-REICHHART and HUGUES RENAULT at the Institut de Biologie Moléculaire des Plantes (IBMP, Strasbourg, France). The yeast (*Saccharomyces cerevisiae*) construct was generated by PCR amplification from complementary DNA prepared from *B. distachyon* spikes using primers listed in **Appendix 5**. The PCR fragment of *Bradi1g75310* was integrated into the yeast

expression vector pYeDP60 (**Appendix 1**; Pompon et al., 1996). Constructs were confirmed by sequencing at each step. The WAT11 yeast strain (Pompon et al., 1996) was transformed with pYeDP60 containing the *Bradi1g75310* sequences as described in Gietz and Schiestl (2008). Yeast cultures were grown and P450 expression was induced as described in Pompon et al. (1996). Cells were harvested by centrifugation and manually broken with glass beads (0.45 mm in diameter) in 50 mM Tris-HCl buffer, pH 7.5, containing 1 mM EDTA and 600 mM sorbitol. The homogenate was centrifuged for 10 min at 10,000 g and the resulting supernatant was centrifuged for 1 h at 100,000 g. The pellet consisting of microsomal membranes was resuspended in 50 mM Tris-HCl, pH 7.4, 1 mM EDTA, and 30% (v/v) glycerol and stored at -20°C until use. P450 content of the microsomal preparations was measured by differential spectrophotometry (Cary 14 UV-Vis, Olis) according to Omura and Sato (1964).

I. STRIGOLACTONES DETECTION AND QUANTIFICATION

Detection and quantification of SLs exuded from the roots of *B. distachyon* lines has been made in collaboration with STÉPHANIE BOUTET-MERCEY and GRÉGORY MOUILLE from IJPB (Versailles, France) according to a method adapted from Boutet-Mercey et al. (2017). *B. distachyon* lines were grown hydroponically as describe above and exudation was performed in fresh ¼ MS -KH_2PO_4 medium during 24 h. When necessary, exudates were immediately frozen in liquid nitrogen and conserved at -80°C before analysis. SLs were extracted from liquid medium, complemented with 10 ng of (*rac*)-GR24 (kindly provided by FRANÇOIS-DIDIER BOYER, IJPB, Versailles, France) as internal standard, by adding the same volume of ethyl acetate followed by a manual and vigorous mixing during 10 min. Organic phase was decanted and dried using a rotary evaporator (Rotavapor, Buchi). The solid phase was resuspended in acetonitrile, and conserved at -20°C before analysis according to Boutet-Mercey et al. (2017). Separation was performed on a $BEHC_{18}$ column (2.1x100 mm, particle size 1.7 µm, Waters), using an ACQUITY UPLC I-class system (Waters), and detection on Waters Xevo TQ-S equipped with an ESI source and operated in positive ion mode.

BIBLIOGRAPHY

Abe S, Sado A, Tanaka K, Kisugi T, Asami K, Ota S, Kim H Il, Yoneyama KK, Xie X, Ohnishi T, et al (2014) Carlactone is converted to carlactonoic acid by MAX1 in Arabidopsis and its methyl ester can directly interact with AtD14 in vitro. Proc Natl Acad Sci **111**: 18084–18089

Agusti J, Herold S, Schwarz M, Sanchez P, Ljung K, Dun EA, Brewer PB, Beveridge CA, Sehr EM, Greb T (2011) Strigolactone signaling is required for auxin-dependent stimulation of secondary growth in plants. Proc Natl Acad Sci **108**: 20242–20247

Akiyama K, Matsuzaki K, Hayashi H (2005) Plant sesquiterpenes induce hyphal branching in arbuscular mycorrhizal fungi. Nature **435**: 824–827

Akiyama K, Ogasawara S, Ito S, Hayashi H (2010) Structural requirements of strigolactones for hyphal branching in AM fungi. Plant Cell Physiol **51**: 1104–1117

Al-Babili S, Bouwmeester HJ (2015) Strigolactones, a novel carotenoid-derived plant hormone. Annu Rev Plant Biol **66**: 161–86

Alder A, Jamil M, Marzorati M, Bruno M, Vermathen M, Bigler P, Ghisla S, Bouwmeester H, Beyer P, Al-babili S (2012) The Path from beta-Carotene to Carlactone, a Strigolactone-Like Plant Hormone. Science (80-) **335**: 1348–1351

Alexander NJ, McCormick SP, Waalwijk C, van der Lee T, Proctor RH (2011) The genetic basis for 3-ADON and 15-ADON trichothecene chemotypes in Fusarium. Fungal Genet Biol **48**: 485–495

Alves SC, Worland B, Thole V, Snape JW, Bevan MW, Vain P (2009) A protocol for Agrobacterium-mediated transformation of Brachypodium distachyon community standard line Bd21. Nat Protoc **4**: 638–649

Andrews JH (2017) Comparative ecology of microorganisms and macroorganisms. Brock/Springer Ser Contemp Biosci. doi: 10.1016/0169-5347(92)90057-I

Arite T, Iwata H, Ohshima K, Maekawa M, Nakajima M, Kojima M, Sakakibara H, Kyozuka J (2007) DWARF10, an RMS1/MAX4/DAD1 ortholog, controls lateral bud outgrowth in rice. Plant J **51**: 1019–1029

Arite T, Kameoka H, Kyozuka J (2012) Strigolactone Positively Controls Crown Root Elongation in Rice. J Plant Growth Regul **31**: 165–172

Arite T, Umehara M, Ishikawa S, Hanada A, Maekawa M, Yamaguchi S, Kyozuka J (2009) D14, a strigolactone-Insensitive mutant of rice, shows an accelerated outgrowth of tillers. Plant Cell Physiol **50**: 1416–1424

Arunachalam C, Doohan FM (2013) Trichothecene toxicity in eukaryotes: Cellular and molecular mechanisms in plants and animals. Toxicol Lett **217**: 149–158

Arvalis Institut du Végétal (2018) Baromètre Maladies, Arvalis Institut du Végétal. http://www.barometre-maladies.arvalis-infos.fr/bletendre/

Atoui A, El Khoury A, Kallassy M, Lebrihi A (2012) Quantification of Fusarium graminearum and Fusarium culmorum by real-time PCR system and zearalenone assessment in maize. Int J Food Microbiol **154**: 59–65

Ayliffe M, Singh D, Park R, Moscou M, Pryor T (2013) Infection of Brachypodium distachyon with Selected Grass Rust Pathogens. Mol Plant-Microbe Interact MPMI **946**: 946–957

Bai G, Shaner G (2004) Management and Resistance in Wheat and Barley to Fusarium Head Blight. Annu Rev Phytopathol **42**: 135–161

Bai G, Shaner G (1996) Variation in Fusarium graminearum and Culticar Resistance to Wheat Scab. Plant Dis **80**: 975–979

Bak S, Beisson F, Bishop G, Hamberger B, Höfer R, Paquette S, Werck-Reichhart D (2011) Cytochromes p450. Arabidopsis Book **9**: e0144

Bak S, Kahn RA, Olsen CE, Halkier BA (1997) Cloning and expression in Escherichia coli of the obtusifoliol 14 alpha- demethylase of Sorghum bicolor (L.) Moench, a cytochrome P450 orthologous to the sterol 14 alpha-demethylases (CYP51) from fungi and mammals. Plant J **11**: 191–201

Bar-Yosef O (1998) On the Nature of Transitions: the Middle to Upper Palaeolithic and the Neolithic Revolution. Cambridge Archaeol J **8**: 141

Batard Y, Leret M, Schalk M, Robineau T, Durst F (1998) Molecular cloning and functional expression in yeast of O-de-ethylase from Helianthus tuberosus. Plant J **14**: 111–120

Becher R, Hettwer U, Karlovsky P, Deising HB, Wirsel SGR (2010) Adaptation of Fusarium graminearum to tebuconazole yielded descendants diverging for levels of fitness, fungicide resistance, virulence, and mycotoxin production. Phytopathology **100**: 444–453

Belmondo S, Marschall R, Tudzynski P, López Ráez J a., Artuso E, Prandi C, Lanfranco L (2017) Identification of genes involved in fungal responses to strigolactones using mutants from fungal pathogens. Curr Genet **63**: 201–213

Bernardo A, Bai G, Guo P, Xiao K, Guenzi AC, Ayoubi P (2007) Fusarium graminearum-induced changes in gene expression between Fusarium head blight-resistant and susceptible wheat cultivars. Funct Integr Genomics **7**: 69–77

Besserer A, Puech-Pagès V, Kiefer P, Gomez-Roldan V, Jauneau A, Roy S, Portais JC, Roux C, Bécard G, Séjalon-Delmas N (2006) Strigolactones stimulate arbuscular mycorrhizal fungi by activating mitochondria. PLoS Biol **4**: 1239–1247

Blake SN, Barry KM, Gill WM, Reid JB, Foo E (2016) The role of strigolactones and ethylene in disease caused by Pythium irregulare. Mol Plant Pathol **17**: 680–690

Boari A, Ciasca B, Pineda-Martos R, Lattanzio VMT, Yoneyama K, Vurro M (2016) Parasitic weed management by using strigolactone-degrading fungi. Pest Manag Sci **72**: 2043–2047

Boddu J, Cho S, Kruger WM, Muehlbauer GJ (2006) Transcriptome Analysis of the Barley- *Fusarium graminearum* Interaction. Mol Plant-Microbe Interact **19**: 407–417

Boddu J, Cho S, Muehlbauer GJ (2007) Transcriptome Analysis of Trichothecene-Induced Gene Expression in Barley. Mol Plant-Microbe Interact **20**: 1364–1375

Boenisch MJ, Schäfer W (2011) Fusarium graminearum forms mycotoxin producing infection structures on wheat. BMC Plant Biol **11**: 110

Bolton MD, Kolmer J a., Garvin DF (2008) Wheat leaf rust caused by Puccinia triticina. Mol Plant Pathol **9**: 563–575

Bolwell GP, Bozak K, Zimmerlin A (1994) Plant cytochrome p450. Phytochemistry **37**: 1491–1506

Booker J, Auldridge M, Wills S, McCarty D, Klee H, Leyser O (2004) MAX3/CCD7 Is a Carotenoid Cleavage Dioxygenase Required for the Synthesis of a Novel Plant Signaling Molecule. Curr Biol **14**: 1232–1238

Booker J, Sieberer T, Wright W, Williamson L, Willett B, Stirnberg P, Turnbull C, Srinivasan M, Goddard P, Leyser O (2005) MAX1 encodes a cytochrome P450 family member that acts downstream of MAX3/4 to produce a carotenoid-derived branch-inhibiting hormone. Dev Cell **8**: 443–449

Boutet-Mercey S, Perreau F, Roux A, Clavé G, Pillot J-P, Schmitz-Afonso I, Touboul D, Mouille G, Rameau C, Boyer F-D (2017) Validated Method for Strigolactone Quantification by Ultra High-Performance Liquid Chromatography - Electrospray Ionisation Tandem Mass Spectrometry Using Novel Deuterium Labelled Standards. Phytochem Anal. doi: 10.1002/pca.2714

Bozak KR, O'keefe DP, Christoffersen RE (1992) Expression of a Ripening-Related Avocado (Persea americana) Cytochrome P450 in Yeast. Plant Physiol **100**: 1976–1981

Bozak KR, Yu H, Sirevåg R, Christoffersen RE (1990) Sequence analysis of ripening-related cytochrome P-450 cDNAs from avocado fruit. Proc Natl Acad Sci U S A **87**: 3904–3908

Bragg JN, Wu J, Gordon SP, Guttman ME, Thilmony R, Lazo GR, Gu YQ, Vogel JP (2012) Generation and Characterization of the Western Regional Research Center Brachypodium T-DNA Insertional Mutant Collection. PLoS One. doi: 10.1371/journal.pone.0041916

Brewer PB, Dun E a., Gui R, Mason MG, Beveridge C a. (2015) Strigolactone Inhibition of Branching Independent of Polar Auxin Transport. Plant Physiol **168**: 1820–1829

Brewer PB, Yoneyama K, Filardo F, Meyers E, Scaffidi A, Frickey T, Akiyama K, Seto Y, Dun E a., Cremer JE, et al (2016) LATERAL BRANCHING OXIDOREDUCTASE acts in the final stages of strigolactone biosynthesis in Arabidopsis. Proc Natl Acad Sci **113**: 6301–6306

Brown N a., Urban M, van de Meene AML, Hammond-Kosack KE (2010) The infection biology of Fusarium graminearum: Defining the pathways of spikelet to spikelet colonisation in wheat ears. Fungal Biol **114**: 555–571

Brutnell TP, Bennetzen JL, Vogel JP (2015) *Brachypodium distachyon* and *Setaria viridis* : Model Genetic Systems for the Grasses. Annu Rev Plant Biol **66**: 465–485

Buerstmayr H, Ban T, Anderson JA (2009) QTL mapping and marker-assisted selection for Fusarium head blight resistance in wheat : a review. Plant Breed **128**: 1–26

Buerstmayr H, Steiner B, Hartl L, Griesser M, Angerer N, Lengauer D, Miedaner T, Schneider B, Lemmens M (2003) Molecular mapping of QTLs for Fusarium head blight resistance in spring wheat. II. Resistance to fungal penetration and spread. Theor Appl Genet **107**: 503–508

Cabello-hurtado F, Batard Y, Salau J, Durst F, Pinot F (1998) Cloning , Expression in Yeast, and Functional Characterization of CYP81B1, a Plant Cytochrome P450 That Catalyzes In-chain Hydroxylation of Fatty Acids. **273**: 7260–7267

Cardoso C, Ruyter-Spira C, Bouwmeester HJ (2011) Strigolactones and root infestation by plant-parasitic Striga, Orobanche and Phelipanche spp. Plant Sci **180**: 414–420

Cardoso C, Zhang Y, Jamil M, Hepworth J, Charnikhova T, Dimkpa SON, Meharg C, Wright MH, Liu J, Meng X, et al (2014) Natural variation of rice strigolactone biosynthesis is associated with the deletion of two *MAX1* orthologs. Proc Natl Acad Sci **111**: 2379–2384

Chakraborty S, Newton a. C (2011) Climate change, plant diseases and food security: An overview. Plant Pathol **60**: 2–14

Challis RJ, Hepworth J, Mouchel C, Waites R, Leyser O (2013) A Role for MORE AXILLARY GROWTH1 (MAX1) in Evolutionary Diversity in Strigolactone Signaling Upstream of MAX2. Plant Physiol **161**: 1885–1902

CHAP (2018) CropMonitor, Crop Health and Protection Centre. http://www.cropmonitor.co.uk/

Cheng X, Ruyter-Spira C, Bouwmeester H (2013) The interaction between strigolactones and other plant hormones in the regulation of plant development. Front Plant Sci **4**: 1–16

CIMMYT (2018) International Maize and Wheat Improvement Center Webpage. http://www.cimmyt.org/

Clough SJ, Bent AF (1998) Floral dip: A simplified method for Agrobacterium-mediated transformation of *Arabidopsis thaliana*. Plant J **16**: 735–743

Coleman JOD, Blake-Kalff MMA, Davies TGE (1997) Detoxification of xenobiotics by plants: Chemical modification and vacuolar compartmentation. Trends Plant Sci **2**: 144–151

Cook CE, Whichard LP, Turner B, Wall ME, Egley GH (1966) Germination of Witchweed (Striga lutea Lour.): Isolation and Properties of a Potent Stimulant. Science (80-) **154**: 1189–1190

Cook RJ (2003) Take-all of wheat. Physiol Mol Plant Pathol **62**: 73–86

Cowger C, Patton-Ozkurt J, Brown-Guedira G, Perugini L (2009) Post-anthesis moisture increased Fusarium head blight and deoxynivalenol levels in North Carolina winter wheat. Phytopathology **99**: 320–327

Crawford S, Shinohara N, Sieberer T, Williamson L, George G, Hepworth J, Muller D, Domagalska M a., Leyser O (2010) Strigolactones enhance competition between shoot branches by dampening auxin transport. Development **137**: 2905–2913

Crozier A, Jaganath IB, Clifford MN (2007) Phenols, Polyphenols and Tannins: An Overview. Plant Second Metab Occur Struct Role Hum Diet 1–24

Cui Y, Lee MY, Huo N, Bragg J, Yan L, Yuan C, Li C, Holditch SJ, Xie J, Luo MC, et al (2012) Fine mapping of the Bsr1 barley stripe mosaic virus resistance gene in the model grass brachypodium distachyon. PLoS One. doi: 10.1371/journal.pone.0038333

Curtis BC (2004) Wheat in the world. Food Agric Organ United Nations 1–16

Cuzick A, Urban M, Hammond-Kosack K (2008) Fusarium graminearum gene deletion mutants map1 and tri5 reveal similarities and differences in the pathogenicity requirements to cause disease on Arabidopsis and wheat floral tissue. New Phytol **177**: 990–1000

Czarnecki O, Yang J, Wang X, Wang S, Muchero W, Tuskan G a., Chen JG (2014) Characterization of MORE AXILLARY GROWTH genes in populus. PLoS One. doi: 10.1371/journal.pone.0102757

Dalmais M, Antelme S, Ho-Yue-Kuang S, Wang Y, Darracq O, d'Yvoire MB, Cézard L, Légée F, Blondet E, Oria N, et al (2013) A TILLING Platform for Functional Genomics in Brachypodium distachyon. PLoS One. doi: 10.1371/journal.pone.0065503

David Miller J, Culley J, Fraser K, Hubbard S, Meloche F, Ouellet T, Lloyd Seaman W, Seifert K a., Turkington K, Voldeng H (1998) Effect of tillage practice on fusarium head blight of wheat. Can J Plant Pathol **20**: 95–103

Dean R, Van Kan J a. L, Pretorius Z a., Hammond-Kosack KE, Di Pietro A, Spanu PD, Rudd JJ, Dickman M, Kahmann R, Ellis J, et al (2012) The Top 10 fungal pathogens in molecular plant pathology. Mol Plant Pathol **13**: 414–430

Decker EL, Alder A, Hunn S, Ferguson J, Lehtonen MT, Scheler B, Kerres KL, Wiedemann G, Safavi-Rizi V, Nordzieke S, et al (2017) Strigolactone biosynthesis is

evolutionarily conserved, regulated by phosphate starvation and contributes to resistance against phytopathogenic fungi in a moss, *Physcomitrella patens*. New Phytol. doi: 10.1111/nph.14506

Desjardins AE, Hohn TM, McCormick SP (1993) Trichothecene biosynthesis in Fusarium species: chemistry, genetics, and significance. Microbiol Rev **57**: 595–604

Desmond OJ, Manners JM, Stephens AE, Maclean DJ, Schenk PM, Gardiner DM, Munn AL, Kazan K (2008) The Fusarium mycotoxin deoxynivalenol elicits hydrogen peroxide production, programmed cell death and defence responses in wheat. Mol Plant Pathol **9**: 435–445

Diamond M, Reape TJ, Rocha O, Doyle SM, Kacprzyk J, Doohan FM, McCabe PF (2013) The Fusarium Mycotoxin Deoxynivalenol Can Inhibit Plant Apoptosis-Like Programmed Cell Death. PLoS One. doi: 10.1371/journal.pone.0069542

Didierjean L, Gondet L, Perkins R, Lau S-MC, Schaller H, O'Keefe DP, Werck-Reichhart D (2002) Engineering Herbicide Metabolism in Tobacco and Arabidopsis with CYP76B1, a Cytochrome P450 Enzyme from Jerusalem Artichoke. Plant Physiol **130**: 179–189

Dill-Macky R, Jones RK (2000) The Effect of Previous Crop Residues and Tillage on Fusarium Head Blight of Wheat. Plant Dis **84**: 71–76

Dohn DR, Krieger RI (1984) N-demethylation of p-chloro-N-methylaniline catalyzed by subcellular fractions from the avocado pear (Persea americana). Arch Biochem Biophys **231**: 416–423

Dor E, Joel DM, Kapulnik Y, Koltai H, Hershenhorn J (2011) The synthetic strigolactone GR24 influences the growth pattern of phytopathogenic fungi. Planta **234**: 419–427

Draper J, Mur L a. J, Jenkins G, Ghosh-Biswas GC, Bablak P, Hasterok R, Routledge APM (2001) Brachypodium distachyon. A New Model System for Functional Genomics in Grasses1. Plant Physiol **127**: 1539–1555

Drummond R, Sheehan H, Simons JL, Martinez-Sanchez NM, Turner RM, Putterill J, C SK (2012) The expression of petunia strigolactone pathway genes is altered as part of the endogenous developmental program. Front Plant Sci **2**: 1–14

Drummond RSM, Martinez-Sanchez NM, Janssen BJ, Templeton KR, Simons JL, Quinn BD, Karunairetnam S, Snowden KC (2009) Petunia hybrida CAROTENOID CLEAVAGE DIOXYGENASE7 Is Involved in the Production of Negative and Positive Branching Signals in Petunia. Plant Physiol **151**: 1867–1877

Dubcovsky J, Dvorak J (2007) Genome Plasticity a Key Factor in the Success of Polyploid Wheat Under Domestication. Science (80-) **316**: 1862–1866

Edwards R, Dixon DP, Cummins I, Brazier-Hicks M, Skipsey M (2011) New Perspectives on the Metabolism and Detoxification of Synthetic Compounds in Plants. *In* P Schröder,

CD Collins, eds, Org. Xenobiotics Plants From Mode Action to Ecophysiol. Springer Netherlands, Dordrecht, pp 125–148

ENDURE (2018) EUROWHEAT. http://eurowheat.au.dk/

Enghiad A, Ufer D, Countryman AM, Thilmany DD (2017) An Overview of Global Wheat Market Fundamentals in an Era of Climate Concerns. Int J Agron. doi: 10.1155/2017/3931897

European Commission (2006) EURL-Mycotoxins. https://ec.europa.eu/jrc/en/eurl/mycotoxins

Falter C, Voigt CA (2014) Comparative Cellular Analysis of Pathogenic Fungi with a Disease Incidence in Brachypodium distachyon and Miscanthus x giganteus. Bioenergy Res **7**: 958–973

FAO (2018) Food and Agricultural Organization of the United Nations - Statistics. http://www.fao.org/faostat/en/#home

FDA (2010) Chemical Contaminants, Metals, Natural Toxins & Pesticides Guidance Documents & Regulations. https://www.fda.gov/Food/GuidanceRegulation/GuidanceDocumentsRegulatoryInformation/ChemicalContaminantsMetalsNaturalToxinsPesticides/default.htm

Feldman M (2001) Origin of cultivated wheat. World Wheat B. A Hist. Wheat Breed. pp 3–56

Feldman M (1995) Wheats. *In* J Smartt, N Simmonds, eds, Evol. Crop plants. Harlow, UK: Longman Scientific and Technical, pp 185–192

Fitzgerald TL, Powell JJ, Schneebeli K, Hsia MM, Gardiner DM, Bragg JN, McIntyre CL, Manners JM, Ayliffe M, Watt M, et al (2015) Brachypodium as an emerging model for cereal-pathogen interactions. Ann Bot **115**: 717–731

Foo E, Blake SN, Fisher BJ, Smith J a., Reid JB (2016) The role of strigolactones during plant interactions with the pathogenic fungus Fusarium oxysporum. Planta **243**: 1387–1396

Foo E, Bullier E, Goussot M, Foucher F, Ramean C, Beveridge C (2005) The Branching Gene RAMOSUS1 Mediates Interactions among Two Novel Signals and Auxin in Pea. Plant Cell **17**: 464–474

Foo E, Davies NW (2011) Strigolactones promote nodulation in pea. Planta **234**: 1073–1081

Foroud N a., Eudes F (2009) Trichothecenes in cereal grains. Int J Mol Sci **10**: 147–173

Francl LJ (2001) The..Disease Triangle: A Plant Pathological Paradigm Revisited. Plant Heal Instr. doi: 10.1094/PHI-T-2001-0517-01

Fraser CM, Chapple C (2011) The Phenylpropanoid Pathway in Arabidopsis. Arab B **9**: e0152

Frear D, Swanson H, Tanaka R (1969) N-demethylation of substituted 3-(phenyl)-1-methylureas: Isolation and characterization of a microsomal mixed function oxidase from cotton. Phytochemistry **8**: 2157–2169

Fruhmann P, Skrinjar P, Weber J, Mikula H, Warth B, Sulyok M, Krska R, Adam G, Rosenberg E, Hametner C, et al (2014) Sulfation of deoxynivalenol, its acetylated derivatives, and T2-toxin. Tetrahedron **70**: 5260–5266

Fry WE (1982) Principles of plant disease management. Academic Press

Gabriac B, Werck-Reichhart D, Teutsch H, Durst F (1991) Purification and immunocharacterization of a plant cytochrome P450: The cinnamic acid 4-hydroxylase. Arch Biochem Biophys **288**: 302–309

Gardiner S a., Boddu J, Berthiller F, Hametner C, Stupar RM, Adam G, Muehlbauer GJ (2010) Transcriptome Analysis of the Barley–Deoxynivalenol Interaction: Evidence for a Role of Glutathione in Deoxynivalenol Detoxification. Mol Plant-Microbe Interact **23**: 962–976

Garvin DF (2016) Garvin Lab Brachypodium Information. https://www.ars.usda.gov/midwest-area/stpaul/plant-science-research/people/david-garvin/garvin-lab-brachypodium-information/

Gatti M (2017) Detoxification of mycotoxins as a source of resistance to Fusarium Head blight: from Brachypodium distachyon to Triticum aestivum. Université Paris-Saclay

Gietz RD, Schiestl RH (2008) High-efficiency yeast transformation using the LiAc / SS carrier DNA / PEG method. Nat Protoc **2**: 31–35

Gilbert J, Haber S (2013) Overview of some recent research developments in fusarium head blight of wheat. Can J Plant Pathol **35**: 149–174

Girin T, David LC, Chardin C, Sibout R, Krapp A, Ferrario-Méry S, Daniel-Vedele F (2014) Brachypodium: A promising hub between model species and cereals. J Exp Bot **65**: 5683–5686

Glenn a. E, Hinton DM, Yates IE, Bacon CW (2001) Detoxification of Corn Antimicrobial Compounds as the Basis for Isolating Fusarium verticillioides and Some Other Fusarium Species from Corn. Appl Environ Microbiol **67**: 2973–2981

Godfray HCJ, Beddington JR, Crute IR, Haddad L, Lawrence D, Muir JF, Pretty J, Robinson S, Thomas SM, Toulmin C (2010) Food security: The challenge of feeding 9 billion people. Science (80-) **327**: 812–818

Goff S a (1999) Rice as a model for crop genomics. Genome Stud Mol Genet 86–89

Gomez-Roldan V, Fermas S, Brewer PB, Puech-Pagès V, Dun E a, Pillot J-P, Letisse F, Matusova R, Danoun S, Portais J-C, et al (2008) Strigolactone inhibition of shoot branching. Nature **455**: 189–194

Goswami RS, Kistler HC (2004) Heading for disaster: Fusarium graminearum on cereal crops. Mol Plant Pathol **5**: 515–525

Gottwald S, Samans B, Lück S, Friedt W (2012) Jasmonate and ethylene dependent defence gene expression and suppression of fungal virulence factors: Two essential mechanisms of Fusarium head blight resistance in wheat? BMC Genomics. doi: 10.1186/1471-2164-13-369

Guéguen Y, Mouzat K, Ferrari L, Tissandie E, Lobaccaro JM a., Batt a. M, Paquet F, Voisin P, Aigueperse J, Gourmelon P, et al (2006) Les cytochromes P450: Métabolisme des xénobiotiques, régulation et rôle en clinique. Ann Biol Clin (Paris) **64**: 535–548

Guengerich FP (2001) Common and Uncommon Cytochrome P450 Reactions Related to Metabolism and Chemical Toxicity. Chem Res Toxicol **14**: 611–650

Guenther JC, Trail F (2005) The development and differentiation of Gibberella zeae (anamorph: Fusarium graminearum) during colonization of wheat. Mycologia **97**: 229–237

Gunupuru LR, Perochon a., Doohan FM (2017) Deoxynivalenol resistance as a component of FHB resistance. Trop Plant Pathol **42**: 175–183

Guzman C, Peña RJ, Singh R, Autrique E, Dreisigacker S, Crossa J, Rutkoski J, Poland J, Battenfield S (2016) Wheat quality improvement at CIMMYT and the use of genomic selection on it. Appl Transl Genomics **11**: 3–8

Ha X, Koopmann B, von Tiedemann A (2015) Wheat blast and fusarium head blight display contrasting interaction patterns on ears of wheat genotypes differing in resistance. Phytopathology 1–12

Hallen-Adams HE, Wenner N, Kuldau G a, Trail F (2011) Deoxynivalenol Biosynthesis-Related Gene Expression During Wheat Kernel Colonization by Fusarium graminearum. Phytopathology **101**: 1091–1096

Hannemann F, Bichet A, Ewen KM, Bernhardt R (2007) Cytochrome P450 systems-biological variations of electron transport chains. Biochim Biophys Acta - Gen Subj **1770**: 330–344

Harrison PJ, Bugg TDH (2014) Enzymology of the carotenoid cleavage dioxygenases: Reaction mechanisms, inhibition and biochemical roles. Arch Biochem Biophys **544**: 105–111

Hayward a., Stirnberg P, Beveridge C, Leyser O (2009) Interactions between Auxin and Strigolactone in Shoot Branching Control. Plant Physiol **151**: 400–412

He JW, Bondy GS, Zhou T, Caldwell D, Boland GJ, Scott PM (2015) Toxicology of 3-epi-deoxynivalenol, a deoxynivalenol-transformation product by Devosia mutans 17-2-E-8. Food Chem Toxicol **84**: 250–259

Hedden P, Thomas SG (2012) Gibberellin biosynthesis and its regulation. Biochem J **444**: 11–25

Himmelbach a., Zierold U, Hensel G, Riechen J, Douchkov D, Schweizer P, Kumlehn J (2007) A Set of Modular Binary Vectors for Transformation of Cereals. Plant Physiol **145**: 1192–1200

Höfer R, Boachon B, Renault H, Gavira C, Miesch L, Iglesias J, Ginglinger J-F, Allouche L, Miesch M, Grec S, et al (2014) Dual function of the CYP76 family from Arabidopsis thaliana in the metabolism of monoterpenols and phenylurea herbicides. Plant Physiol **166**: 1149–1161

Höfer R, Dong L, André F, Ginglinger JF, Lugan R, Gavira C, Grec S, Lang G, Memelink J, Van Der Krol S, et al (2013) Geraniol hydroxylase and hydroxygeraniol oxidase activities of the CYP76 family of cytochrome P450 enzymes and potential for engineering the early steps of the (seco)iridoid pathway. Metab Eng **20**: 221–232

Hofstad AN, Nussbaumer T, Akhunov E, Shin S, Kugler KG, Kistler HC, Mayer KFX, Muehlbauer GJ (2016) Examining the Transcriptional Response in Wheat Near-Isogenic Lines to Infection and Deoxynivalenol Treatment. Plant Genome. doi: 10.3835/plantgenome2015.05.0032

Hohn TM, Vanmiddlesworth F (1986) Purification and characterization of the sesquiterpene cyclase trichodiene synthetase from Fusarium sporotrichioides. Arch Biochem Biophys **251**: 756–761

Hu Z, Yamauchi T, Yang J, Jikumaru Y, Tsuchida-Mayama T, Ichikawa H, Takamure I, Nagamura Y, Tsutsumi N, Yamaguchi S, et al (2014) Strigolactone and cytokinin act antagonistically in regulating rice mesocotyl elongation in darkness. Plant Cell Physiol **55**: 30–41

Huang MT, Lu YC, Zhang S, Luo F, Yang H (2016) Rice (Oryza sativa) Laccases Involved in Modification and Detoxification of Herbicides Atrazine and Isoproturon Residues in Plants. J Agric Food Chem **64**: 6397–6406

IMA (2018) MycoBank - International Mycological Association. http://www.mycobank.org

IPNI (2018) The International Plant Names Index. http://www.ipni.org

Ito M, Sato I, Ishizaka M, Yoshida SI, Koitabashi M, Yoshida S, Tsushima S (2013) Bacterial cytochrome P450 System catabolizing the Fusarium toxin deoxynivalenol. Appl Environ Microbiol **79**: 1619–1628

Jagtap UB, Bapat VA (2017) Transgenic Approaches for Building Plant Armor and Weaponry to Combat Xenobiotic Pollutants : Current Trends and Future Prospects. 197–215

Jansen C, von Wettstein D, Schafer W, Kogel K-H, Felk a., Maier FJ (2005) Infection patterns in barley and wheat spikes inoculated with wild-type and trichodiene synthase gene disrupted Fusarium graminearum. Proc Natl Acad Sci **102**: 16892–16897

Jia H, Cho S, Muehlbauer GJ (2009) Transcriptome Analysis of a Wheat Near-Isogenic Line Pair Carrying Fusarium Head Blight–Resistant and –Susceptible Alleles. Mol Plant-Microbe Interact **22**: 1366–1378

Jia H, Millett BP, Cho S, Bilgic H, Xu WW, Smith KP, Muehlbauer GJ (2011) Quantitative trait loci conferring resistance to Fusarium head blight in barley respond differentially to Fusarium graminearum infection. Funct Integr Genomics **11**: 95–102

Jiang L, Liu X, Xiong G, Liu H, Chen F, Wang L, Meng X, Liu G, Yu H, Yuan Y, et al (2013) DWARF 53 acts as a repressor of strigolactone signalling in rice. Nature **504**: 401–405

Johnson a. W, Rosebery G, Parker C (1976) A novel approach to Striga and Orobanche control using synthetic germination stimulants. Weed Res **16**: 223–227

Jones DT, Taylor WR, Thornton JM (1992) The rapid generation of mutation data matricies from protein sequences. Comput Appl Biosci **8**: 275–282

Jones RK (2000) Assessments of Fusarium Head Blight of Wheat and Barley in Response to Fungicide Treatment. Plant Dis **84**: 1021–1030

Kameoka H, Kyozuka J (2017) Spatial regulation of strigolactone function. J Exp Bot 1–10

Karimi M, Inze D, Depicker A (2002) GATEWAY vectors for Agrobacterium-mediated plant transformation. Trends Plant Sci **7**: 193–195

Karlovsky P (2011) Biological detoxification of the mycotoxin deoxynivalenol and its use in genetically engineered crops and feed additives. Appl Microbiol Biotechnol **91**: 491–504

Kazan K, Gardiner DM (2017) Transcriptomics of cereal- *Fusarium graminearum* interactions: What we have learned so far. Mol Plant Pathol 1–41

Keller NP, Turner G, Bennett JW (2005) Fungal secondary metabolism - From biochemistry to genomics. Nat Rev Microbiol **3**: 937–947

Keon J, Antoniw J, Carzaniga R, Deller S, Ward JL, Baker JM, Beale MH, Hammond-Kosack K, Rudd JJ (2007) Transcriptional adaptation of Mycosphaerella graminicola to programmed cell death (PCD) of its susceptible wheat host. Mol Plant Microbe Interact **20**: 178–193

Kettles GJ, Kanyuka K (2016) Dissecting the Molecular Interactions between Wheat and the Fungal Pathogen Zymoseptoria tritici. Front Plant Sci **7**: 1–7

Khan N, Maymon M, Hirsch A (2017) Combating Fusarium Infection Using Bacillus-Based Antimicrobials. Microorganisms **5**: 75

El Khoury AE, Atoui A (2010) Ochratoxin a: General overview and actual molecular status. Toxins (Basel) **2**: 461–493

El Khoury W, Makkouk K (2010) Integrated plant disease managment in developing countries. J Plant Pathol **92**: S4.35–S4.42

Kim JE, Cheng KM, Craft NE, Hamberger B, Douglas CJ (2010) Over-expression of Arabidopsis thaliana carotenoid hydroxylases individually and in combination with a β-carotene ketolase provides insight into in vivo functions. Phytochemistry **71**: 168–178

Klingenberg M (1958) Pigments of rat liver microsomes. Arch Biochem Biophys **75**: 376–386

Klix MB, Verreet JA, Beyer M (2007) Comparison of the declining triazole sensitivity of Gibberella zeae and increased sensitivity achieved by advances in triazole fungicide development. Crop Prot **26**: 683–690

Kluger B, Bueschl C, Lemmens M, Michlmayr H, Malachova A, Koutnik A, Maloku I, Berthiller F, Adam G, Krska R, et al (2015) Biotransformation of the mycotoxin deoxynivalenol in fusarium resistant and susceptible near isogenic wheat lines. PLoS One. doi: 10.1371/journal.pone.0119656

Kohlen W, Charnikhova T, Lammers M, Pollina T, Tóth P, Haider I, Pozo MJ, de Maagd R a., Ruyter-Spira C, Bouwmeester HJ, et al (2012) The tomato *CAROTENOID CLEAVAGE DIOXYGENASE8* (*SlCCD8*) regulates rhizosphere signaling, plant architecture and affects reproductive development through strigolactone biosynthesis. New Phytol **196**: 535–547

Kong L, Anderson JM, Ohm HW (2005) Induction of wheat defense and stress-related genes in response to *Fusarium graminearum*. Genome **48**: 29–40

Kosaka A, Manickavelu A, Kajihara D, Nakagawa H, Ban T (2015) Altered gene expression profiles of wheat genotypes against Fusarium head blight. Toxins (Basel) **7**: 604–620

Kouzai Y, Kimura M, Yamanaka Y, Watanabe M, Matsui H, Yamamoto M, Ichinose Y, Toyoda K, Onda Y, Mochida K, et al (2016) Expression profiling of marker genes responsive to the defence-associated phytohormones salicylic acid, jasmonic acid and ethylene in Brachypodium distachyon. BMC Plant Biol **16**: 1–11

Kowalska K, Habrowska-Górczyńska DE, Piastowska-Ciesielska AW (2016) Zearalenone as an endocrine disruptor in humans. Environ Toxicol Pharmacol **48**: 141–149

Kugler KG, Siegwart G, Nussbaumer T, Ametz C, Spannagl M, Steiner B, Lemmens M, Mayer KFX, Buerstmayr H, Schweiger W (2013) Quantitative trait loci-dependent analysis of a gene co-expression network associated with Fusarium head blight resistance in bread wheat (Triticum aestivum L.). BMC Genomics. doi: 10.1186/1471-2164-14-728

Kumar P, Henikoff S, Ng PC (2009) Predicting the effects of coding non-synonymous variants on protein function using the SIFT algorithm. Nat Protoc **4**: 1073–1082

Kumar S, Stecher G, Tamura K (2017) MEGA7 : Molecular Evolutionary Genetics Analysis Version 7 . 0 for Bigger Datasets. Mol Biol Evol **33**: 1870–1874

Kvesitadze E, Sadunishvili T, Kvesitadze G (2009) Mechanisms of Organic Contaminants Uptake and Degradation in Plants. Int J Biomed Biol Eng **3**: 361–371

Kvesitadze G, Khatisashvili G, Sadunishvili T, Ramsden JJ (2006) The fate of organic contaminants in the plant cell. *In* G Kvesitadze, G Khatisashvili, T Sadunishvili, JJ Ramsden, eds, Biochem. Mech. Detoxif. High. Plants Basis Phytoremediation. Springer, pp 103–166

Kwak YS, Weller DM (2013) Take-all of wheat and natural disease suppression: A review. Plant Pathol J **29**: 125–135

Lacey J, Bateman GL, Mirocha CJ (1999) Effects of infection time and moisture on development of ear blight and deoxynivalenol production by Fusarium spp. in wheat. Ann Appl Biol **134**: 277–283

Lemmens M, Scholz U, Berthiller F, Dall 'asta C, Koutnik A, Schuhmacher R, Adam G, Buerstmayr H, Mesterházy Á, Krska R, et al (2005) The Ability to Detoxify the Mycotoxin Deoxynivalenol Colocalizes With a Major Quantitative Trait Locus for Fusarium Head Blight Resistance in Wheat. Mol Plant-Microbe Interact **18**: 1318–1324

Lepesheva G, Waterman MR (2009) Sterol 14α-Demethylase Cytochrome P450 (CYP51), a P450 in all Biological Kingdoms. Biochim Biophys Acta **6**: 247–253

Li C, Rudi H, Stockinger EJ, Cheng H, Cao M, Fox SE, Mockler TC, Westereng B, Fjellheim S, Rognli O a., et al (2012) Comparative analyses reveal potential uses of Brachypodium distachyon as a model for cold stress responses in temperate grasses. BMC Plant Biol. doi: 10.1186/1471-2229-12-65

Li G, Yen Y (2008) Jasmonate and ethylene signaling pathway may mediate Fusarium head blight resistance in wheat. Crop Sci **48**: 1888–1896

Li H, Lu Y, Wang J, Zhou M (2003) Cloning of beta-tubulin gene from Gibberella zeae and analysis its relationship with carbendazim-resistance. Wei Sheng Wu Xue Bao **43**: 424—429

Li S, Li Y, Smolke CD (2018) Strategies for microbial synthesis of high-value phytochemicals. Nat Chem **10**: 395–404

Li X, Shin S, Heinen S, Dill-Macky R, Berthiller F, Nersesian N, Clemente T, McCormick S, Muehlbauer GJ (2015) Transgenic Wheat Expressing a Barley UDP-Glucosyltransferase Detoxifies Deoxynivalenol and Provides High Levels of Resistance to *Fusarium graminearum*. Mol Plant-Microbe Interact **28**: 1237–1246

Li X, Sun S, Li C, Qiao S, Wang T, Leng L, Shen H, Wang X (2014) The strigolactone-related mutants have enhanced lamina joint inclination phenotype at the seedling stage. J Genet Genomics **41**: 605–608

Li X, Zhang JB, Song B, Li HP, Xu HQ, Qu B, Dang FJ, Liao YC (2010) Resistance to Fusarium head blight and seedling blight in wheat is associated with activation of a cytochrome p450 gene. Phytopathology **100**: 183–191

Lin H, Wang R, Qian Q, Yan M, Meng X, Fu Z, Yan C, Jiang B, Su Z, Li J, et al (2009) DWARF27, an Iron-Containing Protein Required for the Biosynthesis of Strigolactones, Regulates Rice Tiller Bud Outgrowth. Plant Cell Online **21**: 1512–1525

Linsmaier EM, Skoog F (1965) Organic Growth Factor Requirements of Tobacco Tissue Cultures. Physiol Plant **18**: 100–127

Livak KJ, Schmittgen TD (2001) Analysis of relative gene expression data using real-time quantitative PCR and the 2-ΔΔCT method. Methods **25**: 402–408

Lobell DB, Schlenker W, Costa-Roberts J (2011) Climate trends and global crop production since 1980. Science (80-) **333**: 616–620

Longin CFH (2016) Future of Wheat Breeding is Driven by Hybrid Wheat and Efficient Strategies for Pre-Breeding on Quantitative Traits. Res Rev J Bot Sci 32–33

López-Ráez JA, Shirasu K, Foo E (2017) Strigolactones in Plant Interactions with Beneficial and Detrimental Organisms: The Yin and Yang. Trends Plant Sci. doi: 10.1016/j.tplants.2017.03.011

Lu J, Hu J, Zhao G, Mei F, Zhang C (2017) An In-field Automatic Wheat Disease Diagnosis System. 1–15

Lucena M a, Valpuesta V, Romero-aranda R, Mercado J a, Quesada M a (2003) Structural and physiological changes in the roots of tomato plants over-expressing a basic peroxidase. Physiol Plant **118**: 422–429

Luo K, Rocheleau H, Qi PF, Zheng YL, Zhao HY, Ouellet T (2016) Indole-3-acetic acid in Fusarium graminearum: Identification of biosynthetic pathways and characterization of physiological effects. Fungal Biol **120**: 1135–1145

Lupton FGH (1987) History of wheat breeding. *In* FGH Lupton, ed, Wheat Breed. Its Sci. basis. Springer Netherlands, Dordrecht, pp 51–70

Machado AK, Brown NA, Urban M, Kanyuka K, Hammond-Kosack K (2017) RNAi as an emerging approach to control Fusarium Head Blight disease and mycotoxin contamination in cereals. Pest Manag Sci **74**: 790–799

Maier FJ, Miedaner T, Hadeler B, Felk A, Salomon S, Lemmens M, Kassner H, Schäfer W (2006) Involvement of trichothecenes in fusarioses of wheat, barley and maize evaluated by gene disruption of the trichodiene synthase (Tri5) gene in three field isolates of different chemotype and virulence. Mol Plant Pathol **7**: 449–461

Maloy OC (2005) Plant Disease Management. Plant Heal Instr. doi: 10.1094/PHI-I-2005-0202-01

Mandadi KK, Pyle JD, Scholthof KG (2014) Comparative analysis of antiviral responses in Brachypodium distachyon and Setaria viridis reveals conserved and unique outcomes among C3 and C4 plant defenses. Mol Plant Microbe Interact **27**: 1277–1290

Mandadi KK, Scholthof K-BG (2012) Characterization of a viral synergism in the monocot Brachypodium distachyon reveals distinctly altered host molecular processes associated with disease. Plant Physiol **160**: 1432–1452

Martinez C, Buée M, Jauneau A, Bécard G, Dargent R, Roux C (2001) Effects of a fraction from maize root exudates on haploid strains of sporisorium reilianum f. sp. zeae. Plant Soil **236**: 145–153

Marzec M, Muszynska A (2015) In Silico analysis of the genes encoding proteins that are involved in the biosynthesis of the RMS/MAX/D pathway revealed new roles of strigolactones in plants. Int J Mol Sci **16**: 6757–6782

Masuda D, Ishida M, Yamaguchi K, Yamaguchi I, Kimura M, Nishiuchi T (2007) Phytotoxic effects of trichothecenes on the growth and morphology of Arabidopsis thaliana. J Exp Bot **58**: 1617–1626

Matsuoka Y, Vigouroux Y, Goodman MM, Sanchez G J, Buckler E, Doebley J (2002) A single domestication for maize shown by multilocus microsatellite genotyping. Proc Natl Acad Sci U S A **99**: 6080–6084

Matusova R, Rani K, Verstappen F, Franssen M, Beale M, Bouwmeester HJ (2005) The Strigolactone Germination Stimulants of the Plant-Parasitic Striga and Orobanche spp. Are Derived from the Carotenoid Pathway. Plant Physiol **139**: 920–934

Mazaheri-Naeini M, Sabbagh SK, Martinez Y, Séjalon-Delmas N, Roux C (2015) Assessment of Ustilago maydis as a fungal model for root infection studies. Fungal Biol **119**: 145–153

Mazumder PM, Sasmal D (2001) Mycotoxins - limits and regulations. Anc Sci Life **20**: 1–19

McCartney C a., Somers DJ, Fedak G, DePauw RM, Thomas J, Fox SL, Humphreys DG, Lukow O, Savard ME, McCallum BD, et al (2007) The evaluation of FHB resistance QTLs introgressed into elite Canadian spring wheat germplasm. Mol Breed **20**: 209–221

McCormick SP, Stanley AM, Stover N a., Alexander NJ (2011) Trichothecenes: From simple to complex mycotoxins. Toxins (Basel) **3**: 802–814

McLean M (1995) The phytotoxicity of selected mycotoxins on mature, germinating Zea mays embryos. Mycopathologia **132**: 173–183

McMullen M, Bergstrom G, De Wolf E, Dill-macky R, Hershman D, Shaner G, Van Sanford D (2012) Fusarium Head Blight Disease Cycle , Symptoms , and Impact on Grain Yield and Quality Frequency and Magnitude of Epidemics Since 1997. Plant Dis. doi: 10.1094/PDIS-03-12-0291-FE

McMullen M, Halley S, Schatz B, Meyer S, Jordahl J, Ransom J (2008) Integrated strategies for Fusarium head blight management in the United States. Cereal Res Commun **36**: 563–568

Meinke DW (1998) Arabidopsis thaliana: A Model Plant for Genome Analysis. Science (80-) **282**: 662–682

Merhej J, Boutigny a. L, Pinson-Gadais L, Richard-Forget F, Barreau C (2010) Acidic pH as a determinant of TRI gene expression and trichothecene B biosynthesis in Fusarium graminearum. Food Addit Contam Part A **27**: 710–717

Mesterhazy A (1995) Types and components of resistance to Fusarium head blight of wheat. Plant Breed **114**: 377–386

Miransari M, Abrishamchi a., Khoshbakht K, Niknam V (2014) Plant hormones as signals in arbuscular mycorrhizal symbiosis. Crit Rev Biotechnol **34**: 123–133

Mizutani M (2012) Impacts of diversification of cytochrome P450 on plant metabolism. Biol Pharm Bull **35**: 824–832

Mizutani M, Ohta D (2010) Diversification of P450 Genes During Land Plant Evolution. Annu Rev Plant Biol **61**: 291–315

Mizutani M, Sato F (2011) Unusual P450 reactions in plant secondary metabolism. Arch Biochem Biophys **507**: 194–203

Mochida K, Shinozaki K (2013) Unlocking triticeae genomics to sustainably feed the future. Plant Cell Physiol **54**: 1931–1950

Molina J, Sikora M, Garud N, Flowers JM, Rubinstein S, Reynolds A, Huang P, Jackson S, Schaal BA, Bustamante CD, et al (2011) Molecular evidence for a single evolutionary origin of domesticated rice. Proc Natl Acad Sci **108**: 8351–8356

Mondal S, Rutkoski JE, Velu G, Singh PK, Crespo-Herrera L a., Guzmán C, Bhavani S, Lan C, He X, Singh RP (2016) Harnessing Diversity in Wheat to Enhance Grain Yield, Climate Resilience, Disease and Insect Pest Resistance and Nutrition Through Conventional and Modern Breeding Approaches. Front Plant Sci **7**: 1–15

Morikawa T, Mizutani M, Aoki N, Watanabe B, Saga H, Saito S, Oikawa A, Suzuki H, Sakurai T, Shibata D, et al (2006) Cytochrome P450 CYP710A Encodes the Sterol C-22 Desaturase in Arabidopsis and Tomato. PLANT CELL ONLINE **18**: 1008–1022

Mühleisen J, Piepho HP, Maurer HP, Longin CFH, Reif JC (2014) Yield stability of hybrids versus lines in wheat, barley, and triticale. Theor Appl Genet **127**: 309–316

Muhovski Y (2012) Molecular and genetic characterization of Fusarium head blight resistance in winter wheat Centenaire. Université Catholique de Louvain

Murashige T, Skoog F (1962) A Revised Medium for Rapid Growth and Bio Assays with Tobacco Tissue Cultures. Physiol Plant **15**: 473–497

Nagahashi G, Douds DD (2000) Partial separation of root exudate components and their effects upon the growth of germinated spores of AM fungi. Mycol Res **104**: 1453–1464

Nalam VJ, Vales MI, Watson CJW, Kianian SF, Riera-Lizarazu O (2006) Map-based analysis of genes affecting the brittle rachis character in tetraploid wheat (Triticum turgidum L.). Theor Appl Genet **112**: 373–381

Nelson D, Werck-Reichhart D (2011) A P450-centric view of plant evolution. Plant J **66**: 194–211

Nelson DC, Scaffidi a., Dun E a., Waters MT, Flematti GR, Dixon KW, Beveridge C a., Ghisalberti EL, Smith SM (2011) F-box protein MAX2 has dual roles in karrikin and strigolactone signaling in Arabidopsis thaliana. Proc Natl Acad Sci **108**: 8897–8902

Nelson DR (2004) Comparative Genomics of Rice and Arabidopsis. Analysis of 727 Cytochrome P450 Genes and Pseudogenes from a Monocot and a Dicot. Plant Physiol **135**: 756–772

Nelson DR (2009) The cytochrome p450 homepage. Hum Genomics **4**: 59–65

Nelson DR, Ming R, Alam M, Schuler M a. (2008) Comparison of Cytochrome P450 Genes from Six Plant Genomes. Trop Plant Biol **1**: 216–235

Nganje W, Bangsund D, Leistritz F (2002) Estimating the economic impact of a crop disease: the case of Fusarium head blight in US wheat and barley. Natl. Fusarium Head Blight Forum Proc. pp 275–281

Nussbaumer T, Warth B, Sharma S, Ametz C, Bueschl C, Parich a, Pfeifer M, Siegwart G, Steiner B, Lemmens M, et al (2015) Joint Transcriptomic and Metabolomic Analyses Reveal Changes in the Primary Metabolism and Imbalances in the Subgenome Orchestration in the Bread Wheat Molecular Response to Fusarium graminearum. G3 **5**: 2579–2592

O'Driscoll A, Doohan F, Mullins E (2015) Exploring the utility of Brachypodium distachyon as a model pathosystem for the wheat pathogen Zymoseptoria tritici Plant Biology. BMC Res Notes **8**: 1–10

O'keefe DP, Leto KJ (1989) Cytochrome P-450 from the Mesocarp of Avocado (Persea americana). Plant Physiol **89**: 1141–1149

Oerke E-C (2006) Crop losses to pests. J Agric Sci **144**: 31–43

Ogle H (1997) Disease management: exclusion, eradication and elimination. *In* J Brown, H Ogle, eds, Plant Pathog. Plant Dis. Australasian Plant Pathology Society Inc., pp 358–372

Omura T, Sato R (1964) The Carbon Monoxide-biding pigment of Liver Microsomes. J Biol Chem **239**: 2370–2378

Palisot de Beauvois A-M-F-J (1812) Essai d'une nouvelle agrostographie, ou, Nouveaux genres des graminées: avec figures représentant les caractères de tous les genres. 182

Parker C (2009) Observations on the current status of orobanche and striga problems worldwide. Pest Manag Sci **65**: 453–459

Parniske M (2008) Arbuscular mycorrhiza: the mother of plant root endosymbioses. Nat Rev Microbiol **6**: 763–75

Parry DW, Jenkinson P, McLEOD L (1995) Fusarium ear blight (scab) in small grain cereals—a review. Plant Pathol **44**: 207–238

Pasquali M, Migheli Q (2014) Genetic approaches to chemotype determination in type B-trichothecene producing Fusaria. Int J Food Microbiol **189**: 164–182

Pasquet J-C (2014) Détoxication des mycotoxines par les plantes: analyse de l'interaction entre Brachypodium distachyon et Fusarium graminearum. Université Paris-Sud

Pasquet J-C, Changenet V, Macadré C, Boex-Fontvieille E, Soulhat C, Bouchabké-Coussa O, Dalmais M, Atanasova-Pénichon V, Bendahmane A, Saindrenan P, et al (2016) A Brachypodium UDP-glycosytransferase confers root tolerance to deoxynivalenol and resistance to Fusarium infection. Plant Physiol **172**: 559–574

Pasquet J-C, Chaouch S, Macadré C, Balzergue S, Huguet S, Martin-Magniette M-L, Bellvert F, Deguercy X, Thareau V, Heintz D, et al (2014) Differential gene expression and metabolomic analyses of Brachypodium distachyon infected by deoxynivalenol producing and non-producing strains of Fusarium graminearum. BMC Genomics **15**: 629

Paul P a., Lipps PE, Hershman DE, McMullen MP, Draper M a., Madden L V. (2008) Efficacy of Triazole-Based Fungicides for Fusarium Head Blight and Deoxynivalenol Control in Wheat: A Multivariate Meta-Analysis. Phytopathology **98**: 999–1011

Paul PA, Lipps PE, Hershman DE, McMullen MP, Draper MA, Madden L V. (2007) A quantitative review of tebuconazole effect on Fusarium Head Blight and deoxynivalenol content in Wheat. Phytopathology **97**: 211–220

Payros D, Alassane-Kpembi I, Pierron A, Loiseau N, Pinton P, Oswald IP (2016) Toxicology of deoxynivalenol and its acetylated and modified forms. Arch Toxicol **90**: 2931–2957

Peraldi a., Griffe LL, Burt C, Mcgrann GRD, Nicholson P (2014) Brachypodium distachyon exhibits compatible interactions with Oculimacula spp. and Ramularia collo-cygni, providing the first pathosystem model to study eyespot and ramularia leaf spot diseases. Plant Pathol **63**: 554–562

Peraldi A, Beccari G, Steed A, Nicholson P (2011) Brachypodium distachyon: a new pathosystem to study *Fusarium* head blight and other *Fusarium* diseases of wheat. BMC Plant Biol **11**: 100

Pereyra SA, Dill-Macky R, Sims AL (2004) Survival and Inoculum Production of Gibberella zeae in Wheat Residue. Plant Dis **88**: 724–730

Phongdara a, Nakkaew a, Nualkaew S (2012) Isolation of the detoxification enzyme EgP450 from an oil palm EST library. Pharm Biol **50**: 120–127

Pierrel M a, Batard Y, Kazmaier M, Mignottevieux C, Durst F, Werckreichhart D (1994) Catalytic Properties of the Plant Cytochrome-P450 Cyp73 Expressed in Yeast - Substrate-Specificity of a Cinnamate Hydroxylase. Eur J Biochem **224**: 835–844

Pieterse CMJ, Leon-Reyes A, Van der Ent S, Van Wees SCM (2009) Networking by small-molecule hormones in plant immunity. Nat Chem Biol **5**: 308–316

Piisilä M, Keceli M a, Brader G, Jakobson L, Jõesaar I, Sipari N, Kollist H, Palva ET, Kariola T (2015) The F-box protein MAX2 contributes to resistance to bacterial phytopathogens in Arabidopsis thaliana. BMC Plant Biol **15**: 53

Pimentel M, Escudero M, Sahuquillo E, Minaya MÁ, Catalán P (2017) Are diversification rates and chromosome evolution in the temperate grasses (Pooideae) associated with major environmental changes in the Oligocene-Miocene? PeerJ **5**: e3815

Pinot F, Beisson F (2011) Cytochrome P450 metabolizing fatty acids in plants: Characterization and physiological roles. FEBS J **278**: 195–205

Pompon D, Louerat B, Bronine A, Urban P (1996) Yeast expression of animal and plant P450s in optimized redox environments. Methods Enzymol **272**: 51–64

Ponts N, Pinson-Gadais L, Barreau C, Richard-Forget F, Ouellet T (2007) Exogenous H2O2 and catalase treatments interfere with Tri genes expression in liquid cultures of Fusarium graminearum. FEBS Lett **581**: 443–447

Poppenberger B, Berthiller F, Lucyshyn D, Sieberer T, Schuhmacher R, Krska R, Kuchler K, Glössl J, Luschnig C, Adam G (2003) Detoxification of the Fusarium Mycotoxin Deoxynivalenol by a UDP-glucosyltransferase from Arabidopsis thaliana. J Biol Chem **278**: 47905–47914

Powell JJ, Carere J, Fitzgerald TL, Stiller J, Covarelli L, Xu Q, Gubler F, Colgrave ML, Gardiner DM, Manners JM, et al (2017) The Fusarium crown rot pathogen Fusarium pseudograminearum triggers a suite of transcriptional and metabolic changes in bread wheat (Triticum aestivum L.). Ann Bot **119**: 853–867

Rawat N, Pumphrey MO, Liu S, Zhang X, Tiwari VK, Ando K, Trick HN, Bockus WW, Akhunov E, Anderson J a., et al (2016) Wheat Fhb1 encodes a chimeric lectin with agglutinin domains and a pore-forming toxin-like domain conferring resistance to Fusarium head blight. Nat Genet **48**: 1576–1580

Reif JC, Zhang P, Dreisigacker S, Warburton ML, Van Ginkel M, Hoisington D, Bohn M, Melchinger a. E (2005) Wheat genetic diversity trends during domestication and breeding. Theor Appl Genet **110**: 859–864

Renault H, Bassard JE, Hamberger B, Werck-Reichhart D (2014) Cytochrome P450-mediated metabolic engineering: current progress and future challenges. Curr Opin Plant Biol **19**: 27–34

Roach KC, Feretzaki M, Sun S, Heitman J (2014) Unisexual reproduction. Adv Genet **85**: 255–305

Robineau T, Batard Y, Nedelkina S, Cabello-Hurtado F, LeRet M, Sorokine O, Didierjean L, Werck-Reichhart D (1998) The chemically inducible plant cytochrome P450 CYP76B1 actively metabolizes phenylureas and other xenobiotics. Plant Physiol **118**: 1049–1056

Rocha O, Ansari K, Doohan FM (2005) Effects of trichothecene mycotoxins on eukaryotic cells: A review. Food Addit Contam **22**: 369–378

Roelfs AP (1982) Effects of Barberry Eradication on Stem Rust in the United States. Plant Dis **66**: 177

Routledge APM, Shelley G, Smith J V, Talbot NJ, Draper J, Mur LAJ (2004) Magnaporthe grisea interactions with the model grass Brachypodium distachyon closely resemble those with rice (Oryza sativa). Mol Plant Pathol **5**: 253–265

Rozpądek P, Domka AM, Nosek M, Ważny R, Jędrzejczyk RJ, Wiciarz M, Turnau K (2018) The Role of Strigolactone in the Cross-Talk Between Arabidopsis thaliana and the Endophytic Fungus Mucor sp. Front Microbiol **9**: 1–14

Rudd JC, Horsley RD, Mckendry a L, Elias EM (1993) Host Plant Resistance Genes for Fusarium Head Blight : Sources , Mechanisms ,. Crop Sci **41**: 620–627

Rudd JJ, Kanyuka K, Hassani-Pak K, Derbyshire M, Andongabo A, Devonshire J, Lysenko A, Saqi M, Desai NM, Powers SJ, et al (2015) Transcriptome and Metabolite Profiling of the Infection Cycle of *Zymoseptoria tritici* on Wheat Reveals a Biphasic Interaction with Plant Immunity Involving Differential Pathogen Chromosomal Contributions and a Variation on the Hemibiotrophic Lifest. Plant Physiol **167**: 1158–1185

Sabbagh SK (2011) Effect of GR24, a synthetic analogue of strigolactones, on gene expression of solopathogenic strain of sporisorium reilianum. African J Biotechnol **10**: 15739–15743

Sabbagh SK (2008) Adaptation à la pénétration racinaire de deux Ustilaginaceae parasites du mais : Ustilago maydis et Sporisorium reilianum - Analyse microscopique et transcriptomique. Université de Toulouse/France

Sabbagh SK, Mazaheri M, Panjehkeh N, Salari M (2012) Transcriptomic analysis of Sporisorium reilianum in response to the strigolactone analogue GR24. Phytopathol Mediterr **51**: 283–291

Saeed W, Naseem S, Ali Z (2017) Strigolactones Biosynthesis and Their Role in Abiotic Stress Resilience in Plants: A Critical Review. Front Plant Sci **8**: 1–13

Salamini F, Özkan H, Brandolini A, Schäfer-Pregl R, Martin W (2002) Genetics and geography of wild cereal domestication in the near east. Nat Rev Genet **3**: 429–441

Salvioli A, Ghignone S, Novero M, Navazio L, Venice F, Bagnaresi P, Bonfante P (2016) Symbiosis with an endobacterium increases the fitness of a mycorrhizal fungus, raising its bioenergetic potential. ISME J **10**: 130–144

Sandermann H (1992) Plant metabolism of xenobiotics. Trends Biochem Sci **17**: 82–84

Sandermann H (1994) Higher plant metabolism of xenobiotics: the "green liver" concept. Pharmacogenetics **4**: 225–241

Sandoya G V., Buanafina MMDO (2014) Differential responses of Brachypodium distachyon genotypes to insect and fungal pathogens. Physiol Mol Plant Pathol **85**: 53–64

Sang D, Chen D, Liu G, Liang Y, Huang L, Meng X, Chu J, Sun X, Dong G, Yuan Y, et al (2014) Strigolactones regulate rice tiller angle by attenuating shoot gravitropism through inhibiting auxin biosynthesis. Proc Natl Acad Sci **111**: 11199–11204

Satoh K, Yoneyama K, Kondoh H, Shimizu T, Sasaya T, Choi I-R, Yoneyama K, Omura T, Kikuchi S (2013) Relationship between gene responses and symptoms induced by Rice grassy stunt virus. Front Microbiol **4**: 313

Schalk M, Pierrel M, Zimmerlin A, Batard Y, Durst F, Werck-reichhart D (1997) Xenobiotics : Substrates and Inhibitors of the Plant Cytochrome P450. Enzyme **3**: 229–234

Schmeitzl C, Warth B, Fruhmann P, Michlmayr H, Malachová A, Berthiller F, Schuhmacher R, Krska R, Adam G (2015) The metabolic fate of deoxynivalenol and its acetylated derivatives in a wheat suspension culture: Identification and detection of DON-15-O-glucoside, 15-acetyl-DON-3-O-glucoside and 15-acetyl-DON-3-sulfate. Toxins (Basel) **7**: 3112–3126

Schmidt-Heydt M, Magan N, Geisen R (2008) Stress induction of mycotoxin biosynthesis genes by abiotic factors. FEMS Microbiol Lett **284**: 142–149

Schneebeli K, Mathesius U, Watt M (2015) Brachypodium distachyon is a pathosystem model for the study of the wheat disease rhizoctonia root rot. Plant Pathol **64**: 91–100

Schneider C a, Rasband WS, Eliceiri KW (2012) NIH Image to ImageJ : 25 years of image analysis HISTORICAL commentary NIH Image to ImageJ : 25 years of image analysis. Nat Methods **9**: 671–675

Schuler M a., Werck-Reichhart D (2003) Functional Genomics of P450s. Annu Rev Plant Biol **54**: 629–667

Schumacher J, Simon A, Cohrs KC, Viaud M, Tudzynski P (2014) The Transcription Factor BcLTF1 Regulates Virulence and Light Responses in the Necrotrophic Plant Pathogen Botrytis cinerea. PLoS Genet. doi: 10.1371/journal.pgen.1004040

Schüßler a., Chwarzott D, Walker C (2001) A new fungal phylum, the Glomeromy- cota: phylogeny and evolution. Mycol Res **105**: 1413–1421

Schweiger W, Boddu J, Shin S, Poppenberger B, Berthiller F, Lemmens M, Muehlbauer GJ, Adam G (2010) Validation of a Candidate Deoxynivalenol-Inactivating UDP-Glucosyltransferase from Barley by Heterologous Expression in Yeast. Mol Plant-Microbe Interact **23**: 977–986

Schweiger W, Pasquet J-C, Nussbaumer T, Paris MPK, Wiesenberger G, Macadré C, Ametz C, Berthiller F, Lemmens M, Saindrenan P, et al (2013a) Functional characterization of two clusters of Brachypodium distachyon UDP-glycosyltransferases encoding putative deoxynivalenol detoxification genes. Mol Plant Microbe Interact **26**: 781–92

Schweiger W, Steiner B, Ametz C, Siegwart G, Wiesenberger G, Berthiller F, Lemmens M, Jia H, Adam G, Muehlbauer GJ, et al (2013b) Transcriptomic characterization of two major Fusarium resistance quantitative trait loci (QTLs), Fhb1 and Qfhs.ifa-5A, identifies novel candidate genes. Mol Plant Pathol **14**: 772–785

Screpanti C, Yoneyama K, Bouwmeester HJ (2016) Strigolactones and parasitic weed management 50 years after the discovery of the first natural strigolactone strigol: status and outlook. Pest Manag Sci **72**: 2013–2015

Seong KY, Pasquali M, Zhou X, Song J, Hilburn K, McCormick S, Dong Y, Xu JR, Kistler HC (2009) Global gene regulation by Fusarium transcription factors Tri6 and Tri10 reveals adaptations for toxin biosynthesis. Mol Microbiol **72**: 354–367

Seto Y, Sado A, Asami K, Hanada A, Umehara M, Akiyama K, Yamaguchi S (2014) Carlactone is an endogenous biosynthetic precursor for strigolactones. Proc Natl Acad Sci U S A **111**: 1640–5

Shewry PR (2009) Wheat. J Exp Bot **60**: 1537–1553

Shin S, Torres-Acosta J, Heinden J, McCormick S, Lemmens M, Kovalsky Paris M, Berthiller F, Adam G, Muehlbauer G (2012) Transgenic Arabidopsis thaliana expressing a barley methylation and chromatin patterning UDP-glucosyltransferase exhibit resistance to the mycotoxin deoxynivalenol. J Exp Bot **63**: 4731–4740

Shinohara N, Taylor C, Leyser O (2013) Strigolactone Can Promote or Inhibit Shoot Branching by Triggering Rapid Depletion of the Auxin Efflux Protein PIN1 from the Plasma Membrane. PLoS Biol. doi: 10.1371/journal.pbio.1001474

Siminszky B (2006) Plant cytochrome P450-mediated herbicide metabolism. Phytochem Rev **5**: 445–458

Siminszky B, Corbin FT, Ward ER, Fleischmann TJ, Dewey RE (1999) Expression of a soybean cytochrome P450 monooxygenase cDNA in yeast and tobacco enhances the metabolism of phenylurea herbicides. Proc Natl Acad Sci U S A **96**: 1750–1755

Simons KJ, Fellers JP, Trick HN, Zhang Z, Tai YS, Gill BS, Faris JD (2006) Molecular characterization of the major wheat domestication gene Q. Genetics **172**: 547–555

Singh RP, Singh PK, Rutkoski J, Hodson DP, He X, Jørgensen LN, Hovmøller MS, Huerta-Espino J (2016) Disease Impact on Wheat Yield Potential and Prospects of Genetic Control. Annu Rev Phytopathol **54**: 303–22

Smith W (1884) Diseases of Field and Garden Crops, MACMILLAN. London

Snowden KC, Simkin AJ, Janssen BJ, Templeton KR, Loucas HM, Simons JL, Karunairetnam S, Gleave AP, Clark DG, Klee HJ (2005) The Decreased apical dominance1/Petunia hybrida CAROTENOID CLEAVAGE DIOXYGENASE8 gene affects branch production and plays a role in leaf senescence, root growth, and flower development. Plant Cell **17**: 746–59

Soares R, Ricelli A, Fanelli C, Caputo D, de Cesare G, Chu V, Aires-Barros MR, Conde JP (2018) Advances, challenges and opportunities for point-of-need screening of mycotoxins in foods and feeds. Analyst. doi: 10.1039/C7AN01762F

Sorahinobar M, Soltanloo H, Niknam V, Ebrahimzadeh H, Moradi B, Safaie N, Behmanesh M, Bahram M (2017) Physiological and molecular responses of resistant and susceptible wheat cultivars to Fusarium graminearum mycotoxin extract. Can J Plant Pathol **39**: 444–453

Sorefan K, Booker J, Haurogné K, Haurogne K, Goussot M, Bainbridge K, Foo E, Chatfield S, Ward S, Beveridge C, et al (2003) MAX4 and RMS1 are orthologous dioxygenase-like genes that regulate shoot branching in Arabidopsis and pea MAX4 and RMS1 are orthologous dioxygenase-like genes that regulate shoot branching in Arabidopsis and pea. Genes Dev **17**: 1469–1474

Soreng RJ, Peterson PM, Romaschenko K, Davidse G, Teisher JK, Clark LG, Barberá P, Gillespie LJ, Zuloaga FO (2017) A worldwide phylogenetic classification of the Poaceae (Gramineae) II: An update and a comparison of two 2015 classifications. J Syst Evol **55**: 259–290

Soriano JM, González L, Catalá a. I (2005) Mechanism of action of sphingolipids and their metabolites in the toxicity of fumonisin B1. Prog Lipid Res **44**: 345–356

Steinberg G (2015) Cell biology of Zymoseptoria tritici: Pathogen cell organization and wheat infection. Fungal Genet Biol **79**: 17–23

Steiner B, Kurz H, Lemmens M, Buerstmayr H (2009) Differential gene expression of related wheat lines with contrasting levels of head blight resistance after Fusarium graminearum inoculation. Theor Appl Genet **118**: 753–764

Steinkellner S, Lendzemo V, Langer I, Schweiger P, Khaosaad T, Toussaint JP, Vierheilig H (2007) Flavonoids and strigolactones in root exudates as signals in symbiotic and pathogenic plant-fungus interactions. Molecules **12**: 1290–1306

Stes E, Depuydt S, De Keyser A, Matthys C, Audenaert K, Yoneyama K, Werbrouck S, Goormachtig S, Vereecke D (2015) Strigolactones as an auxiliary hormonal defence mechanism against leafy gall syndrome in Arabidopsis thaliana. J Exp Bot **66**: 5123–5134

Stes E, Francis I, Pertry I, Dolzblasz A, Depuydt S, Vereecke D (2013) The leafy gall syndrome induced by Rhodococcus fascians. FEMS Microbiol Lett **342**: 187–195

Stirnberg P, van De Sande K, Leyser HMO (2002) MAX1 and MAX2 control shoot lateral branching in Arabidopsis. Development **129**: 1131–41

Sudakin DL (2003) Trichothecenes in the environment: Relevance to human health. Toxicol Lett **143**: 97–107

Sun H, Tao J, Gu P, Xu G, Zhang Y (2016) The role of strigolactones in root development. Plant Signal Behav **11**: e1110662

Teich AH, Nelson K (1984) Survey of Fusarium head blight and possible effects of cultural practices in wheat fields in Lambton County in 1983. Can Plant Dis Surv **64**: 11–13

Teutsch HG, Hasenfratz MP, Lesot a, Stoltz C, Garnier JM, Jeltsch JM, Durst F, Werck-Reichhart D (1993) Isolation and sequence of a cDNA encoding the Jerusalem artichoke cinnamate 4-hydroxylase, a major plant cytochrome P450 involved in the general phenylpropanoid pathway. Proc Natl Acad Sci U S A **90**: 4102–6

The Arabidopsis Genome Initiative (2000) Analysis of the genome sequence of the flowering plant Arabidopsis thaliana. Nature **408**: 796–815

The International Brachypodium Initiative (2010) Genome sequencing and analysis of the model grass Brachypodium distachyon. Nature **463**: 763–768

Thompson JD, Higgins DG, Gibson TJ (1994) CLUSTAL W: Improving the sensitivity of progressive multiple sequence alignment through sequence weighting, position-specific gap penalties and weight matrix choice. Nucleic Acids Res **22**: 4673–4680

Thornton LE, Peng H, Neff MM (2011) Rice CYP734A cytochrome P450s inactivate brassinosteroids in Arabidopsis. Planta **234**: 1151–1162

Torres-Vera R, García JM, Pozo MJ, López-Ráez J a. (2014) Do strigolactones contribute to plant defence? Mol Plant Pathol **15**: 211–216

Torriani SFF, Melichar JPE, Mills C, Pain N, Sierotzki H, Courbot M (2015) Zymoseptoria tritici: A major threat to wheat production, integrated approaches to control. Fungal Genet Biol **79**: 8–12

Trail F (2009) For blighted waves of grain: Fusarium graminearum in the postgenomics era. Plant Physiol **149**: 103–110

Umehara M, Hanada A, Yoshida S, Akiyama K, Arite T, Takeda-Kamiya N, Magome H, Kamiya Y, Shirasu K, Yoneyama K, et al (2008) Inhibition of shoot branching by new terpenoid plant hormones. Nature **455**: 195–200

Valitova JN, Sulkarnayeva a G, Minibayeva F V (2016) Plant Sterols: Diversity, Biosynthesis, and Physiological Functions. Biochemistry (Mosc) **81**: 819–834

Vallabhaneni R, Bradbury LMT, Wurtzel ET (2010) The carotenoid dioxygenase gene family in maize, sorghum, and rice. Arch Biochem Biophys **504**: 104–111

Viefhues A, Heller J, Temme N, Tudzynski P (2014) Redox systems in Botrytis cinerea: impact on development and virulence. Mol Plant Microbe Interact **27**: 858–74

Vilmorin MH (1880) Essais De Croisement Entre Blés Différents. Bull la Société Bot Fr **27**: 356–361

Vogel J, Bragg J (2009) Brachypodium distachyon, a New Model for the Triticeae. *In* G Feuillet, C. and Muehlbauer, ed, Genet. Genomics Triticeae. Springer, New York, pp 427–449

Vogel J, Hill T (2008) High-efficiency Agrobacterium-mediated transformation of Brachypodium distachyon inbred line Bd21-3. Plant Cell Rep **27**: 471–478

Vogel JP, Tuna M, Budak H, Huo N, Gu YQ, Steinwand M a. (2009) Development of SSR markers and analysis of diversity in Turkish populations of Brachypodium distachyon. BMC Plant Biol **9**: 1–11

Walter S, Doohan F (2011) Transcript profiling of the phytotoxic response of wheat to the Fusarium mycotoxin deoxynivalenol. Mycotoxin Res **27**: 221–230

Walter S, Nicholson P, Doohan FM (2010) Action and reaction of host and pathogen during Fusarium head blight disease. New Phytol **185**: 54–66

Wang Y, Bouwmeester HJ (2018) Structural diversity in the strigolactones. J Exp Bot. doi: https://doi.org/10.1093/jxb/ery091

Wang Y, Li Q, He Z (2004) Blast fungus-induction and developmental and tissue-specific expression of a rice P450. Chinese Sci Bull **49**: 131–135

Waters MT, Brewer PB, Bussell JD, Smith SM, Beveridge CA (2012) The Arabidopsis ortholog of rice DWARF27 acts upstream of MAX1 in the control of plant development by strigolactones. Plant Physiol. doi: 10.1104/pp.112.196253

Waters MT, Gutjahr C, Bennett T, Nelson DC (2017) Strigolactone Signaling and Evolution. Annu Rev Plant Biol **68**: 291–322

Watt M, Schneebeli K, Dong P, Wilson IW (2009) The shoot and root growth of Brachypodium and its potential as a model for wheat and other cereal crops. Funct Plant Biol **36**: 960–969

Wegulo SN, Baenziger PS, Hernandez Nopsa J, Bockus WW, Hallen-Adams H (2015) Management of Fusarium head blight of wheat and barley. Crop Prot **73**: 100–107

Werck-Reichhart D, Bak S, Paquette S (2002) Cytochromes p450. Arabidopsis Book **1**: e0028

Wevar Oller AL, Agostini E, Talano M a., Capozucca C, Milrad SR, Tigier H a., Medina MI (2005) Overexpression of a basic peroxidase in transgenic tomato (Lycopersicon esculentum Mill. cv. Pera) hairy roots increases phytoremediation of phenol. Plant Sci **169**: 1102–1111

Williams JH, Phillips TD, Jolly PE, Stiles JK, Jolly CM, Aggarwal D (2004) Human aflatoxin in developing countries: a review of toxicology, exposure, potential health consequences, and interventions. Am J Clin Nutr **80**: 1106–1122

Xiang W, Wang X, Ren T (2006) Expression of a wheat cytochrome P450 monooxygenase cDNA in yeast catalyzes the metabolism of sulfonylurea herbicides. **85**: 1–6

Yamada T, Kambara Y, Imaishi H, Ohkawa H (2000) Molecular cloning of novel cytochrome P450 species induced by chemical treatments in cultured tobacco cells. Pestic Biochem Physiol **68**: 11–25

Yamada Y, Furusawa S, Nagasaka S, Shimomura K, Yamaguchi S, Umehara M (2014) Strigolactone signaling regulates rice leaf senescence in response to a phosphate deficiency. Planta **240**: 399–408

Yao R, Ming Z, Yan L, Li S, Wang F, Ma S, Yu C, Yang M, Chen L, Chen L, et al (2016) DWARF14 is a non-canonical hormone receptor for strigolactone. Nature **536**: 469–473

Yoneyama K, Mori N, Sato T, Yoda A, Xie X, Okamoto M, Iwanaga M, Ohnishi T, Nishiwaki H, Asami T, et al (2018) Conversion of carlactone to carlactonoic acid is a conserved function of MAX1 homologs in strigolactone biosynthesis. New Phytol. doi: 10.1111/nph.15055

Yoneyama K, Xie X, Sekimoto H, Takeuchi Y, Ogasawara S, Akiyama K, Hayashi H, Yoneyama K (2008) Strigolactones, host recognition signals for root parasitic plants and arbuscular mycorrhizal fungi, from Fabaceae plants. New Phytol **179**: 484–494

Yoshida M, Nakajima T, Tomimura K, Suzuki F, Arai M, Miyasaka A (2012) Effect of the Timing of Fungicide Application on Fusarium Head Blight and Mycotoxin Contamination in Wheat. Plant Dis **96**: 845–851

Young O, Beevers H (1976) Mixed function oxidases from germinating castor bean endosperm. Phytochemistry **15**: 379–385

Zhang Y, Cheng X, Wang Y, Díez-Simón C, Flokova K, Bimbo A, Bouwmeester HJ, Ruyter-Spira C (2018) The tomato *MAX1* homolog, *SlMAX1* , is involved in the biosynthesis of tomato strigolactones from carlactone. New Phytol. doi: 10.1111/nph.15131

Zhang Y, van Dijk ADJ, Scaffidi A, Flematti GR, Hofmann M, Charnikhova T, Verstappen F, Hepworth J, van der Krol S, Leyser O, et al (2014) Rice cytochrome P450 MAX1 homologs catalyze distinct steps in strigolactone biosynthesis. Nat Chem Biol **10**: 1028–1033

Zhao J, Wang M, Chen X, Kang Z (2016) Role of Alternate Hosts in Epidemiology and Pathogen Variation of Cereal Rusts. Annu Rev Phytopathol **54**: 207–228

Zimdahl RL (2018) Weed Classification. Fundam. Weed Sci. Academic Press, pp 49–61

Zimin A V., Puiu D, Hall R, Kingan S, Clavijo BJ, Salzberg SL (2017) The first near-complete assembly of the hexaploid bread wheat genome, Triticum aestivum. Gigascience 1–7

Zou J, Zhang S, Zhang W, Li G, Chen Z, Zhai W, Zhao X, Pan X, Xie Q, Zhu L (2006) The rice HIGH-TILLERING DWARF1 encoding an ortholog of Arabidopsis MAX3 is required for negative regulation of the outgrowth of axillary buds. Plant J **48**: 687–696

Zwanenburg B, Blanco-Ania D (2018) Strigolactones: new plant hormones in the spotlight. J Exp Bot. doi: 10.1093/jxb/erx487

Zwanenburg B, Regeling H, Van Tilburg-Joukema CW, Van Oss B, Molenveld P, De Gelder R, Tinnemans P (2016) Securing Important Strigolactone Key Structures: Orobanchol and 5-Deoxystrigol. European J Org Chem **2016**: 2163–2169

APPENDICES

APPENDIX 1: BINARY VECTORS USED IN THIS STUDY

pIPKb002 (adapted from Himmelbach et al., 2007)

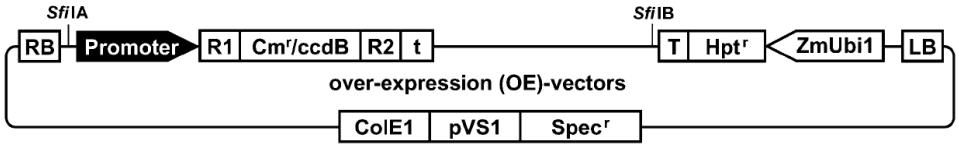

Promoter refers to the *ZmUBI1* strong and constitutive promoter. The cDNA of the *Bradi1g75310* gene has been introduced between the two sequences used for homologous recombination, R1 and R2 (*att*R1 and *att*R2). RB/LB: Right (R) and Left (L) T-DNA borders; Cm^r/ccdB: genes conferring resistance towards chloramphenicol (positive selection marker) and encoding toxic ccdB protein (negative selection marker); t: *Agrobacterium tumefasciens nos* transcriptional termination signal; T: CaMV 35S transcriptional terminal signal; Hpt^r: gene conferring resistance towards hygromycin (positive selection marker); ColE1: origin of replication for *Escherichia coli*; pVS1: origin of replication for *A. tumefaciens*; $Spec^r$ gene conferring resistance towards spectinomycin.

pK7WG2.0 (T-DNA, adapted from Karimi et al., 2002)

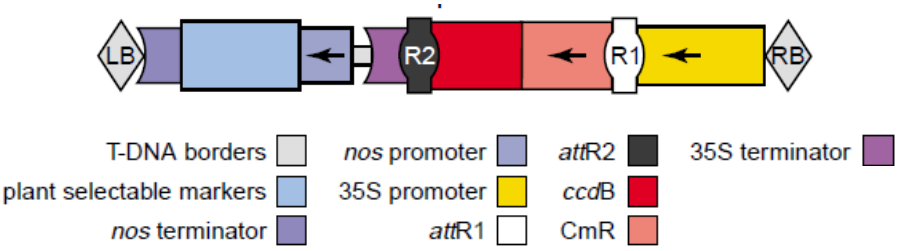

Plant selectable markers referees to *hpt* gene conferring resistance towards hygromycin *in planta*. The cDNAs of the interest were introgressed between the two sequences used for homologous recombination, R1 and R2 (*att*R1 and *att*R2). Other abbreviations are explained above.

pYeDP60 adapted from Pompon et al., 1996)

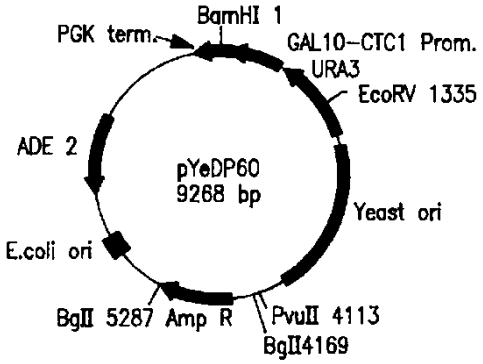

The cDNA of the *Bradi1g75310* gene has been introgressed at the BamHI site. PGK term.: phosphoglycerate kinase transcriptional termination signal; ADE 2: auxotrophy selection marker for adenine; E. coli ori: bacterial replication origin; Amp R: gene conferring resistance to ampicillin; Yeast ori: yeast replication origin; URA3: auxotrophy selection marker for uracil; GAL10-CTC1 Prom.: strong hybrid galactose-inducible promoter.

APPENDIX 2: EXPRESSION PATTERN OF CYP711A ENCODING GENES

Bradi1g75310 (*BdCYP711A29*)

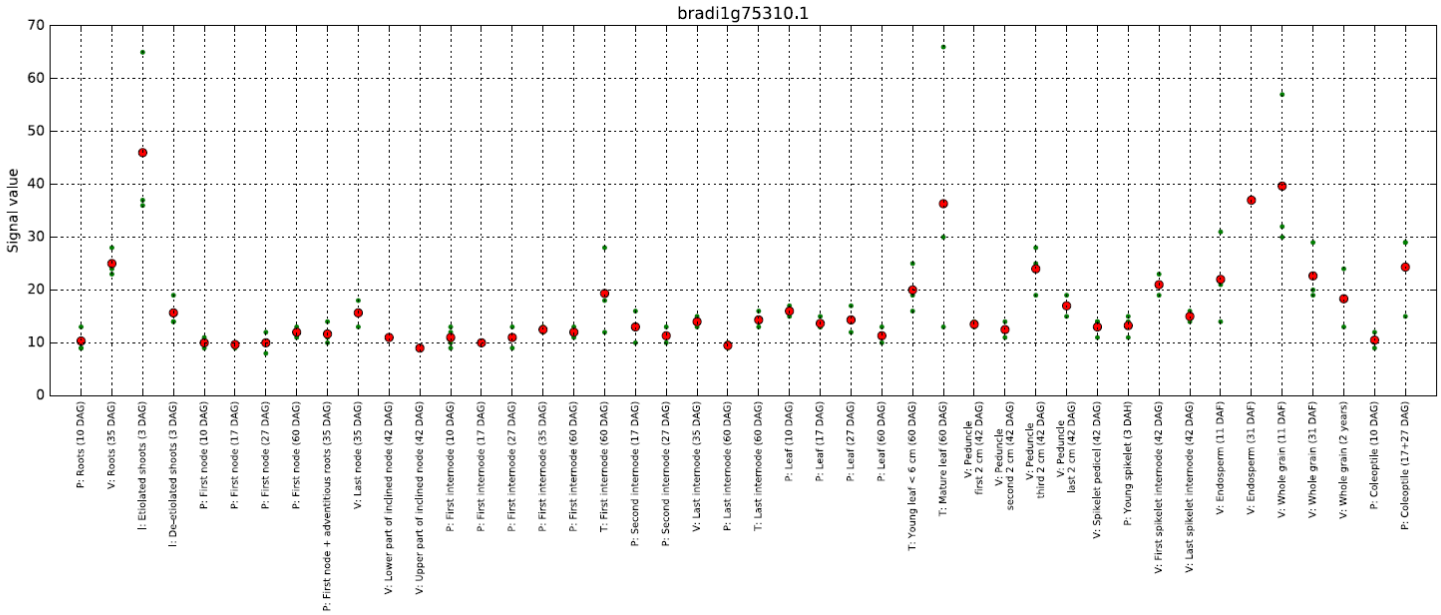

Os01g0700900 (*OsCYP711A2*)

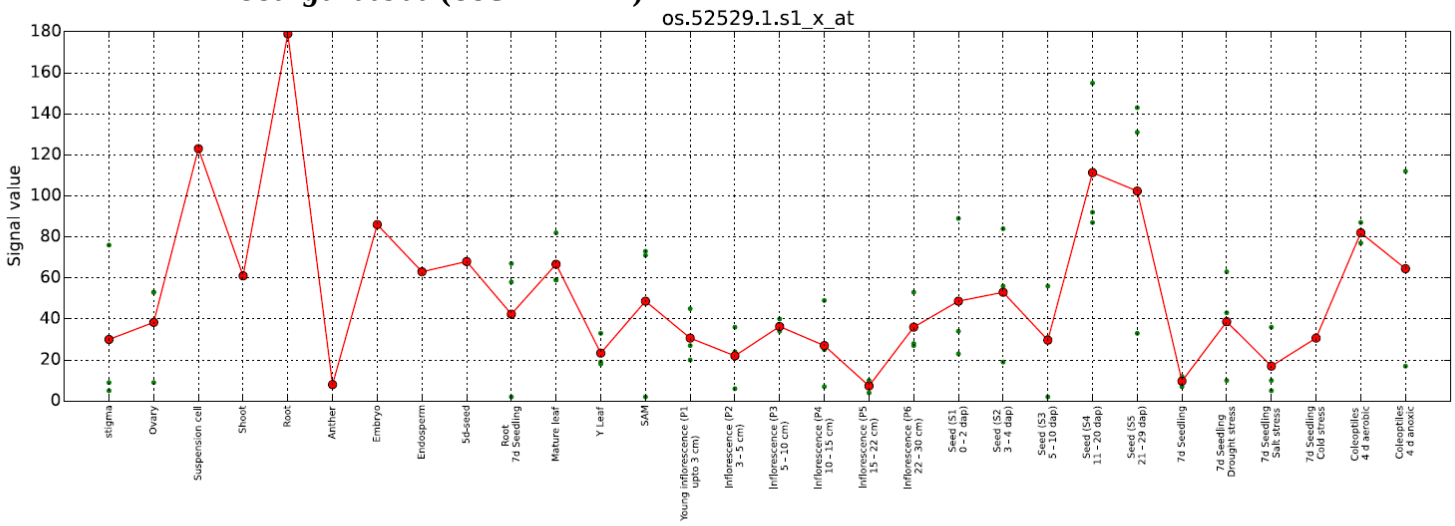

Os01g0701400 (*OsCYP711A3*)

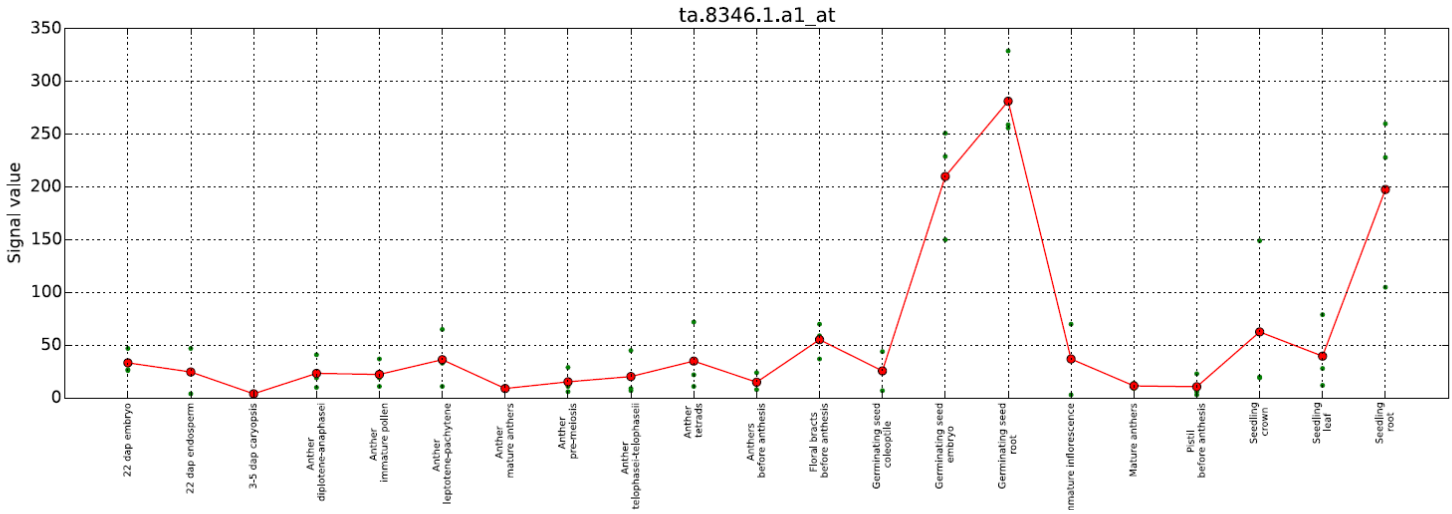

***Os02g0221900* (*OsCYP711A5*)**

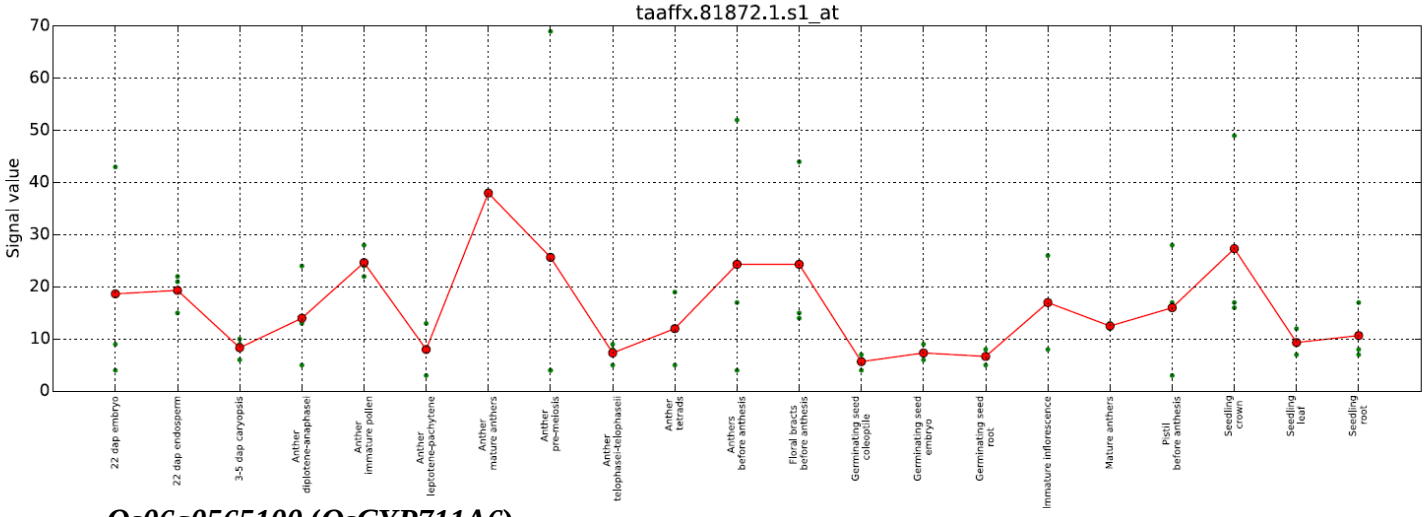

***Os06g0565100* (*OsCYP711A6*)**

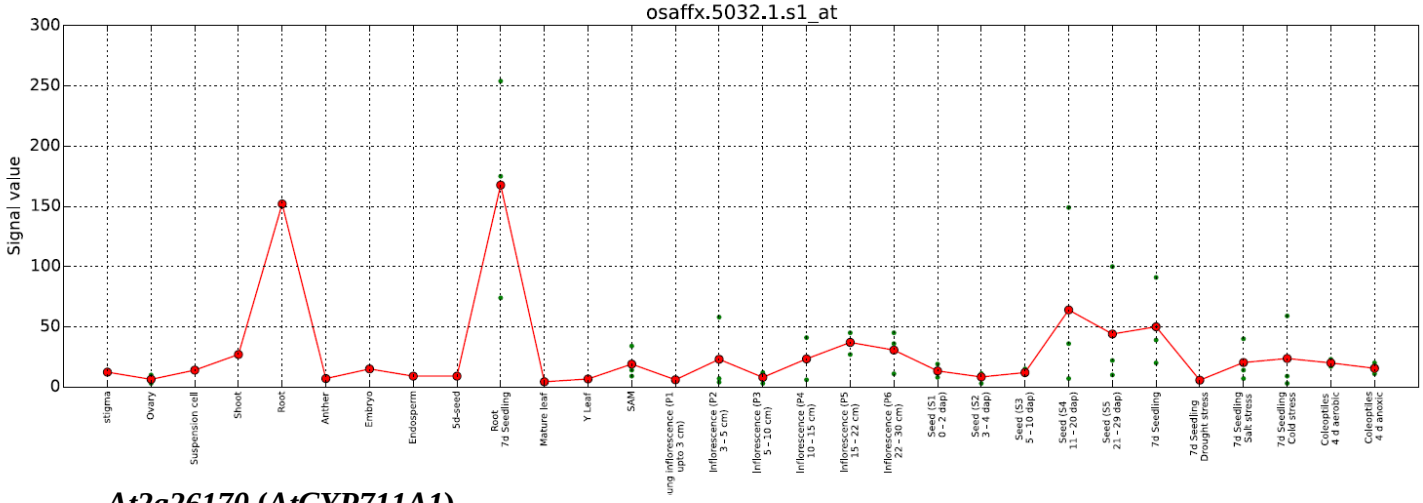

***At2g26170* (*AtCYP711A1*)**

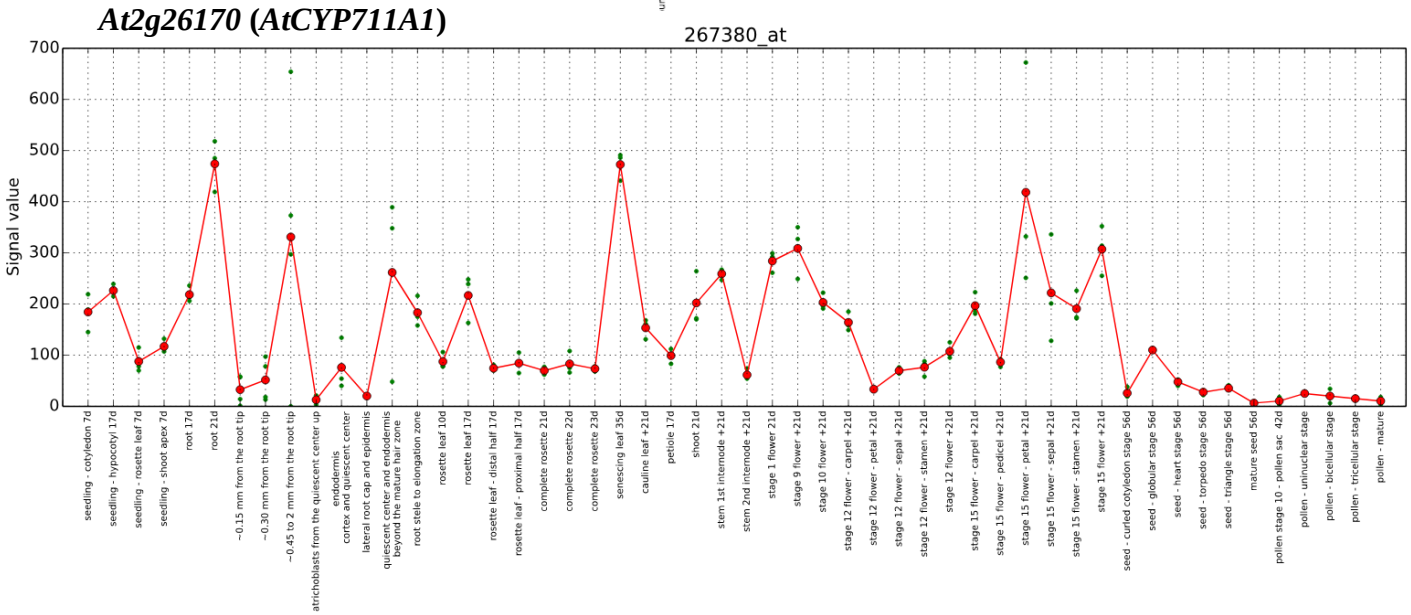

Data were collected from the PlaNet web service hosted by the Max Planck Institute of Potsdam (Germany; http://aranet.mpimp-golm.mpg.de/). *Bd: B. distachyon; Os: O. sativa; At: A. thaliana.*

APPENDIX 3: LIST OF THE PLANT LINES USED IN THE STUDY

Species	Line name	Line Type	Impact	Reference
Brachypodium distachyon	Bd21-3	Wild type	-	Vogel and Hill, 2008
	OE-CYP11.29 OE-CYP12.20	Transformant in a Bd21-3 genetic background	Over-expression of the *Bradi1g75310* gene (independent lines)	This study
	CYP11.26	Null segregant in a Bd21-3 genetic background	WT allele and expression level for each BdCYP711A copies, undergone the same regeneration processes as transformant lines	This study
	M5374#135	TILLING mutant in a Bd21-3 genetic background	Truncated BdCYP711A29 protein (STOP codon) R450*	This study
	WT5374#135		Wild-type allele for the *Bradi1g75310* gene	
	M8687#12		Mutated BdCYP711A29 protein, P431S	
	WT8687#2		Wild-type allele for the *Bradi1g75310* gene	
Arabidopsis thaliana	Col-0	Wild type	-	-
	max1-1	TILLING mutant in a Col-0 genetic background	Knock out mutant for the *MAX1* gene due to a point mutation in the *At2g26170* gene	Stirnberg et al., 2002
	max1-1-35S::MAX1	*max1-1* line genetically complemented with the cDNA of the *MAX1* gene placed under the control of the 35S promoter	Complementation of *max1-1* phenotypes (positive control)	Challis et al., 2013
	max1-1-BdCYP711A5 (3 lines from *#1-4* to *#15-1*)	Transformants in a *max1-1* genetic background	Ectopic expression of the *Bradi3g08630* gene (independant lines)	This study
	max1-1-BdCYP711A6 (3 lines from *#3-2* to *#7-3*)		Ectopic expression of the *Bradi1g37730* gene (independant lines)	
	max1-1-BdCYP711A29 (9 lines from *#1-5* to *#33-6*)		Ectopic expression of the *Bradi1g75310* gene (independant lines)	
	max1-1-BdCYP711A30 (7 lines from *#1-4* to *#13-3*)		Ectopic expression of the *Bradi4g08970* gene (independant lines)	
	max1-1-BdCYP711A31 (2 lines: *#1-7* and *#5-4*)		Ectopic expression of the *Bradi4g09040* gene (independant lines)	

APPENDIX 4: CULTURE MEDIA COMPOSITION

Plant culture media composition

Self-made Murashige and Skoog medium 50X +/- Pi

NH_4NO_3	105 mM	KI	25 µM
KNO_3	95 mM	$ZnSO_4.7H_2O$	150 µM
$CaCl_2.2H_2O$	15 mM	$Na_2MoO_4.2H_2O$	5 µM
$MgSO_4.7H_2O$	7.5 mM	$CoCl_2.6H_2O$	0.5 µM
H_3BO_4	500 µM	$CuSO_4.H_2O$	0.5 µM
$MnSO_4.H_2O$	500 µM		

The medium is autoclaved 20 minutes at 120°C. Then, 10 µM filter sterilized $FeCl_2$ and if needed, 1 mM filter sterilized KH_2PO_4 are added.

Linsmaier and Skoog medium 1X

Murashige and Skoog basal salts (Duchefa Biochemie)	1X
Sucrose	87.6 mM
Agar	0.7%

The medium is autoclaved 20 minutes at 120°C. Then, 555 µM filter sterilized myo-inositol and 0.3 µM filter sterilized thiamine hydrochloride are added.

Fungal culture media composition

Potato Dextrose Agar (PDA) & Potato Dextrose Broth (PDB) 1X

1 L of water containing 200 g of potatoes is boiled during 1 h. The medium is filtered on cotton and 20 g of glucose (and 20 g of agar for PDA) are added. The volume is adjusted to 1 liter before being autoclaved for 20 minutes at 120 ° C.

Mung Bean medium 1X

1 L of water containing 40 g of mung beans is boiled during 10 min. The medium is filtered, and it is autoclaved for 20 minutes at 120 ° C.

APPENDIX 5: LIST OF THE PRIMERS USED IN THE STUDY

Organism	Gene	Oligonucleotide name	Use in the study	Polarity	Sequence (5' → 3')	Product length (pb)
Brachypodium distachyon	*Bradi3g08360* (*BdCYP711A5*)	Bd3g08356_EI-ATG-2	Cloning	Forward	GGAATTCATGGCGGCCATTACCAACTGCT	1611
		Bd3g08356_EV-TAA-2		Revers	GAGATATCTCAGTCGTTCGTCCTCCTGATGG	
		BdCYP711A5qF	RT-PCR	Forward	TTCGGCCCTCAATCTCAATCCC	65
		BdCYP711A5qR		Revers	TGGTCCAGGTACGGGAATTTCG	
	Bradi1g37730 (*BdCYP711A6*)	Bd1g37730_DI-ATG	Cloning	Forward	AATTTAAAATGGCACCAGTTGGGGAATGGCT	2330 (ADNg)
		Bd1g37730_EI-TAA		Revers	GGAATTCCTAGACGGCCTCATTGCGCG	1608 (ADNc)
		BdCYP711A6qF	RT-PCR	Forward	TGCACATGTACCGGAGATTCGTG	131
		BdCYP711A6qR		Revers	ATTGCGCGTCAGCCTCTTGATG	
	Bradi1g75310 (*BdCYP711A29*)	Bd1g75310_BI5'ATG	Cloning	Forward	GAGGATCCATGGAGTCGCCATTGG	2347 (gDNA)
		Bd1g75310_EV3'TAA		Revers	CCGATATCTTAGTGCTCTTCTCGATCG	1621 (cDNA)
		Bd1g75310qF	qPCR	Forward	GCTACGTCTTCAGGCACTCC	103
		Bd1g75310qR		Revers	CGATCGATGACTTGGAGCTT	
		CYP711A29-F1	TILLING	Forward	TTCCCTACACGACGCTCTTCCGATCTCGGCCACATCAATTTTCATT	452 (ADNg)
		CYP711A29-R		Revers	AGTTCAGACGTGTGCTCTTCCGATCTTTAGTGCTCTTCTCGATCGA	/ (ADNc)
	Bradi4g08970 (*BdCYP711A30*)	Bd4g08970_BI-ATG	Cloning	Forward	CGGGATCCATGGGGATGCTGCCGATG	2061 (ADNg)
		Bd4g08970_EV-TAA		Revers	CCGATATCCTATTCCTTATGCCTGTGGATGAC	1603 (ADNc)
		BdCYP711A30qF	RT-PCR	Forward	CACGGCCCTGTCTTTAGGTTTC	/ (ADNg)
		BdCYP711A30qR		Revers	TGAACTTTCTGATCCCGACTTGCC	94 (ADNc)
	Bradi4g09040 (*BdCYP711A31*)	Bd4g09040_5'EV-ATG-4	Cloning	Forward	GGATATCATGATGGGCGGCGTGGGAGT	4318 (ADNg)
		Bd4g09040_3'EI-TAA-3		Revers	CCGAATTCTCATGCATTCCTCTCAATGACATGGAG	1593 (ADNc)
		BdCYP711A31qF	RT-PCR	Forward	AGAAGCATGCCTAGTCCCATCC	/ (ADNg)
		BdCYP711A31qR		Revers	TTTGCCATCTTGTGTCCCTGGTG	79 (ADNc)
	Bradi5g17660 (*BdMAX3*)	Bradi5g17660.1_F	qPCR	Forward	ATGTCGCCAATGGGTCAACG	/ (ADNg)
		Bradi5g17660.1_R		Revers	TTTGTCTTCGGATACCGCATACTC	137 (ADNc)
	Bradi2g49670 (*BdMAX4*)	Bradi2g49670.1_F	qPCR	Forward	TCGTCTCTGCTTCTTGCATACTG	75
		Bradi2g49670.1_R		Revers	TGCACAAACATCCACGTACAGG	
	Bradi4g00660 (*UBC18*)	UBC18qF	qPCR (Housekeeping gene)	Forward	ACCCTCTACGCTGGTGAGAC	223 (gDNA)
		UBC18qR		Revers	TGCTGTAAATGTGCGGATG	118 (cDNA)
	Bradi4g41850 (*ACT7*)	ACT7qF	qPCR (Housekeeping gene)	Forward	CCTGAAGTCCTTTTCCAGCC	188
		ACT7qR		Revers	AGGGCAGTGATCTCCTTGCT	
	Bradi1g39190 (*PR9*)	Bd1g39190_f	qPCR	Forward	TCCGACCAGGCTCTCTAC	122
		Bd1g39190_r		Revers	GCTATGTTCCCCATCTTGAC	
	Bradi3g47110 (*PAL6*)	Bradi3g47110q-F	qPCR	Forward	CCAAACAATTAAGGAGATCAATTAGAA	167 (ADNg)
		Bradi3g47110q-r		Revers	CCCGAATACTGGAAAGTAAGATACA	86 (ADNc)
Fusarium graminearum	18S	R18SqF	qPCR (Housekeeping gene)	Forward	GTCCGGCCGGGCCTTTCC	68
		R18SqR		Revers	AAGTCCTGTTTCCCCGCCACGC	
Arabidopsis thaliana	*At3g18780* (*ACT2*)	AtACT2qF	RT-PCR (Housekeeping gene)	Forward	AATCACAGCACTTGCACCA	100
		AtACT2qR		Revers	GAGGGAAGCAAGAATGGAAC	

[a] *Bd*, *Brachypodium distachyon*; *Fg*, *Fusarium graminearum*; *At*, *Arabidopsis thaliana*

[b] For, forward; Rev, reverse

université PARIS-SACLAY | ÉCOLE DOCTORALE Sciences du végétal : du gène à l'écosystème

Titre : Vers de nouveaux rôles pour les cytochromes P450 et les strigolactones dans la fusariose des épis de *Brachypodium distachyon*

Résumé : La fusariose des épis est l'une de maladies les plus dommageables des céréales tempérées et est principalement causée par le champignon toxinogène *Fusarium graminearum* (*Fg*). Ces dix dernières années, de nombreuses études ont rapporté l'induction transcriptionnelle de gènes de la plante codant pour des cytochromes P450 (P450) en réponse l'infection par *Fg*. Les P450s constituent une famille enzymatique impliquée dans de nombreuses voies métaboliques, certaines avec des intérêts potentiels dans la résistance face aux maladies. Nous avons utilisé la petite graminée modèle *Brachypodium distachyon* (*Bd*) pour caractériser fonctionnellement le premier gène codant pour un P450 induit chez la plante au cours de la fusariose des épis par l'utilisation de lignées altérées dans la séquence ou l'expression du gène *Bradi1g75310* codant le P450 BdCYP711A29.

Nous avons montré qu'en plus d'être un facteur de sensibilité à la maladie, le gène *Bradi1g75310* est impliqué dans une voie de biosynthèse hormonale chez *Bd*, celle des strigolactones (SLs). En effet, en plus de complémenter génétiquement les phénotypes aériens de la lignée mutante *max1-1* d'*Arabidopsis thaliana* altérée dans le gène homologue *MAX1* (*AtCYP711A1*), une lignée de *Bd* surexprimant *Bradi1g75310* (lignée OE) exsude davantage d'orobanchol, une SL spécifique, que la lignée sauvage ou mutante. Une analyse préliminaire de l'impact direct de l'orobanchol sur la croissance de *Fg* semble indiquer une activation des étapes précoces du développement du champignon (germination) qui pourrait être à l'origine de l'induction plus rapide de gènes de défenses observée chez une lignée OE de *Bradi1g75310*. Nous avons également montré que les 4 paralogues de *Bradi1g75310* chez *Bd*, qui codent également pour des CYP711A, sont tous capable de complémenter la lignée *max1-1* et avons généré du matériel végétal fondamental pour la poursuite de l'étude de la diversification des SLs chez la plante monocotylédone modèle *Bd*.

Au global, ce projet constitue une première étape dans la caractérisation de l'implication des P450 dans la réponse de la plante face à l'infection par *Fg* en plus de donner de nouveaux indices concernant le rôle des SLs dans les interactions plante-pathogène. Les résultats obtenus au cours de ce travail de thèse pourront permettre l'amélioration de caractères tant développementaux que de résistance à la fusariose chez les céréales cultivées.

Mots clés : Fusariose des épis, *Brachypodium distachyon*, *Fusarium graminearum*, Cytochromes P450, Strigolactones, Génomique fonctionnelle

Title: Towards New Roles for Cytochrome P450s and Strigolactones in Fusarium Head Blight of *Brachypodium distachyon*

Abstract: Fusarium Head Blight (FHB) is one of the most important diseases of temperate cereals and is mostly caused by the toxin producing-fungus *Fusarium graminearum* (*Fg*). This last decade, several studies reported the transcriptional activation of cereal cytochrome P450-encoding genes (P450s) in response to *Fg* infection. P450s constitute an enzymatic family participating in very diverse metabolic pathways with potential interest for disease resistance. We used the model temperate cereal *Brachypodium distachyon* (*Bd*) to functionally characterize the first FHB-induced P450-encoding gene using *Bd* lines altered in the locus or gene expression of the *Bradi1g75310* gene encoding the BdCYP711A29 P450.

We showed that in addition to be a plant susceptibility factor towards the disease, the *Bradi1g75310* gene is involved in the hormonal biosynthetic pathway of strigolactones (SLs) in *Bd*. Indeed, in addition to genetically complement the shoot phenotypes of the *Arabidopsis thaliana* mutant line for the homologous gene *MAX1* (*AtCYP711A1*, *max1-1* line), a *Bd* line which overexpresses the *Bradi1g75310* gene (OE) exudes more orobanchol, a specific SL, compared to wild-type or mutant lines. Preliminary analysis of the direct impact of orobanchol on *Fg* growth suggests an activation of early fungal development (germination) likely to induce faster induction of defense-related genes during FHB, observed in *Bradi1g75310* OE line. We showed that the four paralogs of *Bradi1g75310* encoding BdCYP711A P450s are all able to genetically complement *max1-1* line and provide important plant material for studying SLs diversification in the model monocot *B. distachyon*.

Overall, this project constitutes a first step in the characterization of P450s involvement in plant response towards *Fg* infection in addition to give new evidences about the role of SLs in plant-pathogen interactions. Results obtained during this Ph.D. project will allow the improvement of both developmental and FHB-related traits in cereal crops.

Keywords: Fusarium Head Blight, *Brachypodium distachyon*, *Fusarium graminearum*, Cytochrome P450s, Strigolactones, Functional genomics